HYDRAZONE LIGANDS FOR IRIDIUM CATALYZED C–H BORYLATIONS OF FLUOROARENES: STRATEGIES FOR ENHANCING RATES AND SELECTIVITIES

By

Christopher Daniel Peruzzi

A DISSERTATION

Submitted to
Michigan State University
in partial fulfillment of the requirements
for the degree of

Chemistry – Doctor of Philosophy

2024

ABSTRACT

Aryl boronic acids and esters are valuable intermediates for the broad chemistry community as building blocks for synthesis due to the wide variety of valuable transformations the C–B bond. The state-of-the-art methodology for generating these compounds is through iridium-catalyzed C–H activation borylation (CHB). Traditional systems activate the least sterically hinder C–H bond to activate, but many systems have been developed that can selectively activate ortho, meta, and para to several functional groups. To date, however, there are a limited number of systems using iridium that can selectively activate fluorinated aromatics due to its weak electrostatic interactions and small atomic size. The work described within detail a novel dipyridyl hydrazone ligand (dmadph) that can borylate fluoroarenes with increased selectivity for C–H activation meta to fluorine. This ligand also generates catalysts that are significantly more active than those generated using the most common ligand, 4,4′-di-*tert*-butyl-2,2′-bipyridine (dtbpy).

Investigations into this novel ligand framework led to the discovery of an unusual effect of hydrogen pressure generated during CHB on the observed regioselectivity of the reaction, further increasing C–H activation meta to fluorine. The hydrogen pressure generated during CHB enabled an iridium-catalyzed transfer borylation, or isodesmic borylation, of arenes. These are the first examples reported that demonstrate these effects in iridium-catalyzed systems. Due to the activity of the catalysts generated with dmadph, the pre-assembled catalyst was synthesized and isolated and revealed an unusual coordination mode to iridium. Parallel conversion kinetic isotope effect experiments revealed a primary kinetic isotope effect for the C–H borylation. NMR experiments during catalysis, however, identified an Ir–fluoroaryl complex, suggesting it is a resting state for the transfer borylation process and thus operates separate to the canonical CHB mechanism.

ACKNOWLEDGEMENTS

This past nearly six years in graduate school I have grown substantially as both a person and a chemist. This journey was long, arduous, but totally worth it and I would not have made it without the support and guidance of the many people I have known and met along the way.

I want to first and foremost thank my advisors, Professors Rob Maleczka and Mitch Smith, for their unwavering support, guidance, and freedom they gave me to explore my projects. The opportunity I have had to work within a collaborative project over the course of my graduate journey was one of the best experiences I could ask for. They taught me not only how to do chemistry, but most importantly how to think about the chemistry I am doing and to focus on the important findings. I am extremely thankful to have worked with both of them. To my group, Anshu, Arzoo, Pauline, Thomas, and previous group members thank you for the friendship, memories, and support over the years – I don't think we would've made it without each other! To MSU's awesome team of support specialists, Dan Holmes, Li Xie, Richard Staples, and Anna Osborn – you guys keep MSU running and without your help nobody could make it out. Last but certainly not least, thank you to my committee, Xuefei, Karen, and Jim for your guidance and support throughout my journey.

To my parents, Luigi and Julie, I am forever grateful for your unconditional love and support throughout these years, I could not have done it without you both. To my sister, Lauren, and brothers, Mike and Kyle, having you guys always be there to support me and pick me up when I was looking down kept me going to make it to the end. And Mike, without your lead starting at Grand Valley, I would not be where I am today or even started my journey with chemistry. I can't thank you enough for showing me what the chemistry world has to offer. To my grandparents, Luigi, Jeanne, Henry and Janet, I know I was always the one you were worried about – I am happy

that finally you all can see I did it, I know you all are looking down at me and watching. I love and miss you all every day.

Lastly, to Pauline Mansour, my rock and my partner – I couldn't have done this journey without you being here. Whether that was you being in the lab and pushing me towards my next goals, or the brief vacations to Lake Michigan or the GRC in Rhode Island (I consider it a vacation as well as a learning experience, it was too beautiful there!) you were instrumental to my success. Through the good and the bad times starting even at GVSU, you have always been there for me and I wouldn't want it any other way. I look forward to all the memories we will continue to make.

TABLE OF CONTENTS

LIST OF TABLES

LIST OF SCHEMES

LIST OF FIGURES

LIST OF ABBREVIATIONS

$[M]^+$	molecular ion peak
μL	microliters
bpy	butyl
Bu	C–H activation/borylation
CHB	C–H activation/borylation
cod	1,5-cyclooctadiene
Cp	cyclopentadienyl
Cy	cyclohexyl
DCM	dichloromethane
DFT	density functional theory
dmadph	2,2'-(hydrazineylidenemethylene)bis(N,N-dimethylpyridin-4-amine)
dmadpm	2,2'-methylenebis(N,N-dimethylpyridin-4-amine)
dppe	1,2-bis(diphenylphosphino)ethane
dtbpy	4,4’-di-tert-butyl-2,2’-bipyridine
eg	ethylene glycol
EI	electron ionization
equiv	equivalents
FWHM	full width at half maximum
GC-MS	Gas Chromatography-Mass Spectroscopy
h	hours
J	coupling constant
KIE	kinetic isotope effect

m	meta
Me	methyl
MeCN	acetonitrile
MHz	megahertz
min	minutes
mL	milliliters
mol	moles
mp	melting point
NCI	non-covalent interaction
NMR	nuclear magnetic resonance
o	ortho
p	para
Ph	phenyl
pin	pinacolate
pKa	acid dissociation constant at logarithmic scale
ppm	parts per million
R	remaining attachment to molecule
RDS	rate determining step
rt	room temperature
THF	tetrahydrofuran
tmphen	3,4,7,8-tetramethyl-1,10-phenanthroline
TON	turnover number

CHAPTER 1.

INTRODUCTION

1.1. Synthetic Utility and Applications of Organoboronates

Organoboronates are desirable intermediates across many disciplines of chemistry due to their exceptional versatility as building blocks towards final molecules of interest. They are able to undergo a variety of transformations[1,2] (**Scheme 1.2.1**) and can tolerate many reaction conditions depending on the oxo group attached to boron.[3] Notably, the Nobel prize winning Suzuki-Miyaura cross-coupling,[4,5] one of the most widely used reactions in medicinal chemistry,[6] requires a boronic acid or ester precursor. While C–C bond formation is important, transformations of the C(sp^2)–B bond via amination,[7–9] halogenation,[10] cyanation,[11] and oxidation[10,12] can also be performed. Transformations of C(sp^3)–B bonds via 1,2-boronate rearrangements,[1,13] heterocycle formation,[14] and cross-coupling reactions[14] are actively studied as ways to build complex molecules.

Scheme 1.1.1. Synthetic utility of C(sp^2)- and C(sp^3)-borylated Compounds

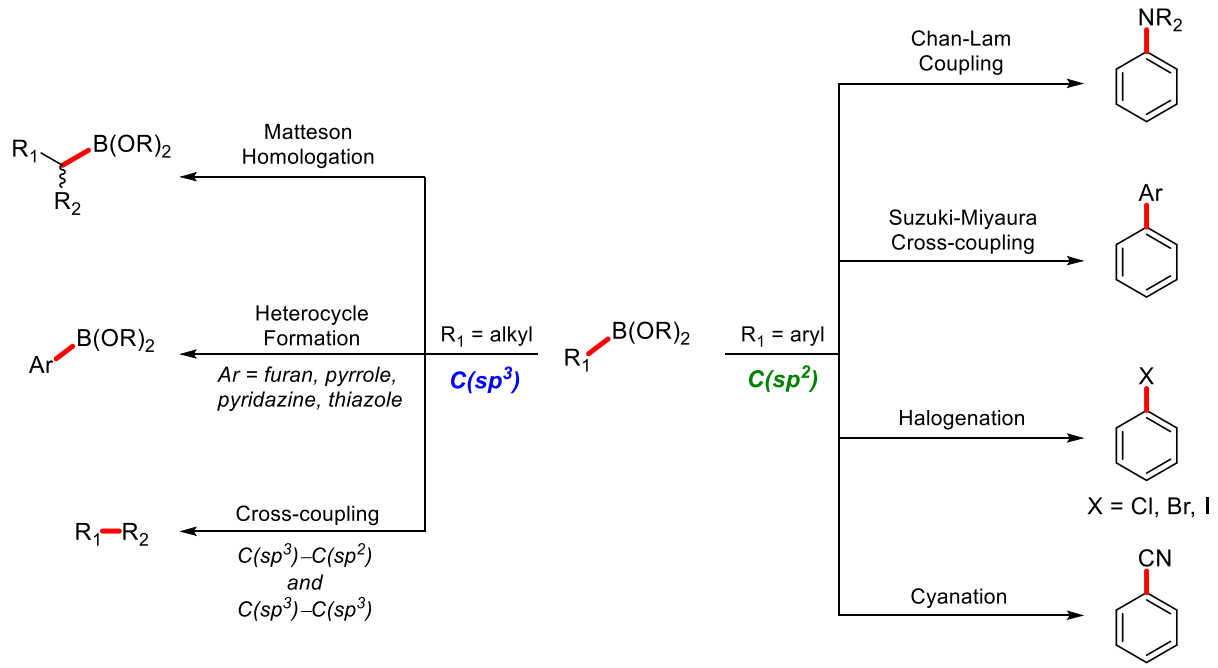

With the obvious desire to generate organoboronic esters as tools for synthesis outlined in **Scheme 1.2.1**, first the C–B bond must be synthesized. The traditional methodologies to synthesize these compounds typically involved a Miyaura borylation,[15] lithiation of an aryl halide or direct C–H lithiation followed by subsequent quenching with triisopropylborate. Early direct C–H activation routes both stoichiometric[16] and catalytic[17] required photochemical conditions to generate the products and a catalyst only requiring heat would offer substantial advantages.

Scheme 1.2.1. First thermocatalytic C–H borylation catalyzed by $Cp^*Ir^{III}(PMe_3)(H)(Bpin)$

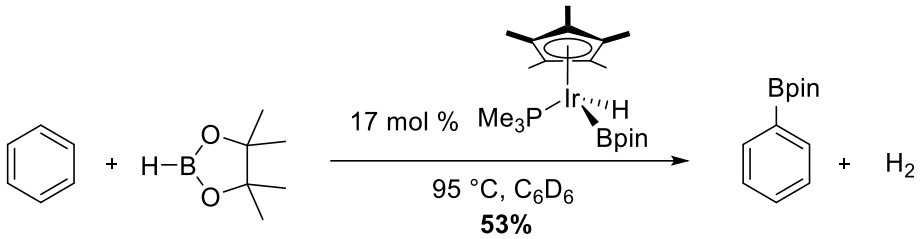

The first discovery of the thermocatalytic C–H borylation by a transition metal catalyst was made by Iverson and Smith in 1999.[18] The catalyst, while not particularly active only achieving about three turnovers, inspired the community to further study the iridium-catalyzed systems. The system was greatly improved upon in 2002, when the Smith and Maleczka collaboration found that by employing a chelating, neutral phosphine donor, the turnover numbers (TON = 4500) greatly increased.[19] Other seminal findings from this work were the proposal of an Ir^{III}/Ir^{V} mechanism over an Ir^{I}/Ir^{III} mechanism and the ability to telescope a borylation with a Suzuki-Miyaura cross-coupling in one pot, showing the Ir catalysis was compatible with halogenated aromatics preferentially activating the C–H bond over the C–X bond.

1.2. Mechanism of C–H Borylation by Ir^{III}

Subsequently after the finding that a chelating neutral donor ligand was essential to generating highly active catalysts towards C–H activation and borylation, Hartwig and co-workers found that utilizing a bipyridine generated extraordinarily active catalysts.[20] The ligand used in

their study, 4,4′-di-*tert*-butyl-2,2′-bipyridine (dtbpy), notably, is the state-of-the-art ligand used today and its analog, 2,2′-bipyridine has been used for extensive computational analysis.[21] Importantly, this analysis from Sakaki and co-workers supported the initial proposal from Smith and Maleczka that the mechanism operates in an Ir^{III}/Ir^{V} catalytic cycle.

Scheme 1.3.1. Proposed mechanism for the activation and borylation of R–H bonds

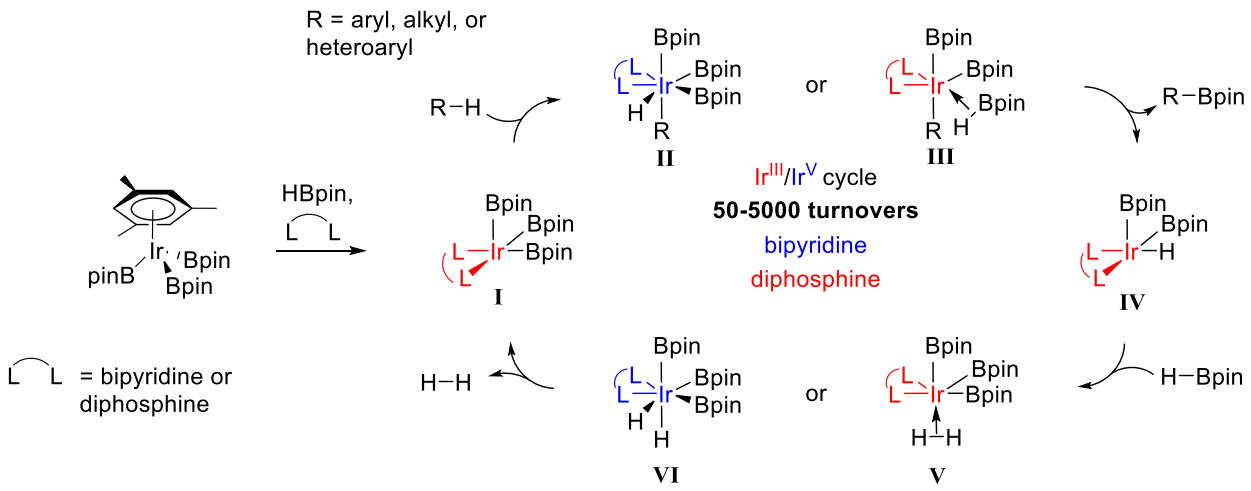

The mechanism was also empirically studied through careful kinetic analysis by the Hartwig group in 2005.[22] They were able to isolate a resting state of the proposed active catalyst **I** with addition of an excess of *cis*-cyclooctene (COE) that they were able to crystallize and use for their kinetic analysis. They found that COE reversibly dissociates from the iridium center to generate the active 16 e^- $L_2Ir(Bpin)_3$, which oxidatively adds a C–H bond to yield the somewhat unusual Ir^V intermediate **II**. This then goes on to reductively eliminate the borylated arene generating the bis(boryl)monohydride **IV**, which after oxidative addition of pinacolborane, yields intermediate **VI**. The catalyst is regenerated from reductive elimination of H_2 from **VI**, closing the catalytic cycle.

Importantly, this mechanism is distinct from the mechanism when a diphosphine ligand is used in place of a bipyridine. Careful examination and NMR analysis by the Smith and Maleczka

group[23] identified several intermediates along the catalytic cycle where intermediates **III** and **V** are operating. The NMR analysis revealed that the agostic complexes are active and present during catalysis, and the mechanism is operating via σ-bond metathesis rather than oxidative addition and reductive elimination. Also revealed and described in this work was that intermediate **IV** and other hydridoiridium(boryls) are active for C–H borylation and not just complex **I**, though their exact competence has not been fully evaluated to date.

1.3. Regioselectivity of Iridium-catalyzed C–H Borylations

1.3.1. General Selectivity of Ir-catalyzed CHBs and Ortho-selective Methodologies

Regioselectivity in iridium-catalyzed CHBs is generally governed by steric effects. [21,22,24] This means that for a given monosubstituted arene, when using a neutral chelating donor ligand, statistical ratio of 2:1 of the meta and para borylated products are generated.[20,25] This is because, as shown in **Scheme 1.4.1**, with a chelating ligand, a 16 e^- Ir^{III} complex is generated, leaving available only one open coordination site for C–H activation. However, if a ligand system were created where a second coordination site could open, this would allow the possibility of a directing group (DG) to coordinate to the metal to direct C–H activation.

Scheme 1.4.1. Ligand field around Ir^{III} active catalyst and consequences on regioselectivity

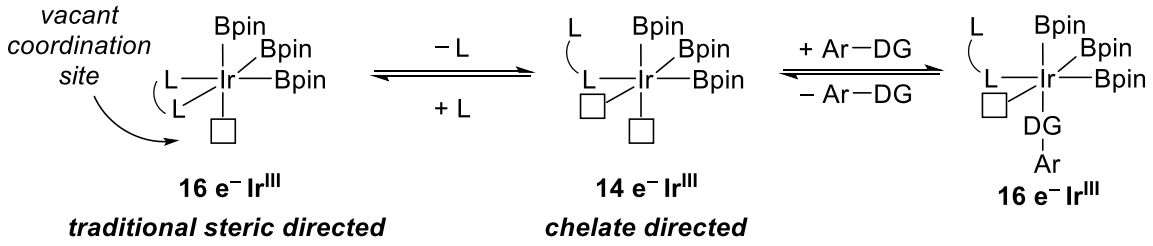

Towards this aim, several CHB systems have been created varying the ligand framework to allow the opening of a second coordination site. The "hemilabile" type ligands shown in **Figure 1.4.1** have been pioneered by Lassaletta[26] and Clark[27] for chelate directed borylations. They

propose that one of the arms of the ligand is able to freely dissociate from the metal center during catalysis, allowing coordination of a directing group, i.e. benzylamines[27], hydrazones[29], and phenylpyridines.[26]

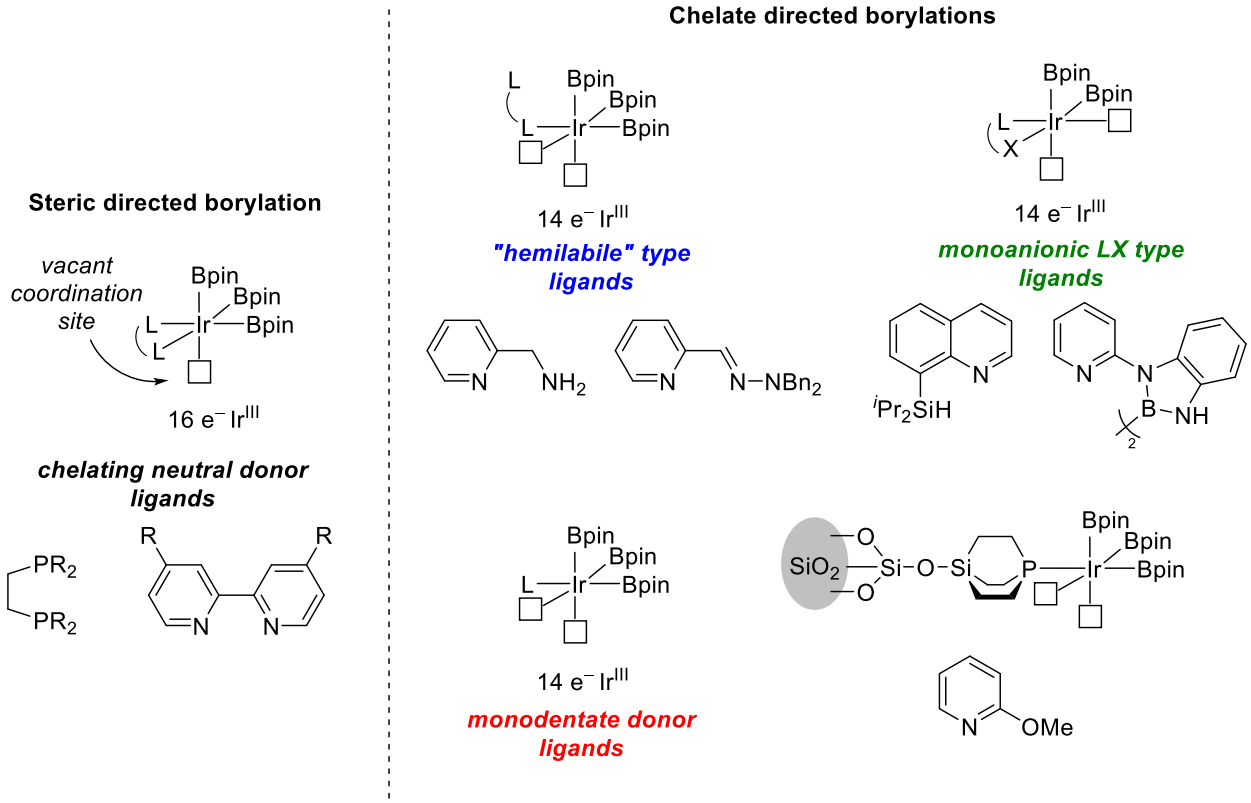

Figure 1.4.1. Steric and chelate borylation catalysts and their ligands

The second type of ligands that can be used to generate 14 e^- Ir^{III} intermediates, are monoanionic LX ligand frameworks. Unlike the neutral ligands previously discussed, these ligands have an anionic arm of the ligand such as a hydrosilane[31] or diboron[30,31] which after oxidative addition yields the silyl and boryl iridium species respectively. Thus, to satisfy the oxidation state and coordination sphere of iridium, only two boryls (Bpin) can add to the iridium, yielding the chelate directed catalyst for borylation.

Lastly, the third ligand set that has been utilized for directed ortho borylations are monodentate ligands. Simply, by controlling the stoichiometry a simple monodentate ligand will

allow the coordination of the DG to yield chelate directed borylations. Generally, however, these ligand systems suffer from poor activity, especially in the case of 2-methoxypyridine.[32] The Si-SMAP ligand developed by Sawamura[33] was proven to be extremely effective for the ortho borylation of esters and functional groups that are much more weakly coordinating like chlorides and methoxymethyl ethers.

1.3.2. Meta- and Para-selective CHBs Utilizing Non-covalent Interactions

While directing effects can be powerful methods to achieve highly selective ortho borylations, strategies to selectively activate C–H bonds meta and para to functional groups is considerably more difficult. Directing groups covalently attach to the metal to direct catalysis in these methods, however, strategies involving non-covalent interactions (NCIs) are being developed as a way to address meta and para activation. Hydrogen bonding (**Figure 1.4.2**) is one such NCI that has been used by the Kanai group[34] and Phipps group[35] to enable meta borylations of aryl amides and benzylamines respectively. The Kanai group appended a bipyridine ligand with a urea which hydrogen bonds with the carbonyl of the substrate, directing C–H activation meta to the amide with exceptional selectivities (up to >99:1). Similarly, the sulfonate group on the ligand utilized by Phipps hydrogen bonds to protected benzyl, phenethyl, and phenylpropylamines with excellent selectivity (up to 20:1 meta:ortho).

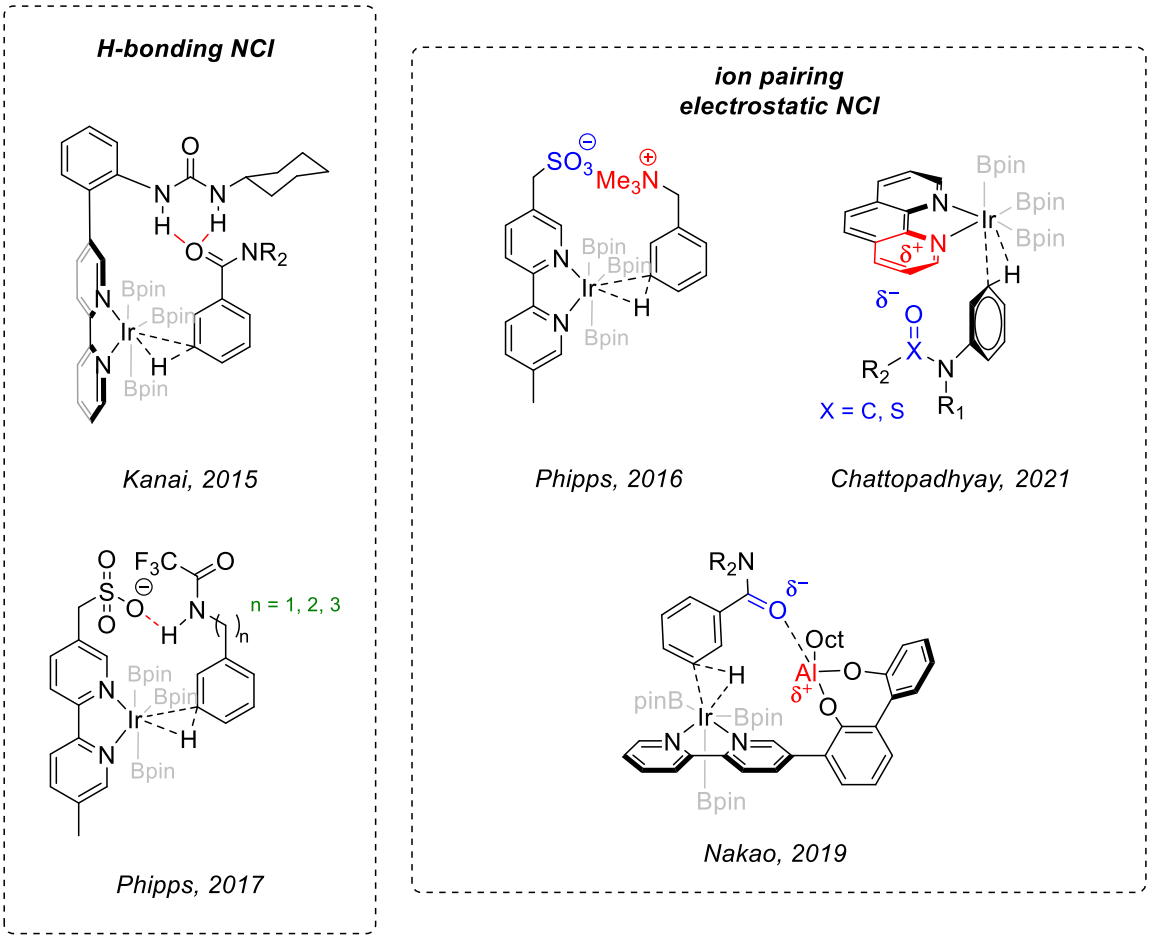

Figure 1.4.2. Strategies for meta-selective C–H activation and borylation

Another powerful non-covalent interaction used to direct CHBs meta is ion pairing effects. These effects can be due to full positive and negative charges, such as in Phipps[36] work that uses the same sulfonated bipyridine used in H-bond directed CHB to ion pair with positively charged quaternary ammonium salts enabling meta direction. These can also be due to partial charges such as those found in the work from the Chattopadhyay group[37] and Nakao group.[38] The Chattopadhyay group utilized an electrostatic interaction from the electron poor phenanthroline ligand on iridium and the electron rich sulfamate or amide of the substrate directing meta CHBs. The Nakao group used a completely different approach by introducing a Lewis acid co-catalyst that attaches to the bipyridine ligand on iridium to direct the borylation. The amide in this work

interacts with the Lewis acid, aluminum, to direct borylation meta for amides and C3-directed borylations of pyridines.

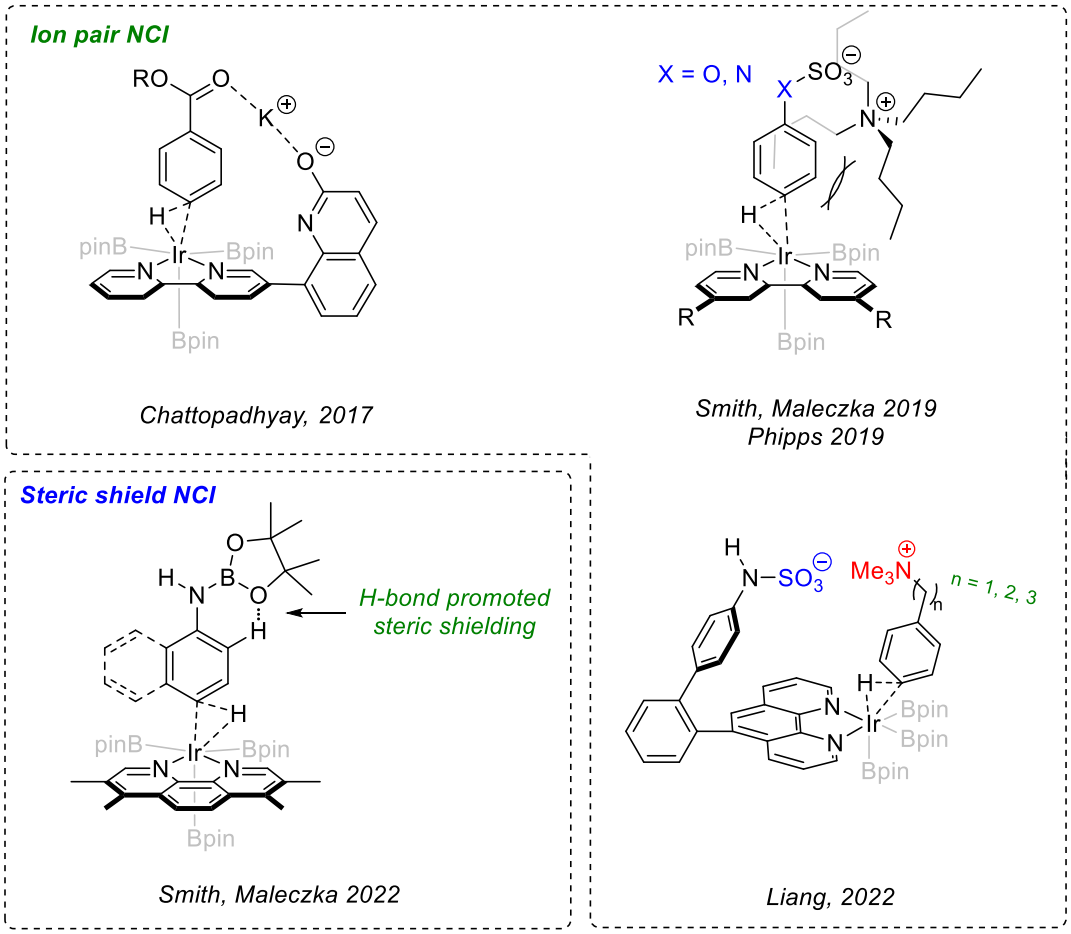

Figure 1.4.3. Strategies for para-selective C–H activation and borylation

Non-covalent interactions have also been utilized for effective directed para borylations (**Figure 1.4.3**). The most commonly used NCI for these transformations has been in using ion pairing. One of the first examples for para selective borylations came from the Chattopadhyay group, where they modified their bipyridine ligand to have a deprotonated quinolinol where the metal countercation, potassium, can pair to the partial negative charge of the carbonyl on esters directing borylation para.[39] A separate approach of this ion pairing directed catalysis from the Phipps[40] and Smith and Maleczka groups[41] concurrently. Phenols, anilines, benzylamines and

benzyl alcohols were converted to their respective sulfonates and paired with a bulky counteraction in tetrabutylammonium. This bulky countercation then sterically blocks the ortho and meta site, only enabling selective functionalization at the para position. The effect of the length of the alkyl chain of the cation further asserts this steric blocking, as shorter alkyl chains than butyl (propyl, ethyl…) erode the para selectivity. Notably, these methodologies can utilize the most commonly used ligands for borylation, 4,4′-disubstituted bipyridines, and only requires sulfonation of the substrates to direct the catalyst, which can easily be removed after borylation. The Liang group used a similar approach as seen in the meta selective borylations, ion pairing benzylammoniums with a sulfonate on a modified phenanthroline ligand to now direct the borylation to the para position.[42] The final novel approach utilizing a NCI to enable para borylations of anilines, indoles, and quinolines was demonstrated by the Smith and Maleczka groups.[43] Formal *N*-borylation of these arenes and (hetero)arenes enables a H-bond between the oxygen of the pinacolate and the ortho C–H bond, which in turn acts as a steric shield of the ortho and meta C–H sites.

1.4. Conclusions

Overall, iridium catalyzed C–H activation borylation is a robust, well-established method for the functionalization of arenes. It has become the state-of-the-art method for complex molecule diversification and molecule building for the wide array of transformations that these organoboronates can undergo. Through the years, many methodologies have been developed to address regioselectivity and for a wide variety of substrates, selective activation of the ortho, meta, and para C–H bonds are achievable, often through the use of attractive non-covalent interactions. Selective activations of fluorinated arenes and (hetero)arenes remain a significant challenge and efforts in iridium-catalyzed methods for highly selective CHBs of these substrates will be discussed and explored in the following chapters.

REFERENCES

(1) Thomas, S. P.; French, R. M.; Jheengut, V.; Aggarwal, V. K. Homologation and Alkylation of Boronic Esters and Boranes by 1,2-Metallate Rearrangement of Boronate Complexes. *Chem. Rec.* **2009**, *9* (1), 24–39.

(2) Jana, R.; Pathak, T. P.; Sigman, M. S. Advances in Transition Metal (Pd, Ni, Fe)-Catalyzed Cross-Coupling Reactions Using Alkyl-Organometallics as Reaction Partners. *Chem. Rev.* **2011**, *111* (3), 1417–1492.

(3) Lennox, A. J. J.; Lloyd-Jones, G. C. Selection of Boron Reagents for Suzuki-Miyaura Coupling. *Chem. Soc. Rev.* **2014**, *43* (1), 412–443.

(4) Miyaura, N.; Yamada, K.; Suzuki, A. A New Stereospecific Cross-Coupling by the Palladium-Catalyzed Reaction of 1-Alkenylboranes with 1-Alkenyl or 1-Alkynyl Halides. *Tetrahedron Lett.* **1979**, *20* (36), 3437–3440.

(5) Miyaura, N.; Suzuki, A. Stereoselective Synthesis of Arylated (E)-Alkenes by the Reaction of Alk-1-Enylboranes with Aryl Halides in the Presence of Palladium Catalyst. *J. Chem. Soc. Chem. Commun.* **1979**, No. 19, 866–867.

(6) Brown, D. G.; Boström, J. Analysis of Past and Present Synthetic Methodologies on Medicinal Chemistry: Where Have All the New Reactions Gone? *J. Med. Chem.* **2016**, *59* (10), 4443–4458.

(7) Evans, D. A.; Katz, J. L.; West, T. R. Synthesis of Diaryl Ethers through the Copper-Promoted Arylation of Phenols with Arylboronic Acids. An Expedient Synthesis of Thyroxine. *Tetrahedron Lett.* **1998**, *39* (19), 2937–2940.

(8) Lam, P. Y. S.; Clark, C. G.; Saubern, S.; Adams, J.; Winters, M. P.; Chan, D. M. T.; Combs, A. New Aryl/Heteroaryl C–N Bond Cross-Coupling Reactions via Arylboronic Acid/Cupric Acetate Arylation. *Tetrahedron Lett.* **1998**, *39* (19), 2941–2944.

(9) Chan, D. M. T.; Monaco, K. L.; Wang, R.-P.; Winters, M. P. New N- and O-Arylations with Phenylboronic Acids and Cupric Acetate. *Tetrahedron Lett.* **1998**, *39* (19), 2933–2936.

(10) Zhu, C.; Falck, J. R. Transition-Metal-Free Ipso-Functionalization of Arylboronic Acids and Derivatives. *Adv. Synth. Catal.* **2014**, *356* (11–12), 2395–2410.

(11) Liskey, C. W.; Liao, X. B.; Hartwig, J. F. Cyanation of Arenes via Iridium-Catalyzed Borylation. *J. Am. Chem. Soc.* **2010**, *132* (33), 11389–11391.

(12) Norberg, A. M.; Smith, M. R., III; Maleczka, R. E., Jr. Practical One-Pot C-H Activation/Borylation/Oxidation: Preparation of 3-Bromo-5-Methylphenol on a Multigram Scale. *Synthesis-Stuttgart* **2011**, *2011* (6), 857–859.

(13) Sharma, H. A.; Essman, J. Z.; Jacobsen, E. N. Enantioselective Catalytic 1,2-Boronate Rearrangements. *Science* **2021**, *374* (6568), 752–757.

(14) Fyfe, J. W. B.; Watson, A. J. B. Recent Developments in Organoboron Chemistry: Old Dogs, New Tricks. *Chem* **2017**, *3* (1), 31–55.

(15) Ishiyama, T.; Ishida, K.; Miyaura, N. Synthesis of Pinacol Arylboronates via Cross-Coupling Reaction of Bis(Pinacolato)Diboron with Chloroarenes Catalyzed by Palladium(0)–Tricyclohexylphosphine Complexes. *Tetrahedron* **2001**, *57* (49), 9813–9816.

(16) Waltz, K. M.; He, X.; Muhoro, C.; Hartwig, J. F. Hydrocarbon Functionalization by Transition Metal Boryls. *J. Am. Chem. Soc.* **1995**, *117* (45), 11357–11358.

(17) Chen, H. Y.; Hartwig, J. F. Catalytic, Regiospecific End-Functionalization of Alkanes: Rhenium-Catalyzed Borylation under Photochemical Conditions. *Angewandte Chemie-International Edition* **1999**, *38* (22), 3391–3393.

(18) Iverson, C. N.; Smith, M. R., III. Stoichiometric and Catalytic B−C Bond Formation from Unactivated Hydrocarbons and Boranes. *J. Am. Chem. Soc.* **1999**, *121* (33), 7696–7697.

(19) Cho, J.-Y.; Tse, M. K.; Holmes, D.; Maleczka, R. E., Jr; Smith, M. R., III. Remarkably Selective Iridium Catalysts for the Elaboration of Aromatic C-H Bonds. *Science* **2002**, *295* (5553), 305–308.

(20) Ishiyama, T.; Takagi, J.; Ishida, K.; Miyaura, N.; Anastasi, N. R.; Hartwig, J. F. Mild Iridium-Catalyzed Borylation of Arenes. High Turnover Numbers, Room Temperature Reactions, and Isolation of a Potential Intermediate. *J. Am. Chem. Soc.* **2002**, *124* (3), 390–391.

(21) Tamura, H.; Yamazaki, H.; Sato, H.; Sakaki, S. Iridium-Catalyzed Borylation of Benzene with Diboron. Theoretical Elucidation of Catalytic Cycle Including Unusual Iridium(v) Intermediate. *J. Am. Chem. Soc.* **2003**, *125* (51), 16114–16126.

(22) Boller, T. M.; Murphy, J. M.; Hapke, M.; Ishiyama, T.; Miyaura, N.; Hartwig, J. F. Mechanism of the Mild Functionalization of Arenes by Diboron Reagents Catalyzed by Iridium Complexes. Intermediacy and Chemistry of Bipyridine-Ligated Iridium Trisboryl Complexes. *J. Am. Chem. Soc.* **2005**, *127* (41), 14263–14278.

(23) Ghaffari, B.; Vanchura, B. A.; Chotana, G. A.; Staples, R. J.; Holmes, D.; Maleczka, R. E., Jr.; Smith, M. R., III. Reversible Borylene Formation from Ring Opening of Pinacolborane and Other Intermediates Generated from Five-Coordinate Tris-Boryl Complexes: Implications for Catalytic C–H Borylation. *Organometallics* **2015**, *34* (19), 4732–4740.

(24) Mkhalid, I. A. I.; Barnard, J. H.; Marder, T. B.; Murphy, J. M.; Hartwig, J. F. C-H Activation for the Construction of C-B Bonds. *Chem. Rev.* **2010**, *110* (2), 890–931.

(25) Cho, J.-Y.; Iverson, C. N.; Smith, M. R., III. Steric and Chelate Directing Effects in Aromatic Borylation. *J. Am. Chem. Soc.* **2000**, *122* (51), 12868–12869.

(26) Ros, A.; Estepa, B.; López-Rodríguez, R.; Álvarez, E.; Fernández, R.; Lassaletta, J. M. Use of Hemilabile N,N Ligands in Nitrogen-Directed Iridium-Catalyzed Borylations of Arenes. *Angew. Chem. Int. Ed. Engl.* **2011**, *50* (49), 11724–11728.

(27) Roering, A. J.; Hale, L. V. A.; Squier, P. A.; Ringgold, M. A.; Wiederspan, E. R.; Clark, T. B. Iridium-Catalyzed, Substrate-Directed C-H Borylation Reactions of Benzylic Amines. *Org. Lett.* **2012**, *14* (13), 3558–3561.

(28) López-Rodríguez, R.; Ros, A.; Fernández, R.; Lassaletta, J. M. Pinacolborane as the Boron Source in Nitrogen-Directed Borylations of Aromatic N,N-Dimethylhydrazones. *J. Org. Chem.* **2012**, *77* (21), 9915–9920.

(29) Ghaffari, B.; Preshlock, S. M.; Plattner, D. L.; Staples, R. J.; Maligres, P. E.; Krska, S. W.; Maleczka, R. E., Jr.; Smith, M. R., III. Silyl Phosphorus and Nitrogen Donor Chelates for Homogeneous Ortho Borylation Catalysis. *J. Am. Chem. Soc.* **2014**, *136* (41), 14345–14348.

(30) Wang, G.; Liu, L.; Wang, H.; Ding, Y.-S.; Zhou, J.; Mao, S.; Li, P. N,B-Bidentate Boryl Ligand-Supported Iridium Catalyst for Efficient Functional-Group-Directed C-H Borylation. *J. Am. Chem. Soc.* **2017**, *139* (1), 91–94.

(31) O'Connell, A. C.; Mansour, P. A.; Maleczka, R. E., Jr; Smith, M. R., III. Regiochemical Switching in Ir-Catalyzed C-H Borylation by Altering Ligand Loadings of N,B-Type Diboron Species. *Org. Lett.* **2023**, *25* (45), 8057–8061.

(32) Obligacion, J. V.; Bezdek, M. J.; Chirik, P. J. C(Sp2)-H Borylation of Fluorinated Arenes Using an Air-Stable Cobalt Precatalyst: Electronically Enhanced Site Selectivity Enables Synthetic Opportunities. *J. Am. Chem. Soc.* **2017**, *139* (7), 2825–2832.

(33) Kawamorita, S.; Ohmiya, H.; Hara, K.; Fukuoka, A.; Sawamura, M. Directed Ortho Borylation of Functionalized Arenes Catalyzed by a Silica-Supported Compact Phosphine-Iridium System. *J. Am. Chem. Soc.* **2009**, *131* (14), 5058–5089.

(34) Kuninobu, Y.; Ida, H.; Nishi, M.; Kanai, M. A Meta-Selective C-H Borylation Directed by a Secondary Interaction between Ligand and Substrate. *Nat. Chem.* **2015**, *7* (9), 712–717.

(35) Davis, H. J.; Genov, G. R.; Phipps, R. J. Meta-Selective C-H Borylation of Benzylamine-, Phenethylamine-, and Phenylpropylamine-Derived Amides Enabled by a Single Anionic Ligand. *Angew. Chem. Int. Ed Engl.* **2017**, *56* (43), 13351–13355.

(36) Davis, H. J.; Mihai, M. T.; Phipps, R. J. Ion Pair-Directed Regiocontrol in Transition-Metal Catalysis: A Meta-Selective C-H Borylation of Aromatic Quaternary Ammonium Salts. *J. Am. Chem. Soc.* **2016**, *138* (39), 12759–12762.

(37) Chaturvedi, J.; Haldar, C.; Bisht, R.; Pandey, G.; Chattopadhyay, B. Meta Selective C-H Borylation of Sterically Biased and Unbiased Substrates Directed by Electrostatic Interaction. *J. Am. Chem. Soc.* **2021**, *143* (20), 7604–7611.

(38) Yang, L.; Uemura, N.; Nakao, Y. Meta-Selective C-H Borylation of Benzamides and Pyridines by an Iridium-Lewis Acid Bifunctional Catalyst. *J. Am. Chem. Soc.* **2019**, *141* (19), 7972–7979.

(39) Hoque, M. E.; Bisht, R.; Haldar, C.; Chattopadhyay, B. Noncovalent Interactions in Ir-Catalyzed C-H Activation: L-Shaped Ligand for Para-Selective Borylation of Aromatic Esters. *J. Am. Chem. Soc.* **2017**, *139* (23), 7745–7748.

(40) Mihai, M. T.; Williams, B. D.; Phipps, R. J. Para-Selective C-H Borylation of Common Arene Building Blocks Enabled by Ion-Pairing with a Bulky Countercation. *J. Am. Chem. Soc.* **2019**, *141* (39), 15477–15482.

(41) Montero Bastidas, J. R.; Oleskey, T. J.; Miller, S. L.; Smith, M. R., III; Maleczka, R. E., Jr. Para-Selective, Iridium-Catalyzed C-H Borylations of Sulfated Phenols, Benzyl Alcohols, and Anilines Directed by Ion-Pair Electrostatic Interactions. *J. Am. Chem. Soc.* **2019**, *141* (39), 15483–15487.

(42) Lu, S.; Zheng, T.; Ma, J.; Deng, Z.; Qin, S.; Chen, Y.; Liang, Y. Para-Selective C-H Borylation of Aromatic Quaternary Ammonium and Phosphonium Salts. *Angew. Chem. Int. Ed Engl.* **2022**. https://doi.org/10.1002/anie.202201285.

(43) Montero Bastidas, J. R.; Chhabra, A.; Feng, Y.; Oleskey, T. J.; Smith, M. R., III; Maleczka, R. E. Steric Shielding Effects Induced by Intramolecular C–H⋯O Hydrogen Bonding: Remote Borylation Directed by Bpin Groups. *ACS Catal.* **2022**, *12* (4), 2694–2705.

CHAPTER 2.

A HYDRAZONE LIGAND FOR IRIDIUM-CATALYZED C–H BORYLATION: ENHANCED REACTIVITY AND SELECTIVITY FOR FLUORINATED ARENES

2.1. Introduction

Ir-catalyzed C–H borylation (CHB) has become a ubiquitous, state of the art method for the direct formation of both alkyl and aryl boronic esters. There are few systems capable, however, of achieving high selectivity in direct borylations of fluoroarenes. The highly selective reactions are limited to cases where oxidative addition is reversible ("ortho fluorine effect"),[1–3] directing groups are installed onto the substrate[4,5], or borylation-deborylation strategies[6] and the majority are ortho-selective.[7–10] With the prominence of fluorine in pharmaceuticals[11] and medicinal chemistry,[12] developing C–H functionalizations with complementary selectivities to the existing methods is important.

The major challenges with site selectivity arise from the intrinsic properties associated with fluorine. Fluorine is only 20% larger than hydrogen[13] causing poor steric discrimination in the context of Ir-catalyzed CHBs,[14–16] and is nonpolarizable[13] preventing strong electrostatic interactions to guide selectivity. Furthermore, experimental work from Jones, Perutz, and co-workers[2] (**Scheme 2.1**) and subsequent computational studies from Eisenstein demonstrated that across many transition metal–fluoroaryl complexes, the metal–carbon bond strength increases with increasing *ortho* fluorine substituents.[1,17] Their findings suggest that, generally, regioselectivity for C–H activation is thermodynamically favored at sites *proximal* to F. Prior work from our group[18,19] also has shown that, in agreement with increased metal–carbon bond strengths, the more acidic C–H bonds are more reactive. Thus an electronically enhanced selectivity for borylation ortho-to-F should be found. The clash of the electronic and thermodynamic preference for ortho-

to-F selectivity with the steric selectivity of CHBs often result in, poor regioselectivity for the CHB of fluoroarenes when utilizing Ir without the use of blocking groups[20] or directing effects.

Scheme 2.1. Challenges in selective fluoroarene C–H activations

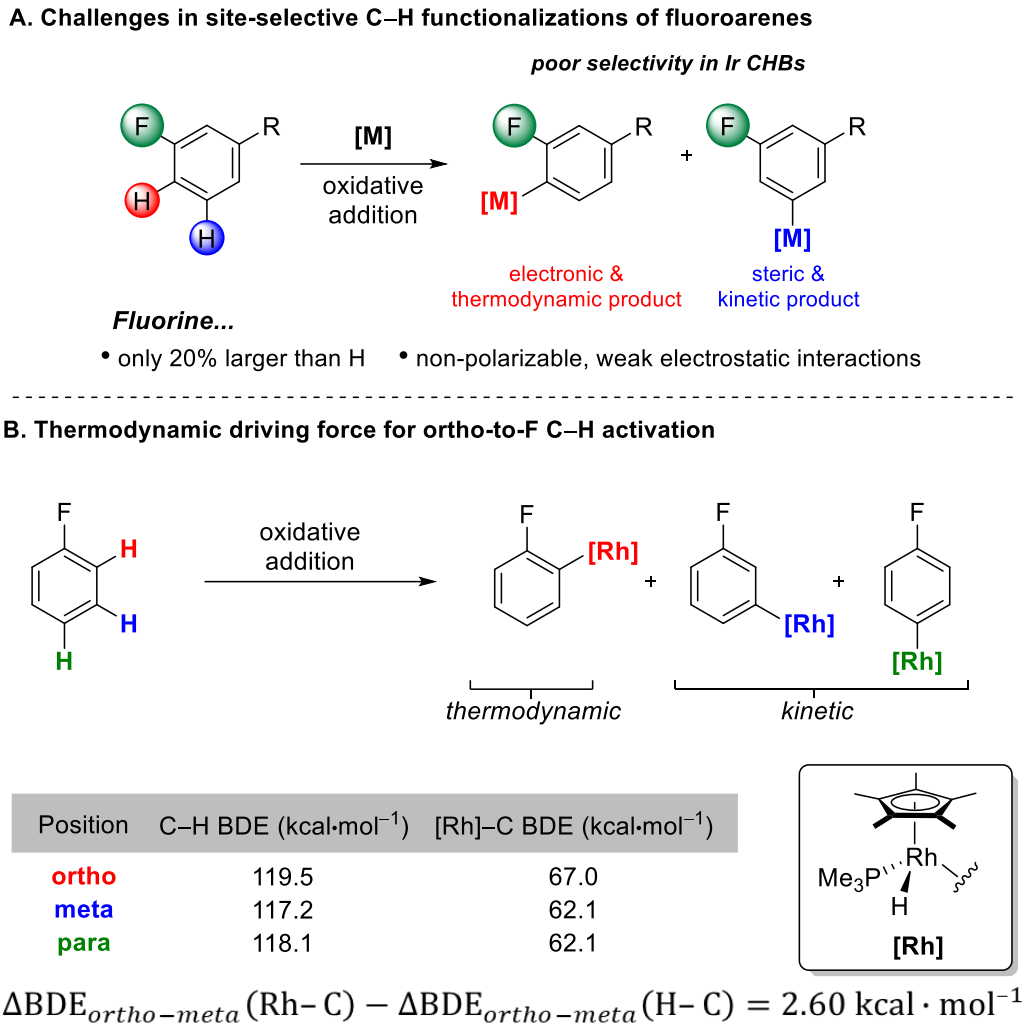

$$\Delta\mathrm{BDE}_{ortho-meta}(\mathrm{Rh-C}) - \Delta\mathrm{BDE}_{ortho-meta}(\mathrm{H-C}) = 2.60\ \mathrm{kcal}\cdot\mathrm{mol}^{-1}$$

Thermodynamically, there is a small difference in the bond dissociation energies of the C–H bonds in fluorobenzene (<2.5 kcal·mol–1).[1] To achieve kinetic control, the barrier that leads to the thermodynamic product must be at least 2.5 kcal·mol–1 (at 298K) higher than the barrier leading to the kinetic product. Moreover, the reaction must be run under conditions where equilibrium is not reached. Towards this aim, several CHB systems (**Figure 2.1**) have been developed for their selectivity in non-directed functionalizations of C–H bonds. Recent work by

the Chirik group (**Figure 2.1a**) demonstrated CHBs with an electron deficient Co catalyst bearing a terpyridine ligand enables slow C–H cleavage, affording up to 99:1 meta-to-F site selectivities.[21] This is distinct from their [($^{i\text{Pr}}$PNP)Co] system[3] where high ortho-to-F selectivity is observed. The Driess group also reported a sterically encumbered Co catalyst generated from a pyridine bis-silylene ligand framework that provides high selectivities for meta functionalizations.[22] Notably, these systems utilizing earth abundant cobalt are only amenable to activated, electron deficient arenes. Furthermore, the cobalt based systems do not tolerate heavier halogens due to more favorable C–X cleavage (X = Cl, Br, I).

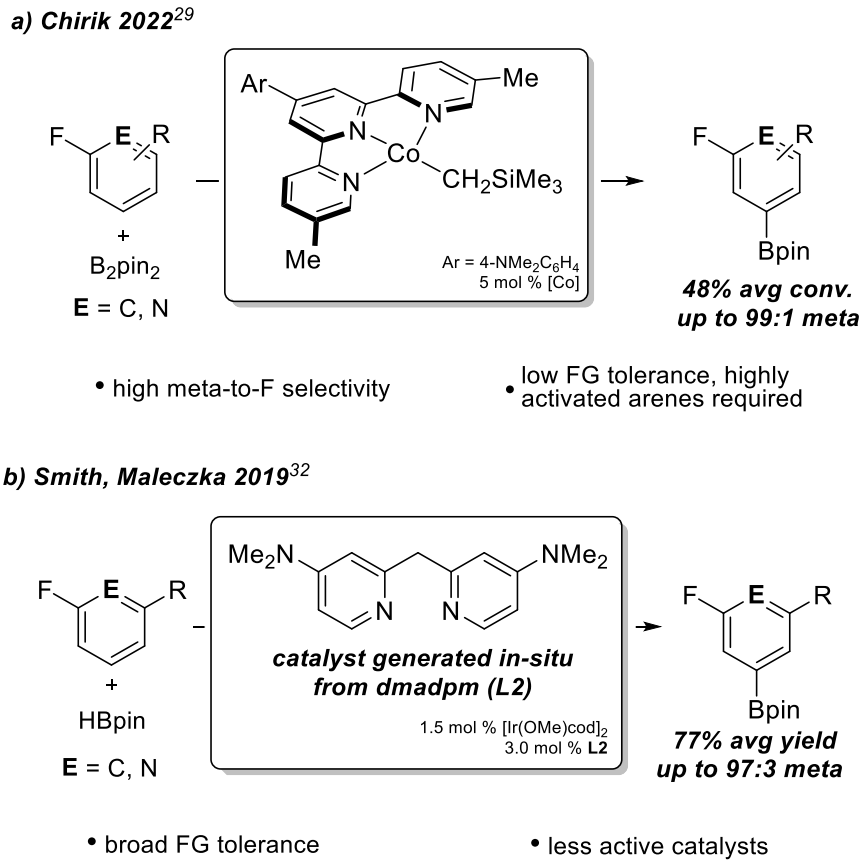

Figure 2.1. Selected examples of catalysts competent for high meta-to-F regioselectivity

A well-known advantage of iridium catalysis is high functional group tolerance, but selective activation meta or para to fluorine via iridium catalysis is underdeveloped.[6,23] Currently, high ortho-to-F selectivity can be achieved with an iridium-terpyridine catalyst that was developed

by Ilies.[9] The only system with high meta-to-F selectivity was developed by our group, utilizing **L2** (**Figure 2.1b**) as the ligand.[23] However, catalysts generated from **L2** are considerably less active than traditional bipyridines or phenanthrolines, requiring at least twice the reaction time for comparable conversions. Thus, we desired to generate a catalyst that achieved both high meta or para to fluorine selectivity and retained activity on the order of iridium catalysts generated from bipyridines such as dtbpy (**L3**).

2.2. Results and Discussion

2.2.1. Optimization of Reaction Conditions

Inspired by prior demonstrations of hydrazone based ligands in Ir-catalyzed CHBs[24,25] and our prior studies of **L1-L2**, **L4** was designed to achieve this goal. Catalysts generated by **L4** were much more reactive than the dipyridylmethane-type ligands (**L1, L2**) and on par with dtbpy (**L3**). Solvent choice proved to be vital to improving meta-to-F selectivity, as using a non-polar solvent (**Scheme 2.2, entries 6-7**) greatly diminishes selectivity. Additionally, there is an effect of temperature on the observed selectivity with lower temperatures improving the meta-to-F selectivity, consistent with kinetic control. This effect is distinct from Ir/bipyridine catalyzed CHBs, where temperature marginally impacts the regioselectivity.[26] Though this effect was observed, 40 °C was the optimal temperature (**Scheme 2, entry 8**) for high activity while maintaining the improved selectivity.

Scheme 2.2. Optimization of borylation conditions[a]

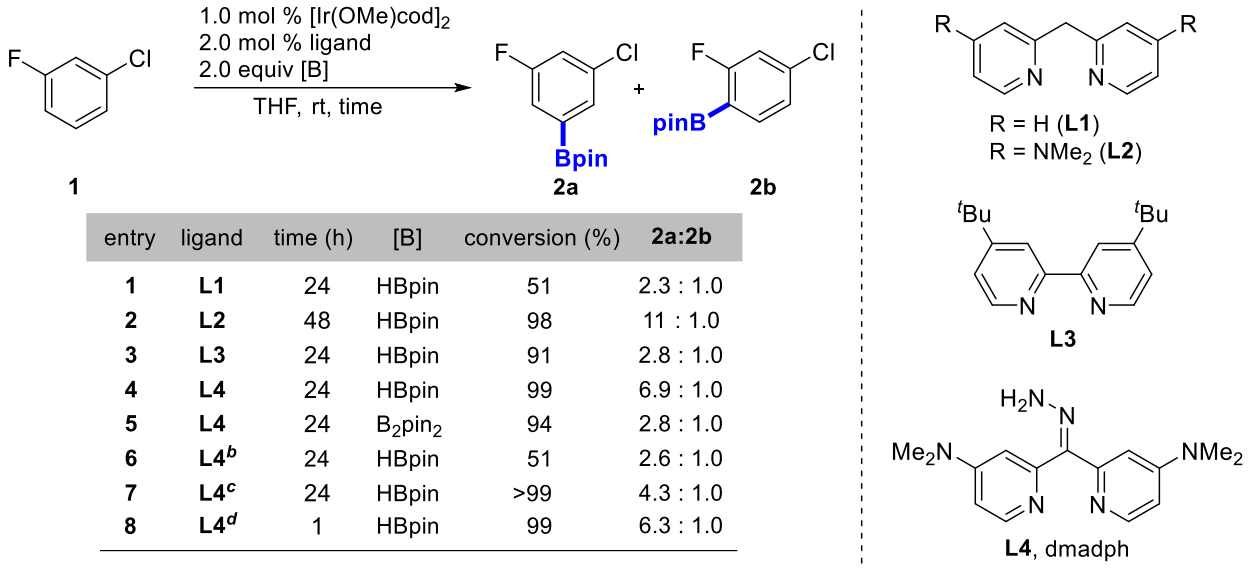

entry	ligand	time (h)	[B]	conversion (%)	2a:2b
1	L1	24	HBpin	51	2.3 : 1.0
2	L2	48	HBpin	98	11 : 1.0
3	L3	24	HBpin	91	2.8 : 1.0
4	L4	24	HBpin	99	6.9 : 1.0
5	L4	24	B_2pin_2	94	2.8 : 1.0
6	L4[b]	24	HBpin	51	2.6 : 1.0
7	L4[c]	24	HBpin	>99	4.3 : 1.0
8	L4[d]	1	HBpin	99	6.3 : 1.0

[a]Reaction conditions: fluoroarene (1.0 mmol), HBpin (2.0 mmol) or B_2pin_2 (1.0 mmol), $[Ir(OMe)cod]_2$ (1.0 mol %), ligand (2.0 mol %), solvent (2.0 mL). [b]n-Hexane used as solvent. [c]CH_2Cl_2 used as solvent. [d]Reaction run at 40 °C. Ratios of products were found with ^{19}F NMR analysis.

2.2.2. Meta-to-F CHBs of Fluoroarenes

Catalysts generated by **L4** afforded improved activity and selectivity for all 1,3-disubstituted arenes examined (**Table 2.1**). Borylations of electron poor substrates **4a-f** were essentially complete within 2 h with kinetic selectivities of up to 18.0:1.0 and high yields. Notably, activated fluoroarenes containing heavier halogens (**4e-f**) are significantly less reactive when using dtbpy as the ancillary ligand. Electron rich substrates **4i-k** still required longer reaction times, however, a nearly 3-fold improvement in both conversion to products and selectivities were found with **L4**. The borylation of fluorobenzene (**4l**) shows improved site selectivity without the influence of other functional groups. We also wanted to examine **5** as a non-fluorinated substrate that typically requires elevated temperatures, prolonged reaction times, and the more reactive borylating reagent (B_2pin_2)[14,26] to achieve good conversion. Under much milder conditions, **L4**

Table 2.1. Meta-selective C–H Borylations of 1,3-Disubstituted Fluorinated and Cyanated Arenes[a]

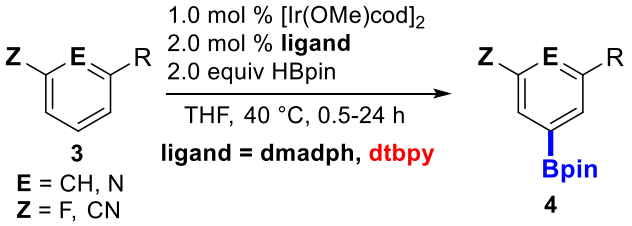

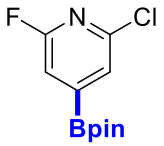

4a
88% (*>20:1.0*), 0.5 h
98% (*5.8:1.0*), 3 h

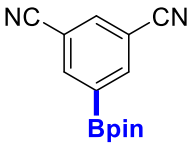

4b
85% (*12.5:1.0*), 0.5 h
90% (*4.4:1.0*), 3 h

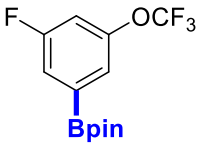

4c
96% (*8.0:1.0*), 2 h
93% (*4.1:1.0*), 14 h

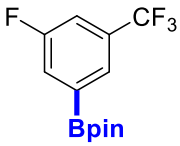

4d
87% (*4.4:1.0*), 2 h
95%, (*1.8:1.0*), 12 h

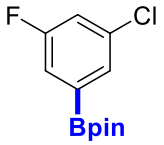

4e
82% (*6.4:1.0*), 1 h
97% (*2.5:1.0*), 18 h

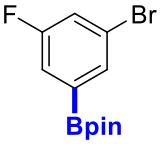

4f
93% (*7.1:1.0*), 2 h
95% (*2.9:1.0*), 20 h

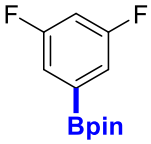

4g
88% (*4.6:1.0:0.9*), 8 h
95%, (*3.3:2.7:1.0*), 12 h

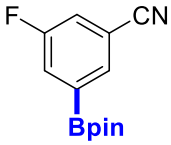

4h
93% (*3.4:1.0*), 2 h
95% (*1.1:1.0*), 6 h

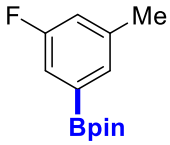

4i
72% (*4.0:1.0*), 24 h
24%, (*1.4:1.0*), 24 h

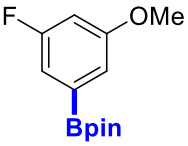

4j
80% (*6.0:1.0*), 24 h
29% (*2.2:1.0*), 24 h

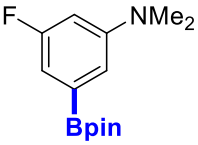

4k
80% (*3.3:1.0*), 24 h
19% (*1.9:1.0*), 24 h

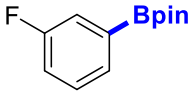

4l[c]
99% (*1.3:**5.4**:1.0*), 3 h
95% (*3.4:**5.2**:1.0*), 24 h

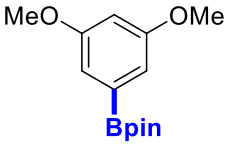

5
72%[d], 24 h
18%, 24 h

[a]Reaction conditions: fluoroarene (3, 1.0 mmol), HBpin (2.0 mmol), $[Ir(OMe)cod]_2$ (1.0 mol %), and ligand (2.0 mol %) in THF (2.5 mL), 40 °C, 0.5-24 h. Isolated yields are reported after column chromatography for dmadph and selectivities are from crude reaction mixtures. Percent conversions found from ^{19}F NMR are reported for dtbpy. Numbers in parentheses correspond to the ratio of meta:ortho to F borylated isomers. [b]Ratio of 5:2,5:4 borylated isomers given in parentheses. [c]5 equiv of fluorobenzene was used to suppress diborylation. Ratio of ortho:meta:para to F borylated isomers given in parentheses. [d]Reaction ran at 65 °C.

achieves 72% conversion in 24 h whereas dtbpy only reaches 18% conversion demonstrating the superior activity of the catalysts generated. Catalyst loading studies were conducted (see section **2.4.4**) to further demonstrate the superior activity of the hydrazone ligand. Excellent conversions were observed with only 0.1/0.2 mol% loadings of [Ir(OMe)cod]$_2$/**L4** respectively. These loadings could be lowered further to 0.01/0.02 mol% at the expense of longer reaction times, as 35% conversion was observed as compared to nearly full conversion at 0.1/0.2 mol%.

Scheme 2.3. Investigations of other fluoroarenes

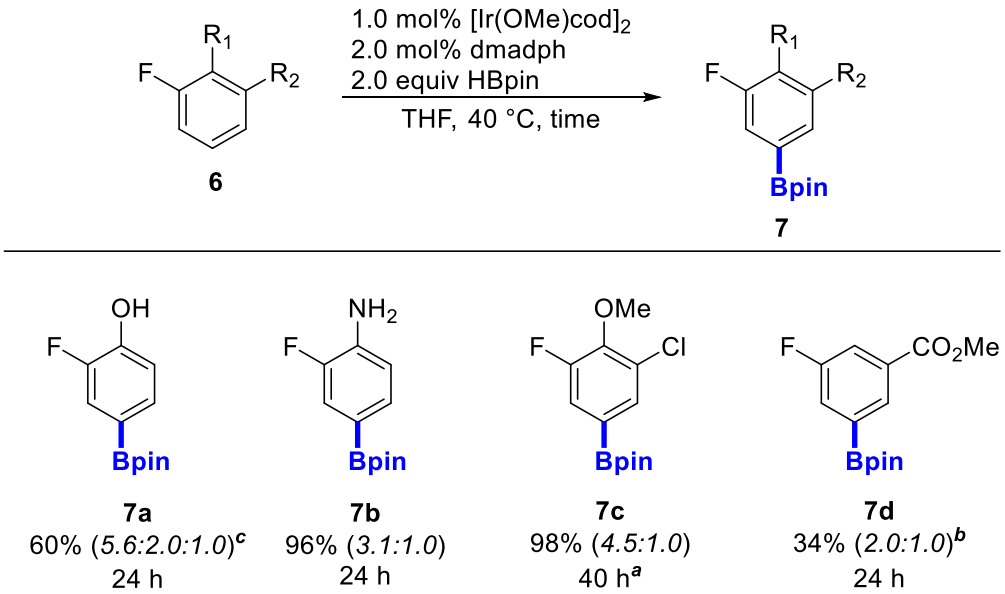

Reaction conditions: fluoroarene (1.0 mmol), HBpin (2.0 mmol), [Ir(OMe)cod]$_2$ (1.0 mol %), and dmadph (2.0 mol %) in THF (2.5 mL), 40 °C. Conversions are listed as determined by ^{19}F NMR. Numbers in parentheses correspond to the ratios of the meta:ortho to F borylated isomers. [a]Reaction run at rt. [b]Some reduction of the ester observed in the ^{1}H NMR. [c]Ratio of products given in parentheses is the meta:para:ortho-to-F borylated isomers.

Other substrates beyond 1,3-disubstituted were also examined under the catalytic conditions in **Scheme 2.4**. The 1,2-disubstituted arenes **7a-7b** bear –OH and –NH$_2$ functional groups, which, first undergo *O*- and *N*-borylation with pinacolborane prior to C–H borylation.[27–29] This reactivity was leveraged to enable para-selective borylations of anilines[27] through intramolecular C–H···O hydrogen bonding of the ortho hydrogen to the oxygen of the N–Bpin group. These conditions were not amenable to phenols, however, which provided no selectivity

(1:1 ratio of para:meta to –OH) for reactions using bipyridines or phenanthrolines as ligands. The meta-to-F selectivity (or para to the phenol) in the case of **7a** was superior for dmadph than when the borylation was done under both conditions previously described by our group.[27,30] Substrate **7b** was not investigated in that work, however the meta-selectivity was moderate. Interestingly, the tri-substituted fluoroarene **7c** showed diminished selectivity compared to 3-fluorochlorobenzene, suggesting an electronic contribution to the observed selectivity from the methoxy group. To determine if esters were tolerated, **7d** was borylated under catalytic conditions and both poor selectivity and activity was observed. The ^{11}B NMR of the crude reaction mixture revealed significant amounts of O–Bpin formation, suggesting reduction of the ester by pinacolborane to the corresponding alcohols. This could be responsible for the poor conversion, as previous work demonstrated lower conversion under the catalytic conditions with only one equivalent of pinacolborane.

Scheme 2.4. Stoichiometric studies of the reactivity of the hydrazone ligand[a]

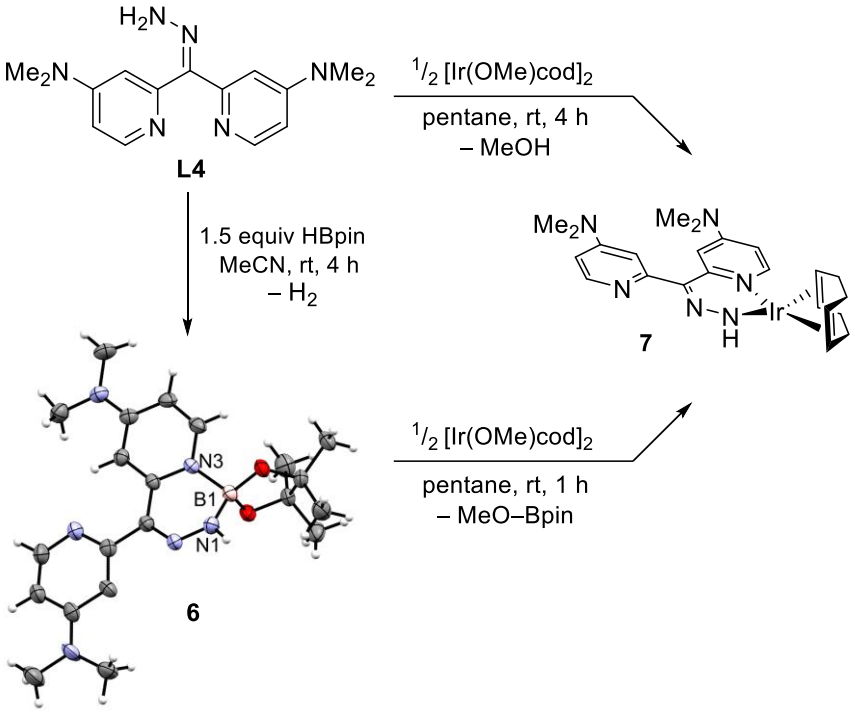

[a]Molecular structure displayed with 50% probability ellipsoids and a partial labelling scheme (co-crystallized CH_3CN and H_2O omitted for clarity). N1–B1 = 1.520 Å, N3–B1 = 1.587 Å

2.2.3. Investigation of the Catalytic Manifold

In trying to rationalize the greatly improved selectivity when using **L4**, we considered the ligand framework and potential structural changes or reactions that could occur during catalysis.[31] As previously described, N–H and O–H sites are rapidly *N*- and *O*-borylated in CHB reactions catalyzed by Ir species with B_2pin_2 or pinacolborane.[27–29] Shown in **Scheme 2.4**, the hydrazone is rapidly *N*-borylated in MeCN without Ir forming a hydrazone-boronate adduct (**6**). A sharp singlet was observed in the ^{11}B NMR (2.96 ppm, $\omega_{1/2}$ = 49 Hz) evidencing the presence of a four-coordinate boron center. This is further validated by ^{1}H NMR, as inequivalent methyl groups of the pinacolate are observed due to hindered rotation of the adduct. Single crystals suitable for Xray crystallography were obtained by crystallization in CH_3CN at –34 °C, unequivocally confirming

the structure. It is noteworthy that with the precatalyst, this reaction occurs on the order of seconds rather than hours.

Scheme 2.5. Alkylation effects on activity and selectivity of CHB

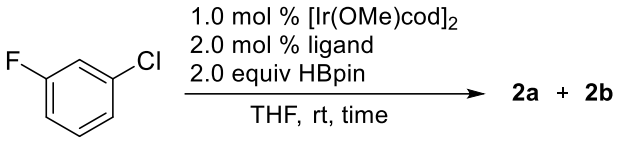

entry	ligand	time (h)	conversion (%)	2a:2b
1	**L4**	12	99	7.0 : 1.0
2	**L5**	27	78	4.0 : 1.0
3	**L6**	12	96	3.0 : 1.0

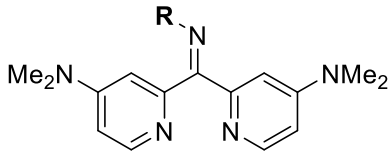

R = NH_2 (**L4**)
R = $NHCH_3$ (**L5**)
R = $N(CH_3)_2$ (**L6**)

We originally hypothesized that the hydrazone-boronate adduct (**6**) formed *in-situ* during borylation and introduced an increased steric demand to the metal that improved selectivities. In practice, the stoichiometric reactions of both **L4** and **6** with $[Ir(OMe)cod]_2$ in pentane leads to exclusive formation of the Ir^I hydrazido **7** (**Scheme 2.4**) and methanol or MeO–Bpin, respectively. While catalytic amounts of material are difficult to characterize, the judicious choice of substrate can allow some analysis of the species generated during the reaction. Thus, the CHB of pentafluorobenzene was monitored via a NMR tube reaction (see section **2.2.10** for details), and ^{11}B NMR evidenced the formation of a new N–B bond during the reaction. Based on this evidence, both hydrogens in the amino hydrazone, **L4,** may be important for the reactivity and selectivity observed. To explore this, we synthesized substituted analogs of **L4** (**Scheme 2.5**). Alkylation of the free amine of the hydrazone in **L5-L6** proved deleterious to both regioselectivity and activity. These results implicate the importance of the amine in hydrazone **L4**. We hypothesize that the hydrazone amine forms both the Ir–hydrazido and the N–Bpin in the active catalyst.

Furthermore, we wanted to determine if the isolated hydrazido **7** and boronate adduct **6** lead to active catalyst formation by comparison with *in-situ* generation in **Table 1**. When both

were used for a borylation of fluorochlorobenzene (**Scheme 2.5**), nearly identical selectivities to those found when generating the catalyst *in-situ* were observed. With these results in mind, a bis(boryl)Ir^{III} is likely operating in a canonical Ir^{III}/Ir^{V} catalytic cycle.

Scheme 2.6. Borylation of fluorochlorobenzene with isolated adduct and Ir^{I} hydrazido[a]

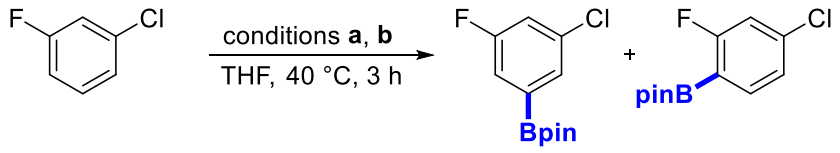

condition	variation	conversion (%)	2a:2b
a	2.0 mol % **7** 2.0 equiv HBpin	75	6.5:1.0
b	1.0 mol % $[Ir(OMe)cod]_2$ 2.0 mol % **6** 2.0 equiv HBpin	80	6.5:1.0

2.3. Conclusions

In summary, a new dipyridyl hydrazone ligand, dmadph, has been used in Ir-catalyzed C–H borylations of fluorinated arenes to afford significantly greater kinetic products than with dtbpy. We have shown dmadph generates catalysts that are *both* more active and selective than those generated from dtbpy. Additionally, HBpin is utilized to increase meta selectivity, an effect that we previously observed with the dipyridylmethane type ligands.[23] This unusual increase in regioselectivity using HBpin with both **L2** *and* **L4** warrants further mechanistic evaluation and investigations are ongoing.

2.4. Experimental

2.4.1. General Information

Pinacolborane (HBpin) (97% stabilized with 1% triethylamine) was purchased commercially and used as received without further purification. The iridium catalyst, bis(η^4-1,5-cyclooctadiene)-di-μ-methoxy-diiridium (I), $[Ir(OMe)(cod)]_2$, was prepared by a literature procedure.[32]

All substrates were obtained commercially and used as received unless otherwise noted.

All reactions were prepared in 3.0 mL Wheaton microreactor vials equipped with stir bars and pressure caps in a glovebox under a nitrogen atmosphere and then transferred to a preheated aluminum block outside of the glovebox. THF and *n*-hexane were obtained from wet stills refluxing over sodium and benzophenone. Methylene chloride and acetonitrile were obtained from dry stills according to the literature procedure.[33]

Reactions were monitored by ^{19}F NMR, and crude reaction ratios were verified by ^{1}H NMR or ^{19}F NMR for fluorine containing substrates. NMR spectra were recorded on a Varian 500 MHz DD2 Spectrometer equipped with a 1H-19F/15N-31P 5mm Pulsed Field Gradient (PFG) Probe. Spectra were taken in deuterated solvents referenced to residual solvent signals in ^{1}H NMR and ^{13}C{^{1}H} NMR. ^{13}C{^{1}H} NMR resonances for the boron-bearing carbon atom were not observed due to quadrupolar relaxation. NMR spectra were processed for display using the MNova software with only phasing and baseline corrections applied. For all NMR spectra, no peaks were manually corrected, suppressed or altered in any form, and unprocessed fids are available upon request.

Single crystal analyses were performed by Michigan State University Center for Crystallographic Research on a Charge Coupled Device (CCD diffractometer).

High-resolution mass spectra were obtained at the Michigan State University Mass Spectrometry Core using electron spray ionization (ESI+). Low resolution GC-MS was obtained on a Shimadzu GCMS-QP2010SE.

Silica used for purification of crude material was standard laboratory grade 230 - 400 mesh designed for flash chromatography applications. Purification of crude materials on a 1 mmol scale was achieved by standard flash chromatography methods employing 2-3 g silica gel plugs in small chromatography columns of dimension approximately 2 x 30 cm. The concentrated crude materials were dissolved in a minimum amount of solvent, applied to the silica gel with a Pasteur pipette and eluted into test tubes. Compounds that eluted were visualized by spotting on TLC plates and irradiating with 254 nm UV light

2.4.2. Preparation of dmadph Ligand

Synthesis of 4-(dimethylamino)picolinic acid hydrogen chloride[34]

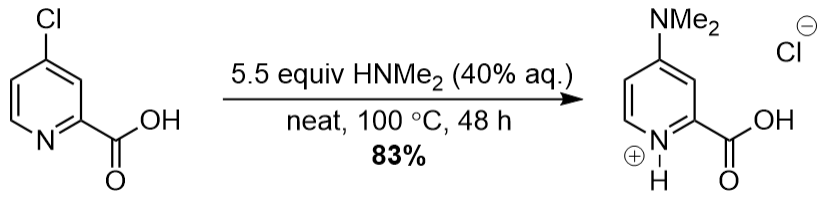

To a 350 mL pressure tube equipped with a stir bar, 4-chloropicolinic acid (18.0 g, 0.114 mol, 1 equiv) was added. Next, dimethylamine (40% in H_2O, 80.0 mL, 0.632 mol, 5.5 equiv) was added directly to the pressure tube. The pressure tube was then sealed and heated at 100 °C for 48 h. After cooling the pressure tube, the pH was adjusted to 11 using 10 M NaOH. The solvent was removed under vacuum, and the resulting solid was extracted with ethyl acetate (3 x 150mL). The solvent was removed on a rotary evaporator to yield the crude 4-(dimethylamino)picolinate. The solid was then recrystallized using a minimal amount of hot HCl (pH = 3) and allowing it to cool

at -10 °C overnight. The resulting pale-yellow needles were filtered and washed with a 50/50 mixture of EtOH/Et_2O until the washings were colorless. The solid was then further dried to yield 4-(dimethylamino)picolinic acid hydrogen chloride (**15.6 g, 83%**) as white crystals (mp 236.0-239.8 °C dec).

The NMR data matches with those previously reported.[34]

^{1}H NMR (500 MHz, D_2O) δ 7.78 (d, *J* = 7.2 Hz, 1H), 7.09 (d, *J* = 2.9 Hz, 1H), 6.68 (dd, *J* = 7.3, 3.0 Hz, 1H), 3.00 (s, 6H).

^{13}C{^{1}H} NMR (126 MHz, D_2O) δ 162.9, 157.9, 139.4, 138.4, 108.0, 107.6, 39.7, 39.5.

Synthesis of ethyl-4-(dimethylamino)picolinate

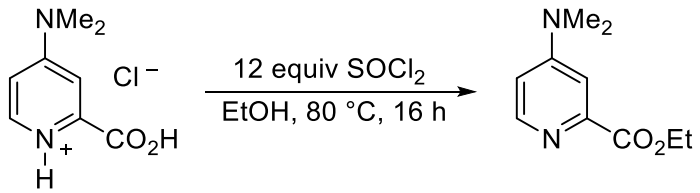

The title compound was synthesized according to a known literature procedure[34] for the analogous methyl ester, with a slight modification to the work up procedure.

A 250 mL 3-neck round bottom flask was equipped with a Dimroth condenser, pressure equalized addition funnel, and a stir bar. 4-(Dimethylamino)picolinic acid hydrogen chloride (5.127 g, 25.3 mmol, 1 equiv) was weighed into the flask followed by 65 mL of ethanol. Thionyl chloride (22.0 mL, 303.3 mmol, 12 equiv) was added to the addition funnel and the flask was then cooled to 0 °C. Thionyl chloride was added dropwise over a period of 25 minutes while keeping the solution close to 0 °C. When the addition was complete, the solution was brought to reflux for 16 hours. Upon cooling, the solution was quenched using sat. aq. $NaHCO_3$ until pH = 7. The pH was balanced to approximately pH = 10 using 10 M NaOH and the resulting solution was extracted with CH_2Cl_2 (3 x 60 mL). The combined CH_2Cl_2 layers were passed through a plug of basic

alumina and dried over $MgSO_4$. The drying agent was then gravity filtered and the solvent removed under vacuum to yield ethyl-4-(dimethylamino)picolinate (**5.134 g, 88%**) as an orange oil.

^{1}H NMR (500 MHz, $CDCl_3$) δ 8.33 (d, *J* = 5.9 Hz, 1H), 7.39 (d, *J* = 2.7 Hz, 1H), 6.59 (dd, *J* = 5.9, 2.8 Hz, 1H), 4.45 (q, *J* = 7.1 Hz, 2H), 3.05 (s, 6H), 1.43 (t, *J* = 7.1 Hz, 3H).

^{13}C{^{1}H} NMR (126 MHz, $CDCl_3$) δ 166.4, 154.8, 149.8, 148.4, 108.7, 108.1, 61.7, 39.2, 14.4.

Synthesis of bis(4-(dimethylamino)pyridin-2-yl)methanone

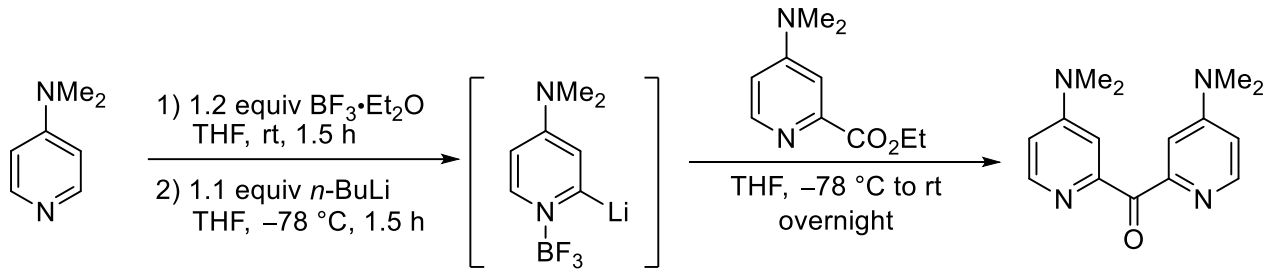

To an oven-dried, 250 mL round bottom flask equipped with a stir bar, 4-(dimethylamino)pyridine (0.7436 g, 6.0 mmol, 1.0 equiv) was added along with 90 mL of dry THF. The clear solution was sparged with N_2 for 30 minutes. After this, $BF_3{\cdot}OEt_2$ (0.890 mL, 7.2 mmol, 1.2 equiv) was added dropwise to the DMAP solution causing it to briefly warm up and turn the clear, colorless solution to a slightly cloudy and yellow solution and stirred for 1 h at room temperature. Afterwards, the mixture was cooled to –78 °C and the temperature was carefully monitored with a thermocouple probe inserted through a septum into the mixture. Next, *n*-BuLi (2.5 M in hexanes, 2.60 mL, 1.1 equiv) was added dropwise via syringe over 20 minutes, ensuring that the temperature did not rise above –70 °C. The solution was stirred cold at –78 °C for 1.5 h. Separately, ethyl-4-(dimethylamino)picolinate was added to a 300 mL, 3-neck round bottom flask equipped with a stir bar. Under nitrogen, 50 mL of THF was added and the solution was cooled to to –78 °C. After 1.5 h of stirring, the lithiated 4-(dimethylamino)pyridine was cannula transferred dropwise to the cooled solution of ethyl-4-(dimethylamino)picolinate, causing the light-yellow solution to become

a deep, golden yellow-orange. The mixture was stirred cold for 1.5 h and then quenched with 1.0 mL of anhydrous EtOH and allowed to come to rt overnight. The solvent was removed on a rotary evaporator and the solid dissolved in CH_2Cl_2 (80 mL) and washed with a 1M KOH/1% ethylene glycol solution (3x30mL). After drying under Na_2SO_4, the solvent was again removed on a rotary evaporator to yield a yellow-white solid which was dissolved in CH_2Cl_2 and washed with EtOAc (3x20 mL). The CH_2Cl_2 was dried again and evaporated to yield a white powder of bis(4-(dimethylamino)pyridin-2-yl)methanone (0.5232 g, 32% yield). The spectral data matched with previously reported literature values.[23]

Synthesis of 2,2'-(hydrazineylidenemethylene)bis(N,N-dimethylpyridin-4-amine) (L4)

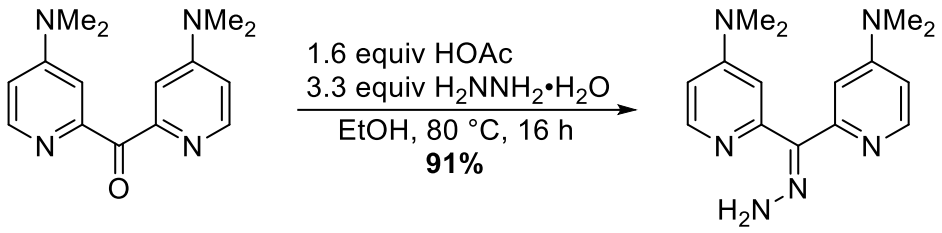

To a 25 mL, heavy walled Schlenk flask equipped with a stir bar, bis(DMAP)methanone (0.523 g, 1.9 mmol, 1 equiv) was added and dissolved in 15 mL of anhydrous ethanol with stirring. At room temperature, acetic acid (0.177 mL, 3.1 mmol, 1.6 equiv) was added via syringe with vigorous stirring, and the color of the solution turned to a pale yellow. Then, hydrazine hydrate (65%, 0.462 mL, 6.2 mmol, 3.3 equiv) was added via a syringe to the solution, which caused it to become an orange color. The reaction was stirred at 70 °C for 4 h and allowed to cool back down to rt. The solvent was then carefully removed under vacuum until a white precipitate formed. The resulting white solid was collected by filtration and washed with several portions of 2-3 mLs of ice-cold isopropanol. The mother liquor was subsequently concentrated to yield a second crop of the white solid, which was also washed with isopropanol. The combined white solids were then

recrystallized in a minimal amount of ^{i}PrOH to yield dmadph (**0.511 g, 91%**) as white needles (mp 149.0-152.0 °C dec.)

^{1}H NMR (500 MHz, $CDCl_3$) δ 8.30 (d, *J* = 6.0 Hz, 1H), 8.20 (d, *J* = 5.9 Hz, 1H), 7.46 (s, 2H), 7.04 (d, *J* = 2.7 Hz, 1H), 6.54 (d, *J* = 2.7 Hz, 1H), 6.47 (dd, *J* = 6.0, 2.7 Hz, 1H), 6.44 (dd, *J* = 5.9, 2.7 Hz, 1H), 3.03 (s, 6H), 2.94 (s, 6H).

^{13}C{^{1}H} NMR (126 MHz, $CDCl_3$) δ 157.3, 154.8, 153.0, 148.7, 148.5, 145.2, 108.1, 106.1, 105.7, 105.0, 39.2, 39.1.

2.4.3. Optimization of Reaction Conditions

Table S2.1. Optimization of Reaction Conditions

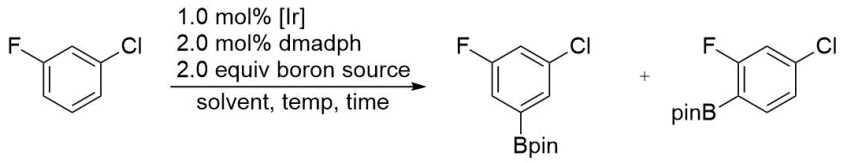

entry	[Ir]	boron source	solvent	temp (°C)	time (h)	%conversion	ratio m : o
1	$[Ir(OMe)cod]_2$	B_2pin_2	THF	25	24	>99	2.9 : 1.0
2	$[Ir(OMe)cod]_2$	HBpin	THF	25	24	>99	7.8 : 1.0
3	$[Ir(OMe)cod]_2$	HBpin	DCM	25	24	>99	4.3 : 1.0
4	$[Ir(Cl)cod]_2$	HBpin	DCM	25	24	71	4.1 : 1.0
5	$[Ir(OMe)cod]_2$	HBpin	THF	40	1	98	6.3 : 1.0
6	$[Ir(Cl)cod]_2$	HBpin	THF	40	1	24	5.9 : 1.0
7	$[Ir(OMe)cod]_2$	HBpin	THF	60	1	>99	4.4 : 1.0
8	$[Ir(OMe)cod]_2$	HBpin	THF	50	2	>99	5.7 : 1.0

Optimized conditions chosen are highlighted in yellow. Ratios of products were determined by ^{19}F NMR analysis of the crude reaction mixtures.

2.4.4. Catalyst Loading Studies

Table S2.2 Catalyst Loading Studies on Conversion and Selectivity

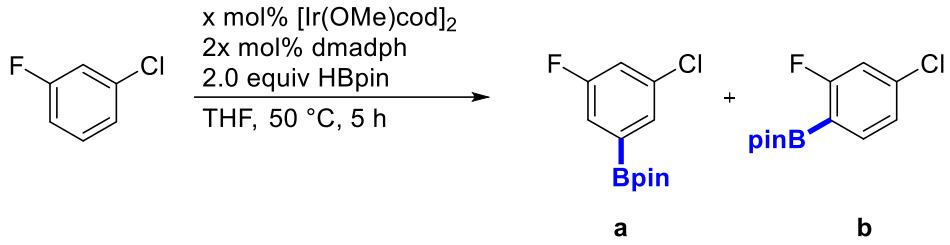

x	conversion	a:b
1	>99%*	7.3 : 1.0
0.25	95%*	7.28 : 1.0
0.1	92%	6.1 : 1.0
0.01	35%	4.7 : 1.0
0.001	n.d.	--

*T = 25 °C, t = 24 h

Ratios of products were determined by ^{19}F NMR analysis of the crude reaction mixtures.

2.4.5. General Procedure for Borylation of Arenes and Hetero(arenes)

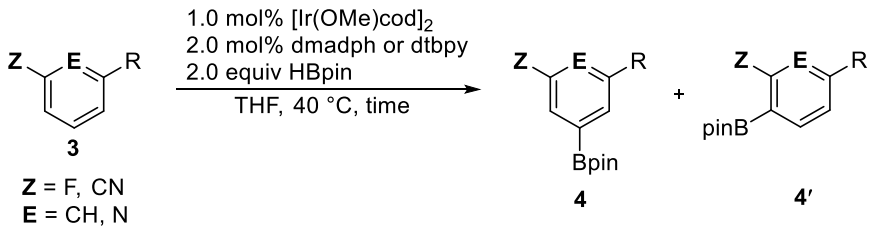

In a nitrogen-filled glovebox, a 3.0 mL Wheaton pressure vial equipped with a stir bar was charged with a 1.0 mL THF solution of $[Ir(OMe)cod]_2$ (6.6 mg, 0.01 equiv). To this solution, pinacolborane (0.290 mL, 2 mmol, 2.0 equiv) was added with a syringe while stirring, turning the light-yellow solution into a golden orange. Then, in a small test tube, a 1.0 mL THF solution of dmadph (5.6 mg, 0.02 equiv) or dtbpy (5.4 mg, 0.02 equiv) was made and added to the iridium solution with a syringe and the solution immediately turned dark red in color. Last, the substrate

was added to this solution and capped. The reaction was heated at 40 °C and stirred in an aluminum heating block on top of a stir plate. Reactions were monitored by ^{19}F and ^{1}H NMR spectroscopies. When reactions were completed, the volatiles were evaporated, and the crude reaction mixtures purified by silica gel chromatography in 100% CH_2Cl_2. The borylated products were isolated as the regioisomeric mixtures.

2.4.6. Characterization of Borylated Products

Borylation of 2-chloro-6-fluoropyridine (4a)

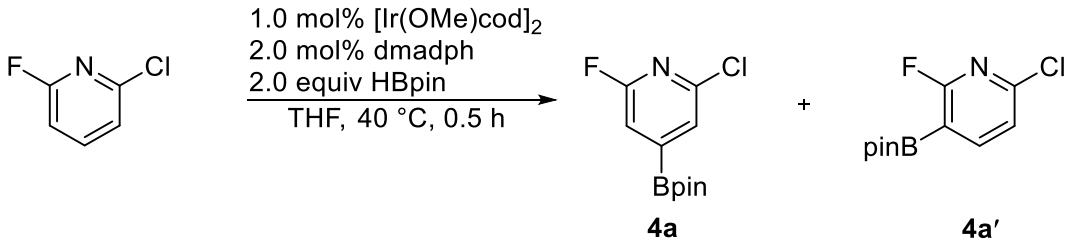

Isolated as a white, crystalline solid (**88%, >20:1.0 m:o selectivity**) after column chromatography in 100% CH_2Cl_2. Conversion was determined from ^{19}F NMR to be >99% at 30 min. The spectral data agree with previously reported literature values.[23] (mp 77.8-80.1 °C)

Selectivity found via ^{19}F NMR of the crude material was >20:1.0 **4a:4a′**.

The selectivity found via ^{19}F NMR for dtbpy was 5.8:1.0 **4a:4a′**.

^{1}H NMR of 4a (500 MHz, $CDCl_3$) δ 7.56 (d, *J* = 1.7 Hz, 1H), 7.20 (d, *J* = 2.6 Hz, 1H), 1.35 (s, 12H)

^{1}H NMR of 4a′ (500 MHz, $CDCl_3$) δ 8.11 (t, *J* = 8.1 Hz, 1H), 7.22 (dd, *J* = 7.5 Hz, 1.6 Hz, 1H), 1.35 (s, 12H)

$^{13}C\{^{1}H\}$ NMR of 4a (126 MHz, $CDCl_3$) δ 162.3 (d, *J* = 247.6 Hz), 148.7 (d, *J* = 12.8 Hz), 126.6 (d, *J* = 4.8 Hz), 112.9 (d, *J* = 33.0 Hz), 85.3, 25.0.

^{19}F NMR of 4a (470 MHz, $CDCl_3$) δ -67.38

^{19}F NMR of 4a′ (470 MHz, $CDCl_3$) δ -55.95

^{11}B NMR (160 MHz, $CDCl_3$) δ 29.69 (br s)

Borylation of isophthalonitrile (4b)

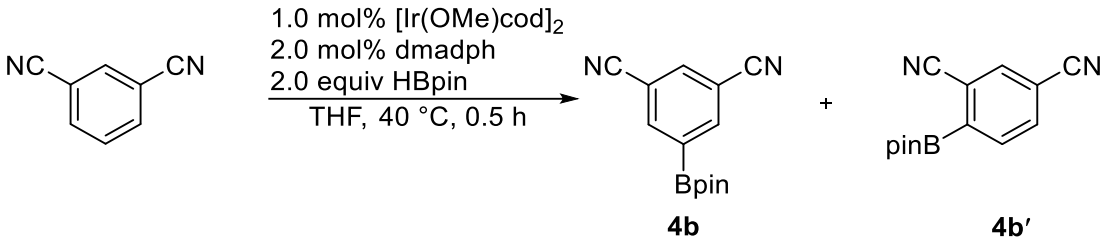

Isolated as a white, crystalline solid (**85%, 14.3:1.0 m:o selectivity**) after column chromatography in 100% CH_2Cl_2. Conversion was determined from ^{19}F NMR to be >99% at 30 min. The spectral data agree with previously reported literature values.[23]

Selectivity found via ^{19}F NMR of the crude material was 12.5:1.0 **4b:4b′**.
The selectivity found via ^{1}H NMR analysis for dtbpy was 4.4:1.0 **4b:4b′**.

^{1}H NMR of 4b (500 MHz, $CDCl_3$) δ 8.26 (d, *J* = 1.6 Hz, 2H), 7.98 (t, *J* = 1.6 Hz, 1H), 1.35 (s, 12H).

^{1}H NMR of 4b′ (500 MHz, $CDCl_3$) δ 8.01 (d, *J* = 7.9 Hz, 1H), 7.96-7.95 (m, 1H), 7.83 (dd, *J* = 7.8, 1.5 Hz, 1H) 1.38 (s, 12H).

^{13}C{^{1}H} NMR of 4b (126 MHz, $CDCl_3$) δ 141.8, 137.1, 116.7, 113.6, 85.3, 24.8.

^{13}C{^{1}H} NMR of 4b′ (126 MHz, $CDCl_3$) δ 136.7, 136.1, 136. 0, 134.4, 118.7, 116.9, 116.7, 115.4, 85.6, 24.8.

^{11}B NMR (160 MHz, $CDCl_3$) δ 29.73 (br s)

Borylation of 3-(trifluoromethoxy)fluorobenzene (4c)

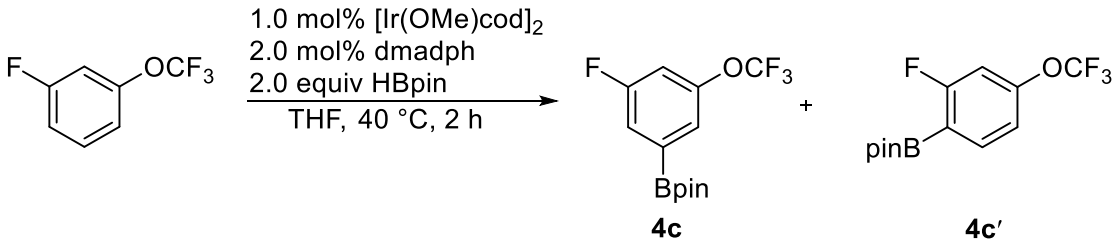

Isolated as a colorless, clear liquid (**96%, 8.0:1.0 m:o selectivity**) after column chromatography in 100% CH_2Cl_2. Conversion was determined from ^{19}F NMR to be >99% at 2 h.

Selectivity found via ^{19}F NMR of the crude material was 8.0:1.0 **4c:4c′.**

The selectivity found via ^{19}F NMR for dtbpy was 4.1:1.0 **4c:4c′.**

^{1}H NMR of 4c (500 MHz, $CDCl_3$) δ 7.44-7.42 (m, 2H), 7.03 (ddd, *J* = 9.0, 2.5, 1.5 Hz, 1H), 1.35 (s, 12H).

^{1}H NMR of 4c′ (500 MHz, $CDCl_3$) δ 7.78 (dd, *J* = 8.5, 1.5 Hz, 1H), 6.99 – 7.02* (m, 1H), 6.92 (dq, *J* = 9.5, 0.9 Hz, 1H), 1.36 (s, 12H).

^{13}C{^{1}H} NMR of 4c (126 MHz, $CDCl_3$) δ 162.4 (d, *J* = 250.1 Hz), 138.0 (d, *J* = 9.7 Hz), 122.3 (d, *J* = 3.1 Hz), 119.5 (d, *J* = 19.3 Hz), 111.6 (d, *J* = 25.0 Hz), 84.5, 24.7.

^{13}C{^{1}H} NMR of 4c′ (126 MHz, $CDCl_3$) δ 167.4 (d, *J* = 254.0 Hz), 149.4 (d, *J* = 9.9 Hz), 121.4, 115.1 (d, *J* = 3.8 Hz), 108.2 (d, *J* = 28.3 Hz), 84.1, 24.7.

^{19}F NMR of 4c (470 MHz, $CDCl_3$) δ -57.92 (3F), -110.87 (1F)

^{19}F NMR of 4c′ (470 MHz, $CDCl_3$) δ -57.81 (3F), -98.93 (1F)

^{11}B NMR (160 MHz, $CDCl_3$) δ 30.06 (br s)

*apparent doublet of quartets with matching coupling constants to the resonance at 6.92 ppm, one of the quartets is buried under the major isomer, however.

Borylation of 3-(trifluoromethyl)fluorobenzene (4d)

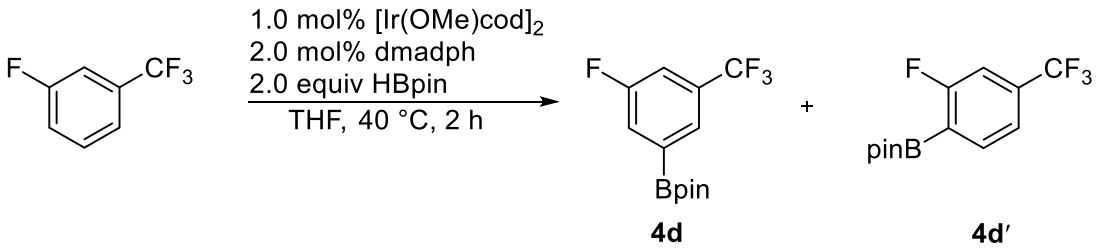

Isolated as a colorless, clear liquid (**87%, 4.4:1.0 m:o selectivity**) after column chromatography in 100% CH_2Cl_2. Conversion was determined from ^{19}F NMR to be >99% at 2 h. The spectral data agree with previously reported literature values.[7,22]

Selectivity found via ^{19}F NMR of the crude material was 4.4:1.0 **4d:4d′.**

The selectivity found via ^{19}F NMR for dtbpy was 1.8:1.0 **4d:4d′.**.

^{1}H NMR of 4d (500 MHz, $CDCl_3$) δ 7.84 (s, 1H), 7.65 (dd, *J* = 8.5, 2.5 Hz, 1H), 7.40-7.37 (m, 1H), 1.36 (s, 12H).

^{1}H NMR of 4d′* (500 MHz, $CDCl_3$) δ 7.86 (t, *J* = 7.0 Hz, 1H), 7.40 (m, 1H), 7.29 (d, *J* = 8.9 Hz, 1H), 1.37 (s, 12H).

^{13}C{^{1}H} NMR of 4d (126 MHz, $CDCl_3$) δ 162.1 (d, *J* = 249.5 Hz), 132.0 (dd, *J* = 33.2, 7.0 Hz), 127.0 (p, *J* = 3.8 Hz), 124.6 (d, *J* = 19.5 Hz), 115.3 (dq, *J* = 24.5, 3.7 Hz), 84.6, 24.8.

^{13}C{^{1}H} NMR of 4d′ (126 MHz, $CDCl_3$) δ 166.7 (d, *J* = 253.2 Hz), 137.6 (d, *J* = 8.3 Hz), 120.4 – 120.1 (m), 112.8 – 112.2 (m), 84.4, 24.8.

^{19}F NMR of 4d (470 MHz, $CDCl_3$) δ -62.69 (3F), -111.94 (1F).

^{19}F NMR of 4d′ (470 MHz, $CDCl_3$) δ -100.52

^{11}B NMR (160 MHz, $CDCl_3$) δ 30.15 (br s)

*Resonance at 7.86 buried under major isomer, assumed triplet from previously reported literature values. Resonance at 7.40 completely buried under major isomer, but visible, matching the chemical shift from previously reported values.[7]

Borylation of 3-fluorochlorobenzene (4e)

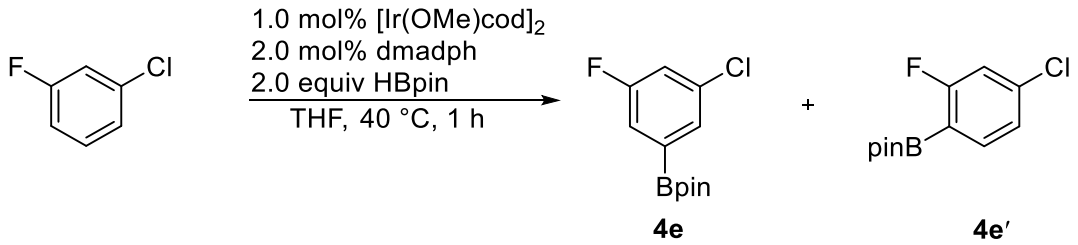

Isolated as a colorless, clear liquid (**82%, 6.1:1.0 m:o selectivity**) after column chromatography in 100% CH_2Cl_2. Conversion was determined from ^{19}F NMR to be 98% at 1 h. The spectral data agree with previously reported literature values.[23]

Selectivity found via ^{19}F NMR of the crude material was 6.4:1.0 **4e:4e′.**

The selectivity found via ^{19}F NMR for dtbpy was 2.5:1.0 **4e:4e′.**.

^{1}H NMR of 4e (500 MHz, $CDCl_3$) δ 7.56 (d, *J* = 1.1 Hz, 1H), 7.37 (dd, *J* = 8.5, 2.0 Hz, 1H), 7.16 (dt, *J* = 8.6, 2.3 Hz, 1H), 1.34 (s, 12H).

^{1}H NMR of 4e′ (500 MHz, $CDCl_3$) δ 7.67 (dd, *J* = 7.8, 6.7 Hz, 1H), 7.14 (dd, *J* = 8.3, 2.0 Hz, 1H), 7.07 (dd, *J* = 9.0, 1.7 Hz, 1H), 1.34 (s, 12H).

^{13}C{^{1}H} NMR of 4e (126 MHz, $CDCl_3$) δ 162.3 (d, *J* = 250.5 Hz), 134.7 (d, *J* = 8.82 Hz), 130.3 (d, *J* = 3.0 Hz), 119.3 (d, *J* = 19.3 Hz), 118.7 (d, *J* = 24.6 Hz), 84.4, 24.8.

^{13}C{^{1}H} NMR of 4e′ (126 MHz, $CDCl_3$) δ 167.1 (d, *J* = 254.7 Hz), 138.4 (d, *J* = 10.6 Hz), 137.6 (d, *J* = 9.2 Hz), 124.1 (d, *J* = 3.4 Hz), 116.1 (d, *J* = 27.6 Hz), 84.0, 24.8.

^{19}F NMR of 4e (470 MHz, $CDCl_3$) δ -111.94

^{19}F NMR of 4e′ (470 MHz, $CDCl_3$) δ -100.52

^{11}B NMR (160 MHz, $CDCl_3$) δ 30.15 (br s)

Borylation of 3-fluorobromobenzene (4f)

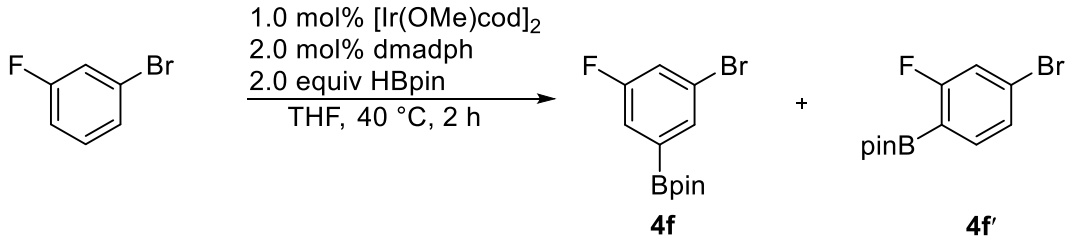

Isolated as a colorless, clear liquid (**93%, 7.2:1.0 m:o selectivity**) after column chromatography in 100% CH_2Cl_2. Conversion was determined from ^{19}F NMR to be 97% at 2 h. The spectral data agree with previously reported literature values.[9]

Selectivity found via ^{19}F NMR of the crude material was 7.1:1.0 **4f:4f′.**

The selectivity found via ^{19}F NMR for dtbpy was 2.9:1.0 **4f:4f′.**

^{1}H NMR of 4f (500 MHz, $CDCl_3$) δ 7.71 (dd, *J* = 1.75, 0.70 Hz, 1H), 7.41 (ddd, *J* = 8.5, 2.5, 0.6 Hz, 1H), 7.32 (ddd, *J* = 8.3, 2.5, 0.60 Hz, 1H), 1.34 (s, 12H).

^{1}H NMR of 4f′ (500 MHz, $CDCl_3$) δ 7.60 (dd, *J* = 8.0, 6.5 Hz, 1H), 7.29 (dd, *J* = 8.0, 1.7 Hz, 1H), 7.23 (dd, *J* = 8.6, 1.7 Hz, 1H), 1.35 (s, 12H).

^{13}C{^{1}H} NMR of 4f (126 MHz, $CDCl_3$) δ 162.3 (d, *J* = 251.6 Hz), 133.3 (d, *J* = 3.1 Hz), 121.6 (d, *J* = 24.4 Hz), 119.7 (d, *J* = 19.3 Hz), 84.4, 24.8.

^{13}C{^{1}H} NMR of 4f′ (126 MHz, $CDCl_3$) δ 166.9 (d, *J* = 255.7 Hz), 137.8 (d, *J* = 8.8 Hz), 127.1 (d, *J* = 3.4 Hz), 126.4 (d, *J* = 10.0 Hz), 119.0 (d, *J* = 27.4 Hz), 84.1, 24.8.

^{19}F NMR of 4f (470 MHz, $CDCl_3$) δ -111.56

^{19}F NMR of 4f′ (470 MHz, $CDCl_3$) δ -100.30

^{11}B NMR (160 MHz, $CDCl_3$) δ 30.11 (br s)

Borylation of 1,3-difluorobenzene (4g)

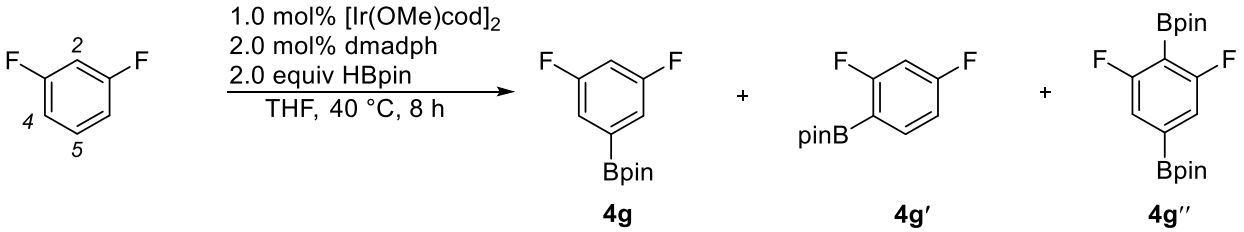

Isolated as a white solid (**88%, 4.3:1.0:0.9 5:4:2,5-diborylated selectivity**) after column chromatography in 100% CH_2Cl_2. Conversion was determined from ^{19}F NMR to be >99% at 8 h. The spectral data agree with previously reported literature values for the 4- and 5-borylated isomers.[18] The resonances at δ -94.1 (corresponding to the 4,6-diborylated isomer) and -100.6 (corresponding to the 2-borylated isomer) represent 2% of the regioisomeric mixture.

Selectivity found via ^{19}F NMR of the crude material was 4.6:1.0:0.9 **4g:4g′:4g″.**

The selectivity found via ^{19}F NMR for dtbpy was 3.3:2.7:1.0 of **4g:4g′:4g′′.**

^{1}H NMR of 4g (500 MHz, $CDCl_3$) δ 7.27 (dt, *J* = 6.1, 2.2 Hz, 2H), 6.86 (tt, *J* = 8.9, 2.4 Hz, 1H), 1.33 (s, 12H).

^{1}H NMR of 4g′ (500 MHz, $CDCl_3$) δ 7.74 – 7.70 (m, 1H), 6.88 – 6.83* (m, 1H), 6.75 (td, *J* = 9.5, 2.3 Hz, 1H), 1.37 (s, 12H).

^{1}H NMR of 4g′′ (500 MHz, $CDCl_3$) δ 7.23 – 7.25 (m, 2H), 1.34 (s, 12H).

^{13}C{^{1}H} NMR of 4g (126 MHz, $CDCl_3$) δ 162.7 (dd, *J* = 249.7, 11.0 Hz), 116.8 (dd, *J* = 17.7, 5.0 Hz), 106.4 (t, *J* = 25.1 Hz), 84.4, 24.8.

^{13}C{^{1}H} NMR of 4g′ (126 MHz, $CDCl_3$) δ 165.7 (dd, *J* = 289.7, 12.2 Hz), 116.7 – 115.9 (m), 111.1 (dd, *J* = 20.2, 3.6 Hz), 103.6 (dd, *J* = 27.9, 24.3 Hz), 83.9, 24.7.

^{19}F NMR of 4g (470 MHz, $CDCl_3$) δ -110.79

^{19}F NMR of 4g′ (470 MHz, $CDCl_3$) δ -98.63, -105.13

^{19}F NMR of 4g′′ (470 MHz, $CDCl_3$) δ -101.80

^{11}B NMR (160 MHz, $CDCl_3$) δ 30.02 (br s)

*Resonance is completely buried underneath the major isomer. An irregular peak shape for the major isomer provides evidence of the resonance and is in agreement with previous reported values.

Borylation of 3-fluorobenzonitrile (4h)

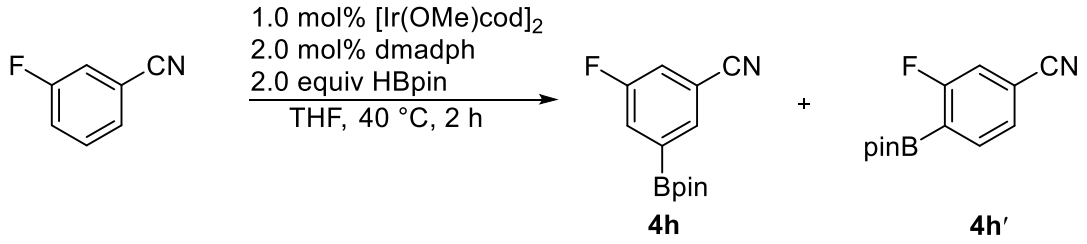

Isolated as a colorless, clear liquid (**93%, 3.5:1.0 m:o selectivity**) after column chromatography in 100% CH_2Cl_2. Conversion was determined from ^{19}F NMR to be >99% at 2 h.

Selectivity found via ^{19}F NMR of the crude material was 3.4:1.0 **4h:4h′.**
The selectivity found via ^{19}F NMR for dtbpy was 1.1:1.0 **4h:4h′.**.

^{1}H NMR of 4h (500 MHz, $CDCl_3$) δ 7.88 (s, 1H), 7.70 (dd, *J* = 8.5, 0.6 Hz, 1H), 7.41 (ddd, *J* = 8.1, 2.6, 1.4 Hz, 1H), 1.35 (s, 12H).

^{1}H NMR of 4h′ (500 MHz, $CDCl_3$) δ 7.62 (t, *J* = 6.7 Hz, 1H), 6.95* (m, 1H), 6.86 (d, *J* = 10.4 Hz, 1H), 1.36 (s, 12H).

^{13}C{^{1}H} NMR of 4h (126 MHz, $CDCl_3$) δ 161.7 (d, *J* = 251.0 Hz), 137.8 (d, *J* = 8.7 Hz), 134.2 (d, *J* = 3.3 Hz), 125.8 (d, *J* = 19.4 Hz), 121.1 (d, *J* = 24.7 Hz), 84.8, 24.7.

^{13}C{^{1}H} NMR of 4h′ (126 MHz, $CDCl_3$) δ 166.2 (d, *J* = 254.7 Hz), 127.2 (d, *J* = 3.7 Hz), 118.7 (d, *J* = 27.6 Hz), 117.4 (d, *J* = 3.0 Hz), 113.5 (d, *J* = 8.5 Hz), 84.6, 24.7.

^{19}F NMR of 4h (470 MHz, $CDCl_3$) δ -111.07

^{19}F NMR of 4h′ (470 MHz, $CDCl_3$) δ -99.87

^{11}B NMR (160 MHz, $CDCl_3$) δ 29.96 (br s)

*Resonance at 6.95 is completely buried under major isomer.

Borylation of 3-fluorotoluene (4i)

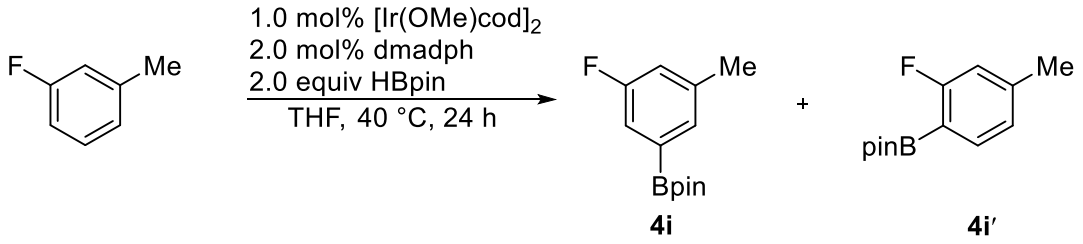

Isolated as a colorless, clear liquid (**72%, 4.2:1.0 m:o selectivity**) after column chromatography in 100% CH_2Cl_2. Conversion was determined from ^{19}F NMR to be >99% at 24 h. The spectral data agree with previously reported literature values.[7]

Selectivity found via ^{19}F NMR of the crude material was 4.0:1.0 **4i:4i′.**

The selectivity found via ^{19}F NMR for dtbpy was 1.4:1.0 **4i:4i′.**.

^{1}H NMR of 4i (500 MHz, $CDCl_3$) δ 7.40 (s, 1H), 7.28 (dd, *J* = 8.9, 2.0 Hz, 1H), 6.98-6.95 (m, 1H), 2.36 (s, 3H), 1.35 (s, 12H).

^{1}H NMR of 4i′ (500 MHz, $CDCl_3$) δ 7.40 (s, 1H), 7.28 (dd, *J* = 8.9, 2.0 Hz, 1H), 6.98-6.95 (m, 1H), 2.36 (s, 3H), 1.35 (s, 12H).

^{13}C{^{1}H} NMR of 4i (126 MHz, $CDCl_3$) δ 162.5 (d, *J* = 246.4 Hz), 139.8 (d, *J* = 7.0 Hz), 136.6 (d, *J* = 8.7 Hz), 131.0 (d, *J* = 2.5 Hz), 118.8 (d, *J* = 20.9 Hz), 117.9 (d, *J* = 19.3 Hz), 84.0, 24.8, 21.1.

^{13}C{^{1}H} NMR of 4i′ (126 MHz, $CDCl_3$) δ 144.3 (d, *J* = 8.7 Hz), 136.6 (d, *J* = 8.7 Hz), 124.5 (d, *J* = 2.8 Hz), 115.8 (d, *J* = 23.9 Hz), 83.7, 24.8, 21.0.

^{19}F NMR of 4i (470 MHz, $CDCl_3$) δ -115.35

^{19}F NMR of 4i′ (470 MHz, $CDCl_3$) δ -103.84

^{11}B NMR (160 MHz, $CDCl_3$) δ 30.53 (br s)

Borylation of 3-fluoroanisole (4j)

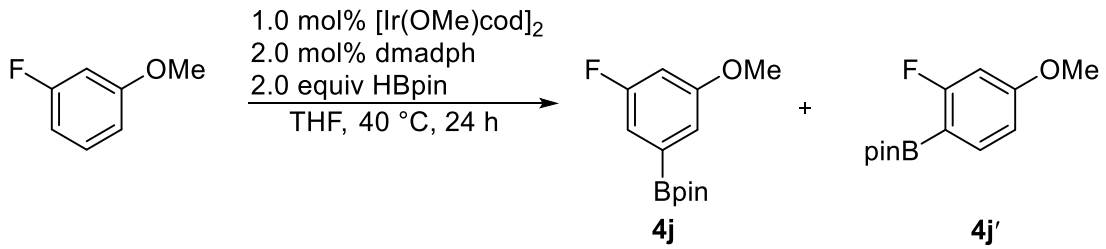

Isolated as a colorless, clear liquid (**80%, 5.8:1.0 m:o selectivity**) after column chromatography in 100% CH_2Cl_2. Conversion was determined from ^{19}F NMR to be 88% at 24 h. The spectral data agree with previously reported literature values.[7]

Selectivity found via ^{19}F NMR of the crude material was 6.0:1.0 **4j:4j′.**

The selectivity found via ^{19}F NMR for dtbpy was 2.2:1.0 **4j:4j′.**

^{1}H NMR 4j (500 MHz, $CDCl_3$) δ 7.10 (d, *J* = 5.0 Hz, 1H), 7.09 (dd, *J* = 8.5, 2.4 Hz, 1H), 6.70 (dt, *J* = 10, 5.0 Hz, 1H), 3.82 (s, 3H), 1.34 (s, 12H).

^{1}H NMR 4j′ (500 MHz, $CDCl_3$) δ 7.65 (dd, *J* = 8.3, 7.2 Hz, 1H), 6.68* (dd, *J* = 2.5 Hz, 1H), 6.57 (dd, *J* = 11.3, 2.3 Hz, 1H), 3.81 (s, 3H), 1.35 (s, 12H).

^{13}C{^{1}H} NMR of 4j (126 MHz, $CDCl_3$) δ 163.2 (d, *J* = 246.3 Hz), 160.5 (d, *J* = 10.3 Hz), 114.7 (d, *J* = 2.5 Hz), 113.3 (d, *J* = 19.7 Hz), 105.1 (d, *J* = 24.7 Hz), 84.1, 55.6, 24.8.

^{13}C{^{1}H} NMR of 4j′ (126 MHz, $CDCl_3$) δ 168.5 (d, *J* = 250.9 Hz), 137.7 (d, *J* = 10.5 Hz), 109.9 (d, *J* = 2.7 Hz), 101.1 (d, *J* = 28.0 Hz), 83.6, 55.5, 24.8.

^{19}F NMR of 4j (470 MHz, $CDCl_3$) δ -57.92 (3F), -110.87 (1F)

^{19}F NMR of 4j′ (470 MHz, $CDCl_3$) δ -57.81 (3F), -98.93 (1F)

^{11}B NMR (160 MHz, $CDCl_3$) δ 30.45 (br s)

*Agrees with previous reported literature values[7], the only coupling constant visible is given, and the other half of the resonance is buried under the major isomer.

Borylation of 3-fluoro-*N*,*N*-dimethylaniline (4k)

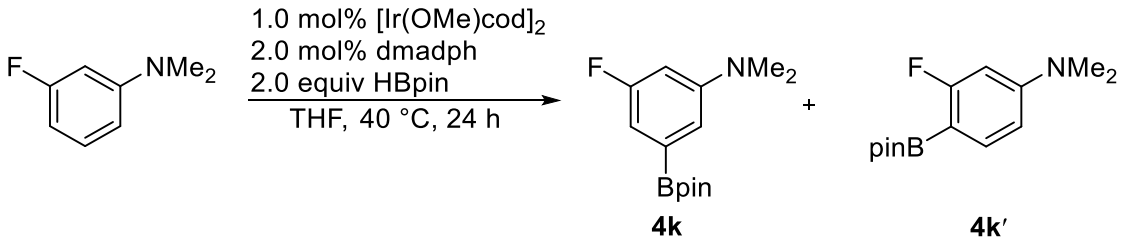

Isolated as a white solid (**93%, 3.1:1.0 m:o selectivity**) after column chromatography in 100% CH_2Cl_2. Conversion was determined from ^{19}F NMR to be 71% at 24 h. The spectral data agree with previously reported literature values.[7]

Selectivity found via ^{19}F NMR of the crude material was 3.3:1.0 **4k:4k′.**
The selectivity found via ^{19}F NMR for dtbpy was 1.9:1.0 **4k:4k′.**.

^{1}H NMR 4k (500 MHz, $CDCl_3$) δ 6.94 (d, *J* = 2.3 Hz, 1H), 6.84 (dd, *J* = 8.5, 2.3 Hz, 1H), 6.49 (dt, *J* = 12.6, 2.3 Hz, 1H), 2.97 (s, 6H), 1.35 (s, 12H).

^{1}H NMR 4k′ (500 MHz, $CDCl_3$) δ 7.59 (t, *J* = 7.9 Hz, 1H), 6.44 (dd, *J* = 8.5, 2.2 Hz, 1H), 6.31 (dd, *J* = 13.4, 2.2 Hz, 1H), 2.98 (s, 6H), 1.35 (s, 12H).

^{19}F NMR of 4k (470 MHz, $CDCl_3$) δ -113.79.

^{19}F NMR of 4k′ (470 MHz, $CDCl_3$) δ -101.65.

^{13}C{^{1}H} NMR of 4k (126 MHz, $CDCl_3$) δ 163.7 (d, *J* = 242.9 Hz), 151.9 (d, *J* = 9.8 Hz), 114.1 (d, *J* = 1.9 Hz), 108.4 (d, *J* = 19.8 Hz), 102.1 (d, *J* = 25.9 Hz), 83.9, 40.5, 24.8.

^{13}C{^{1}H} NMR of 4k′ (126 MHz, $CDCl_3$) δ 163.7 (d, *J* = 242.9 Hz), 151.9 (d, *J* = 9.8 Hz), 114.1 (d, *J* = 1.9 Hz), 108.4 (d, *J* = 19.8 Hz), 102.1 (d, *J* = 25.9 Hz), 83.8 (m), 40.5, 24.8.

^{11}B NMR (160 MHz, $CDCl_3$) δ 30.59 (br s).

Borylation of fluorobenzene (4l)

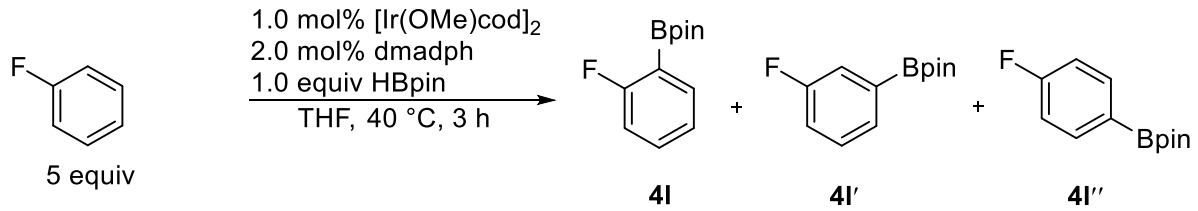

Reaction run with 5-fold excess of substrate. Isolated as a colorless, clear liquid (**99%, 1.4 : 5.5 : 1.0 o:m:p, <5% diborylated isomers**) after column chromatography in 100% CH_2Cl_2. Conversion was determined from ^{19}F NMR to be 98% at 3 h. The NMR spectral data agree with previously reported literature.[22,35] The ^{1}H NMR resonances of the 2-monoborylated isomer and 4-monoborylated isomer were not assigned due to significant overlap with each other and the major isomer.

Selectivity found via ^{19}F NMR of the crude material was 1.3:5.4:1.0 **4l:4l′:4l′′.**
The selectivity found via ^{19}F NMR for dtbpy was 3.4:5.2:1.0 **4l:4l′:4l′′**.

^{1}H NMR of 4l′ (500 MHz, $CDCl_3$) δ 7.56 (dd, *J* = 7.2, 0.5 Hz, 1H), 7.47 (dd, *J* = 9.2, 2.6 Hz, 1H), 7.33 (ddd, *J* = 13.3, 5.5, 2.6 Hz, 1H), 7.13 (m, 1H), 1.34 (s, 12H).

^{13}C{^{1}H} NMR of 4l (126 MHz, $CDCl_3$) δ 167.2 (d, *J* = 250.9 Hz), 136.8 (d, *J* = 7.9 Hz), 133.3 (d, *J* = 8.8 Hz), 123.6 (d, *J* = 3.2 Hz), 115.2 (d, *J* = 23.9 Hz), 83.9, 24.8.

^{13}C{^{1}H} NMR of 4l′ (126 MHz, $CDCl_3$) δ 162.5 (d, *J* = 246.4 Hz), 130.3 (d, *J* = 3.0 Hz), 129.5 (d, *J* = 7.1 Hz), 120.9 (d, *J* = 19.3 Hz), 118.2 (d, *J* = 21.0 Hz), 84.1, 24.8.

^{13}C{^{1}H} NMR of 4l″ (126 MHz, $CDCl_3$) δ 165.1 (d, *J* = 250.2 Hz), 137.0 (d, *J* = 8.2 Hz), 114.8 (d, *J* = 20.2 Hz), 83.9, 24.8.

^{19}F NMR of 4l (470 MHz, $CDCl_3$) δ -102.66

^{19}F NMR of 4l′ (470 MHz, $CDCl_3$) δ -114.22

^{19}F NMR of 4l″ (470 MHz, $CDCl_3$) δ -108.45

^{11}B NMR (160 MHz, $CDCl_3$) δ 30.54 (br s)

Borylation of dimethyl resorcinol (5)

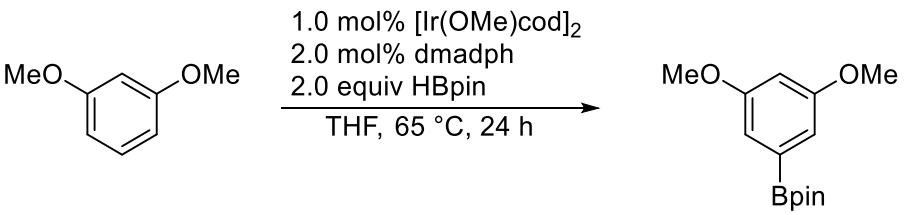

Reaction run at 65 °C, and the conversion at 24 h was determined to be 72% by ^{1}H NMR. Product is known[36] and was not isolated but assigned spectroscopically as the known product.

Borylation of 2-fluorophenol (7a)

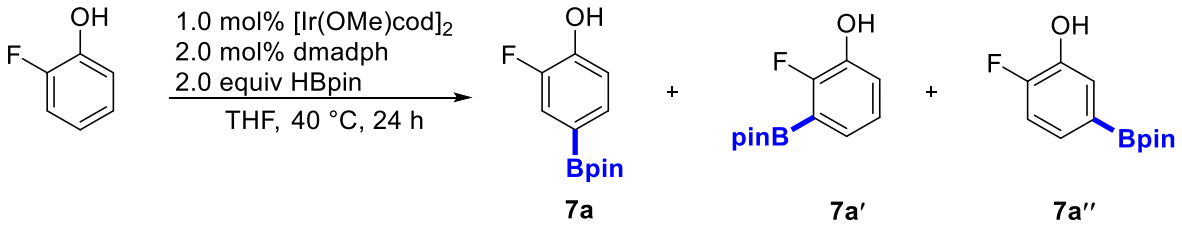

Reaction run according to the general procedure. After stirring for 24 h, the reaction conversion was determined to be 60% by ^{19}F NMR The products were not isolated as this was a scouting reaction to gauge selectivity. The NMR data match previously reported literature values.[30]

^{1}H NMR of 7a* (500 MHz, $CDCl_3$) δ 7.51 – 7.48 (m, 2H), 6.98 (t, *J* = 8.3 Hz, 1 H), 5.38 (br s, 1H), 1.33 (s, 12H)

^{19}F NMR of 7a (470 MHz, $CDCl_3$) δ -142.5

^{19}F NMR of 7a′ (470 MHz, $CDCl_3$) δ -132.5

^{19}F NMR of 7a″ (470 MHz, $CDCl_3$) δ -136.4

^{11}B NMR (160 MHz, $CDCl_3$) δ 29.7 (br s)

*Due to significant overlap in the ^{1}H NMR, products **7a′** and **7a″** were not assigned.

Borylation of 2-fluoroaniline (7b)

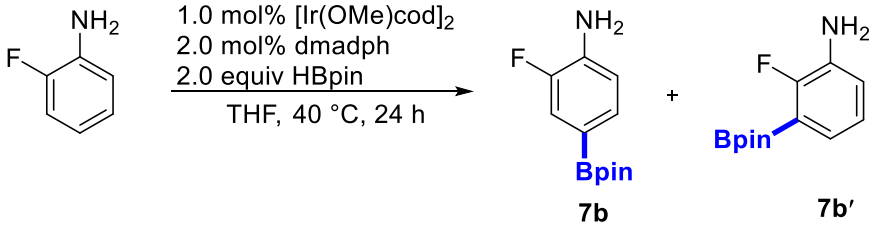

Reaction run according to the general procedure. The products were not isolated as this was a scouting reaction to gauge selectivity. After stirring for 24 h, the reaction conversion was determined to be 96% by ^{19}F NMR. The NMR data match previously reported literature values.[30]

^{1}H NMR of 7b (500 MHz, $CDCl_3$) δ 7.41 – 7.38 (m, 2H), 6.75 (t, *J* = 8.0 Hz), 3.01 (br s, 2H), 1.32 (s, 12 H).

^{1}H NMR of 7b′ (500 MHz, $CDCl_3$) δ 7.09 (ddd, *J* = 7.1, 5.1, 1.7 Hz, 1H), 6.94 (t, *J* = 7.5 Hz, 1H), 6.88 (ddd, *J* = 9.0, 7.8, 1.8 Hz, 1H), 3.70 (br s, 2H), 1.36 (s, 12H).

^{19}F NMR of 7b (470 MHz, $CDCl_3$) δ -137.3

^{19}F NMR of 7b′ (470 MHz, $CDCl_3$) δ -125.6

^{11}B NMR (160 MHz, $CDCl_3$) δ 30.3 (br s)

Borylation of 1-chloro-3-fluoro-2-methoxybenzene (7c)

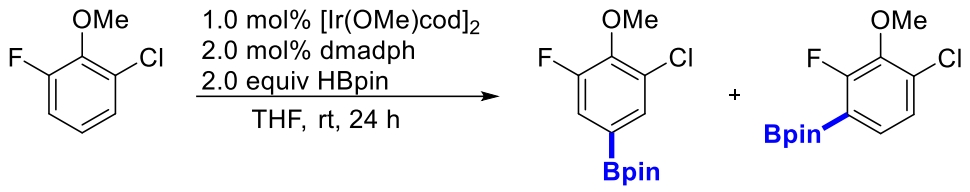

7c **7c′**

Reaction run according to the general procedure at room temperature. After stirring for 24 h, the reaction conversion was determined to be 98% by ^{19}F NMR. The products were not isolated as this was a scouting reaction to gauge selectivity. Product 7c′ was known and matched previously reported literature values.[37]

^{1}H NMR of 7c (500 MHz, $CDCl_3$) δ 7.59 (s, 1H), 7.42 (d, J = 11.1 Hz), 4.00 (s, 3H), 1.33 (s, 12H).

^{1}H NMR of 7c′ (500 MHz, $CDCl_3$) δ 7.35 (dd, J = 8.1, 5.7 Hz, 1H) 7.15 (dd, J = 8.2, 1.2 Hz, 1H), 3.96 (s, 3H), 1.36 (s, 12H).

^{19}F NMR of 7c (470 MHz, $CDCl_3$) δ -129.1

^{19}F NMR of 7c′ (470 MHz, $CDCl_3$) δ -118.1

^{11}B NMR (160 MHz, $CDCl_3$) δ 29.7 (br s)

Borylation of methyl 3-fluorobenzoate (7d)

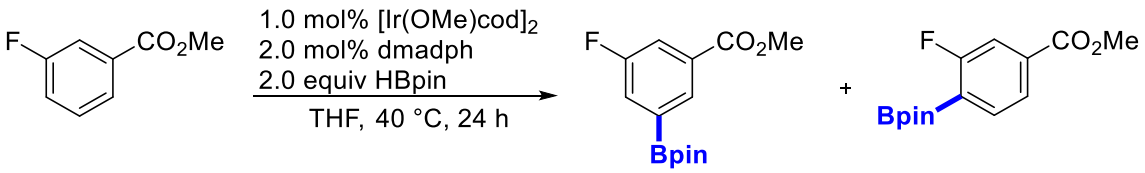

7d **7d′**

Reaction run according to the general procedure. After stirring for 24 h, the reaction conversion was determined to be 34% by ^{19}F NMR. The products were not isolated as this was a scouting reaction to gauge selectivity and functional group tolerance.

^{1}H NMR of 7d (500 MHz, $CDCl_3$)* δ 8.20 (s, 1H), 7.76 – 7.75 (m, 1H), 7.62 – 7.60 (m, 1H), 3.88 (s, 3H), 1.22 (s, 12H).

^{19}F NMR of 7d (470 MHz, $CDCl_3$) δ -113.7

^{19}F NMR of 7d′ (470 MHz, $CDCl_3$) δ -102.4

^{11}B NMR (160 MHz, $CDCl_3$) δ 30.1 (br s)

*Due to significant overlap with **7d** and starting material, product **7d′** was not assigned via ^{1}H NMR.

2.4.7. Preparation of Ir^{I} hydrazido from dmadph and 6

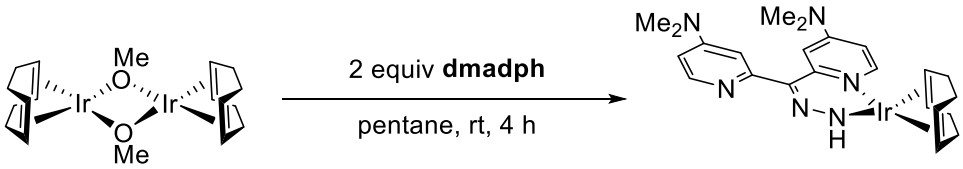

In a N_2 filled glovebox, a 20 mL scintillation vial was charged with $[Ir(OMe)cod]_2$ (0.033 g, 0.05 mmol) and a stir bar. In a small test tube, dmadph (0.028 g, 0.1 mmol) was weighed and suspended in 3.0 mL of pentane. Then, 2.0 mL of pentane was added to the scintillation vial with strong stirring yielding a light-yellow solution. The suspension of dmadph was then added with a pipette, changing the color immediately to a dark red-brown with significant precipitate. The mixture was allowed to stir for 4 hours at room temperature and placed in a freezer at -35 °C overnight. The resulting suspension was filtered over a glass frit funnel (F porosity) and washed with 3x5 mL portions of pentane and dried, yielding a dark maroon solid (0.030 g, **99%** yield) of the Ir^{I} hydrazido **7**.

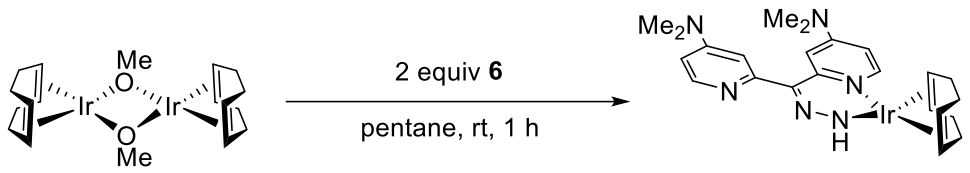

In a N_2 filled glovebox, a 20 mL scintillation vial was charged with $[Ir(OMe)cod]_2$ (0.033 g, 0.05 mmol) and a stir bar. In a small test tube, **6** (0.040 g, 0.1 mmol) was weighed and suspended in 3.0 mL of pentane. Then, 2.0 mL of pentane was added to the scintillation vial with strong stirring yielding a light-yellow solution. The suspension of **6** was then added with a pipette, changing the color immediately to a dark red-brown. The mixture was allowed to stir for 1 hour at room temperature and placed in a freezer at -35 °C overnight. The resulting suspension was filtered over a glass frit funnel (F porosity) and washed with 3x5 mL portions of pentane and dried, yielding a dark maroon solid (0.028 g, **93%** yield) of the Ir^I hydrazido **7**.

^{1}H NMR (500 MHz, THF-*d*$_8$) δ 9.23 (s, 1H), 8.12 (d, *J* = 5.7 Hz, 1H), 7.82 (d, *J* = 7.3 Hz, 1H), 7.49 (d, *J* = 3.1 Hz, 1H), 6.94 (d, *J* = 2.6 Hz, 1H), 6.45 (dd, *J* = 5.8, 2.6 Hz, 1H), 6.40 (dd, *J* = 7.3, 3.1 Hz, 1H), 3.69 – 3.60 (m, 2H), 3.51 – 3.44 (m, 2H), 3.02 (s, 6H), 2.96 (s, 6H), 2.44 – 2.29 (m, 4H), 2.32 – 2.16 (m, 4H).

^{13}C{^{1}H} NMR (126 MHz, THF-*d*$_8$) δ 171.3, 161.5, 154.9, 153.2, 147.6, 147.4, 107.7, 105.7, 104.2, 103.7, 66.9, 62.8, 58.4, 38.2, 37.9, 31.7, 30.5, 24.8.

2.4.8. Borylation of fluorochlorobenzene with 6 and 7

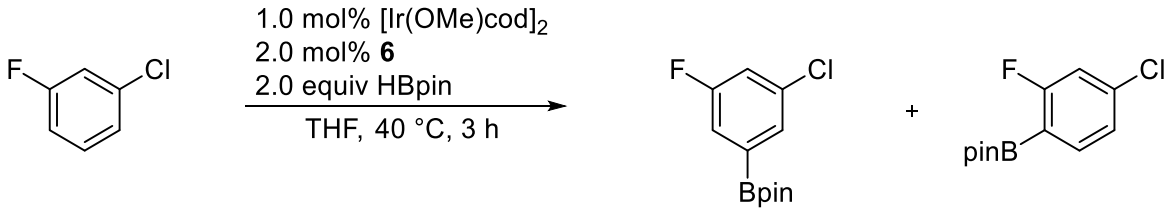

Reaction performed according to the general procedure with the following minor changes: **6** (0.008 g, 0.02 equiv) was weighed into a test tube in place of **L4**/dtbpy, and the reaction was stirred for 3

h. Conversion was found to be 80% by ^{19}F NMR analysis, with a regioisomeric ratio of 6.5:1.0 meta:ortho to F.

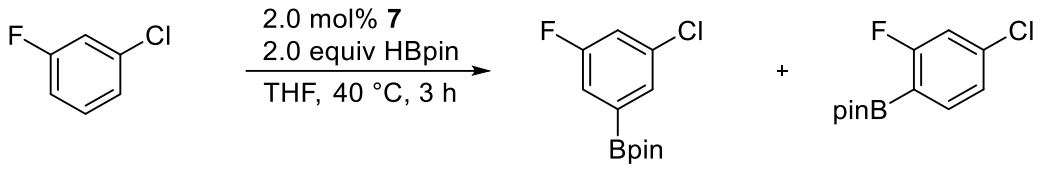

Reaction performed according to the general procedure with the following minor changes: **7** (0.012 g, 0.02 equiv) was weighed into a test tube in place of **L4**/dtbpy and $[Ir(OMe)cod]_2$, and the reaction was stirred at 40 °C for 3 h. Conversion was found to be 75% by ^{19}F NMR analysis, with a regioisomeric ratio of 6.5:1.0 meta:ortho to F.

2.4.9. Preparation of dmadph-borane Adduct for X-ray Crystallography

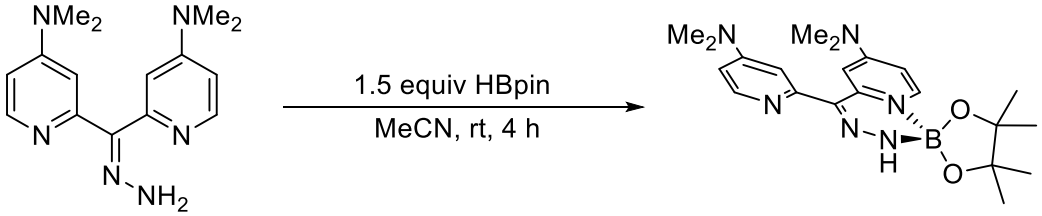

In a N_2 filled glovebox, a 20 mL scintillation vial was charged with a stir bar and dmadph (0.046 g, 0.16 mmol, 1 equiv). Then, 3.0 mL of MeCN was added to the vial and stirred. Afterwards, pinacolborane (0.40 mL, 0.28 mmol, 1.75 equiv) was added with a syringe and stirred for 4 h. The addition of pinacolborane turned the clear, colorless slurry to a light-yellow and caused the solution to warm and bubble. An additional 4.0 mL of MeCN was added to fully dissolve everything and was then stirred for another 20 h. After stirring the scintillation vial was placed in a -34 °C freezer for 2 days and upon returning, yellow needles precipitated (**0.051 g, 78%**) that were suitable for X-ray crystallography.

^{1}H NMR (500 MHz, $CDCl_3$) δ 8.42 (d, *J* = 7.2 Hz, 1H), 8.20 (d, *J* = 5.8 Hz, 1H), 7.52 (d, *J* = 2.4 Hz, 1H), 7.33 (br s, 1 H), 7.04 (d, *J* = 2.2 Hz, 1H), 6.63 (dd, *J* = 7.1, 2.4 Hz, 1H), 6.48 (dd, *J* = 5.6, 2.2 Hz, 1H), 3.06 (s, 6 H), 3.04 (s, 6H), 1.25 (s, 6H), 1.20 (s, 6H).

^{13}C{^{1}H} NMR (126 MHz, $CDCl_3$) δ 157.1, 155.3, 154.9, 147.9, 142.9, 139.6, 105.8, 105.2, 105.1, 102.6 79.5, 39.4, 39.3, 26.8, 26.0.

^{11}B NMR (160 MHz, $CDCl_3$) δ 2.92 (s, $\omega_{1/2}$ = 49 Hz)

HRMS (ESI+) *m/z* calculated for $C_{21}H_{32}N_6O_2B^+$ ($[MH]^+$) 411.2680, found *m/z* 411.2698.

2.4.10. NMR Tube Borylation of Pentafluorobenzene

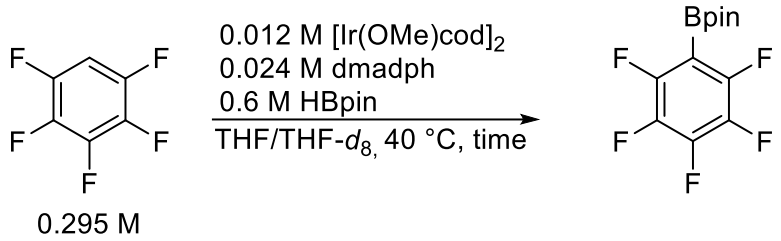

In a N_2 filled glovebox, $[Ir(OMe)cod]_2$ (0.0070 g, 0.01 mmol), dmadph (0.0060 g, 0.02 mmol), were weighed into separate test tubes. Then, 1.0 mL of THF was added to both test tubes. To the solution of Ir, HBpin (300 µL, 2 mmol) was added and shaken briefly, turning the light-yellow solution into a golden-yellow. The solution of Ir and pinacolborane was then pipetted into the solution of dmadph and transferred into a scintillation vial with a stir bar. The combined solution was stirred vigorously for 5 minutes, turning the solution dark red. Using a microsyringe, 400 µL of the combined solution was added to a J-young tube, followed by pentafluorobenzene (20 µL, 0.18 mmol) and 0.3 mL of THF-d_8. The J-young was capped, inverted and thoroughly mixed. The tube was then transferred into a preheated oil bath at 40 °C and monitored by ^{1}H, ^{19}F, and ^{11}B NMR.

See **Figure S58** for the ^{11}B NMR of the reaction at t = 3.5 h. The resonance at δ 25.36 is typical for a N–B bond where boron is 3-coordinate[27].

2.4.11. Crystallographic Data for 6

Slow crystallization of **6** from MeCN in a glovebox at –34 °C provided crystals suitable for X-ray diffraction analysis. Single yellow needle crystals of **6** used as received. A suitable crystal with dimensions 0.38 × 0.10 × 0.04 mm^3 was selected and mounted on a nylon loop with paratone oil on a Bruker APEX-II CCD diffractometer. The crystal was kept at a steady T = 173(1) K during data collection. The structure was solved with the **ShelXT**[38] solution program using dual methods and by using **Olex2**[39] as the graphical interface. The model was refined with **ShelXL**[40] using full matrix least squares minimisation on $\boldsymbol{F}^2$.

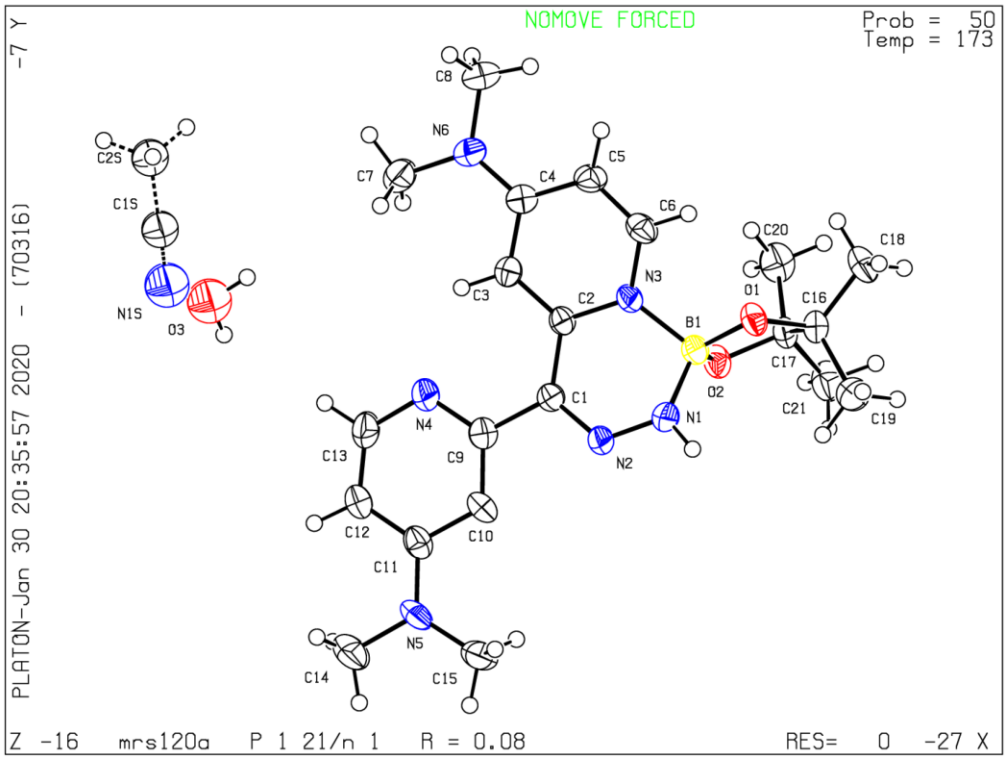

Figure S2.1. Representation of the solid-state structure of 6 at 50% probability ellipsoids. Co-crystallized H_2O and CH_3CN are shown.

Compound	**6**
CCDC	1981016
Formula	$C_{21.4}H_{31.8}BN_{6.2}O_{2.6}$
$D_{calc.}$/ g cm^{-3}	1.236
μ/mm^{-1}	0.669
Formula Weight	428.34
Colour	yellow
Shape	needle
Size/mm^3	0.38×0.10×0.04
T/K	173(1)
Crystal System	monoclinic
Space Group	$P2_1/n$
a/Å	13.9473(5)
b/Å	6.8875(3)
c/Å	24.6074(11)
α/°	90
β/°	103.062(3)
γ/°	90
V/Å^3	2302.67(17)
Z	4
Z'	1
Wavelength/Å	1.54178
Radiation type	CuK$_\alpha$
Θ_{min}/°	3.688
Θ_{max}/°	68.228
Measured Refl's.	18482
Ind't Refl's	4193
Refl's with I > 2(I)	2066
R_{int}	0.1398
Parameters	295
Restraints	5
Largest Peak	0.557
Deepest Hole	-0.263
GooF	1.015
wR_2 (all data)	0.2476
wR_2	0.1965
R_1 (all data)	0.1665
R_1	0.0809

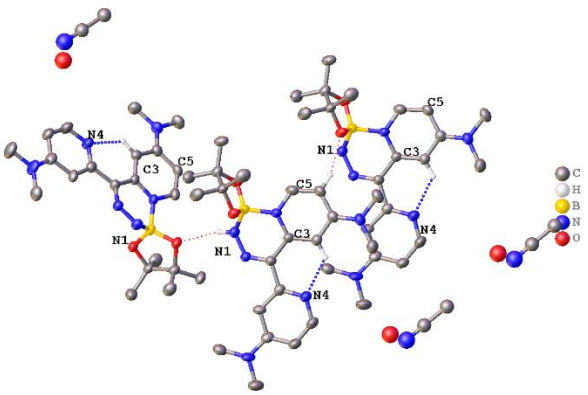

Figure S2.2. The following hydrogen bonding interactions with a maximum D-D distance of 3.2 Å and a minimum angle of 110 ° are present in 6: N1–O1_*1: 3.158 Å, C3–N4: 2.843 Å, C5–O2*_2: 3.179 Å.

2.4.12. NMR Data

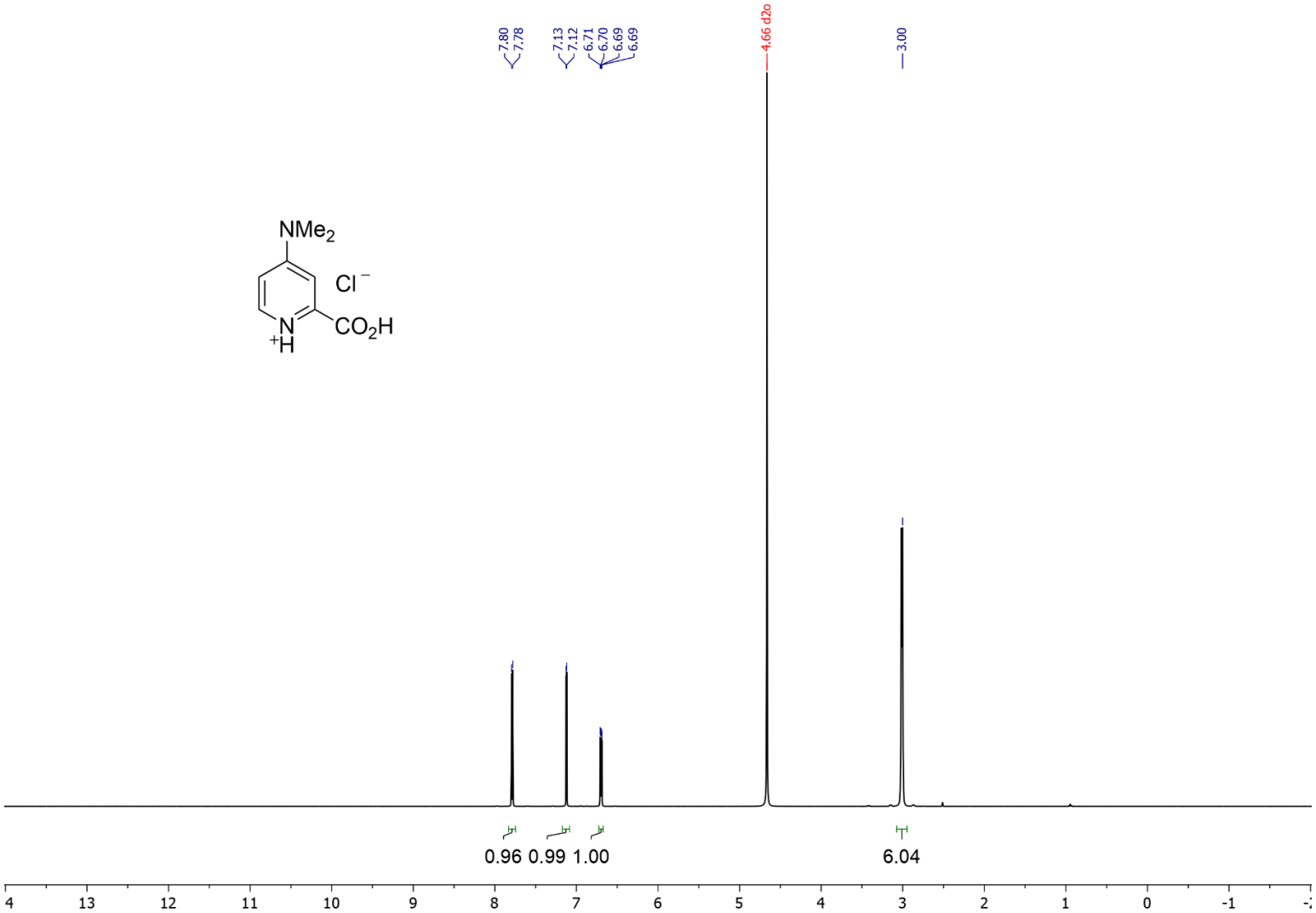

^{1}H NMR of 4-(dimethylamino)picolinic acid hydrogen chloride (500 MHz, D_2O)

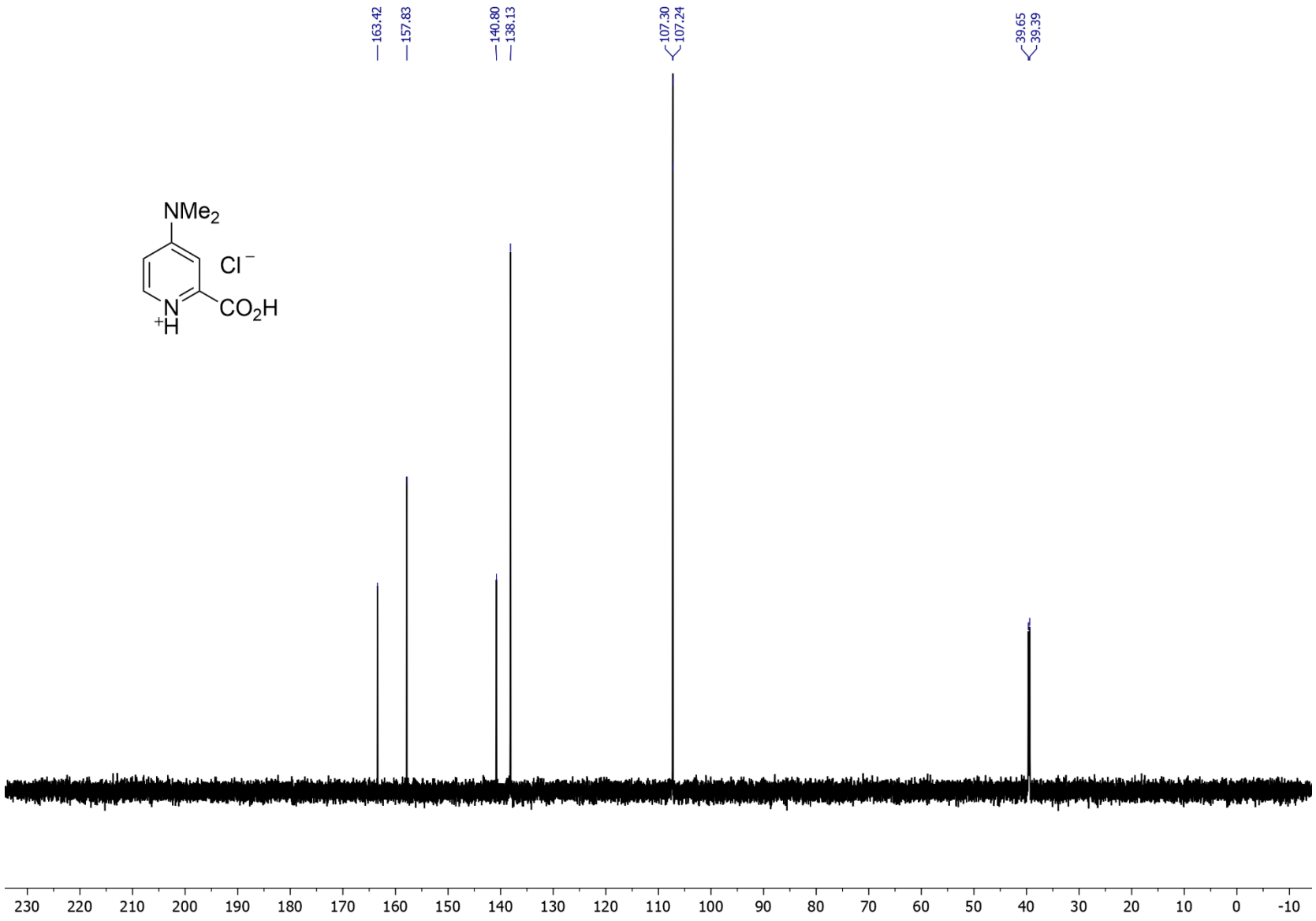

^{13}C NMR of 4-(dimethylamino)picolinic acid hydrogen chloride (125 MHz, D_2O)

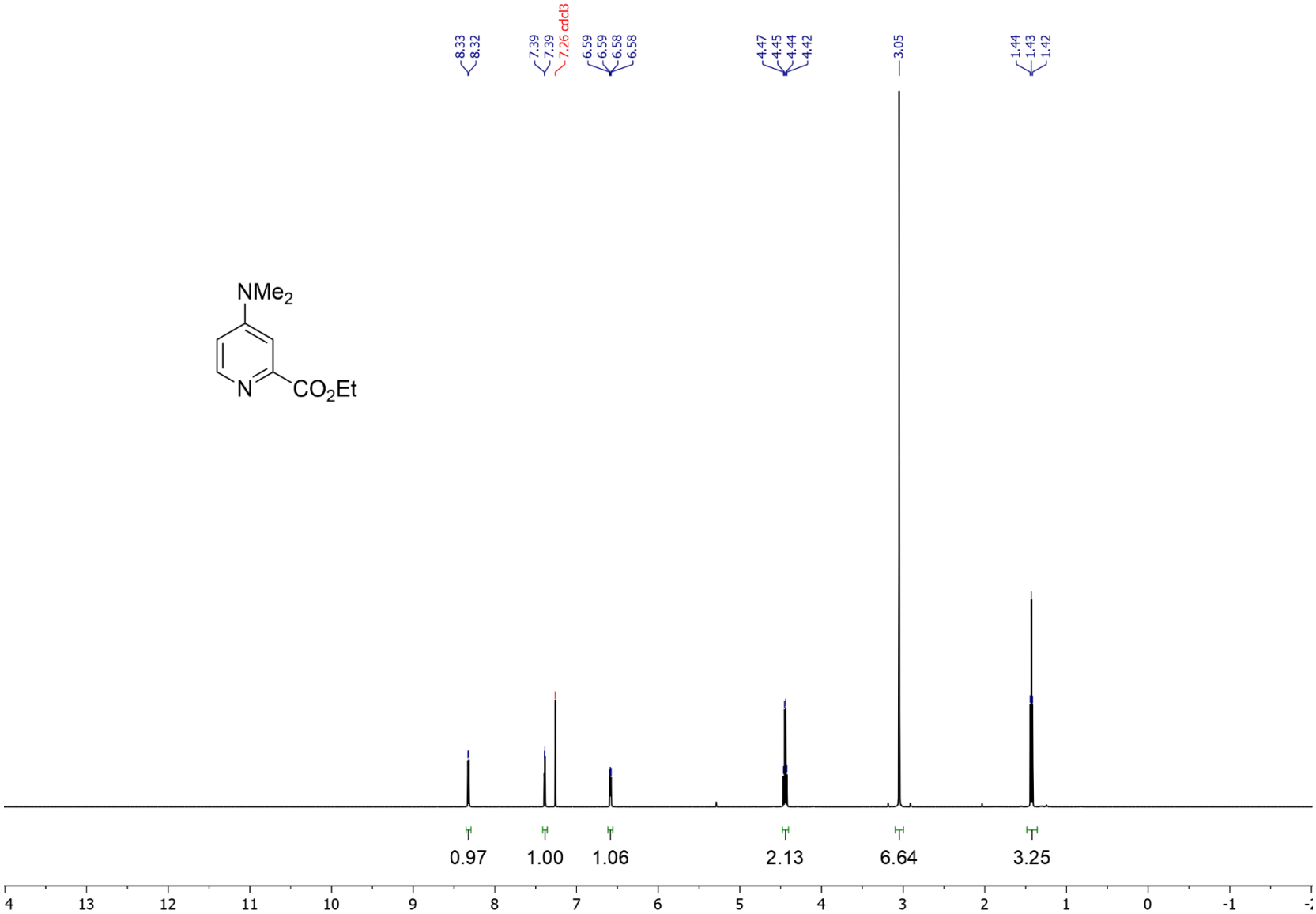

^{1}H NMR of ethyl-4-(dimethylamino)picolinate (500 MHz, $CDCl_3$)

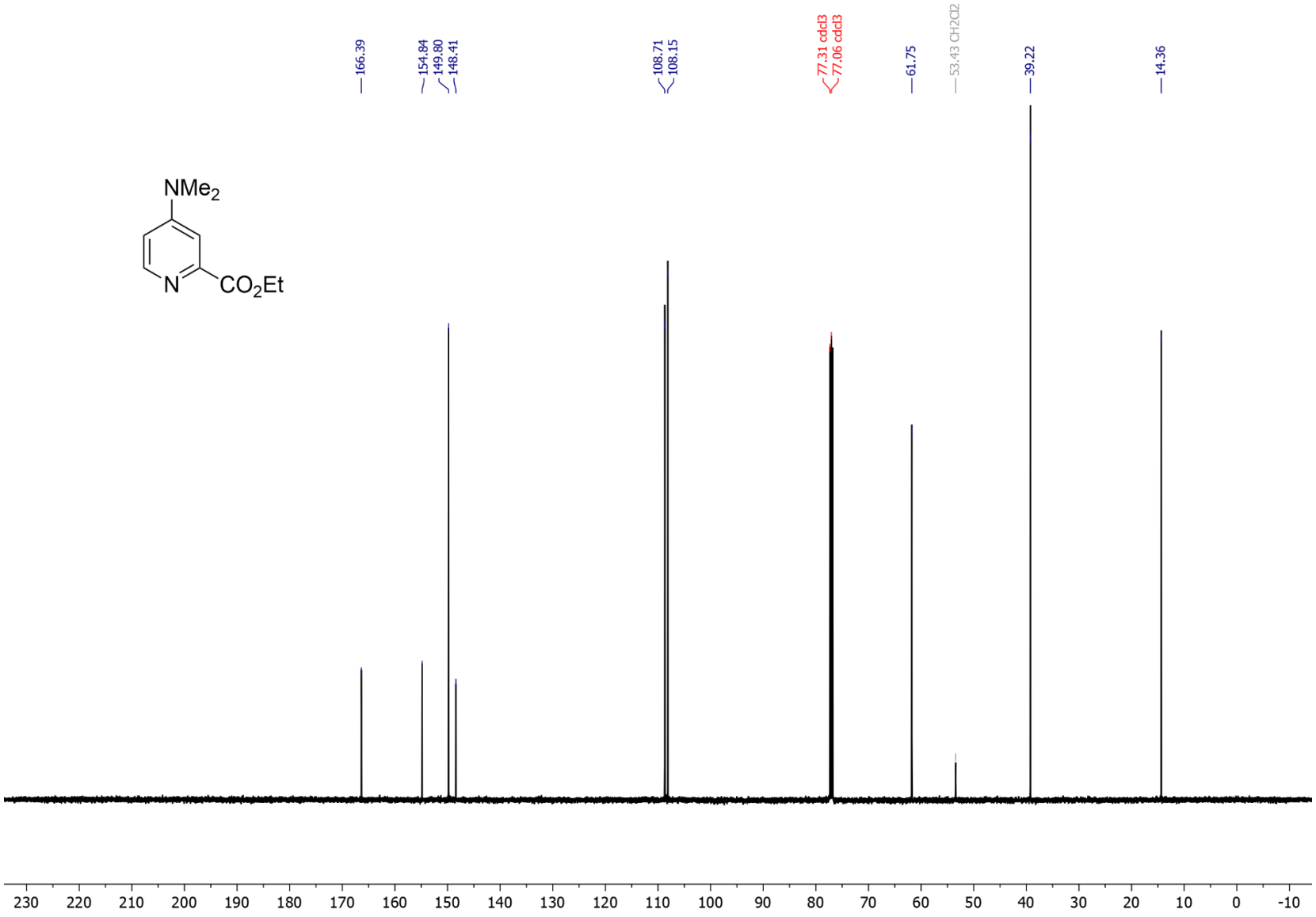

^{13}C NMR of ethyl-4-(dimethylamino)picolinate (125 MHz, $CDCl_3$)

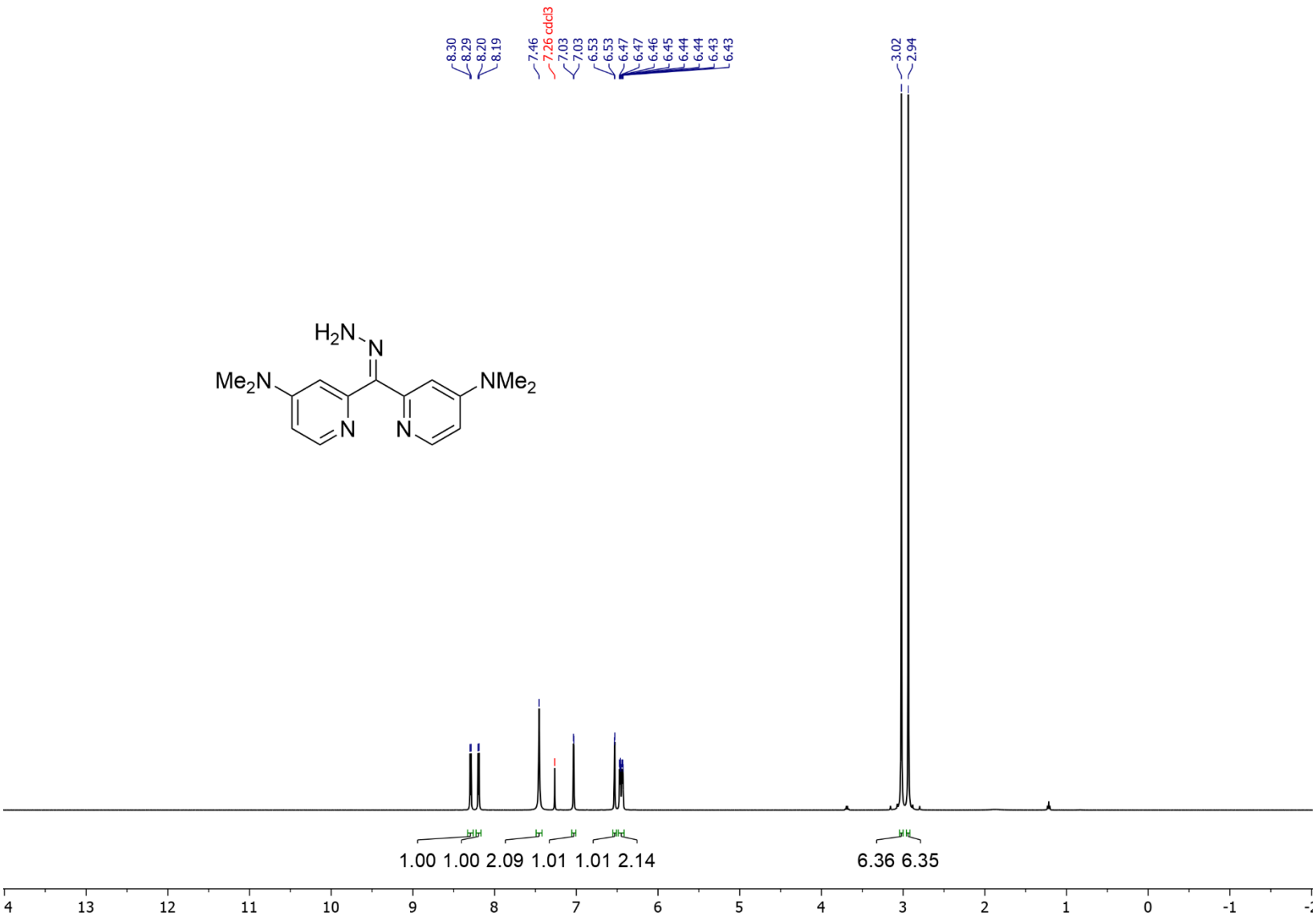

^{1}H NMR of bis((4-dimethylamino)pyridine)methylene hydrazine (dmadph) (500 MHz, $CDCl_3$)

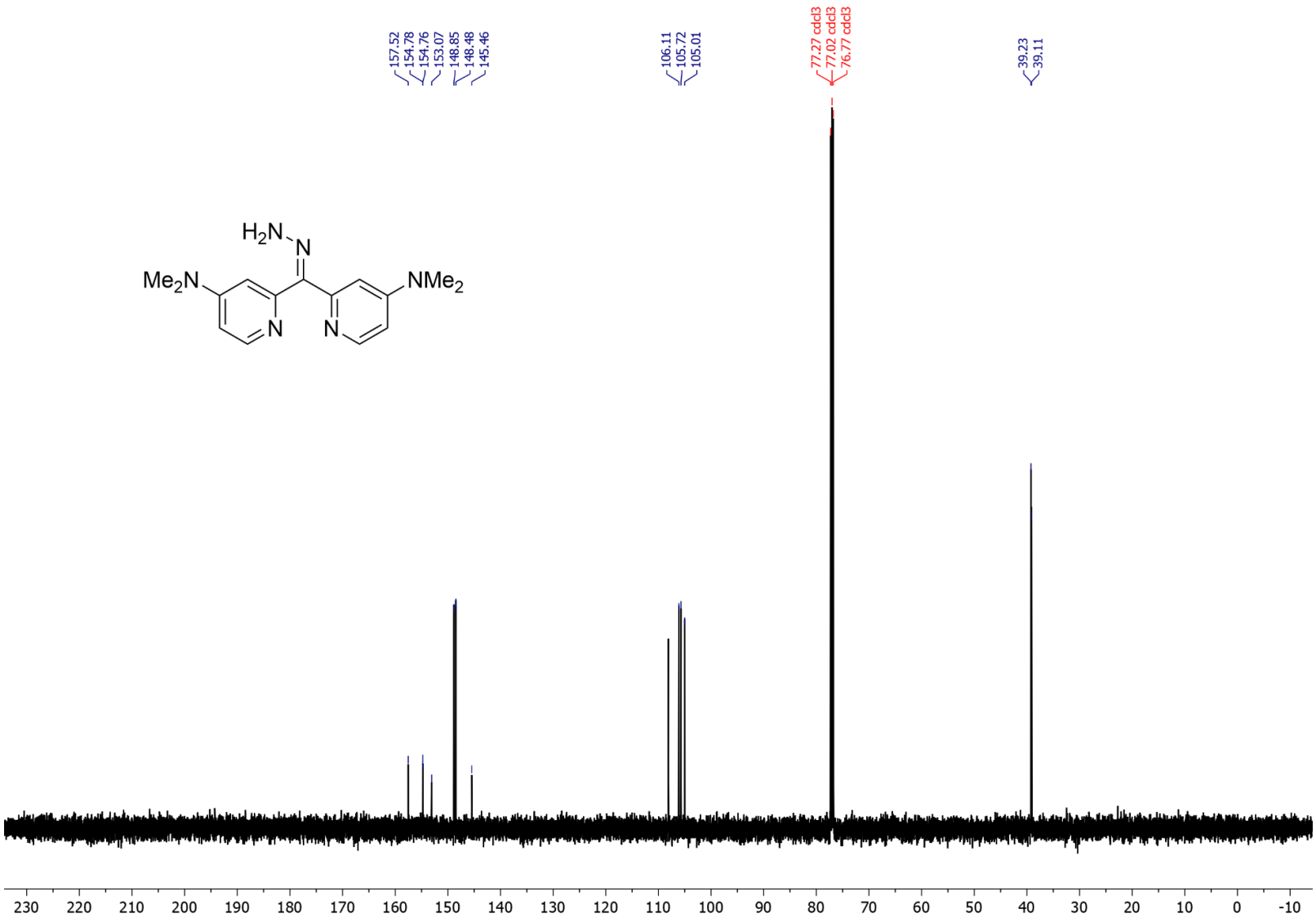

^{13}C NMR of bis((4-dimethylamino)pyridine)methylene hydrazine (dmadph) 125 MHz, $CDCl_3$)

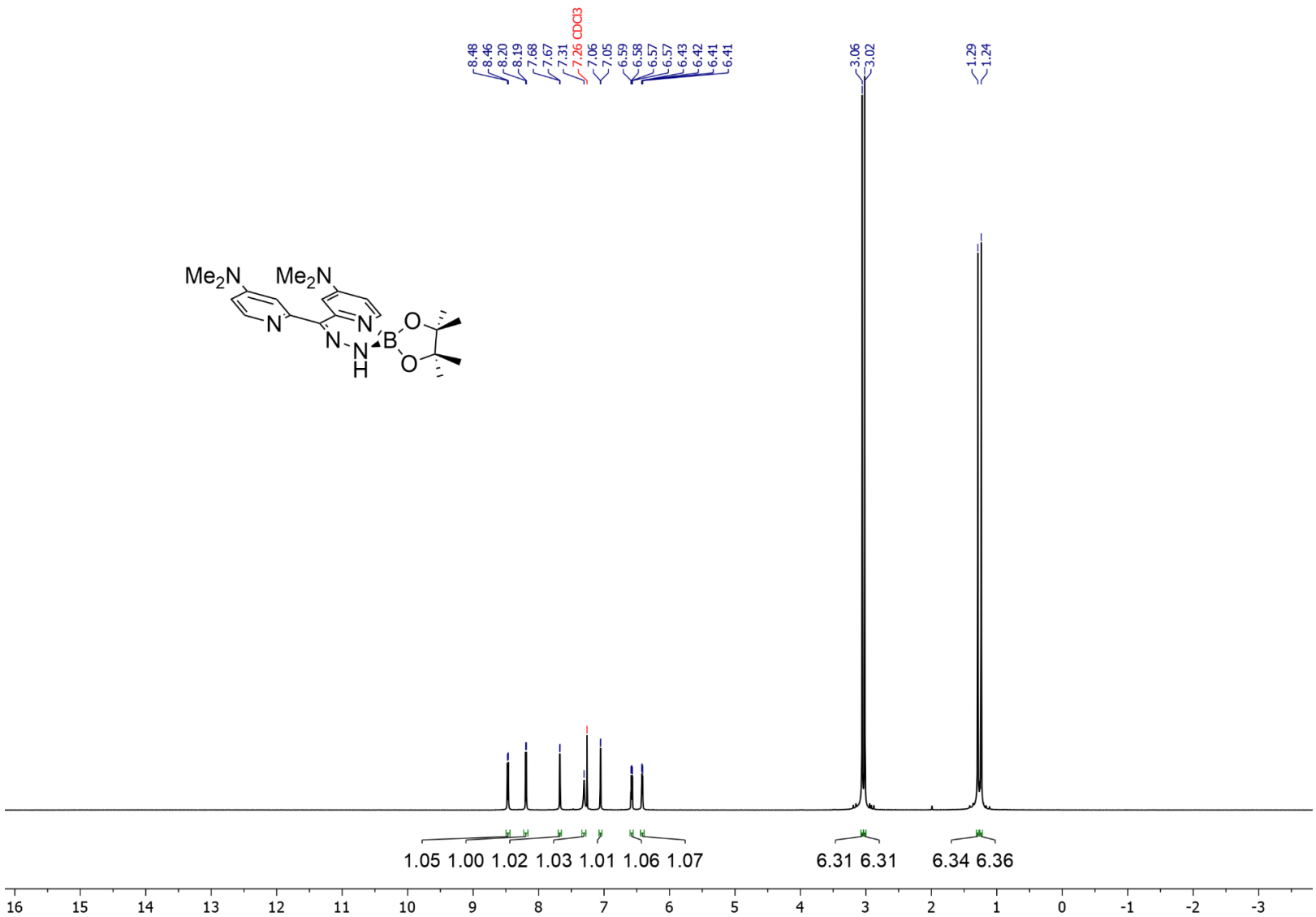

^{1}H NMR of dmadph-HBpin adduct (500 MHz, $CDCl_3$)

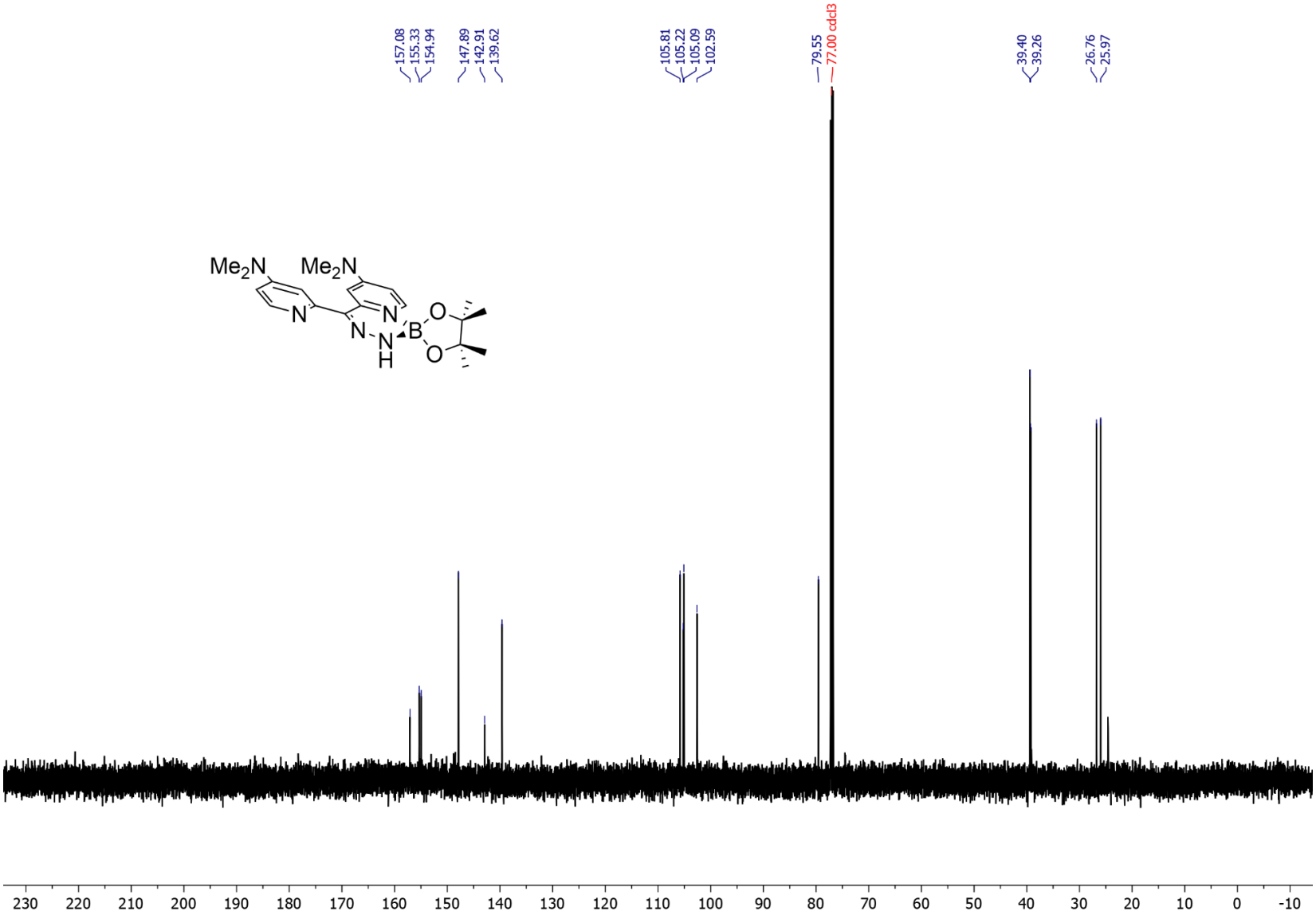

^{13}C NMR of dmadph-HBpin adduct (126 MHz, $CDCl_3$)

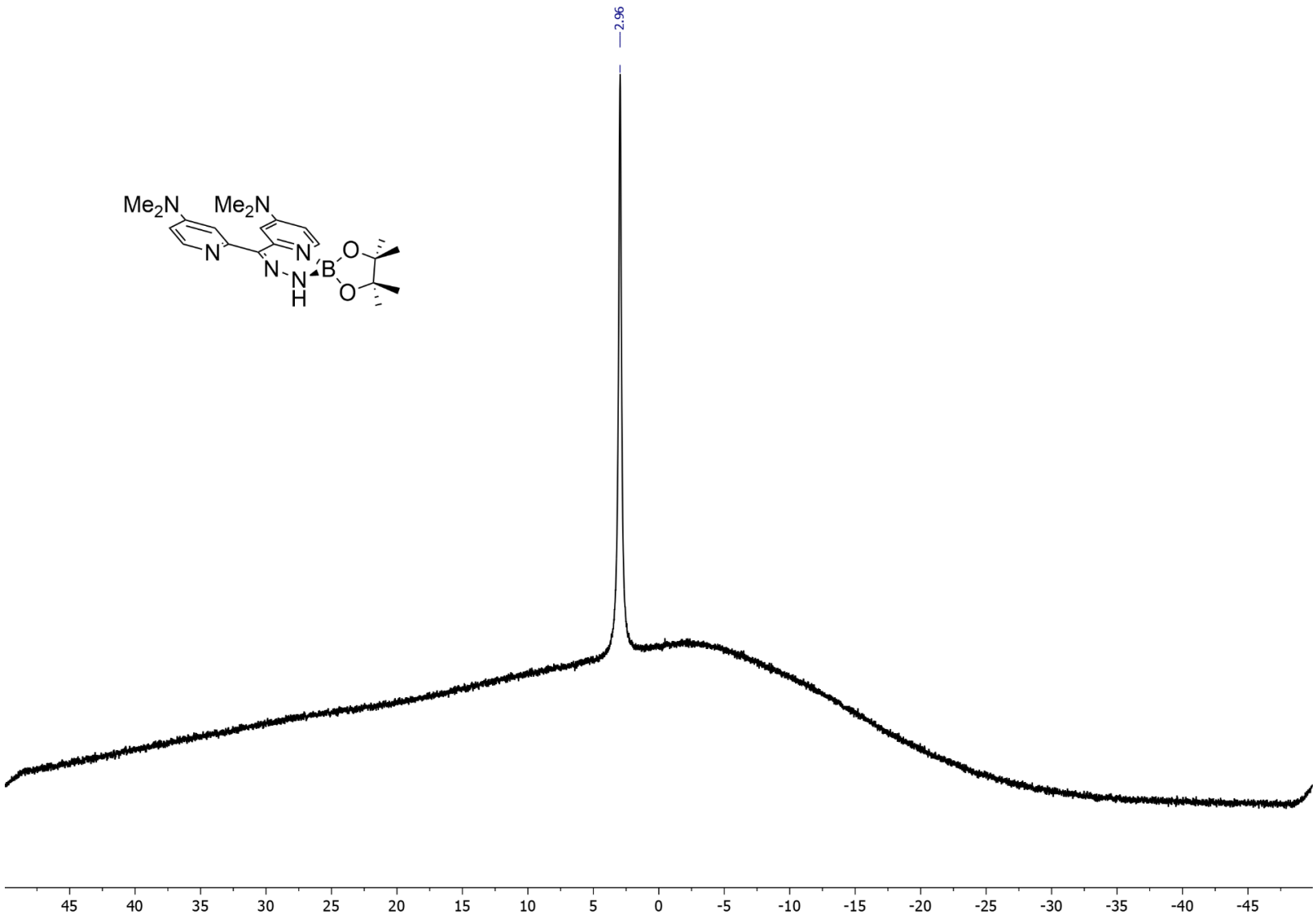

^{11}B NMR of dmadph-HBpin adduct (160 MHz, $CDCl_3$)

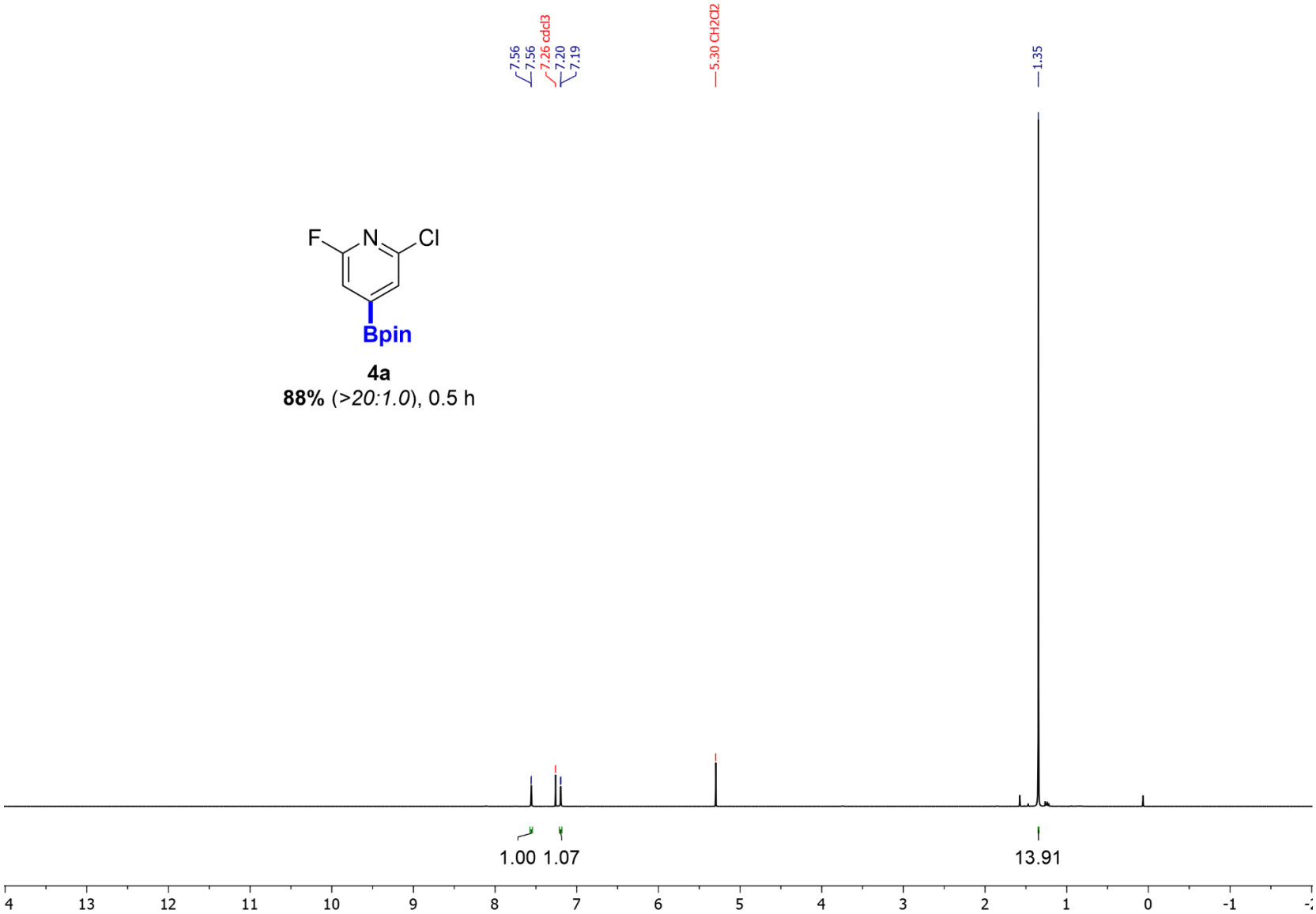

^{1}H NMR of **4a** (500 MHz, $CDCl_3$)

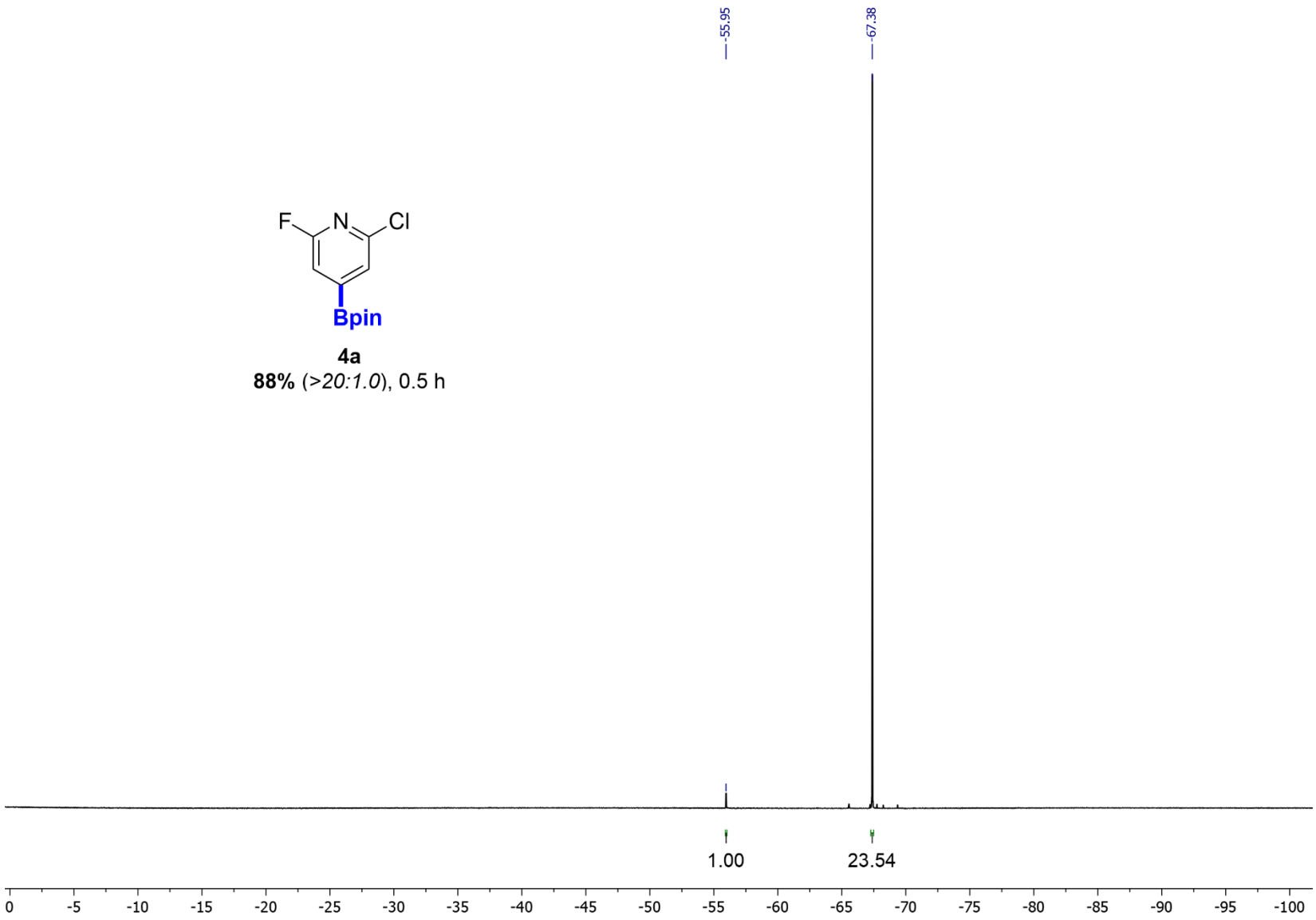

^{19}F NMR of **4a** (470 MHz, $CDCl_3$)

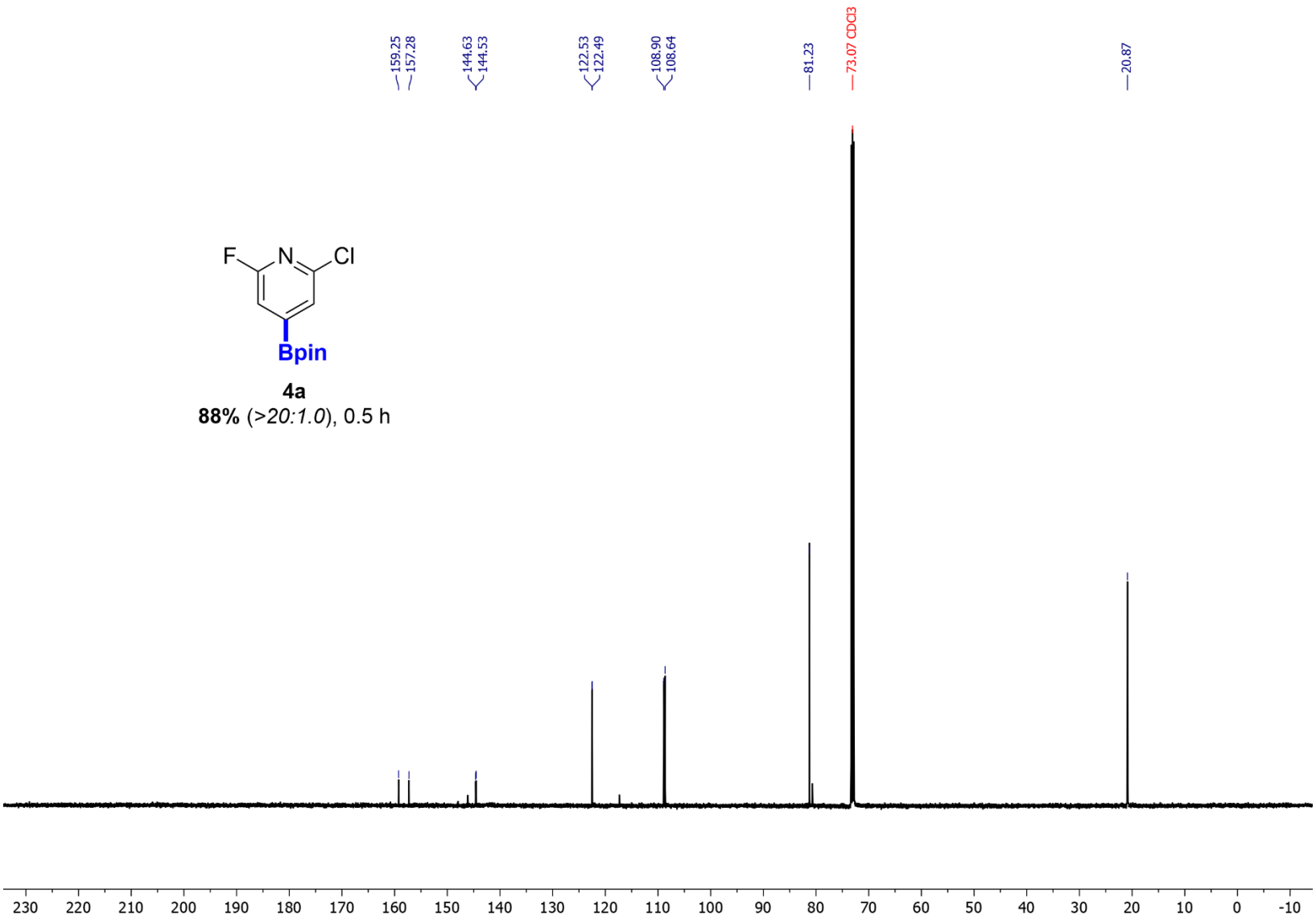

^{13}C NMR of **4a** (126 MHz, $CDCl_3$)

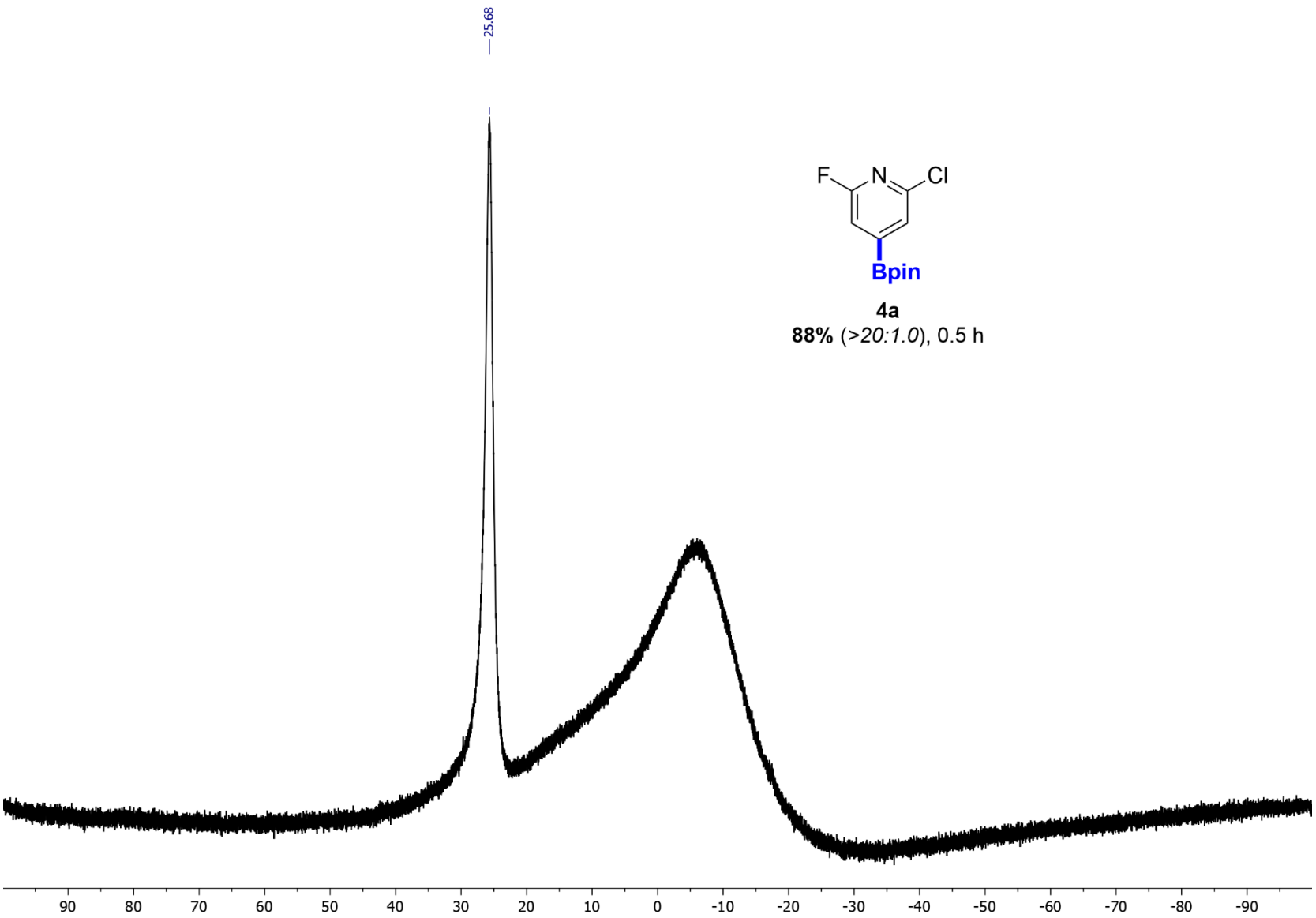

^{11}B NMR of **4a** (160 MHz, $CDCl_3$)

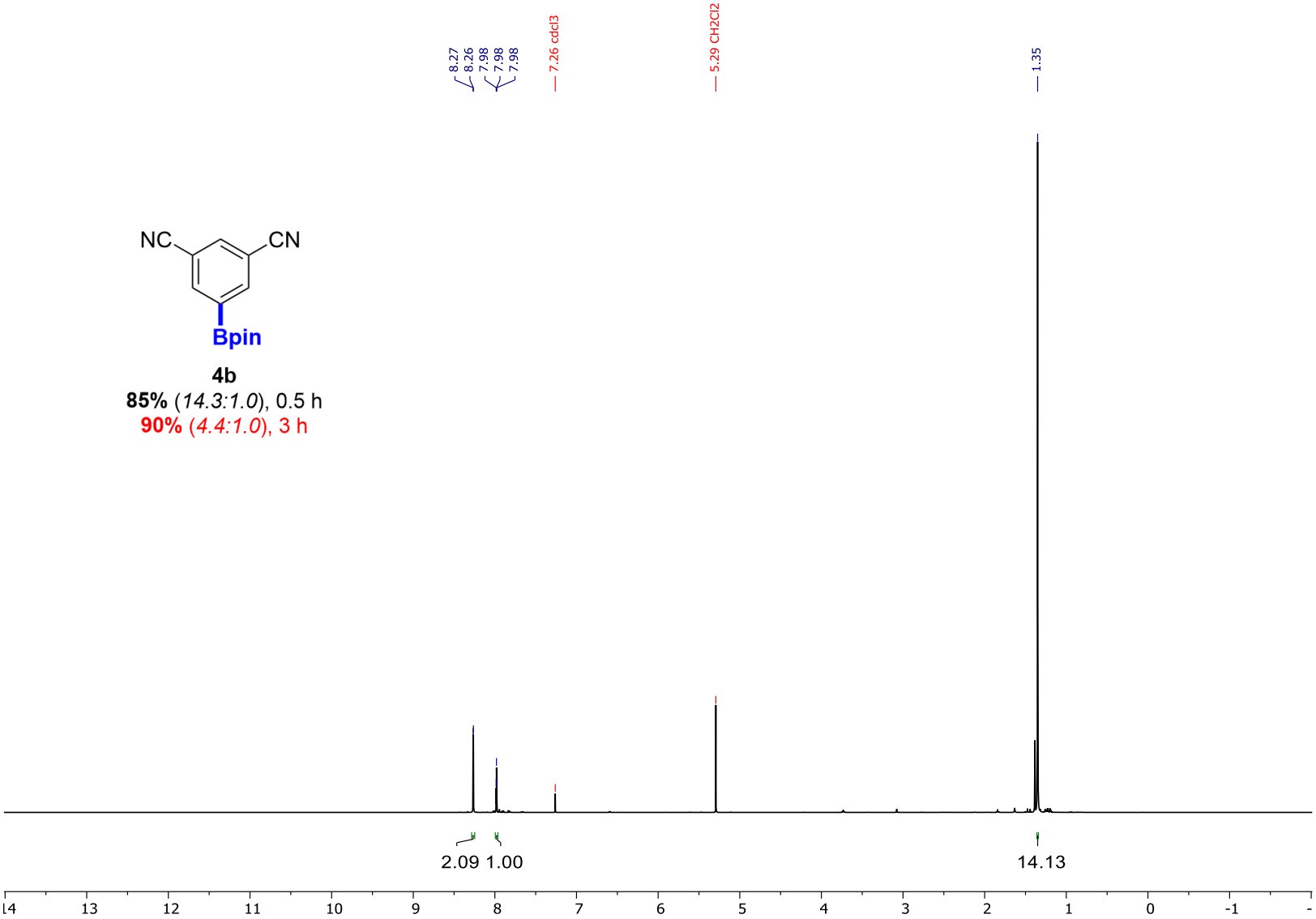

^{1}H NMR of **4b** (160 MHz, $CDCl_3$)

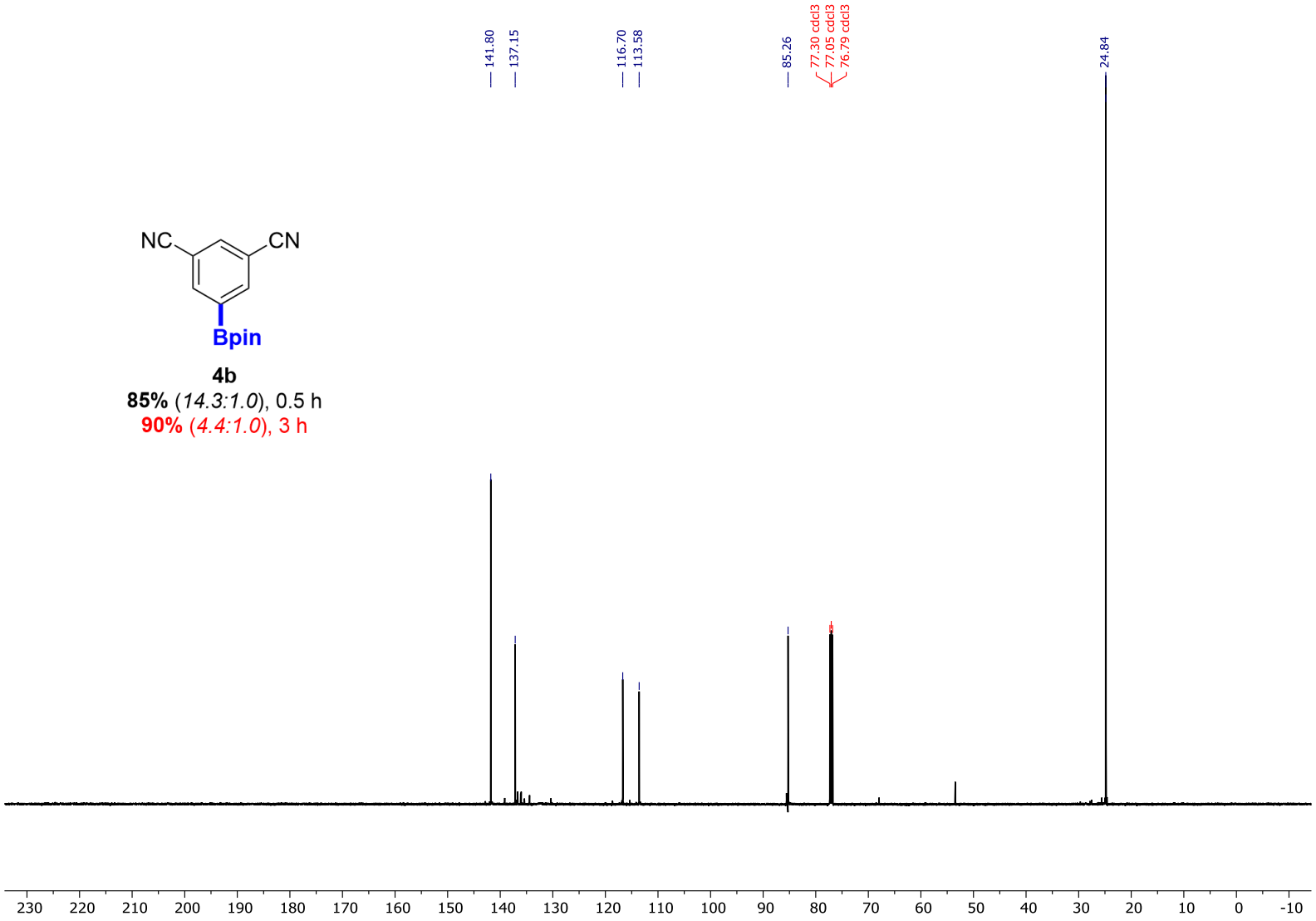

^{13}C NMR of **4b** (126 MHz, $CDCl_3$)

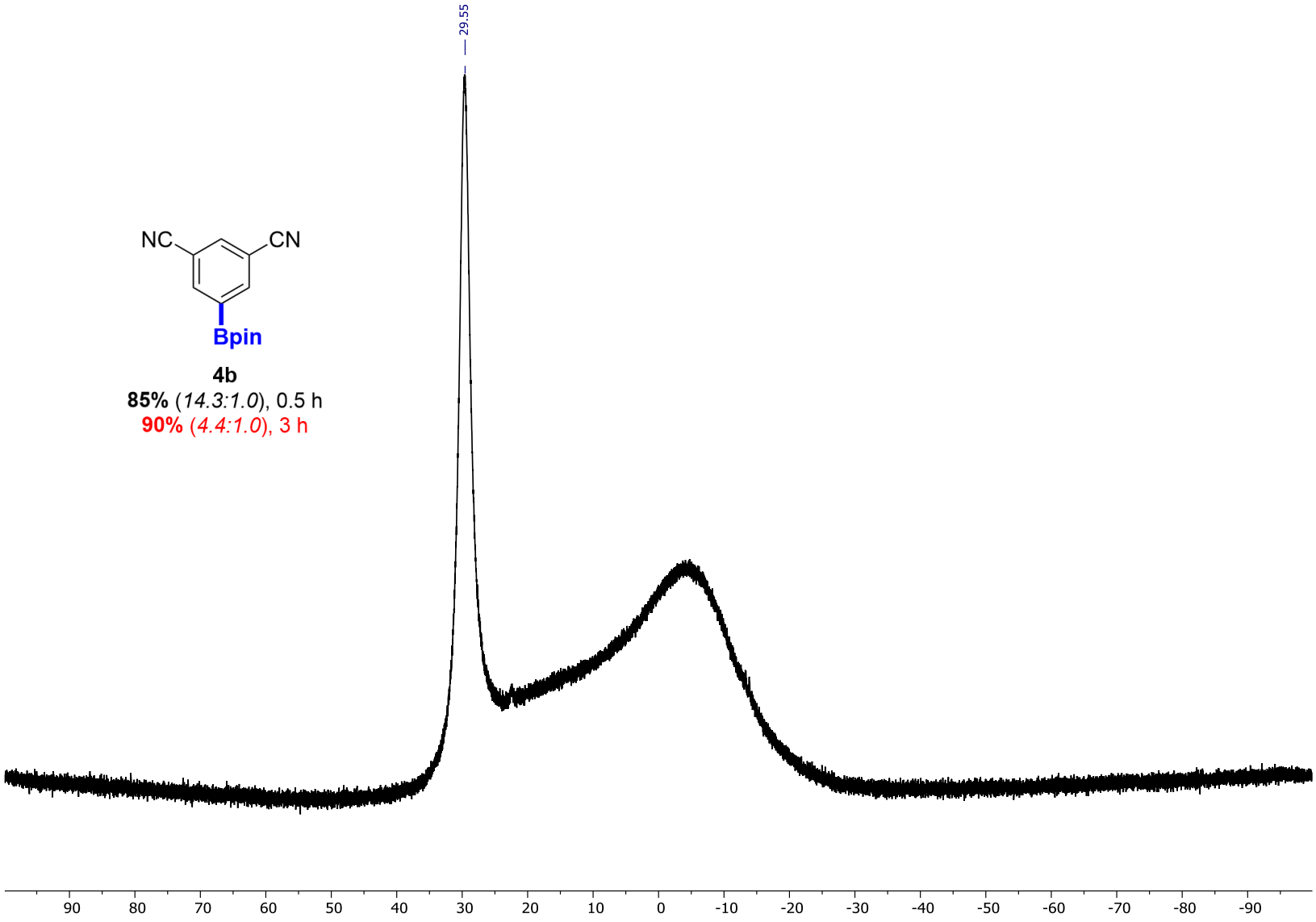

^{11}B NMR of **4b** (160 MHz, $CDCl_3$)

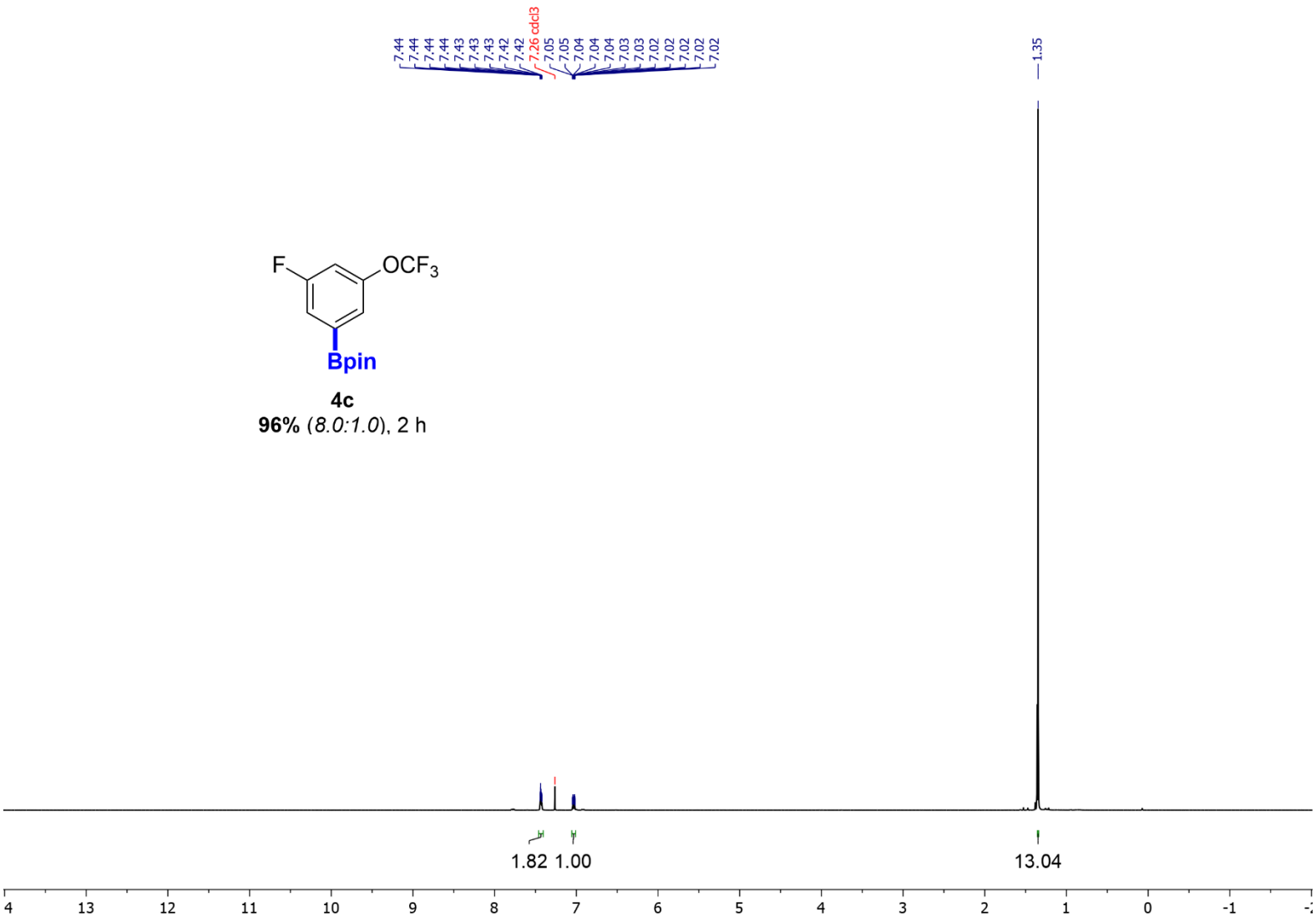

^{1}H NMR of **4c** (500 MHz, $CDCl_3$)

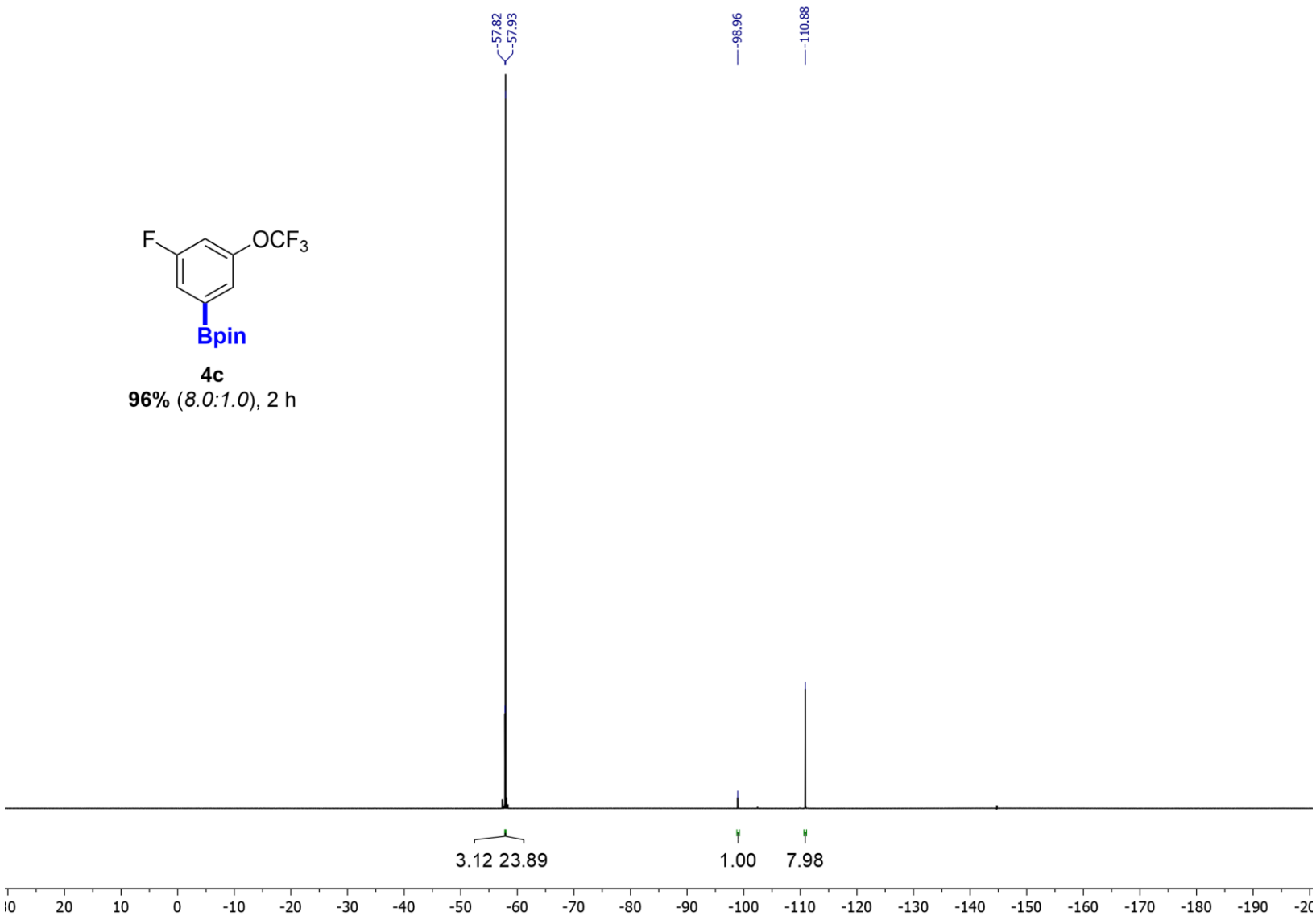

^{19}F NMR of **4c** (470 MHz, $CDCl_3$)

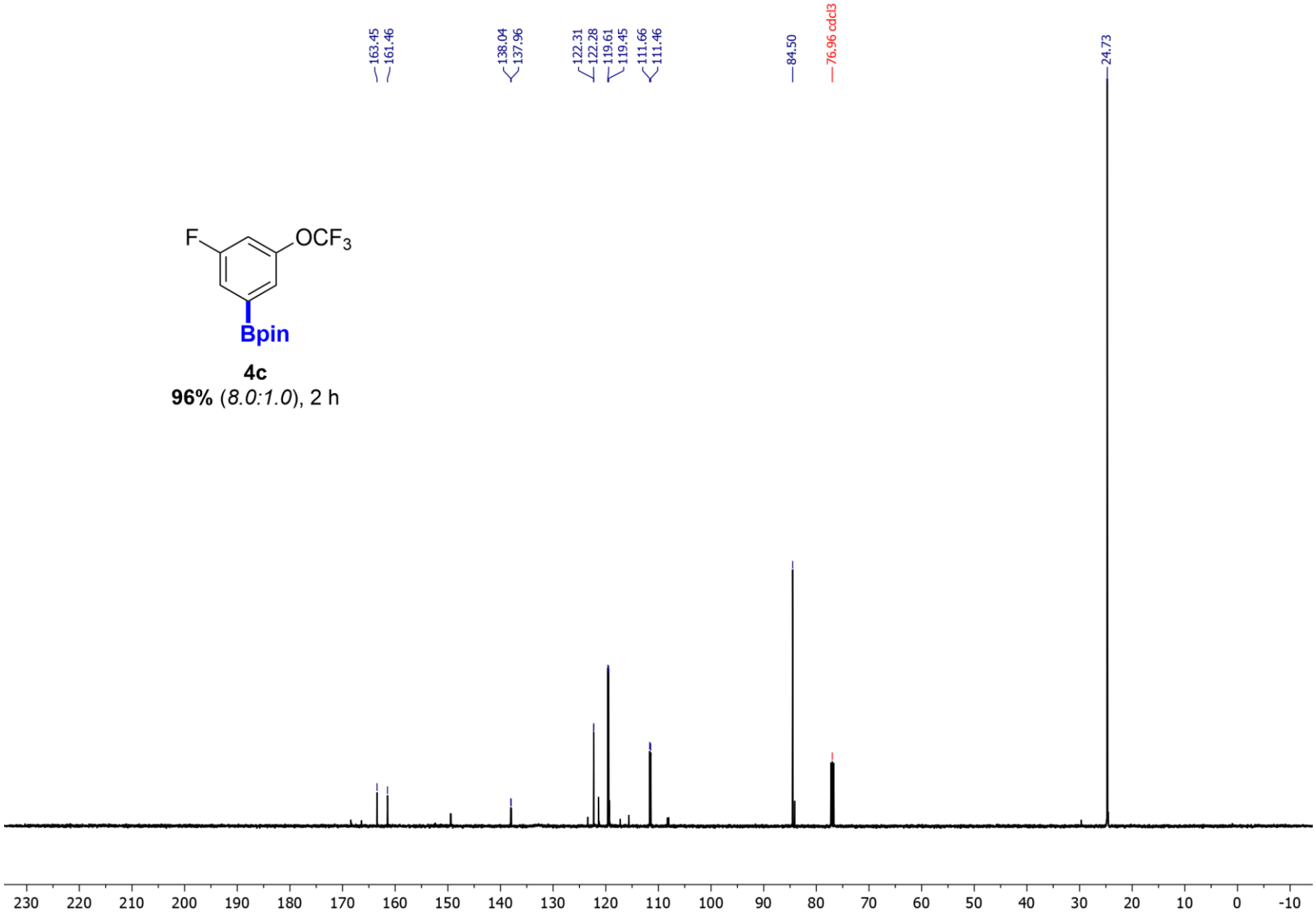

^{13}C NMR of **4c** (126 MHz, $CDCl_3$)

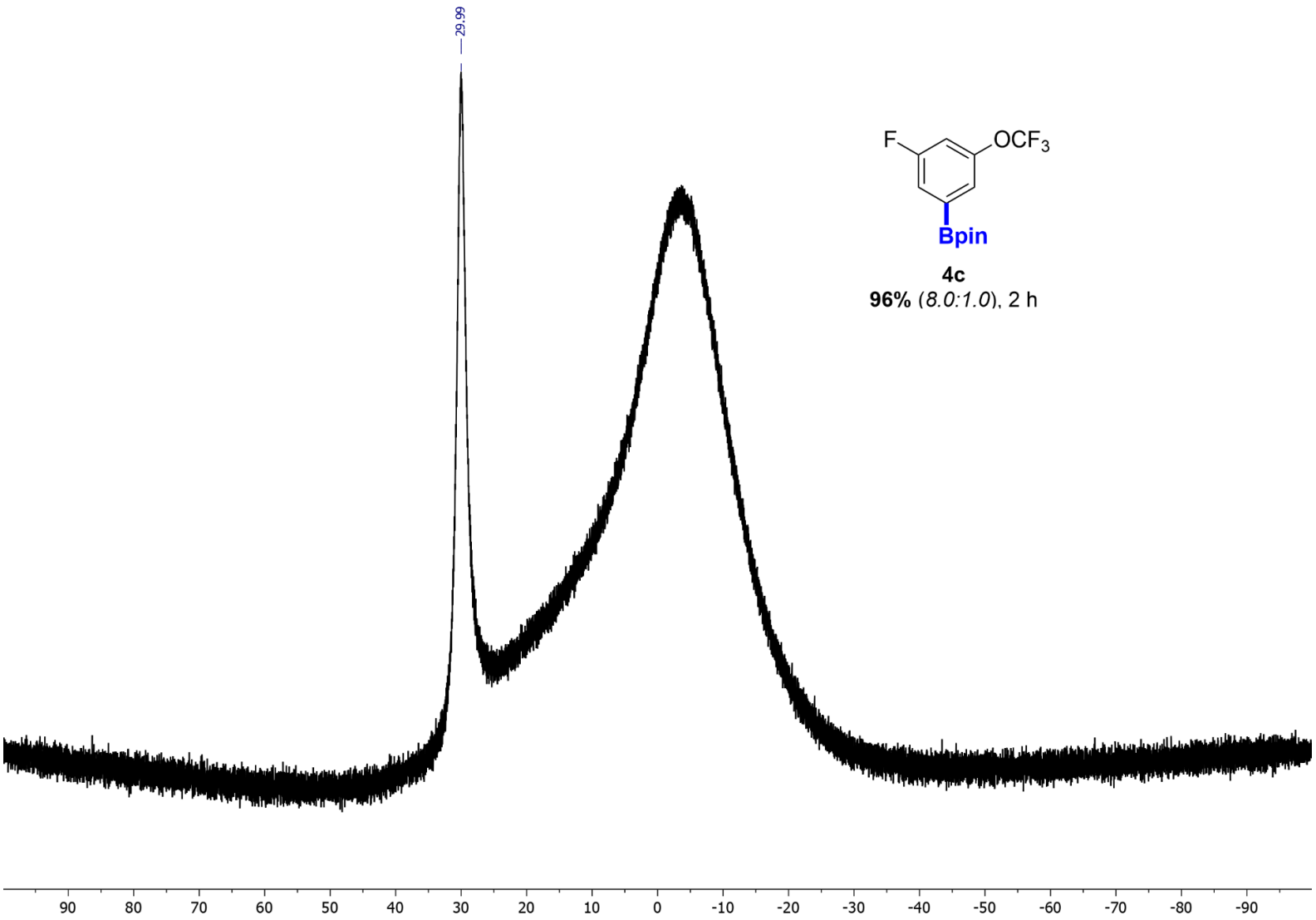

^{11}B NMR of **4c** (160 MHz, $CDCl_3$)

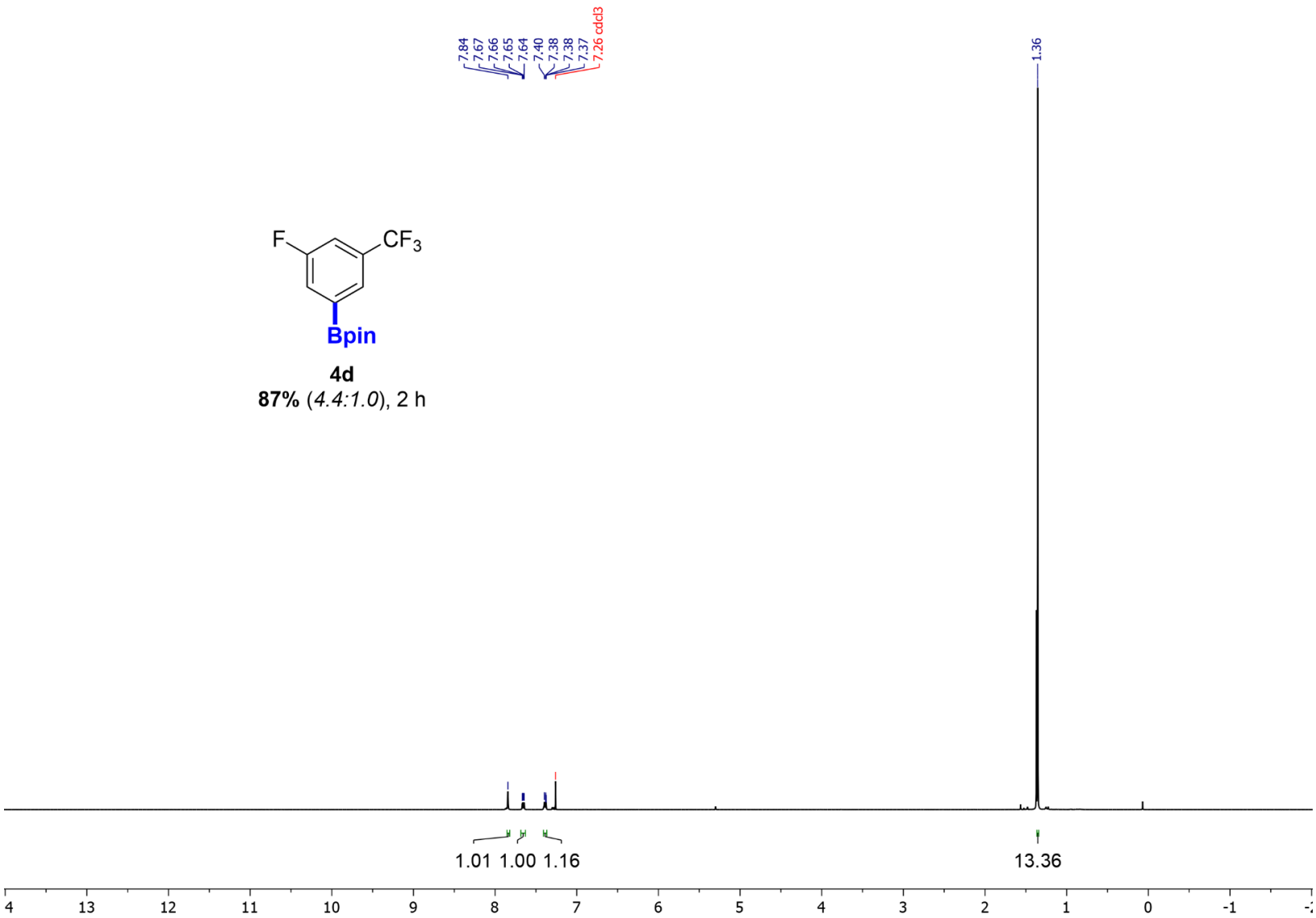

^{1}H NMR of **4d** (500 MHz, $CDCl_3$)

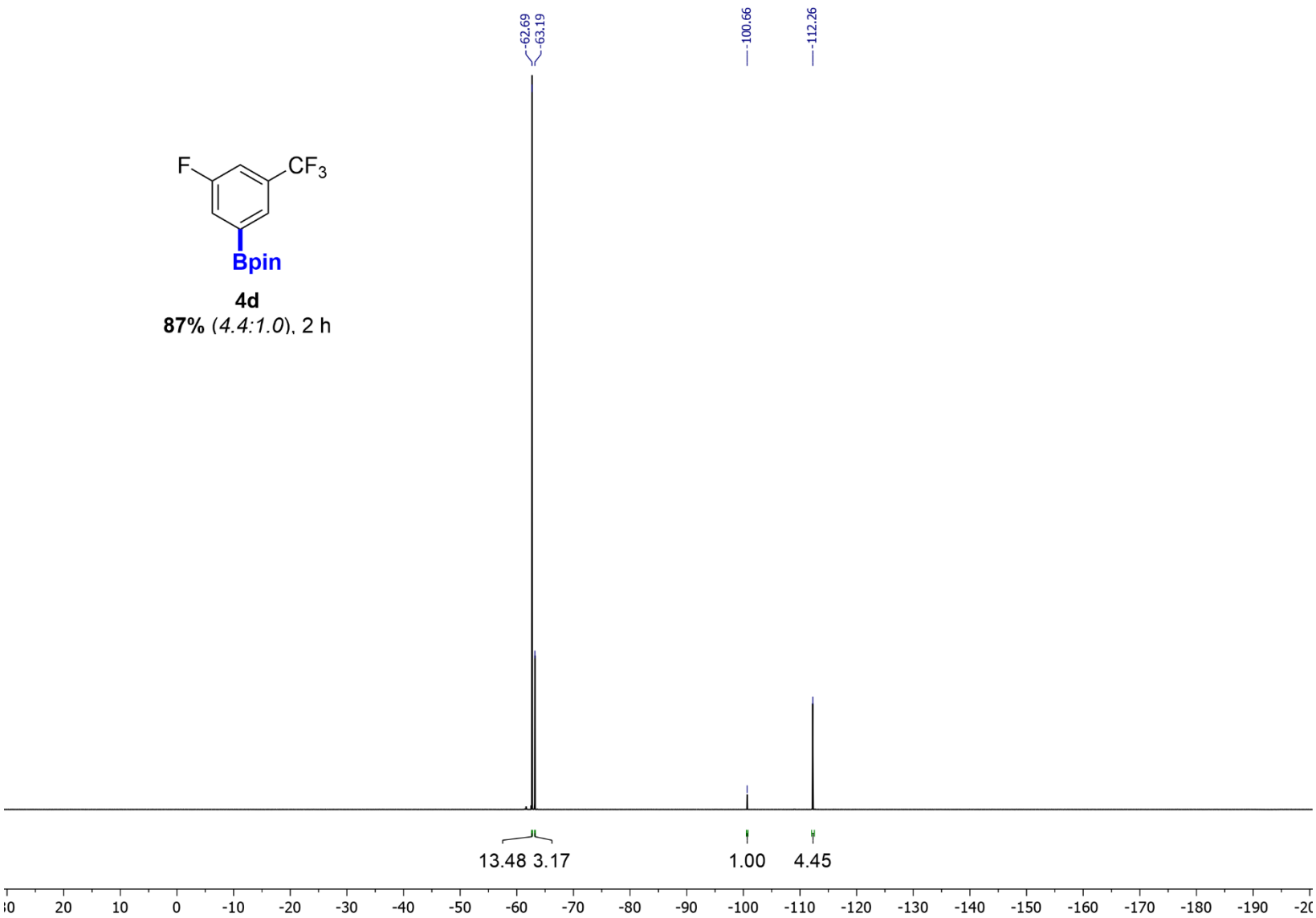

^{19}F NMR of **4d** (470 MHz, $CDCl_3$)

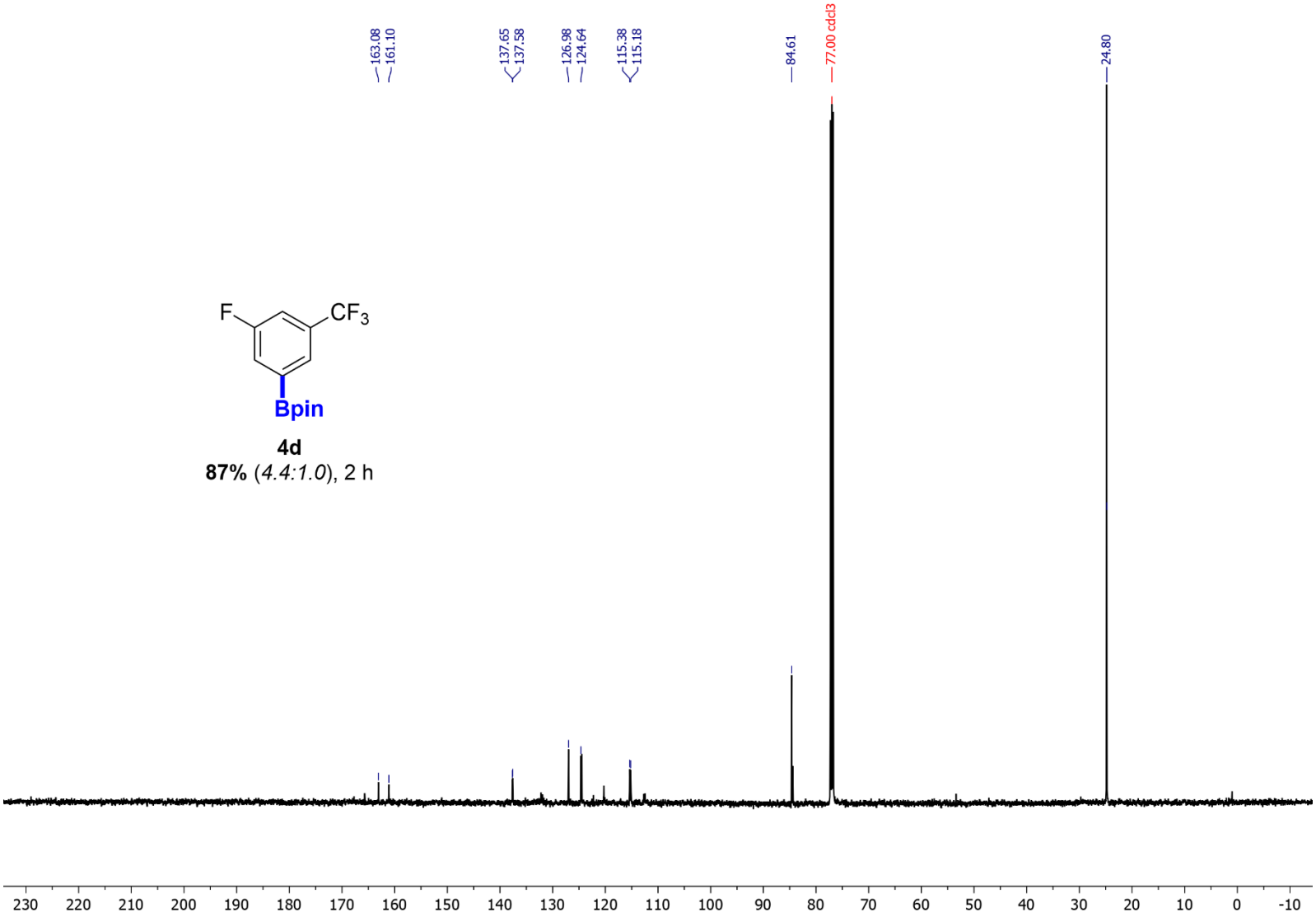

^{13}C NMR of **4d** (126 MHz, $CDCl_3$)

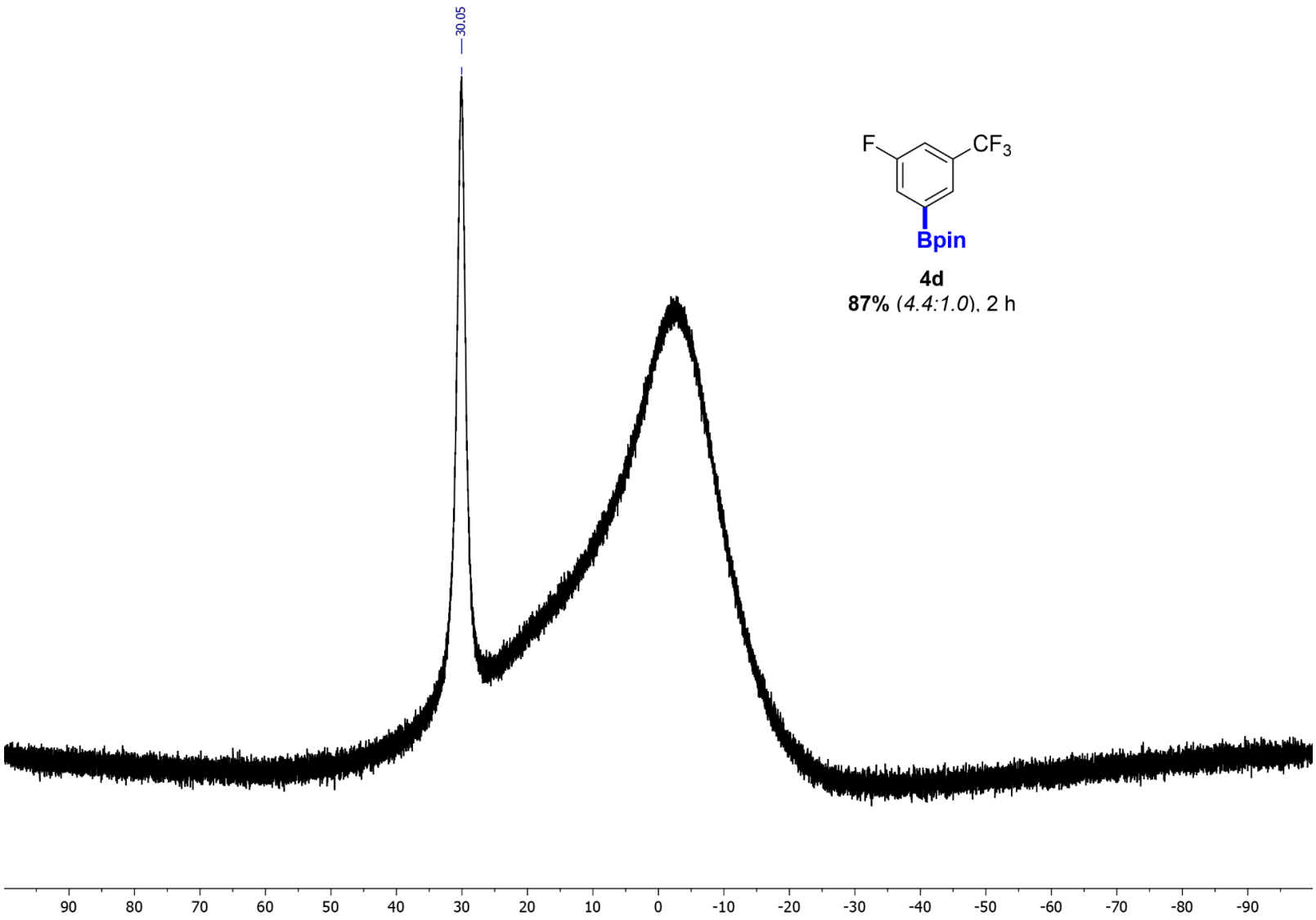

^{11}B NMR of **4d** (160 MHz, $CDCl_3$)

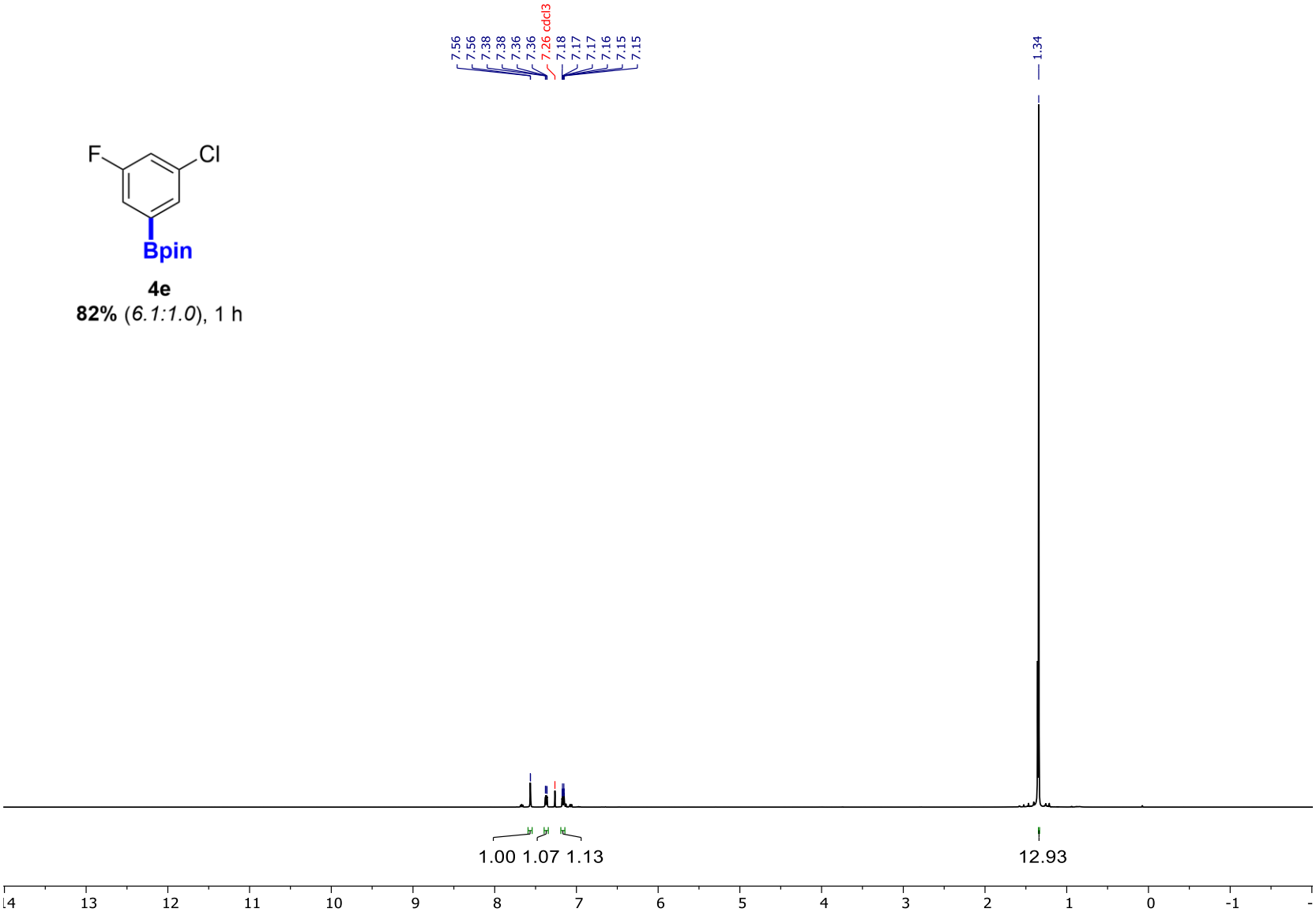

^{1}H NMR of **4e** (500 MHz, $CDCl_3$)

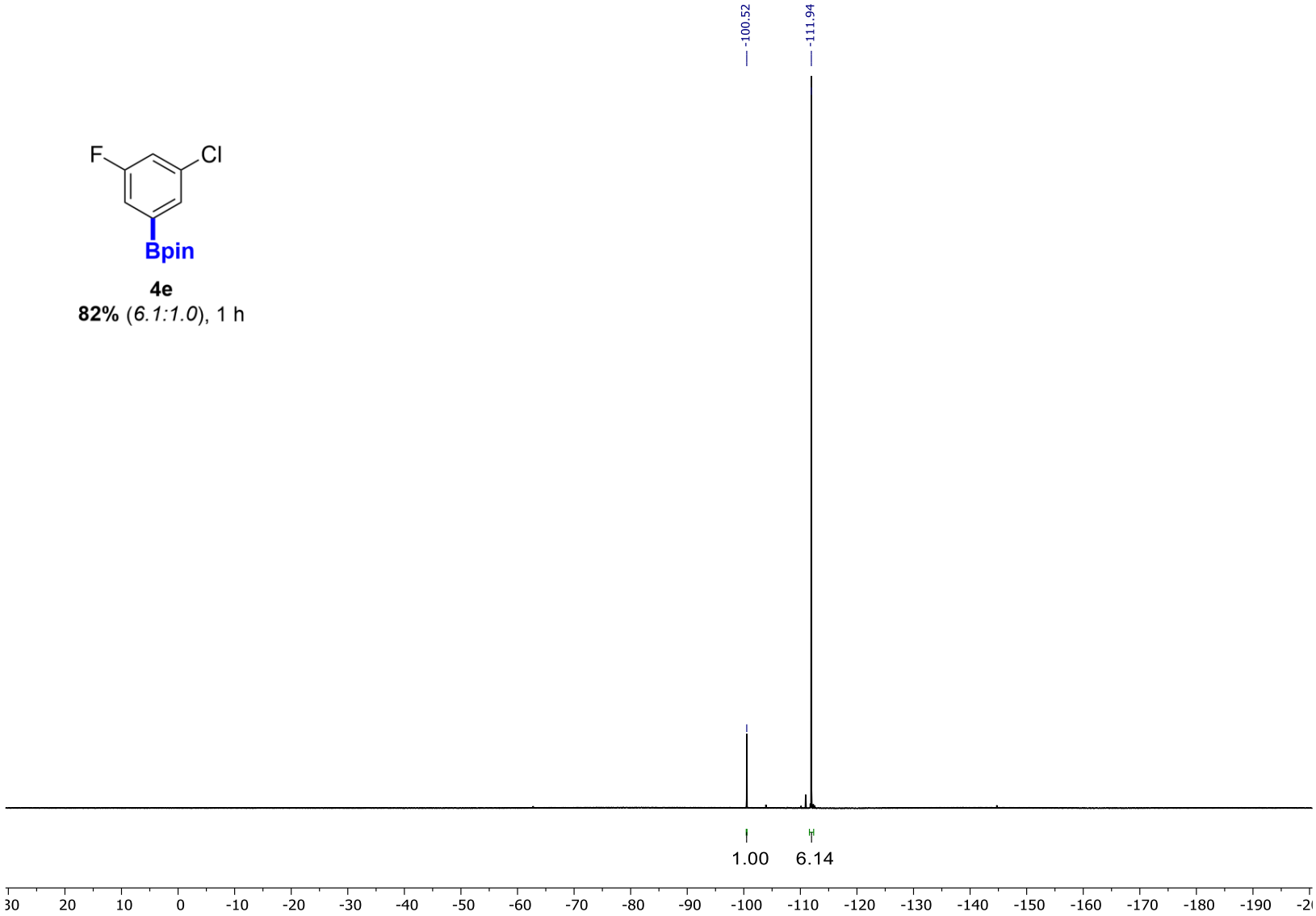

^{19}F NMR of **4e** (470 MHz, $CDCl_3$)

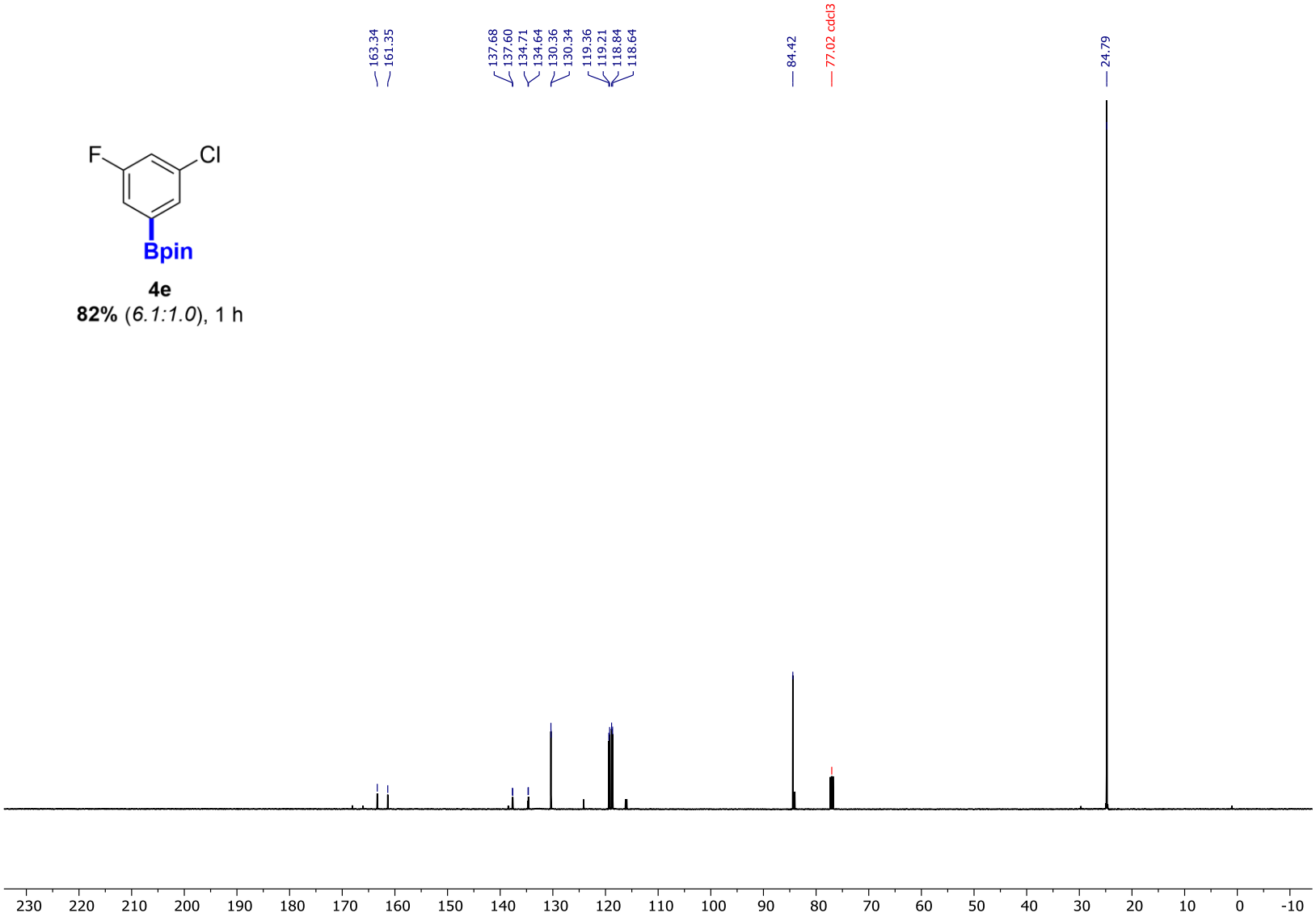

^{13}C NMR of **4e** (126 MHz, $CDCl_3$)

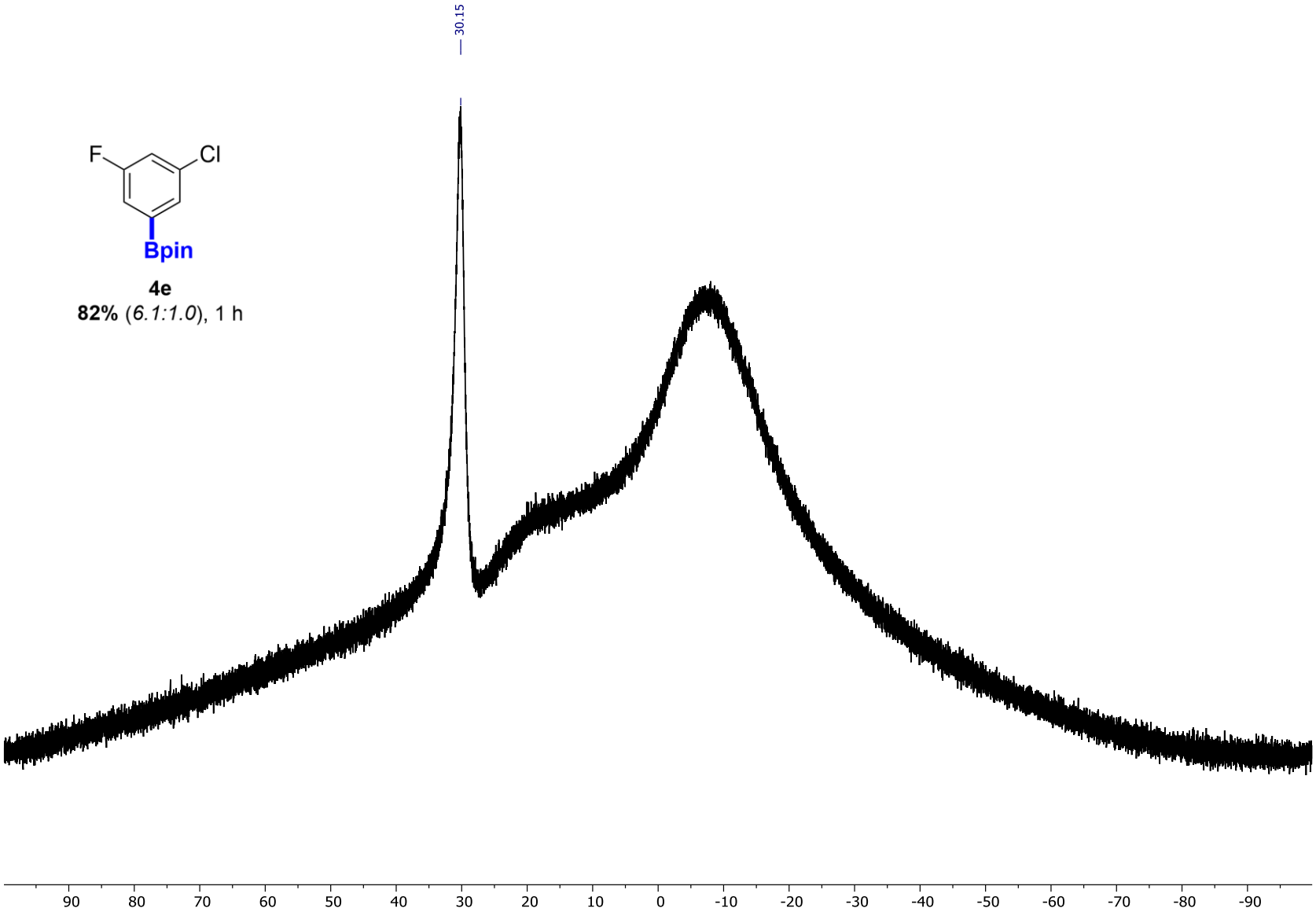

^{11}B NMR of **4e** (160 MHz, $CDCl_3$)

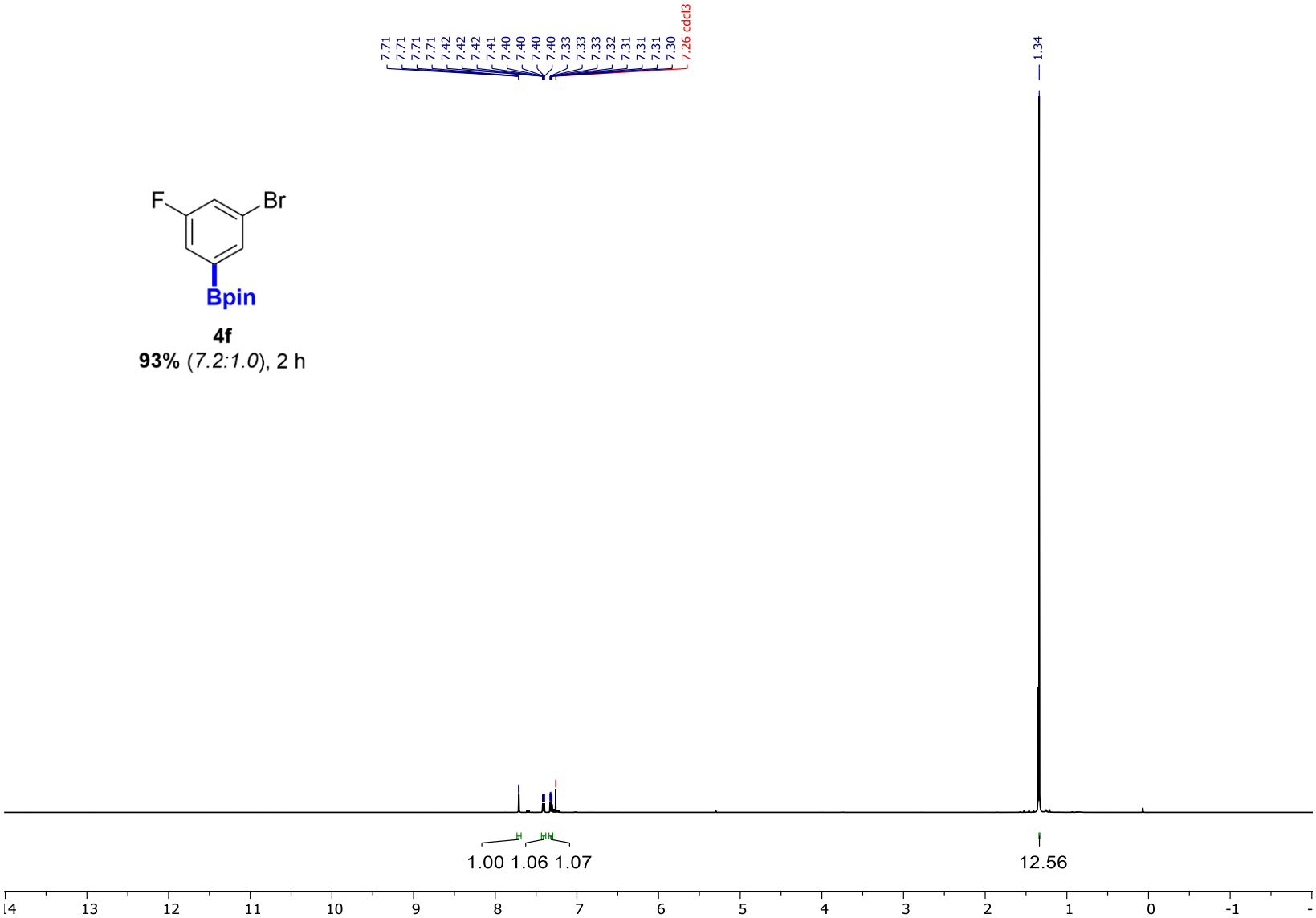

^{1}H NMR of **4f** (500 MHz, $CDCl_3$)

4f
93% (*7.2:1.0*), 2 h

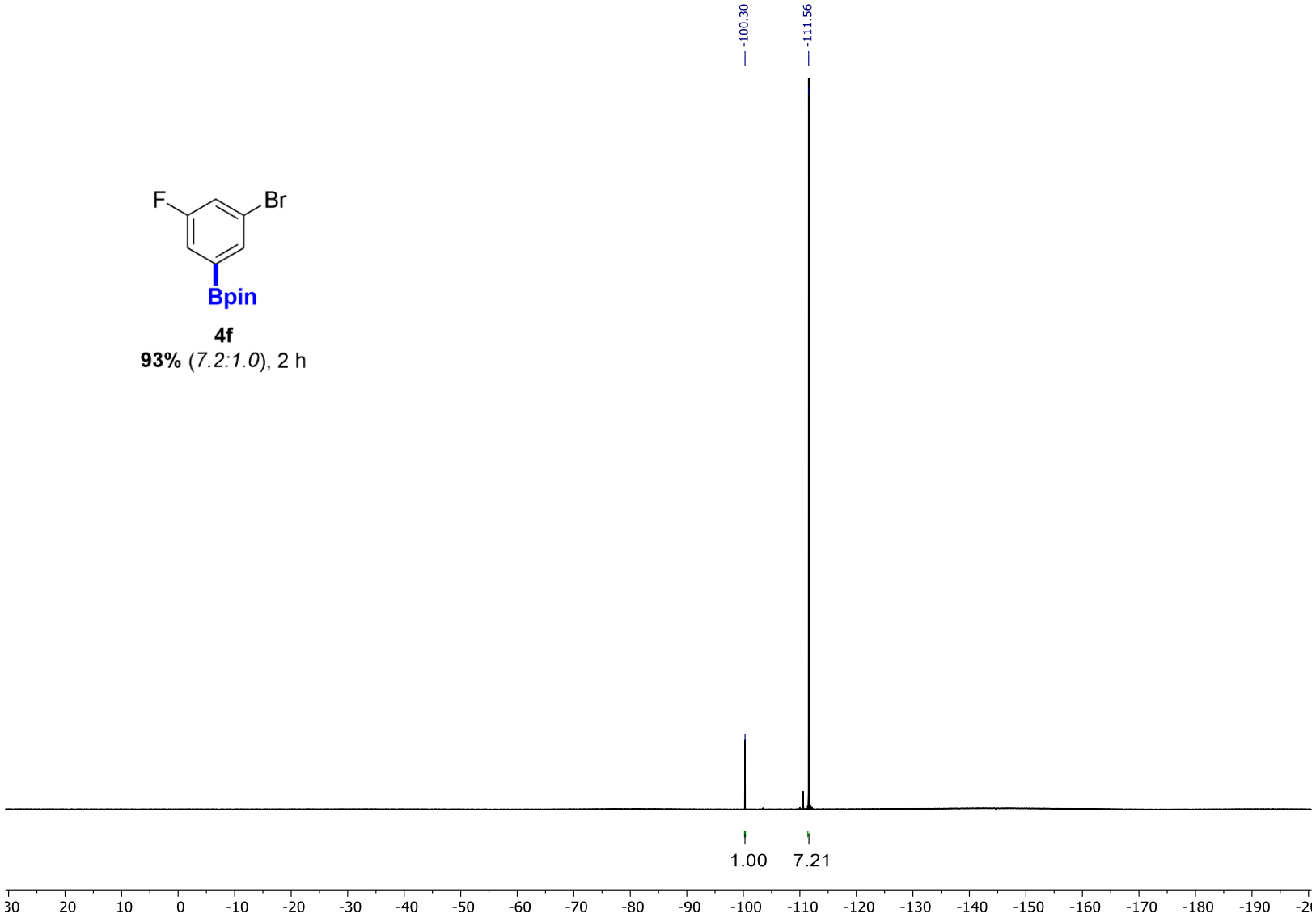

^{19}F NMR of **4f** (470 MHz, $CDCl_3$)

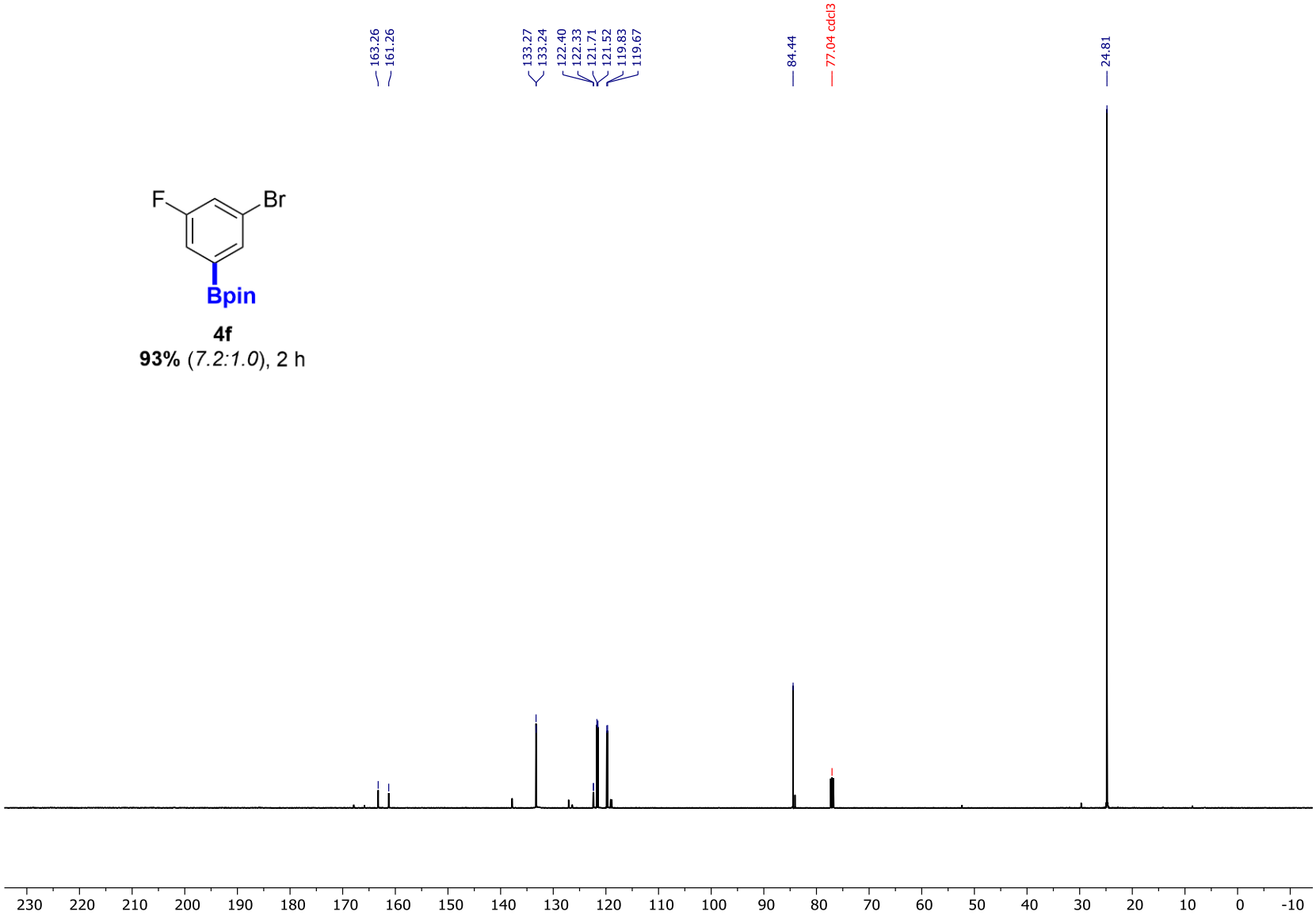

^{13}C NMR of **4f** (126 MHz, $CDCl_3$)

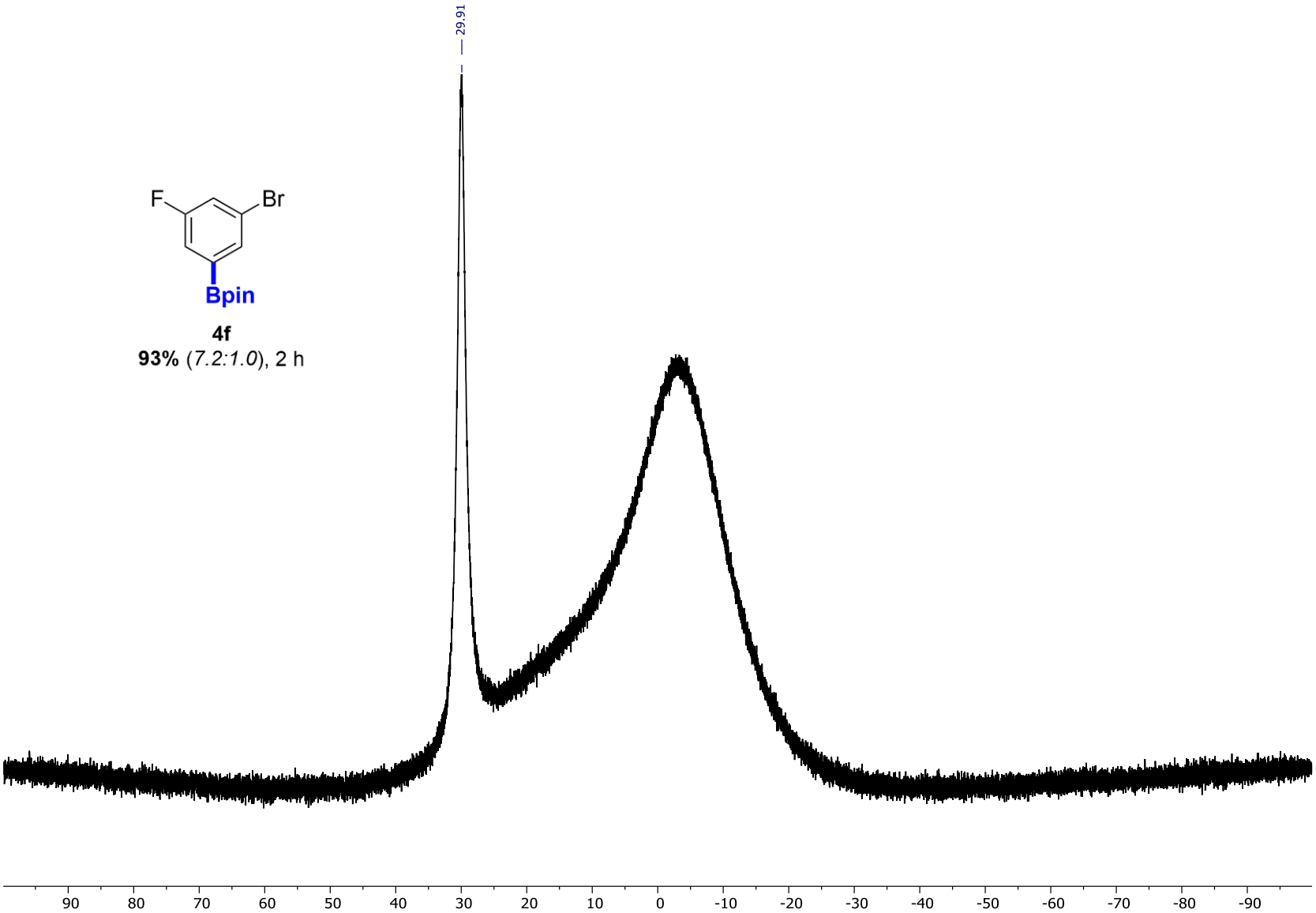

^{11}B NMR of **4f** (160 MHz, $CDCl_3$)

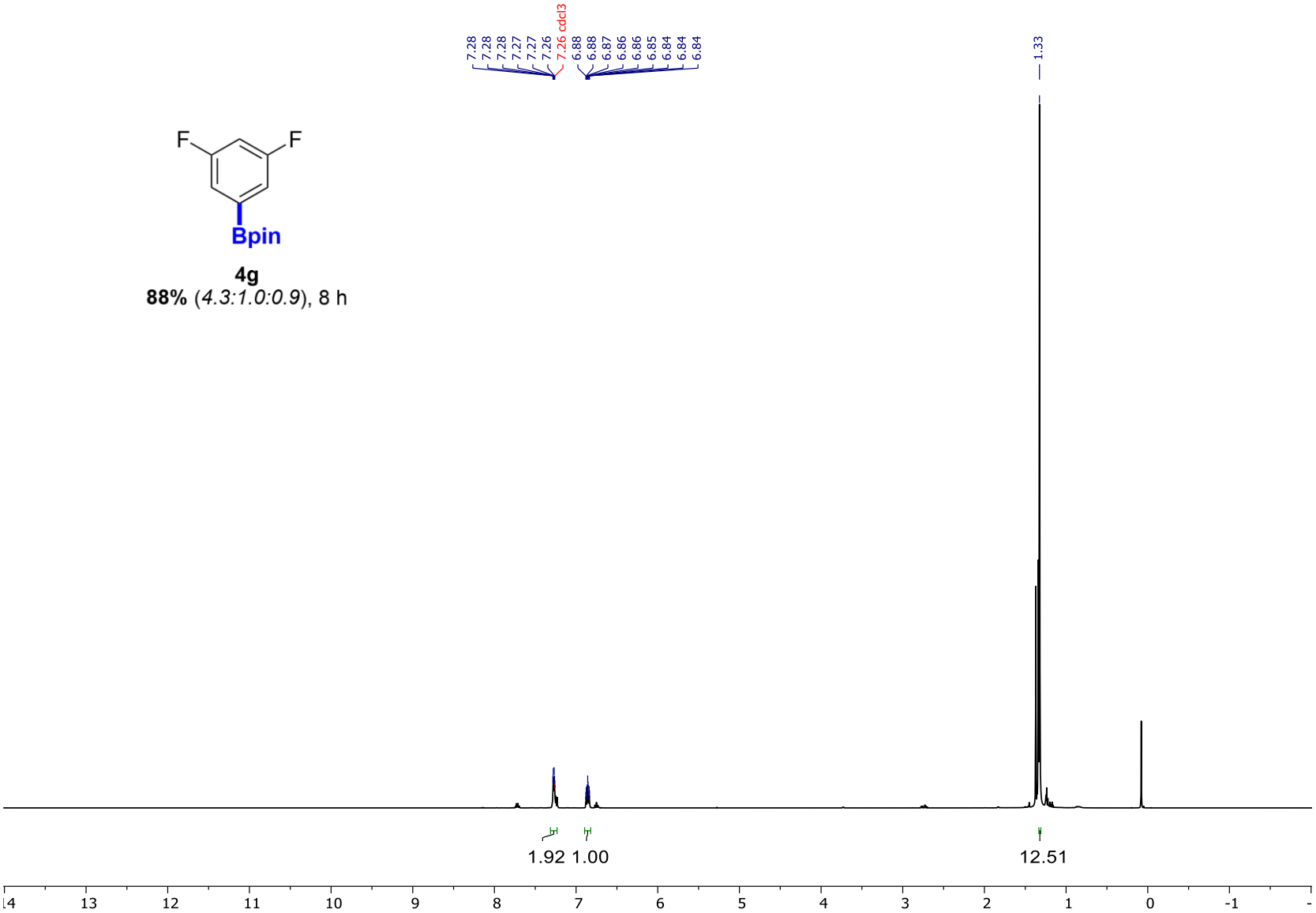

^{1}H NMR of **4g** (500 MHz, $CDCl_3$)

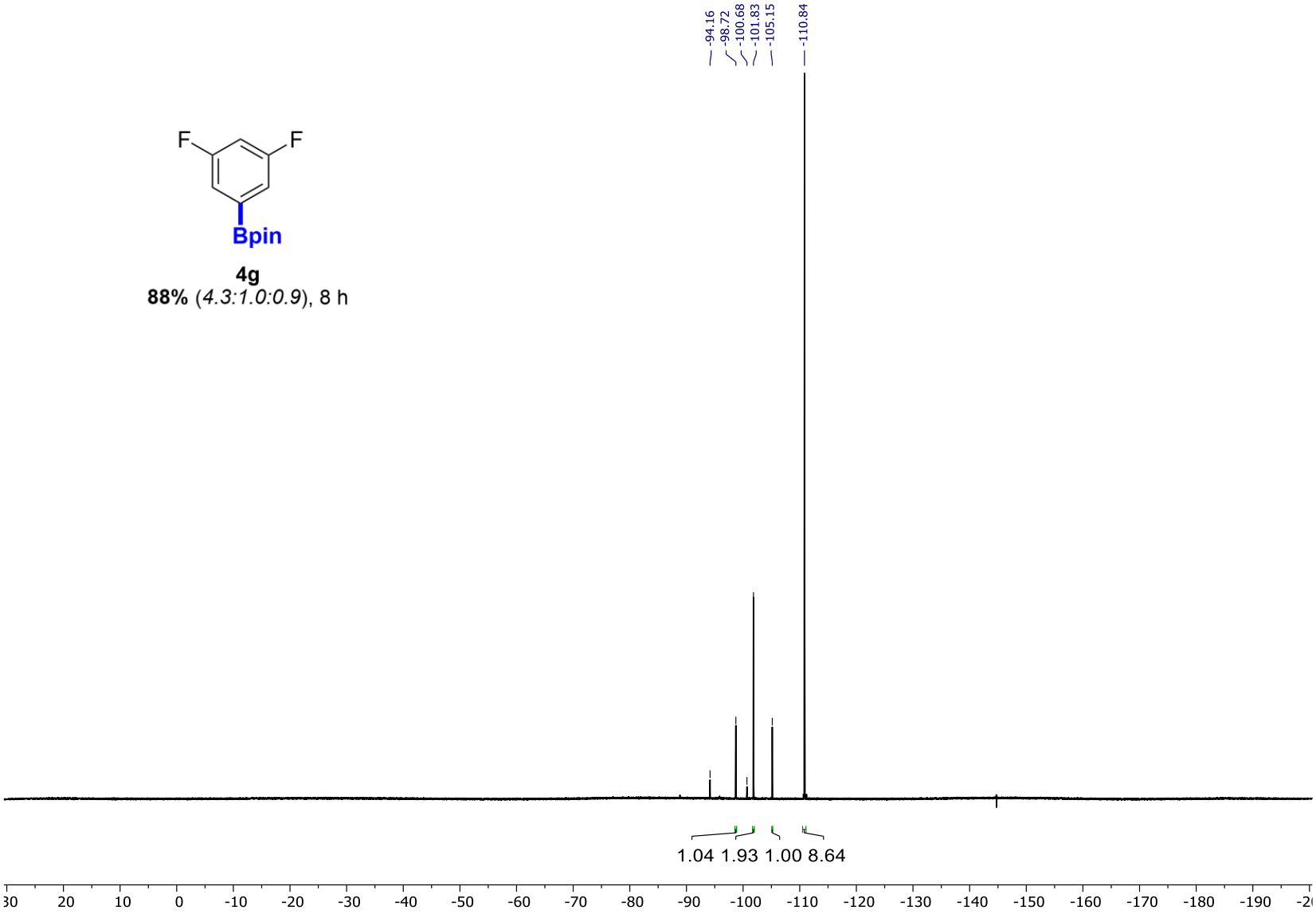

^{19}F NMR of **4g** (470 MHz, $CDCl_3$)

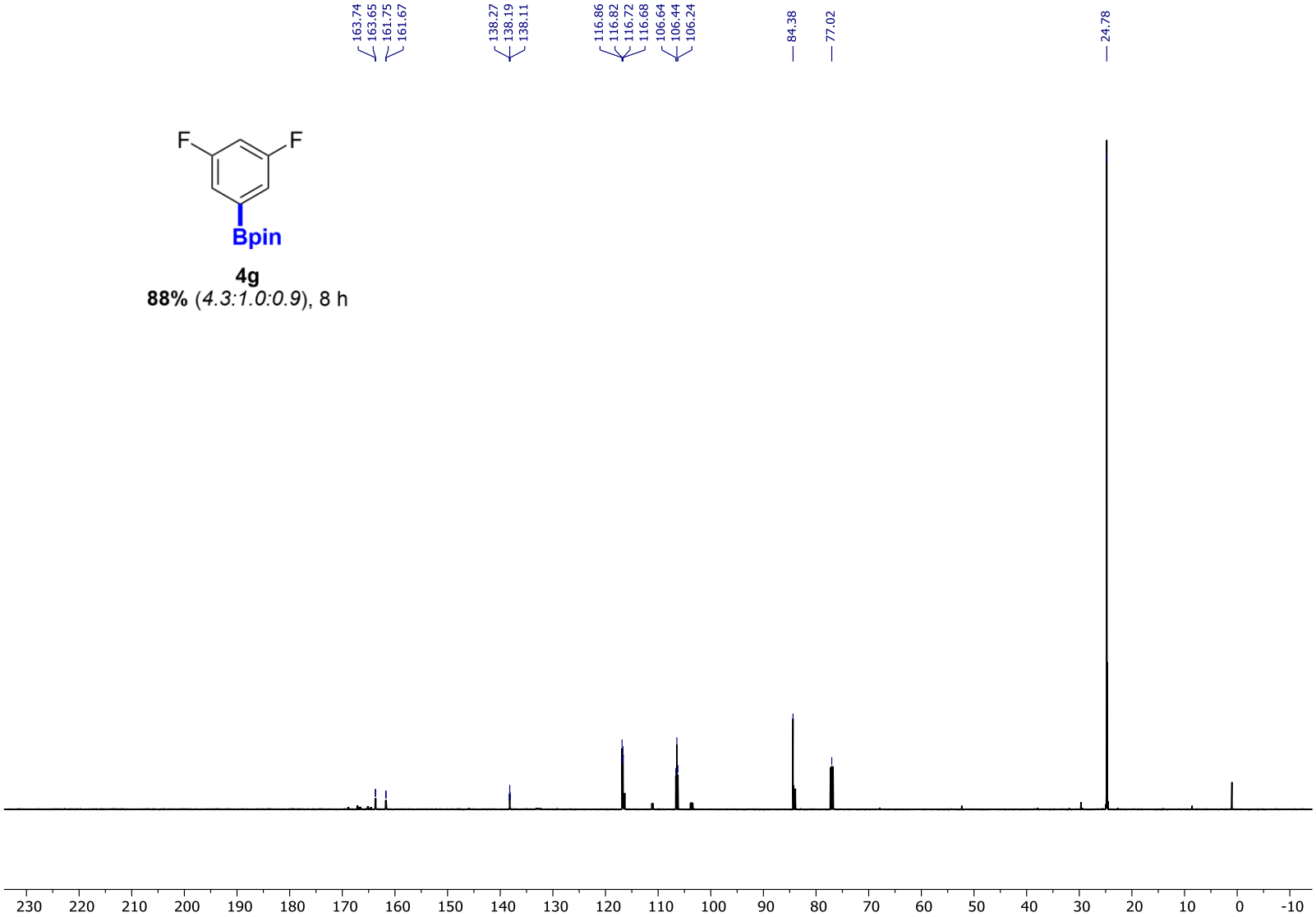

^{13}C NMR of **4g** (126 MHz, $CDCl_3$)

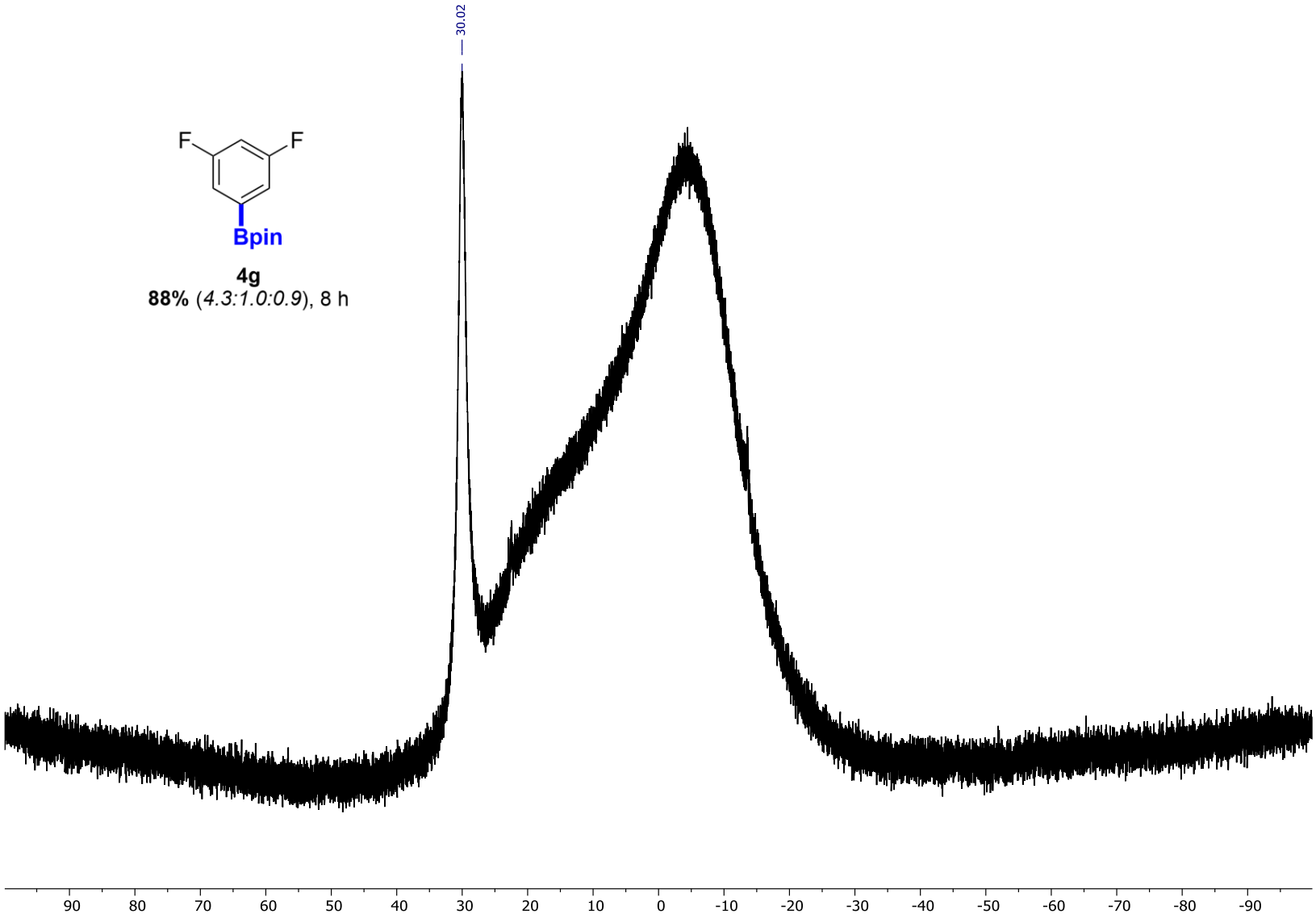

^{11}B NMR of **4g** (160 MHz, $CDCl_3$)

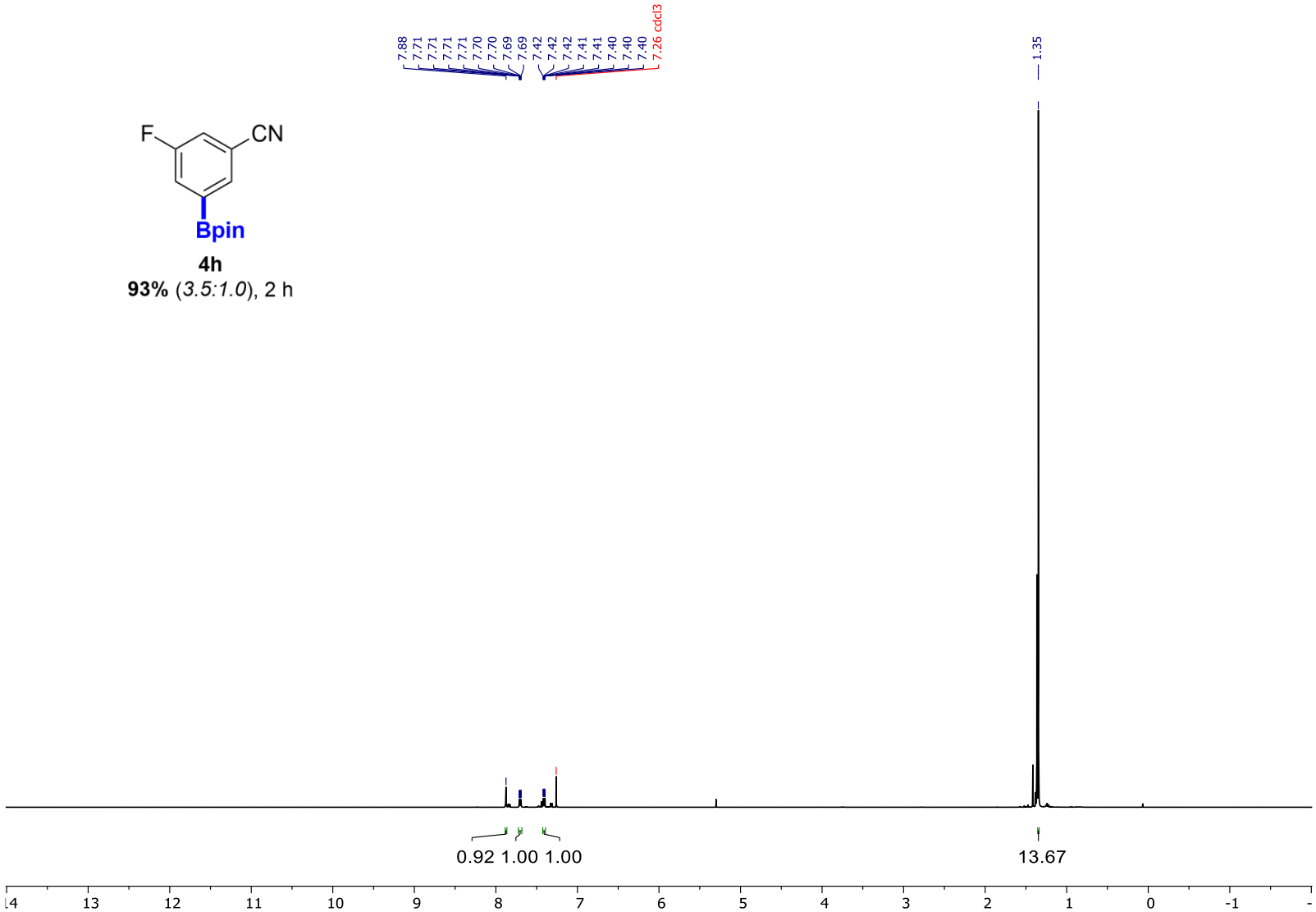

^{1}H NMR of **4h** (500 MHz, $CDCl_3$)

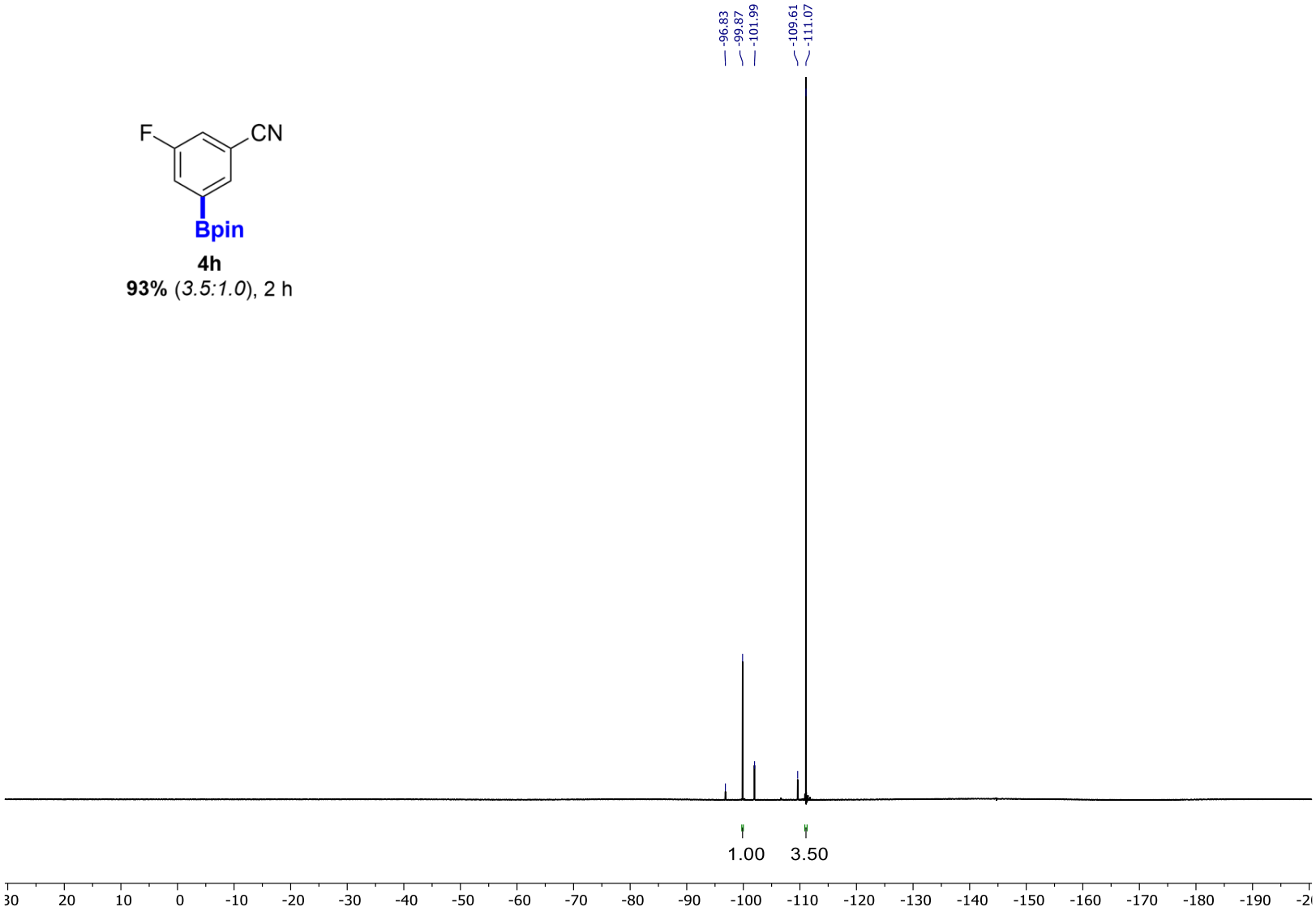

^{19}F NMR of **4h** (470 MHz, $CDCl_3$)

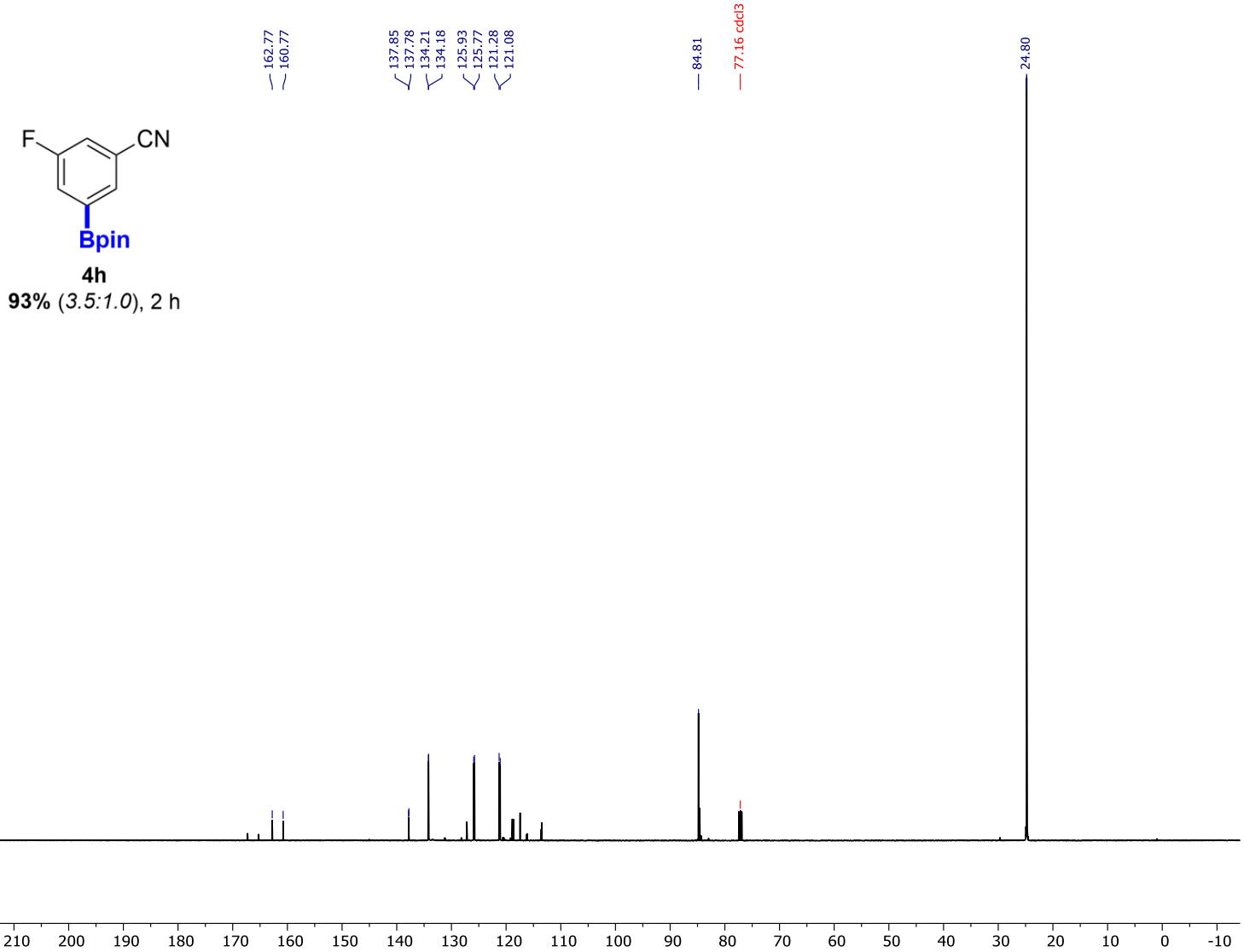

^{13}C NMR of **4h** (126 MHz, $CDCl_3$)

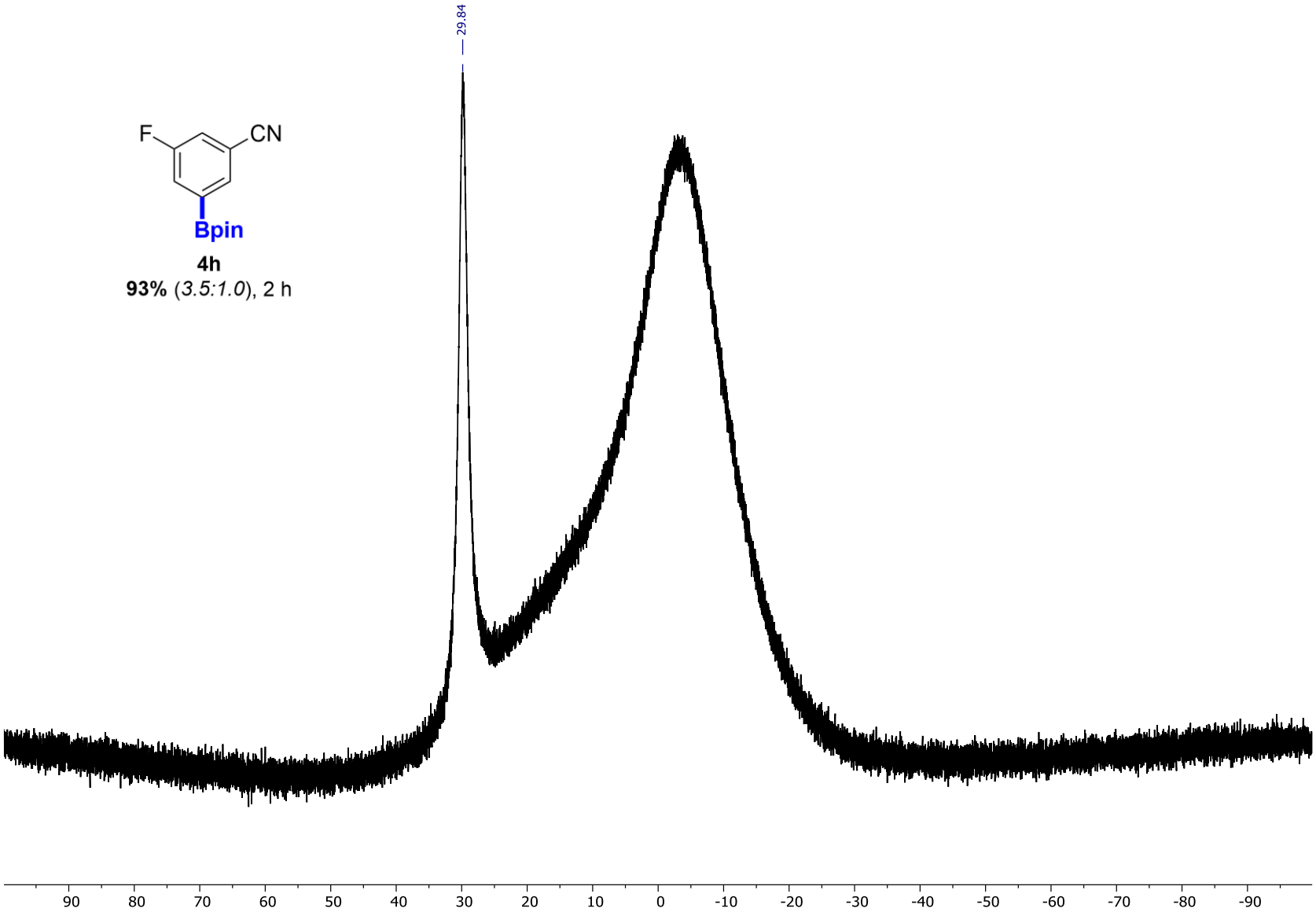

^{11}B NMR of **4h** (160 MHz, $CDCl_3$)

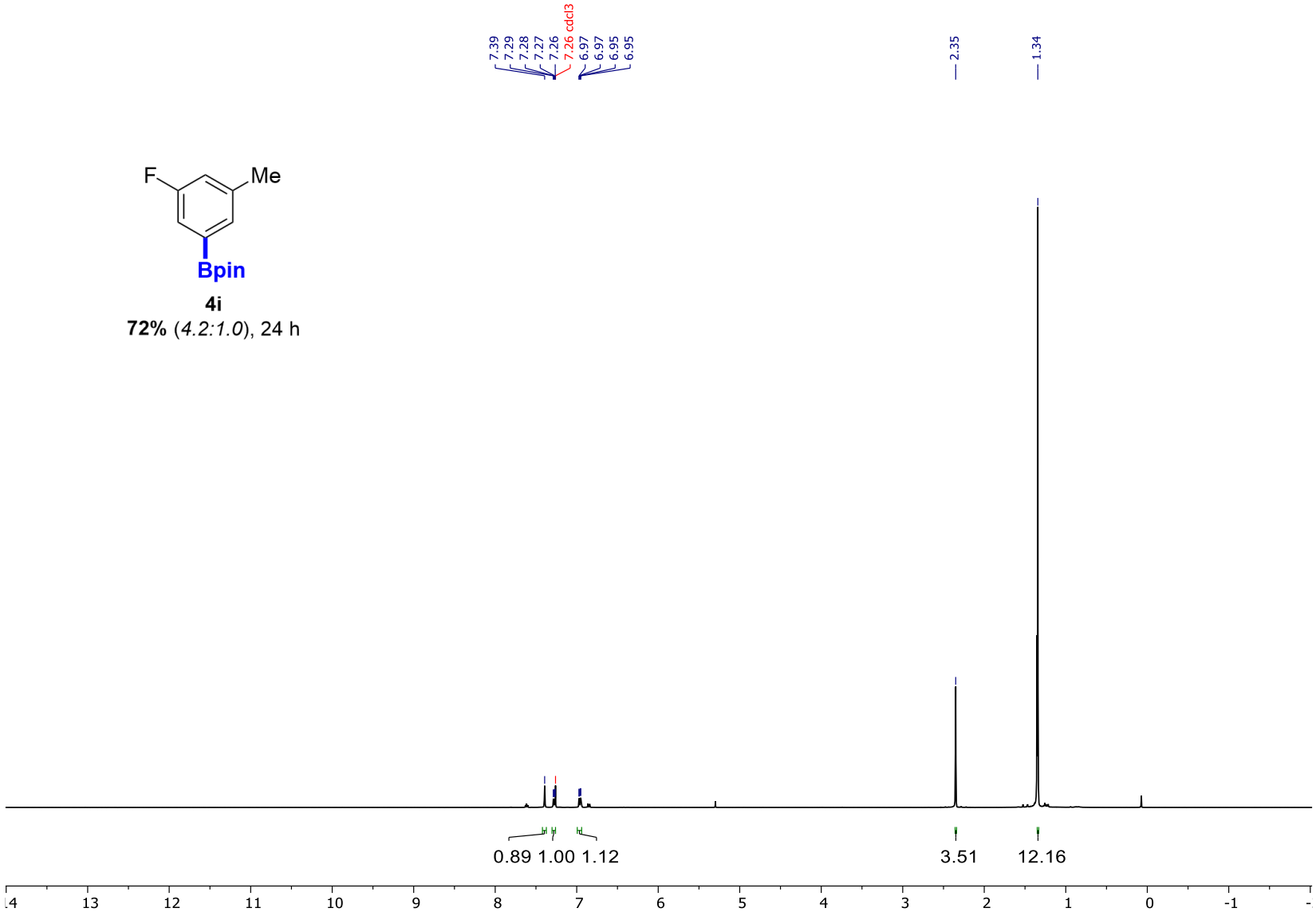

^{1}H NMR of **4i** (500 MHz, $CDCl_3$)

4i

72% (*4.2:1.0*), 24 h

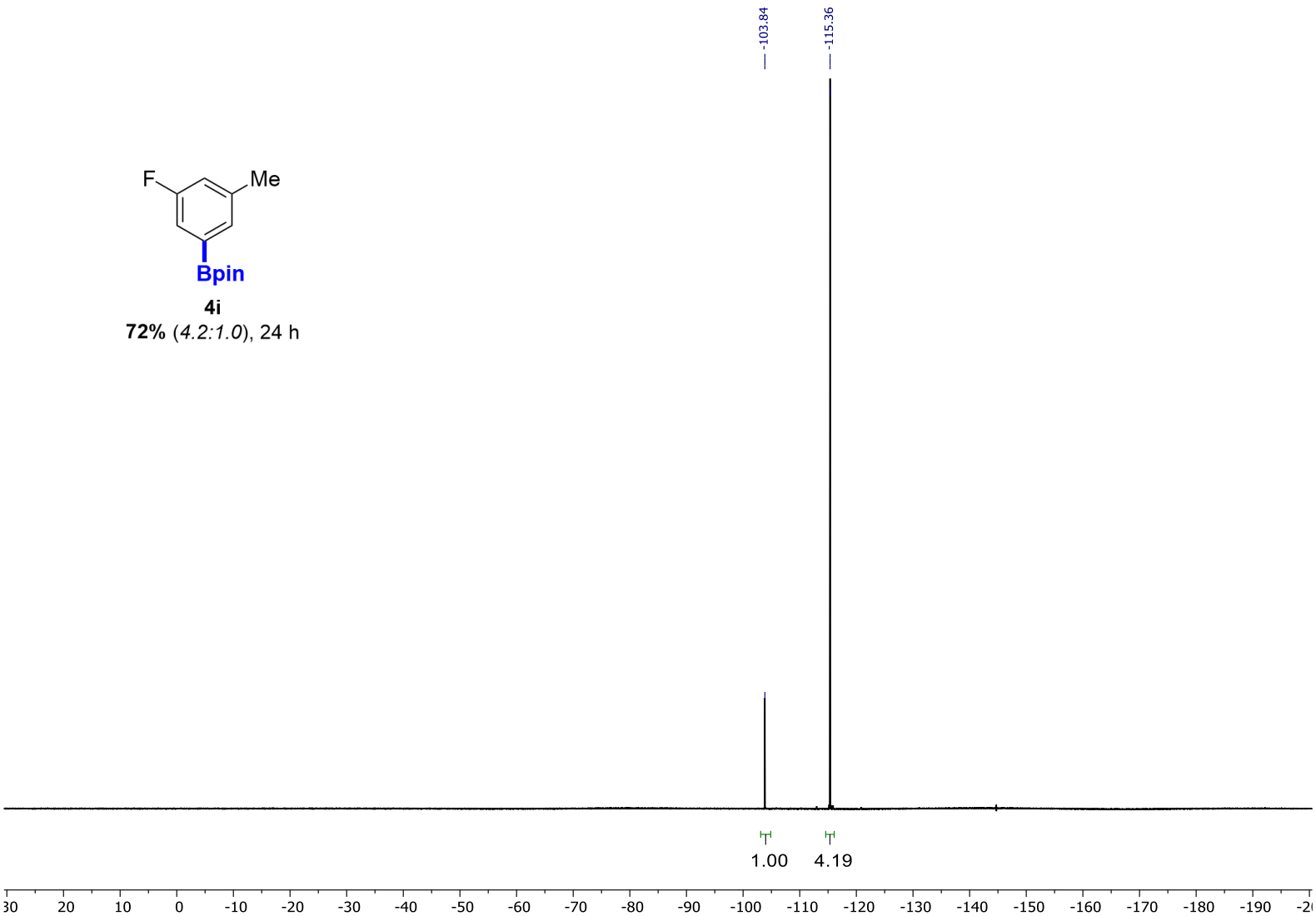

^{19}F NMR of **4i** (470 MHz, $CDCl_3$)

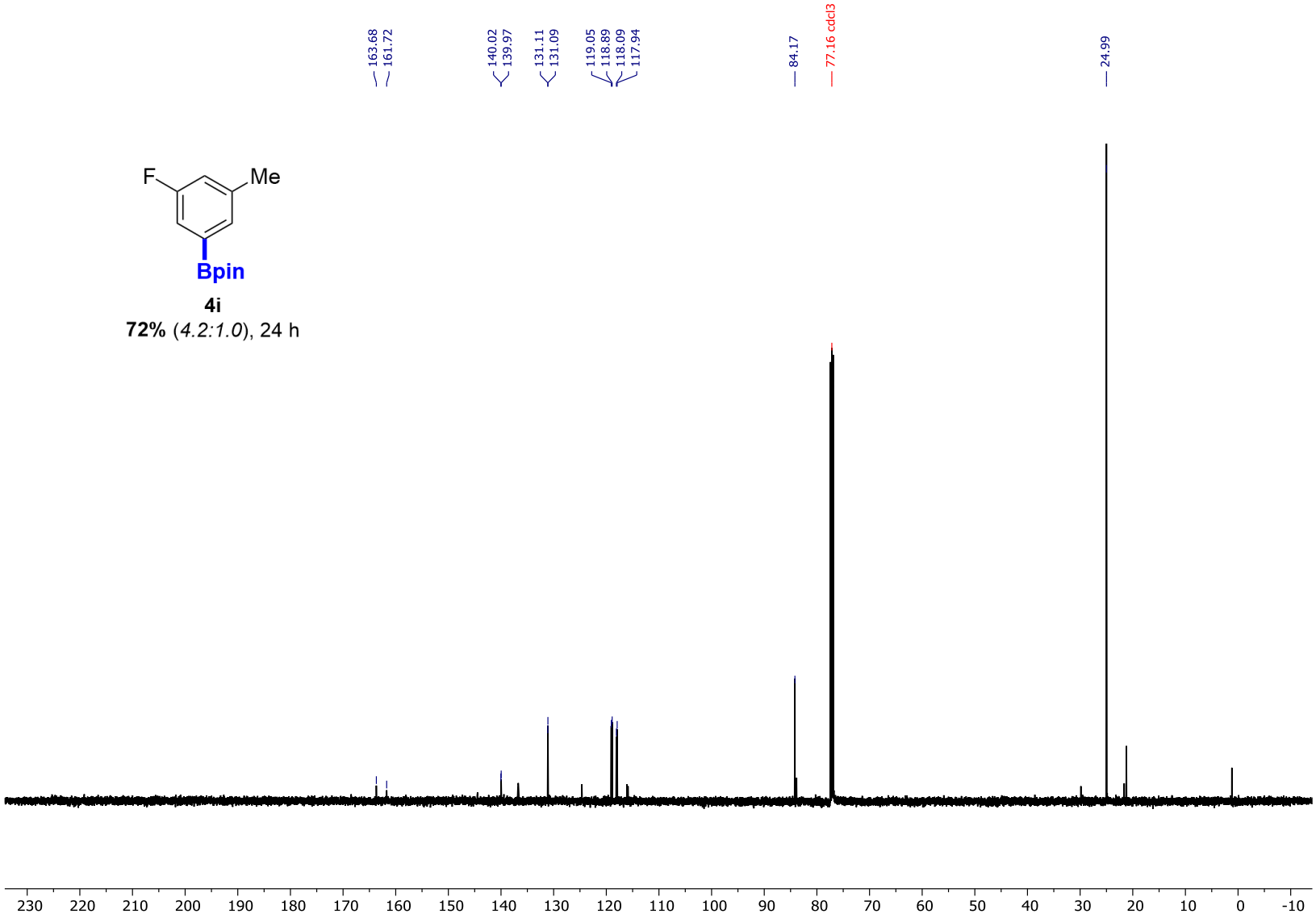

^{13}C NMR of **4i** (126 MHz, $CDCl_3$)

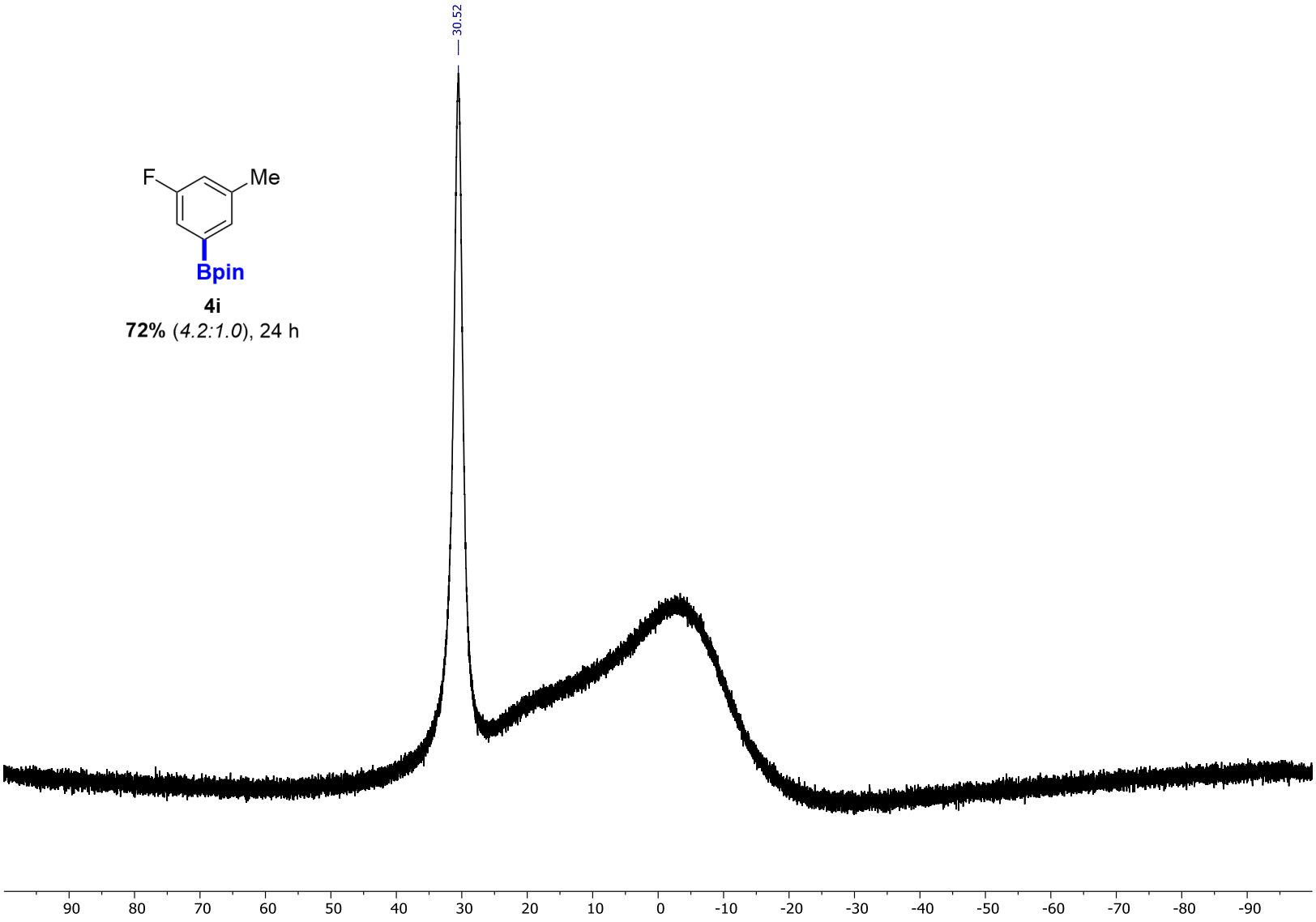

^{11}B NMR of **4i** (160 MHz, $CDCl_3$)

4j

80% (*5.8:1.0*), 24 h

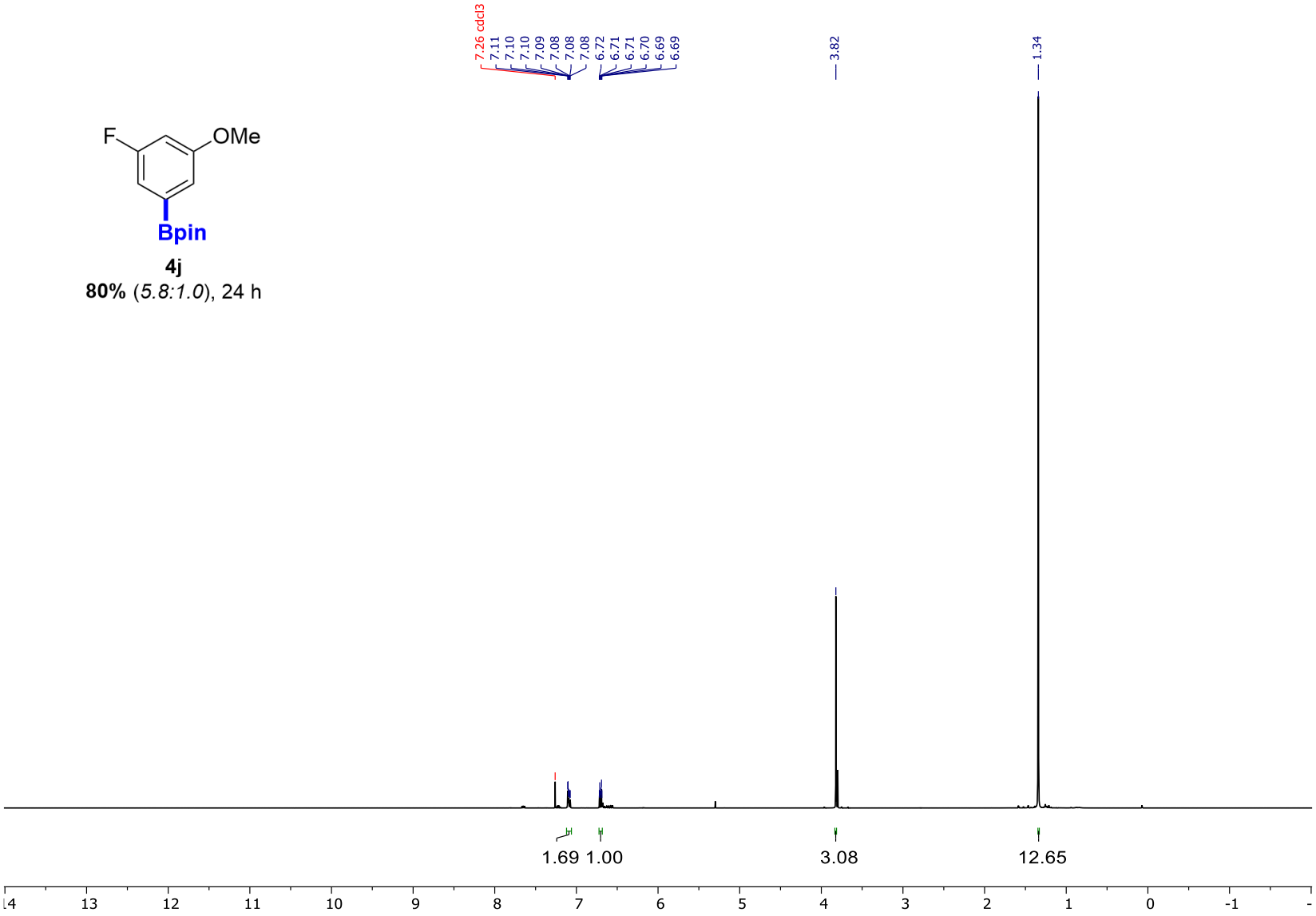

^{1}H NMR of **4j** (500 MHz, $CDCl_3$)

4j
80% (*5.8:1.0*), 24 h

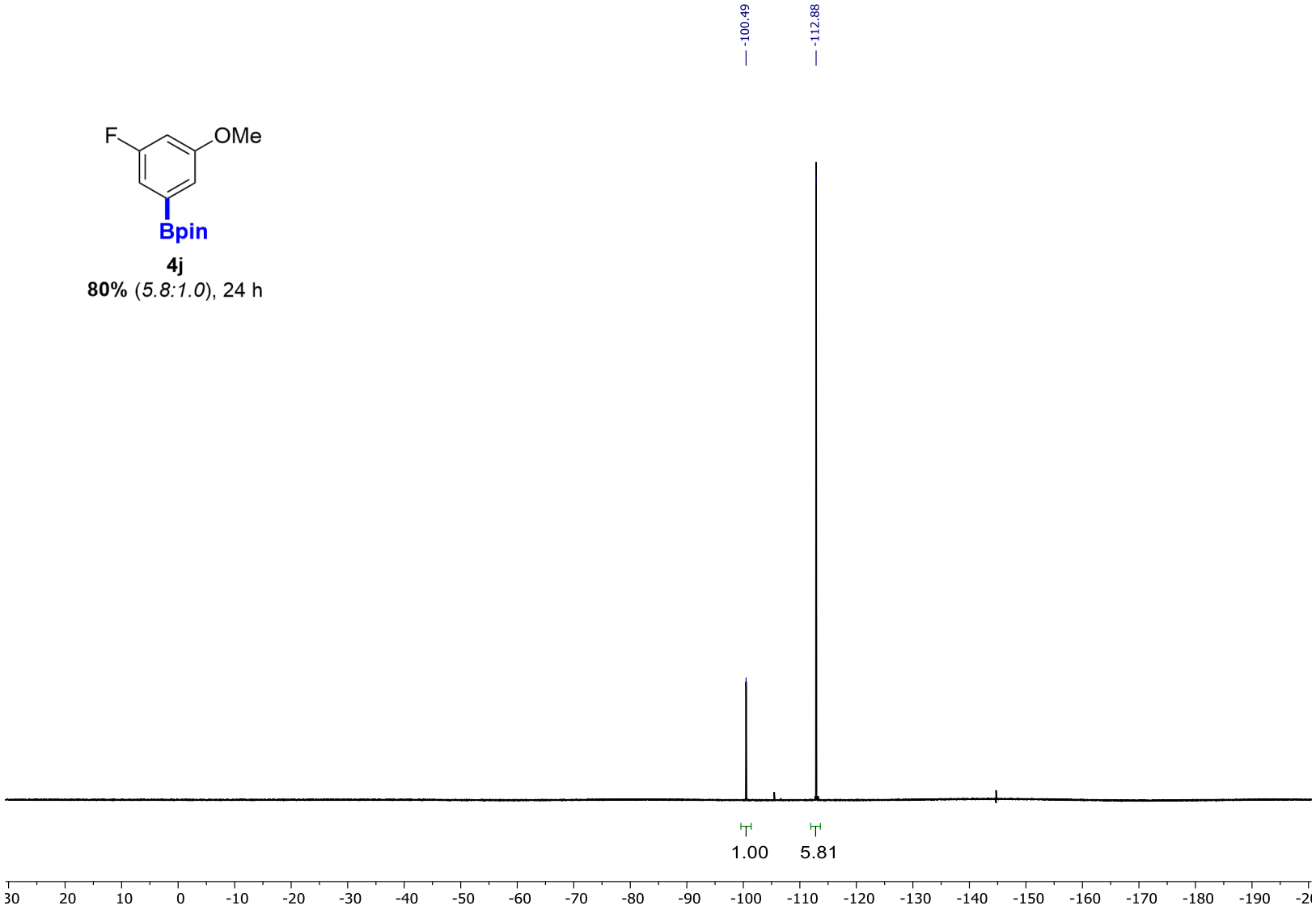

^{19}F NMR of **4j** (470 MHz, $CDCl_3$)

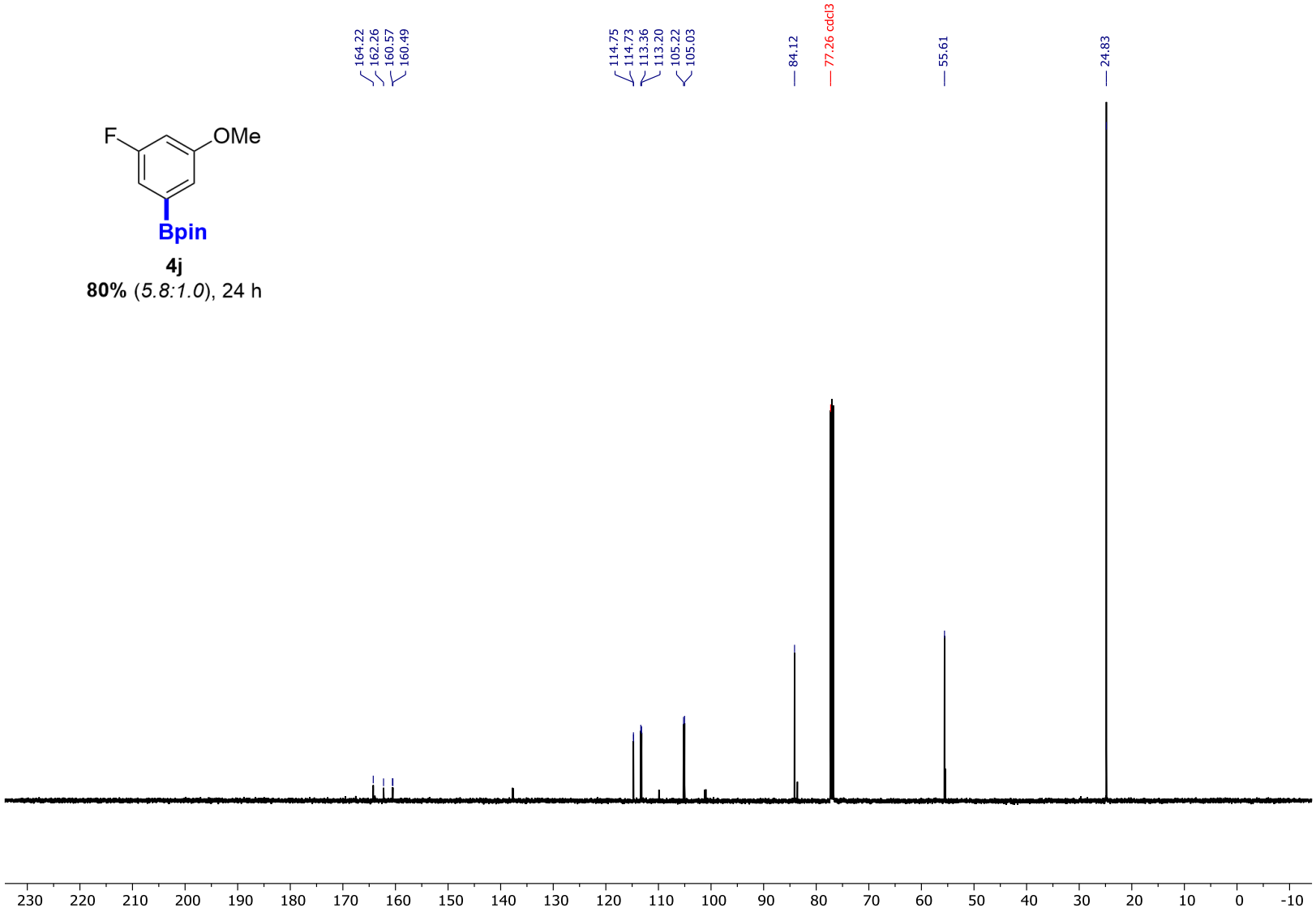

^{13}C NMR of **4j** (126 MHz, $CDCl_3$)

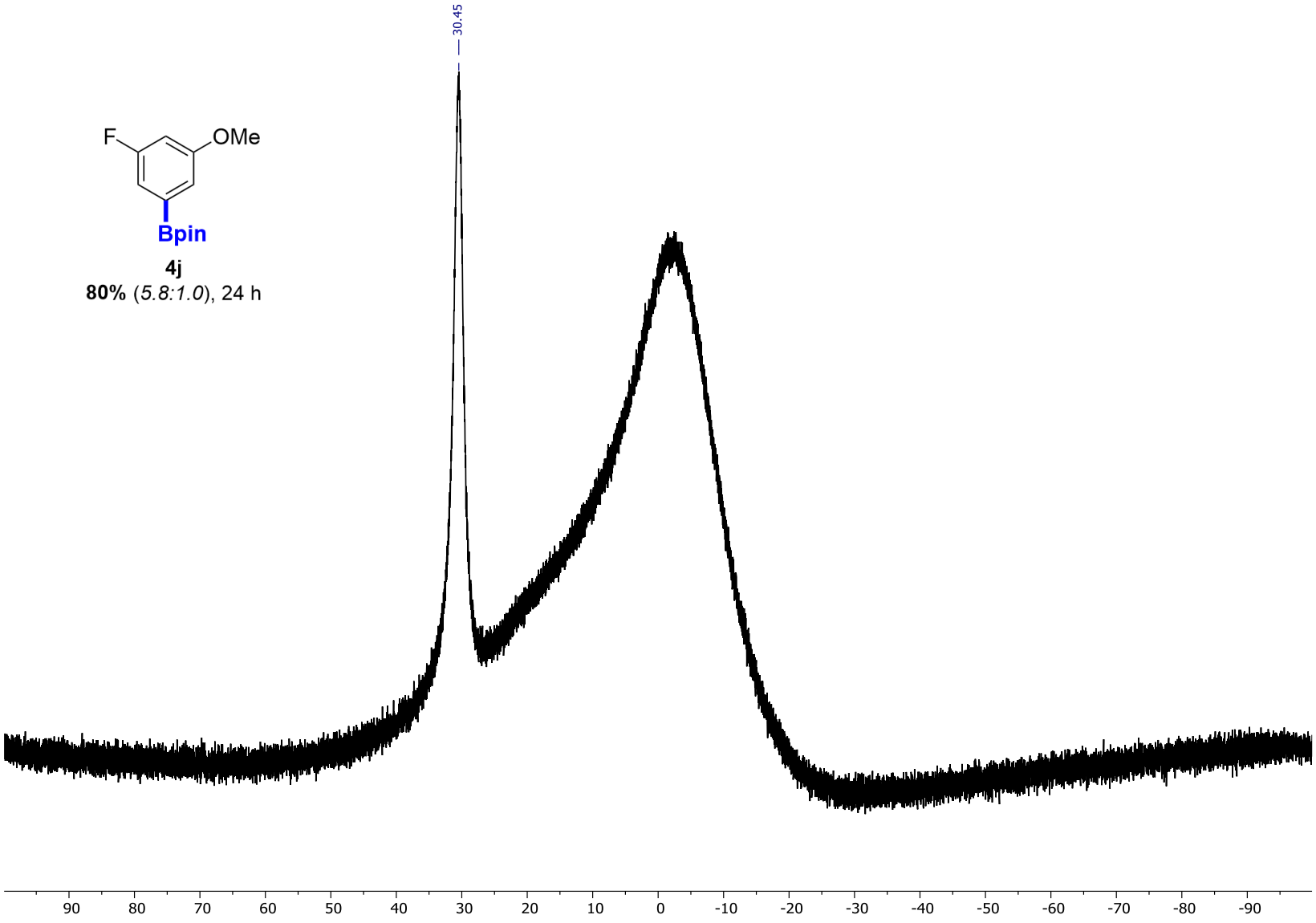

^{11}B NMR of **4j** (160 MHz, $CDCl_3$)

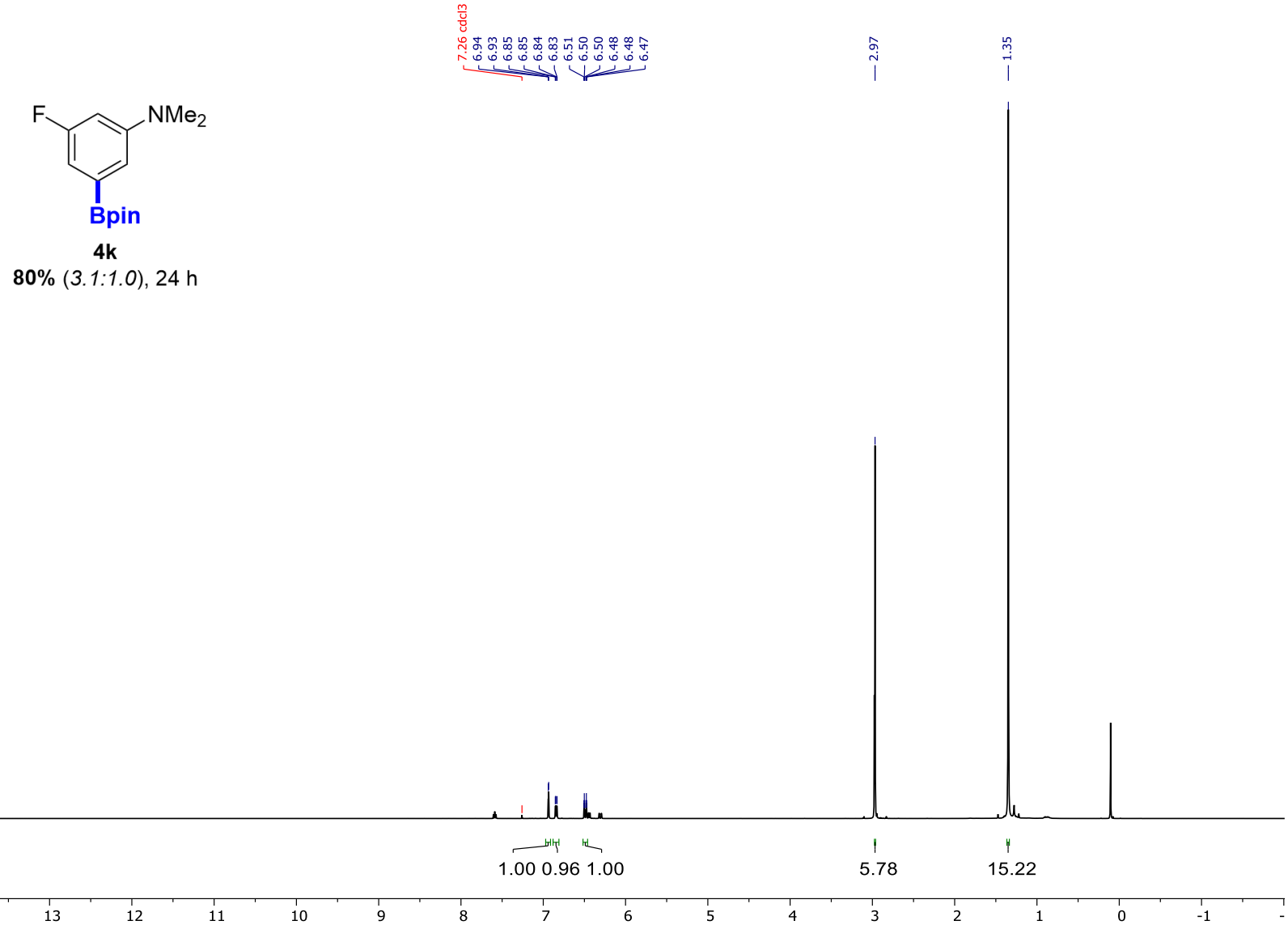

^{1}H NMR of **4k** (500 MHz, $CDCl_3$)

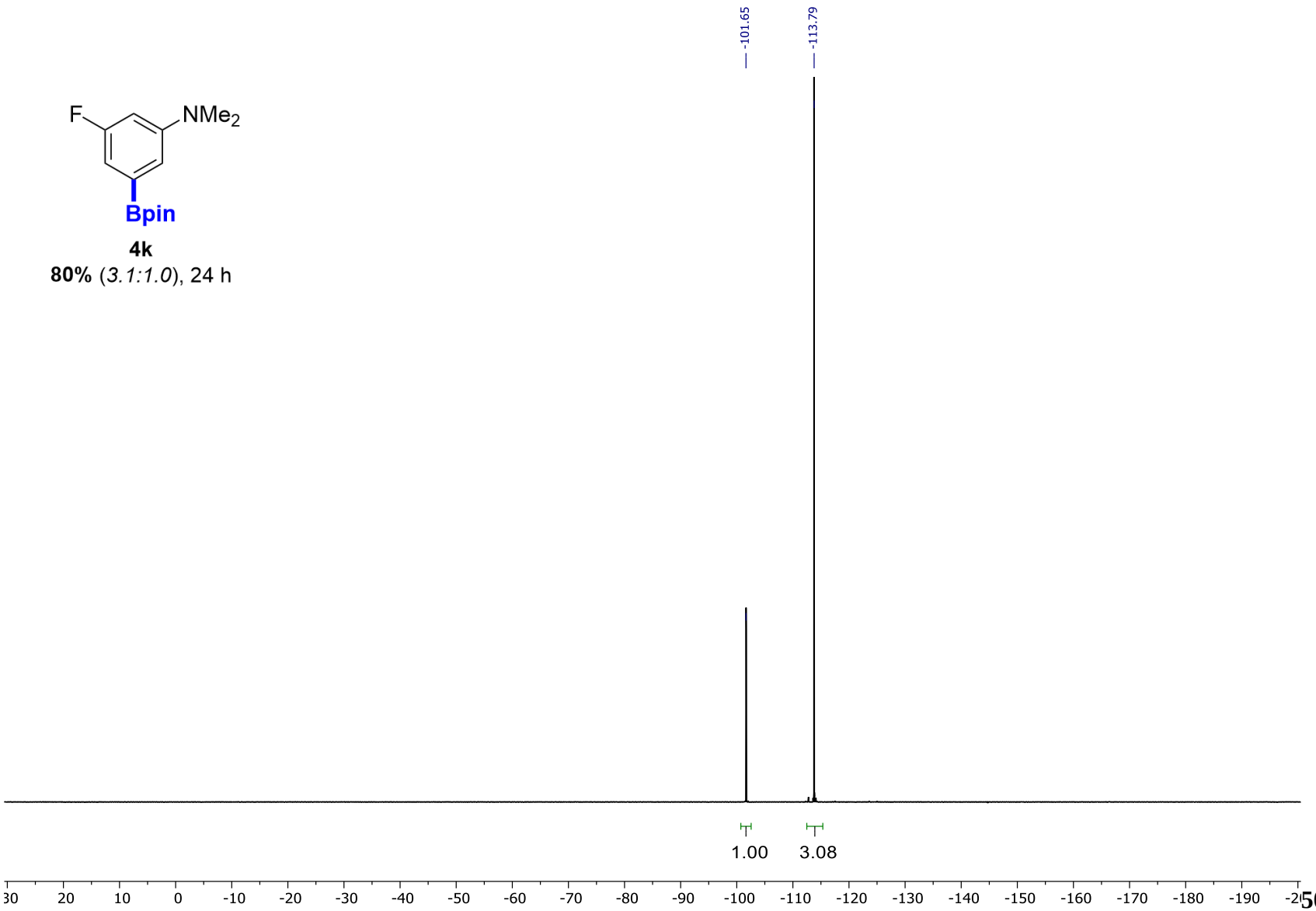

50.

^{19}F NMR of **4k** (470 MHz, $CDCl_3$)

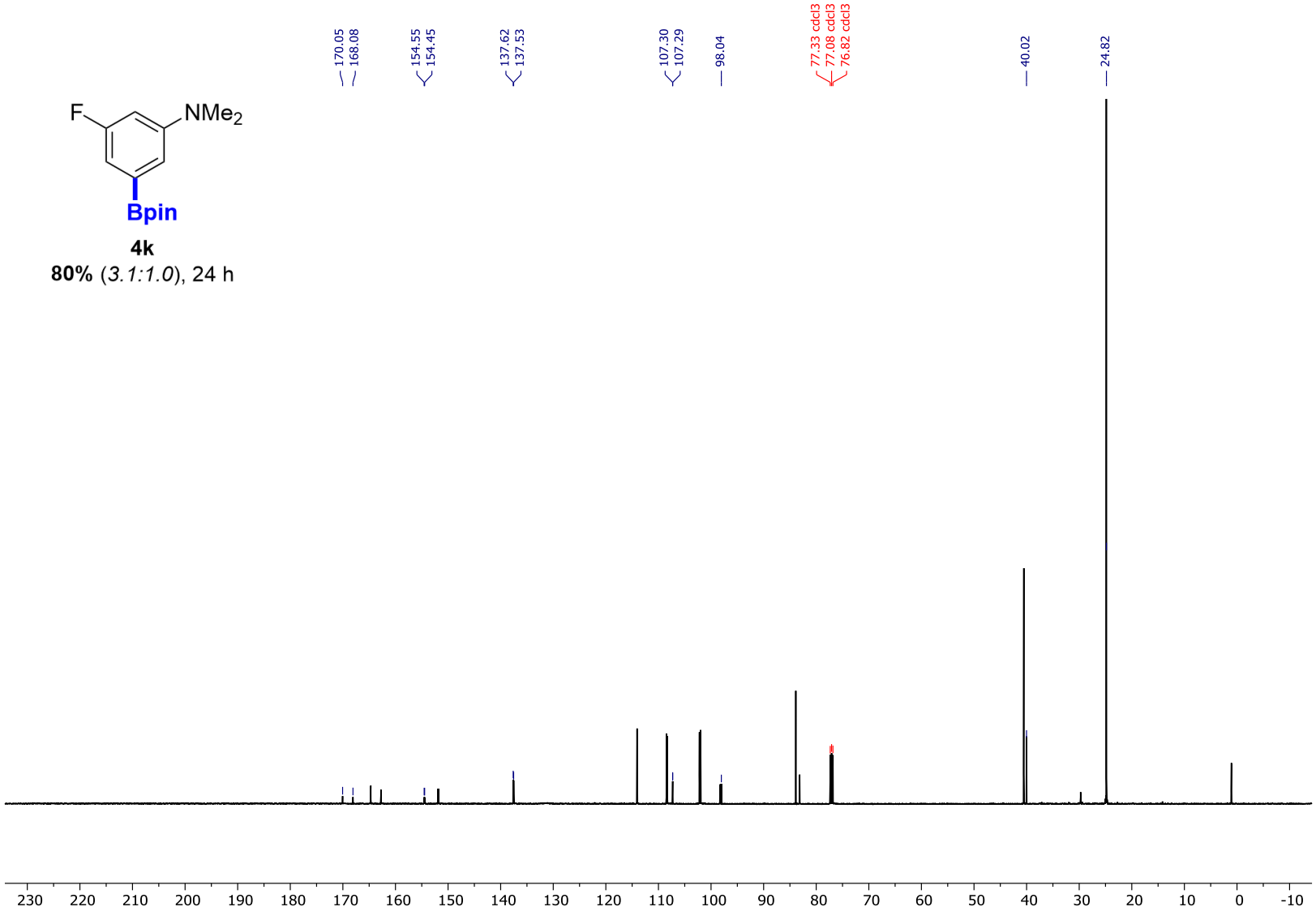

^{13}C NMR of **4k** (126 MHz, $CDCl_3$)

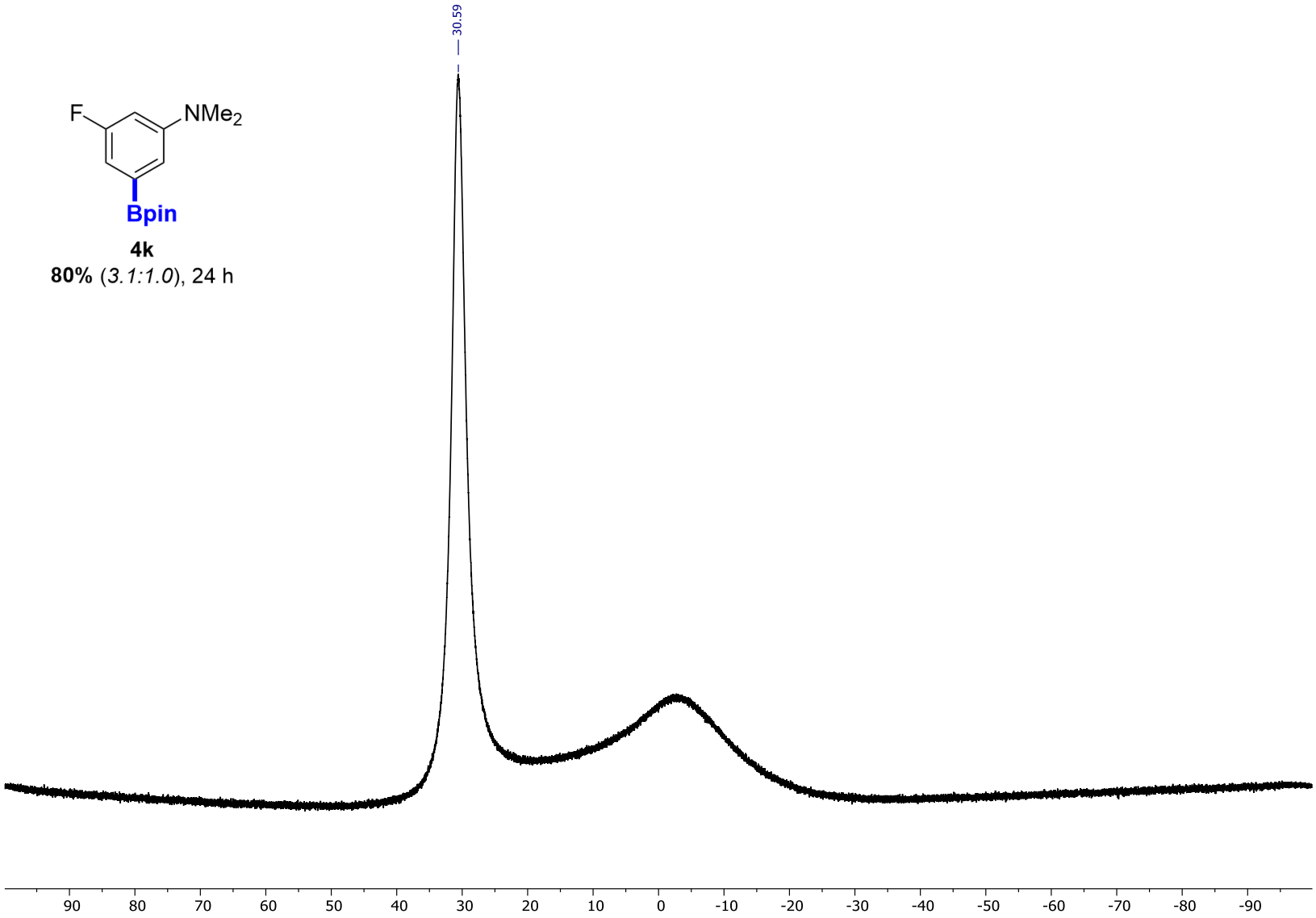

^{11}B NMR of **4k** (160 MHz, $CDCl_3$)

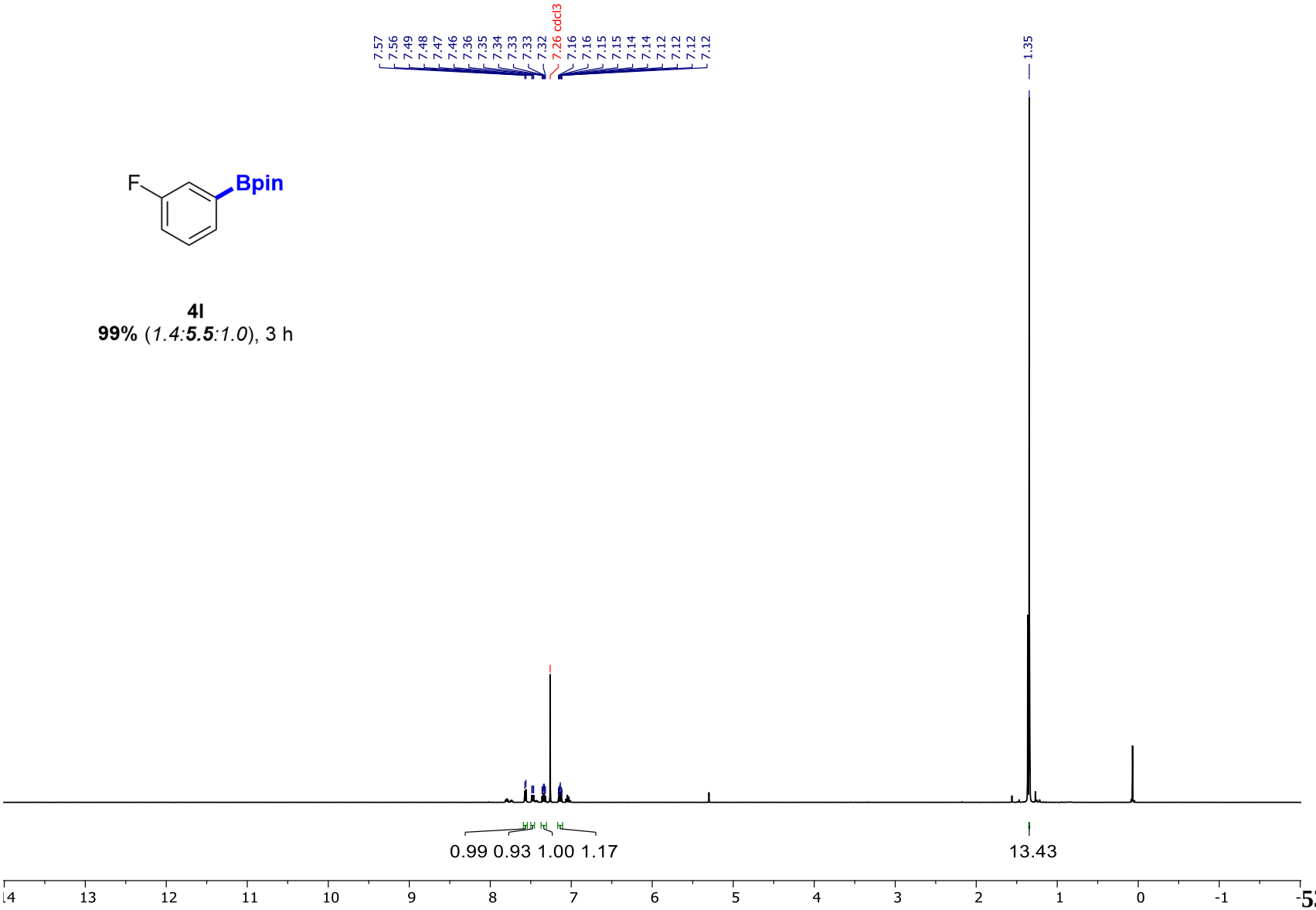

-53.

^{1}H NMR of **4l** (500 MHz, $CDCl_3$)

4l
99% (*1.4*:***5.5***:*1.0*), 3 h

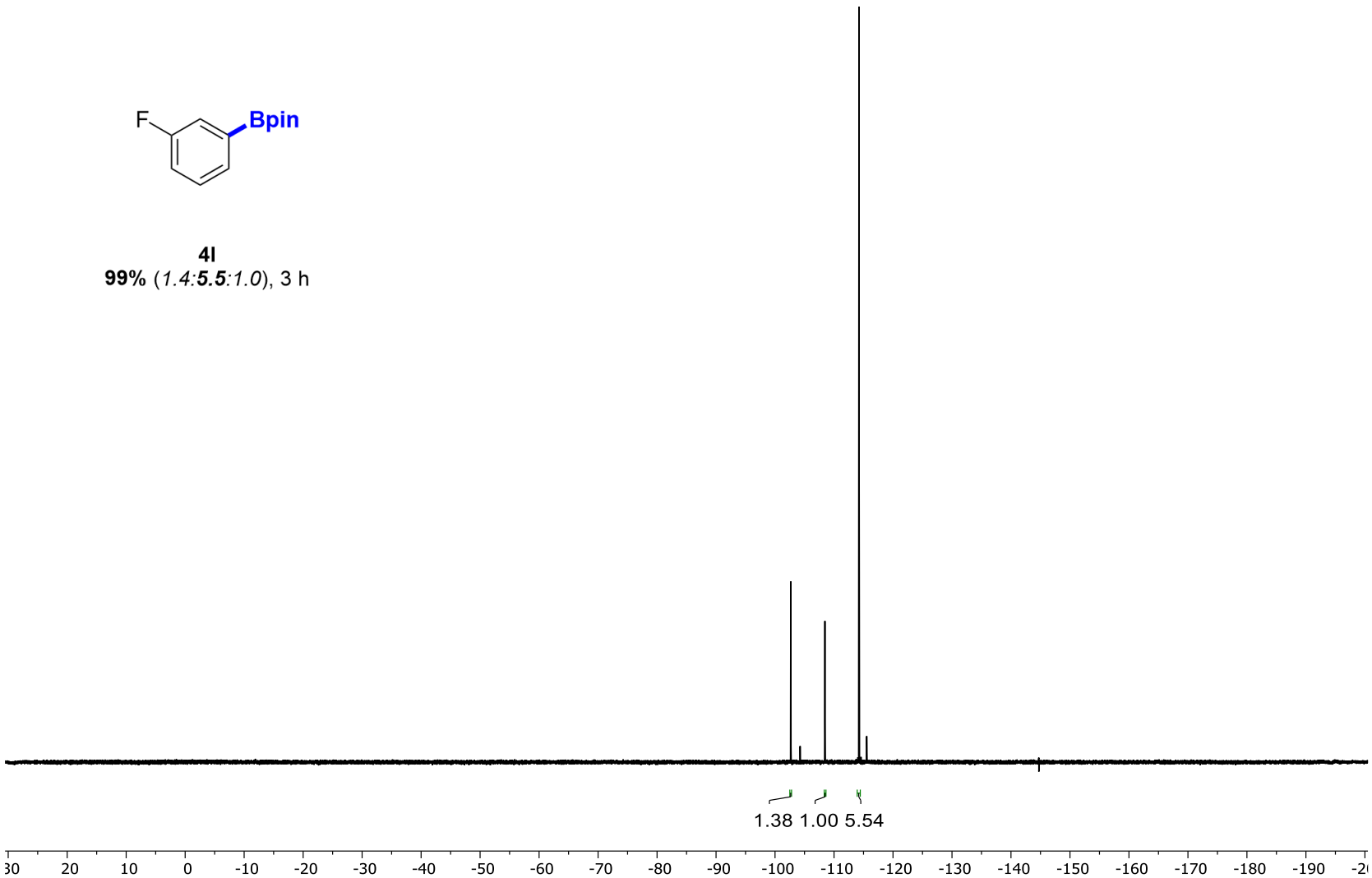

^{19}F NMR of **4l** (470 MHz, $CDCl_3$)

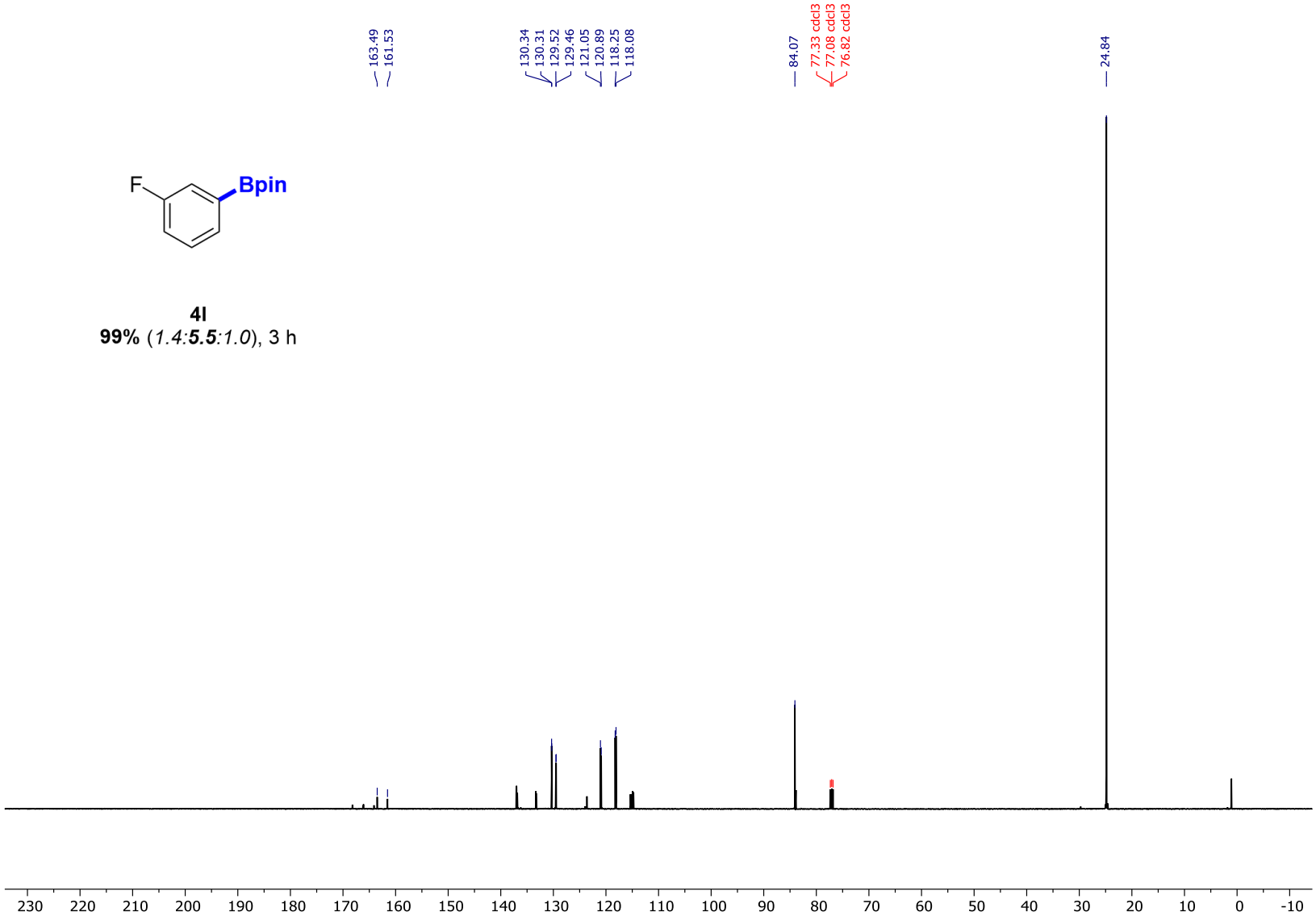

^{13}C NMR of **4l** (126 MHz, $CDCl_3$)

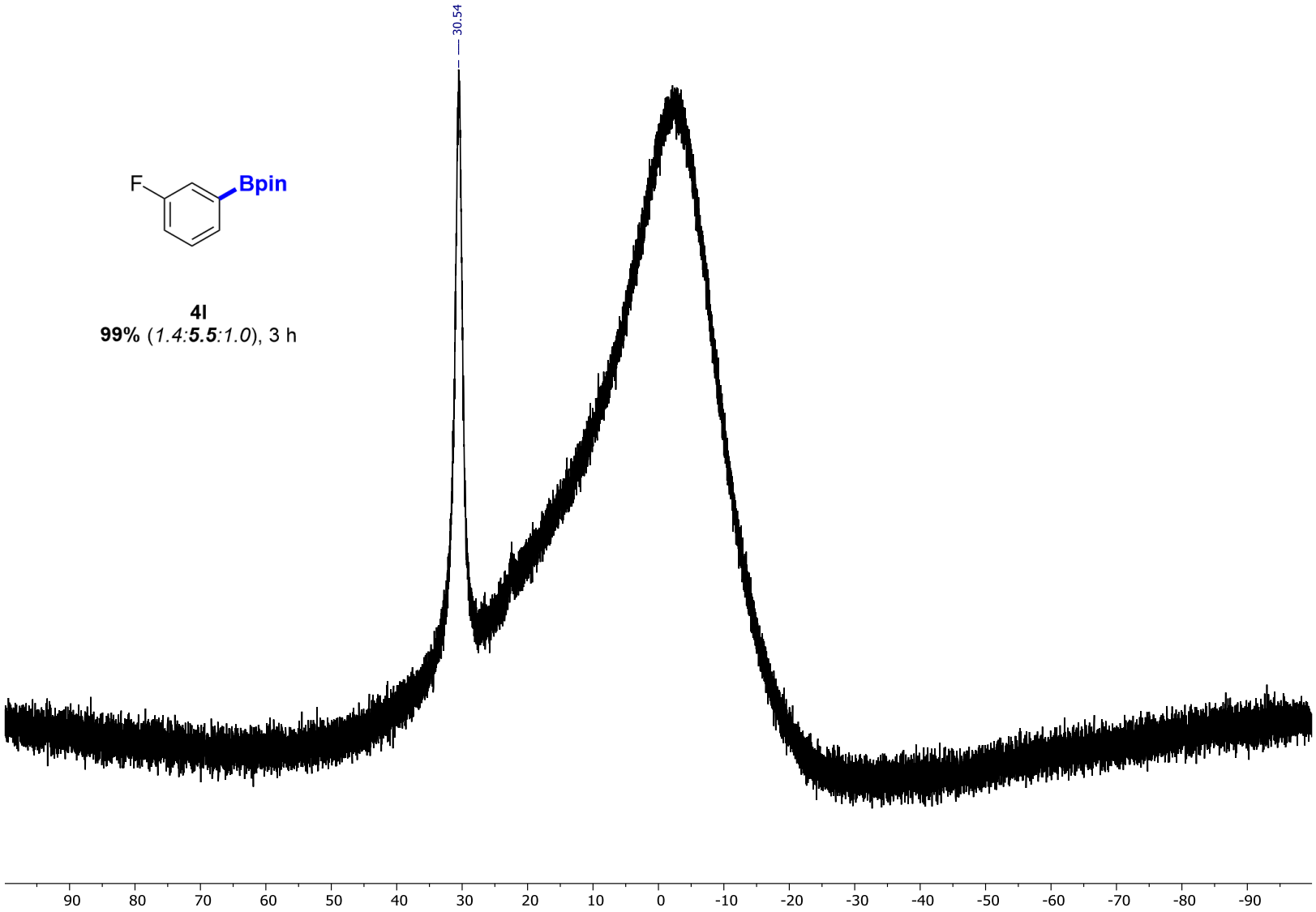

^{11}B NMR of **4l** (160 MHz, $CDCl_3$)

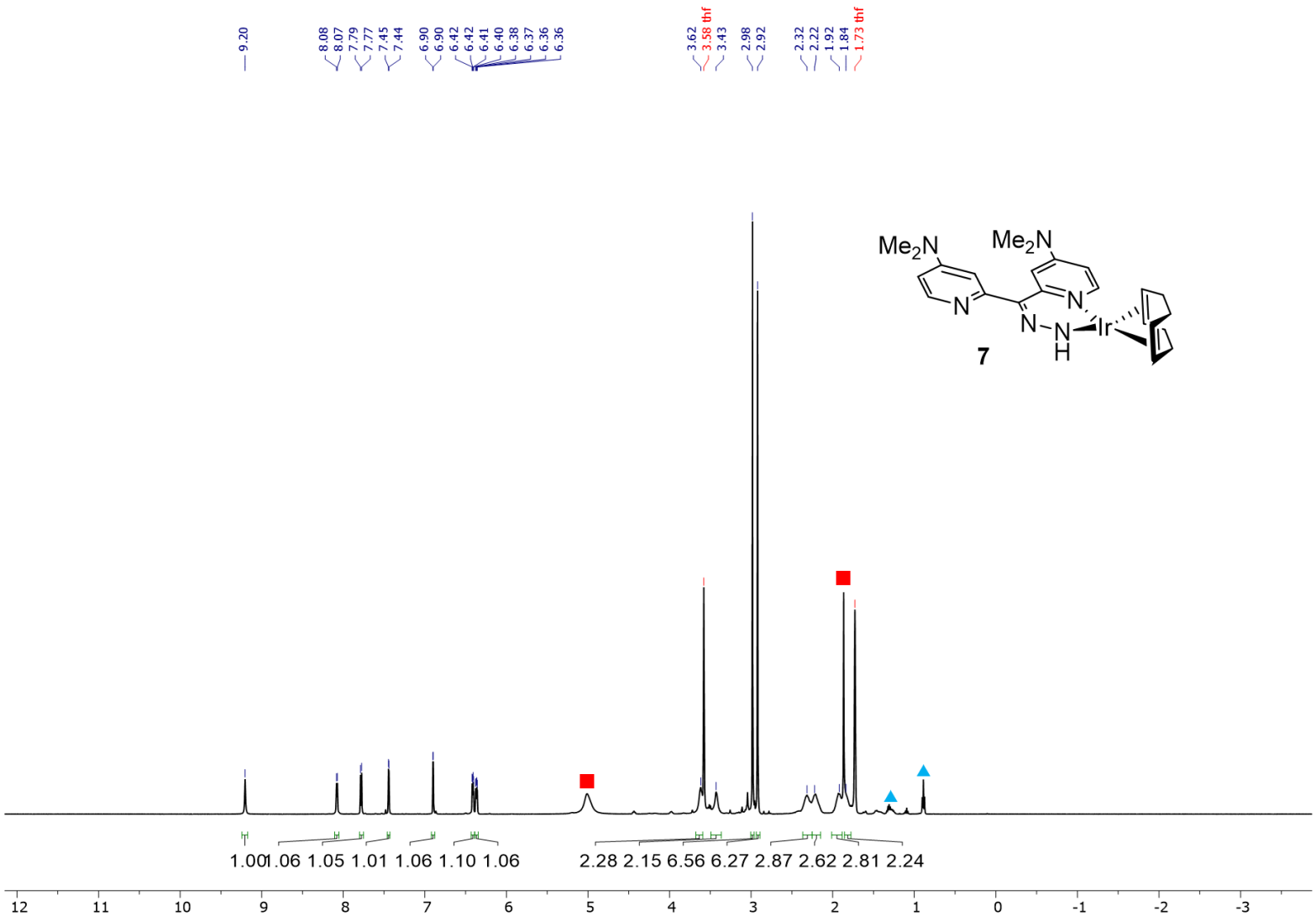

^{1}H NMR of **7** (500 MHz, THF-d_8). Blue triangles (▲) represent impurities from NMR solvent. Red squares (■) represent impurities found after isolation.

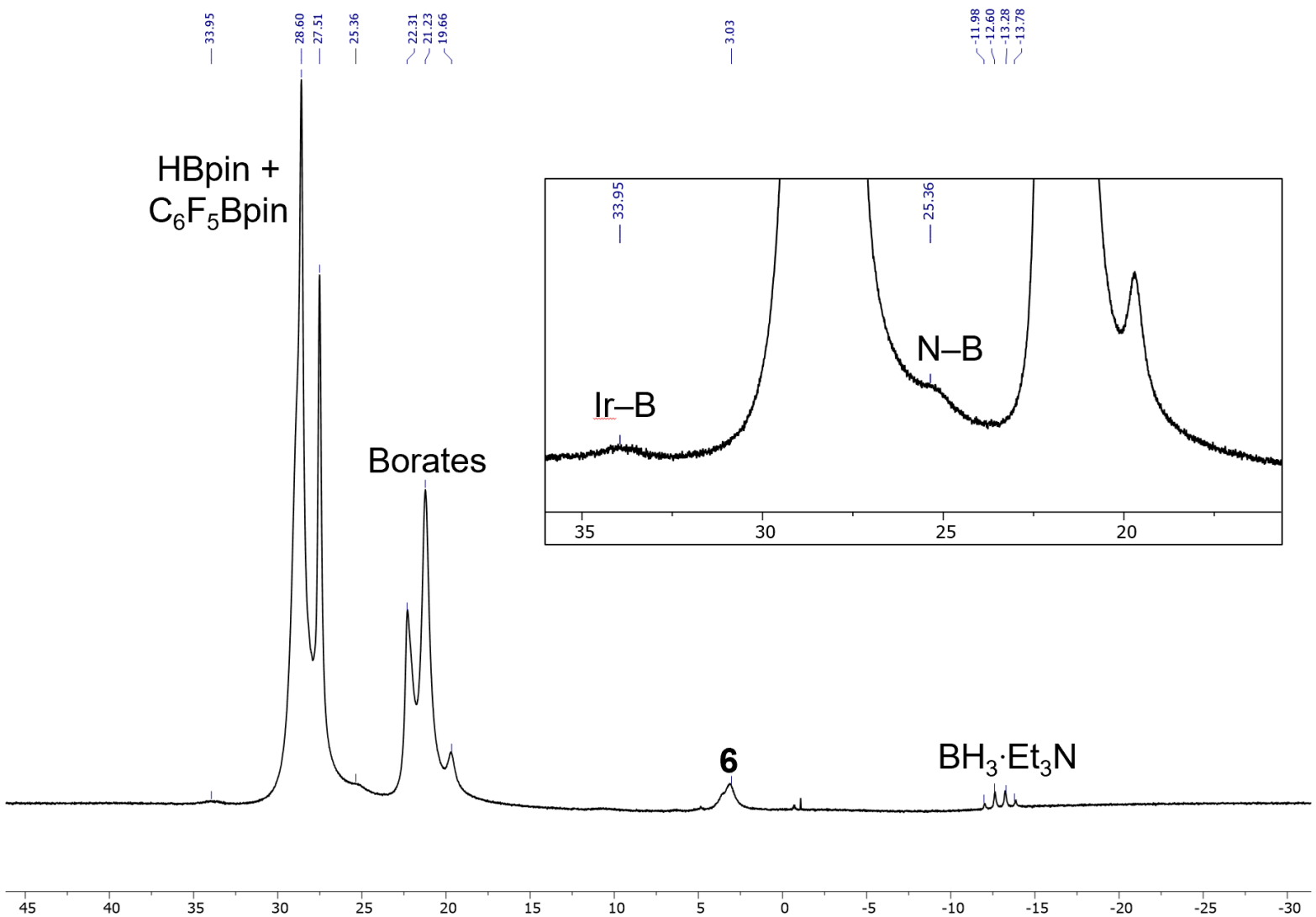

Annotated ^{11}B NMR (500 MHz, THF/THF-d_8) of NMR tube borylation of pentafluorobenzene.

REFERENCES

(1) Clot, E.; Mégret, C.; Eisenstein, O.; Perutz, R. N. Exceptional Sensitivity of Metal-Aryl Bond Energies to Ortho-Fluorine Substituents: Influence of the Metal, the Coordination Sphere, and the Spectator Ligands on M-C/H-C Bond Energy Correlations. *J. Am. Chem. Soc.* **2009**, *131* (22), 7817–7827.

(2) Evans, M. E.; Burke, C. L.; Yaibuathes, S.; Clot, E.; Eisenstein, O.; Jones, W. D. Energetics of C-H Bond Activation of Fluorinated Aromatic Hydrocarbons Using a [Tp'Rh(CNneopentyl)] Complex. *J. Am. Chem. Soc.* **2009**, *131* (37), 13464–13473.

(3) Pabst, T. P.; Obligacion, J. V.; Rochette, É.; Pappas, I.; Chirik, P. J. Cobalt-Catalyzed Borylation of Fluorinated Arenes: Thermodynamic Control of C(Sp2)-H Oxidative Addition Results in Ortho-to-Fluorine Selectivity. *J. Am. Chem. Soc.* **2019**, *141* (38), 15378–15389.

(4) Wang, G.; Liu, L.; Wang, H.; Ding, Y.-S.; Zhou, J.; Mao, S.; Li, P. N,B-Bidentate Boryl Ligand-Supported Iridium Catalyst for Efficient Functional-Group-Directed C-H Borylation. *J. Am. Chem. Soc.* **2017**, *139* (1), 91–94.

(5) Ros, A.; Fernández, R.; Lassaletta, J. M. Functional Group Directed C–H Borylation. *Chem. Soc. Rev.* **2014**, *43* (10), 3229–3243.

(6) Kallepalli, V. A.; Gore, K. A.; Shi, F.; Sanchez, L.; Chotana, G. A.; Miller, S. L.; Maleczka, R. E., Jr.; Smith, M. R., III. Harnessing C–H Borylation/Deborylation for Selective Deuteration, Synthesis of Boronate Esters, and Late Stage Functionalization. *J. Org. Chem.* **2015**, *80* (16), 8341–8353.

(7) Obligacion, J. V.; Bezdek, M. J.; Chirik, P. J. C(Sp2)-H Borylation of Fluorinated Arenes Using an Air-Stable Cobalt Precatalyst: Electronically Enhanced Site Selectivity Enables Synthetic Opportunities. *J. Am. Chem. Soc.* **2017**, *139* (7), 2825–2832.

(8) Takaya, J.; Ito, S.; Nomoto, H.; Saito, N.; Kirai, N.; Iwasawa, N. Fluorine-Controlled C-H Borylation of Arenes Catalyzed by a PSiN-Pincer Platinum Complex. *Chem. Commun.* **2015**, *51* (100), 17662–17665.

(9) Kuleshova, O.; Asako, S.; Ilies, L. Ligand-Enabled, Iridium-Catalyzed Ortho-Borylation of Fluoroarenes. *ACS Catal.* **2021**, *11* (10), 5968–5973.

(10) Eisenstein, O.; Milani, J.; Perutz, R. N. Selectivity of C-H Activation and Competition between C-H and C-F Bond Activation at Fluorocarbons. *Chem. Rev.* **2017**, *117* (13), 8710–8753.

(11) Wang, J.; Sánchez-Roselló, M.; Aceña, J. L.; del Pozo, C.; Sorochinsky, A. E.; Fustero, S.; Soloshonok, V. A.; Liu, H. Fluorine in Pharmaceutical Industry: Fluorine-Containing Drugs Introduced to the Market in the Last Decade (2001-2011). *Chem. Rev.* **2014**, *114* (4), 2432–2506.

(12) Gillis, E. P.; Eastman, K. J.; Hill, M. D.; Donnelly, D. J.; Meanwell, N. A. Applications of Fluorine in Medicinal Chemistry. *J. Med. Chem.* **2015**, *58* (21), 8315–8359.

(13) Meanwell, N. A. Fluorine and Fluorinated Motifs in the Design and Application of Bioisosteres for Drug Design. *J. Med. Chem.* **2018**, *61* (14), 5822–5880.

(14) Boller, T. M.; Murphy, J. M.; Hapke, M.; Ishiyama, T.; Miyaura, N.; Hartwig, J. F. Mechanism of the Mild Functionalization of Arenes by Diboron Reagents Catalyzed by Iridium Complexes. Intermediacy and Chemistry of Bipyridine-Ligated Iridium Trisboryl Complexes. *J. Am. Chem. Soc.* **2005**, *127* (41), 14263–14278.

(15) Tamura, H.; Yamazaki, H.; Sato, H.; Sakaki, S. Iridium-Catalyzed Borylation of Benzene with Diboron. Theoretical Elucidation of Catalytic Cycle Including Unusual Iridium(v) Intermediate. *J. Am. Chem. Soc.* **2003**, *125* (51), 16114–16126.

(16) Green, A. G.; Liu, P.; Merlic, C. A.; Houk, K. N. Distortion/Interaction Analysis Reveals the Origins of Selectivities in Iridium-Catalyzed C–H Borylation of Substituted Arenes and 5-Membered Heterocycles. *J. Am. Chem. Soc.* **2014**, *136* (12), 4575–4583.

(17) Tanabe, T.; Brennessel, W. W.; Clot, E.; Eisenstein, O.; Jones, W. D. Synthesis, Structure, and Reductive Elimination in the Series Tp'Rh(PR3)(Ar(F))H; Determination of Rhodium-Carbon Bond Energies of Fluoroaryl Substituents. *Dalton Trans.* **2010**, *39* (43), 10495–10509.

(18) Chotana, G. A.; Rak, M. A.; Smith, M. R., III. Sterically Directed Functionalization of Aromatic C-H Bonds: Selective Borylation Ortho to Cyano Groups in Arenes and Heterocycles. *J. Am. Chem. Soc.* **2005**, *127* (30), 10539–10544.

(19) Vanchura, B. A., II; Preshlock, S. M.; Roosen, P. C.; Kallepalli, V. A.; Staples, R. J.; Maleczka, R. E., Jr.; Singleton, D. A.; Smith, M. R., III. Electronic Effects in Iridium C-H Borylations: Insights from Unencumbered Substrates and Variation of Boryl Ligand Substituents. *Chem. Commun.* **2010**, *46* (41), 7724–7726.

(20) Jayasundara, C. R. K.; Unold, J. M.; Oppenheimer, J.; Smith, M. R., III; Maleczka, R. E., Jr. A Catalytic Borylation/Dehalogenation Route to o-Fluoro Arylboronates. *Org. Lett.* **2014**, *16* (23), 6072–6075.

(21) Pabst, T. P.; Chirik, P. J. Development of Cobalt Catalysts for the Meta-Selective C(Sp2)-H Borylation of Fluorinated Arenes. *J. Am. Chem. Soc.* **2022**, *144* (14), 6465–6474.

(22) Ren, H.; Zhou, Y.-P.; Bai, Y.; Cui, C.; Driess, M. Cobalt-Catalyzed Regioselective Borylation of Arenes: N-Heterocyclic Silylene as an Electron Donor in the Metal-Mediated Activation of C−H Bonds. *Chem. Eur. J.* **2017**, *23* (24), 5663–5667.

(23) Miller, S. L.; Chotana, G. A.; Fritz, J. A.; Chattopadhyay, B.; Maleczka, R. E., Jr; Smith, M. R., III. C-H Borylation Catalysts That Distinguish Between Similarly Sized Substituents Like Fluorine and Hydrogen. *Org. Lett.* **2019**, *21* (16), 6388–6392.

(24) Ros, A.; Estepa, B.; López-Rodríguez, R.; Álvarez, E.; Fernández, R.; Lassaletta, J. M. Use of Hemilabile N,N Ligands in Nitrogen-Directed Iridium-Catalyzed Borylations of Arenes. *Angew. Chem. Int. Ed. Engl.* **2011**, *50* (49), 11724–11728.

(25) Tagata, T.; Nishida, M. Aromatic C-H Borylation Catalyzed by Iridium/2,6-Diisopropyl-N-(2-Pyridylmethylene)Aniline Complex. *Adv. Synth. Catal.* **2004**, *346* (13–15), 1655–1660.

(26) Preshlock, S. M.; Ghaffari, B.; Maligres, P. E.; Krska, S. W.; Maleczka, R. E., Jr; Smith, M. R., III. High-Throughput Optimization of Ir-Catalyzed C-H Borylation: A Tutorial for Practical Applications. *J. Am. Chem. Soc.* **2013**, *135* (20), 7572–7582.

(27) Montero Bastidas, J. R.; Chhabra, A.; Feng, Y.; Oleskey, T. J.; Smith, M. R., III; Maleczka, R. E. Steric Shielding Effects Induced by Intramolecular C–H⋯O Hydrogen Bonding: Remote Borylation Directed by Bpin Groups. *ACS Catal.* **2022**, *12* (4), 2694–2705.

(28) Preshlock, S. M.; Plattner, D. L.; Maligres, P. E.; Krska, S. W.; Maleczka, R. E., Jr.; Smith, M. R., III. A Traceless Directing Group for C-H Borylation. *Angew. Chem. Int. Ed.* **2013**, *52* (49), 12915–12919.

(29) Chattopadhyay, B.; Dannatt, J. E.; Andujar-De Sanctis, I. L.; Gore, K. A.; Maleczka, R. E., Jr; Singleton, D. A.; Smith, M. R., III. Ir-Catalyzed Ortho-Borylation of Phenols Directed by Substrate-Ligand Electrostatic Interactions: A Combined Experimental/in Silico Strategy for Optimizing Weak Interactions. *J. Am. Chem. Soc.* **2017**, *139* (23), 7864–7871.

(30) Montero Bastidas, J. R.; Oleskey, T. J.; Miller, S. L.; Smith, M. R., III; Maleczka, R. E., Jr. Para-Selective, Iridium-Catalyzed C-H Borylations of Sulfated Phenols, Benzyl Alcohols, and Anilines Directed by Ion-Pair Electrostatic Interactions. *J. Am. Chem. Soc.* **2019**, *141* (39), 15483–15487.

(31) Oeschger, R. J.; Larsen, M. A.; Bismuto, A.; Hartwig, J. F. Origin of the Difference in Reactivity between Ir Catalysts for the Borylation of C–H Bonds. *J. Am. Chem. Soc.* **2019**, *141* (41), 16479–16485.

(32) Uson, R.; Oro, L. A.; Cabeza, J. A.; Bryndza, H. E.; Stepro, M. P. Dinuclear Methoxy, Cyclooctadiene, and Barrelene Complexes of Rhodium(I) and Iridium(I): Kirschner/Inorganic. In *Inorganic Syntheses*; Kirschner, S., Ed.; Inorganic Syntheses; John Wiley & Sons, Inc.: Hoboken, NJ, USA, 1985; Vol. 231, pp 126–130.

(33) Pangborn, A. B.; Giardello, M. A.; Grubbs, R. H.; Rosen, R. K.; Timmers, F. J. Safe and Convenient Procedure for Solvent Purification. *Organometallics* **1996**, *15* (5), 1518–1520.

(34) Yeoh, K. K.; Chan, M. C.; Thalhammer, A.; Demetriades, M.; Chowdhury, R.; Tian, Y.-M.; Stolze, I.; McNeill, L. A.; Lee, M. K.; Woon, E. C. Y.; Mackeen, M. M.; Kawamura, A.; Ratcliffe, P. J.; Mecinović, J.; Schofield, C. J. Dual-Action Inhibitors of HIF Prolyl Hydroxylases That Induce Binding of a Second Iron Ion. *Org. Biomol. Chem.* **2013**, *11* (5), 732–745.

(35) Obligacion, J. V.; Semproni, S. P.; Chirik, P. J. Cobalt-Catalyzed C–H Borylation. *J. Am. Chem. Soc.* **2014**, *136* (11), 4133–4136.

(36) Wang, G.; Xu, L.; Li, P. Double N,B-Type Bidentate Boryl Ligands Enabling a Highly Active Iridium Catalyst for C–H Borylation. *J. Am. Chem. Soc.* **2015**, *137* (25), 8058–8061.

(37) Newby, J. A.; Blaylock, D. W.; Witt, P. M.; Pastre, J. C.; Zacharova, M. K.; Ley, S. V.; Browne, D. L. Design and Application of a Low-Temperature Continuous Flow Chemistry Platform. *Org. Process Res. Dev.* **2014**, *18* (10), 1211–1220.

(38) Sheldrick, G. M. SHELXT - Integrated Space-Group and Crystal-Structure Determination. *Acta Crystallogr A Found Adv* **2015**, *71* (Pt 1), 3–8.

(39) Dolomanov, O. V.; Bourhis, L. J.; Gildea, R. J.; Howard, J. A. K.; Puschmann, H. OLEX2: A Complete Structure Solution, Refinement and Analysis Program. *J. Appl. Crystallogr.* **2009**, *42* (2), 339–341.

(40) Sheldrick, G. M. A Short History of SHELX. *Acta Crystallogr. A* **2008**, *64* (Pt 1), 112–

CHAPTER 3.

HYDROGEN PRESSURE EFFECTS IN IRIDIUM-CATALYZED BORYLATIONS WITH A DI-PYRIDYL HYDRAZONE LIGAND: EVIDENCE OF TRANSFER BORYLATION AND EQUILIBRIUM

3.1. Introduction

Traditional C–H activation borylation via group 8-9 transition metal catalysts typically operate under the two principal mechanisms: oxidative addition and reductive elimination or σ-bond metathesis. The metal first reacts with the functionalizing reagent, either a diboron (B_2gly_2, gly = glycolate) or a borane (HBgly) to generate the metal boryl complex that performs the direct borylation reaction. Diborons are generally well tolerated by most functional groups, but boranes such as pinacolborane can be problematic for some reactive functional groups. Moreover, utilizing diborons does not avoid this problem, as stoichiometric amounts of boranes are generated after CHB. In efforts to avoid their generation to allow more broad functional group tolerance, hetero(aryl) or vinyl boronate esters are being investigated as a boron source in functional group transfer catalysis. This relatively new concept for borylation was found and investigated by the Fontaine[1,2] and Dydio[3] groups with organocatalysts and transition metal catalysts respectively and, accordingly, operate in distinct mechanisms.

The Fontaine group demonstrated 2-mercaptopyridine as a simple, though not ideal, catalyst for the isodesmic borylation of pyrroles, indoles, and thiophenes from 2-furyl(Bcat) (**Figure 3.1.1A**). This isodesmic approach is driven by thermodynamic equilibrium, as the borylated products are favored over 2-furyl(Bcat) by 1-4 kcal·mol^{-1}.[1] Furthermore, furan can be removed from the mixture due to its volatility, taking advantage of Le Chatelier's principle to further drive the reaction.

Notably, this methodology can access electron-rich aromatics unlike prior aminoborane systems,[4] though, the reaction of *N*,*N*-dimethylaniline only reached 9% conversion. Simple alkyl substituted thiophenes and furans were marginal in their reactivity. While these select substrates did not work well under the catalytic conditions, substituted pyrroles and indoles were excellent candidates for transfer borylations. Olefins, alkynes, nitriles, and halogens were all tolerant of the conditions of borylation underscoring the compatibility of reactive functional groups to the catalysis.

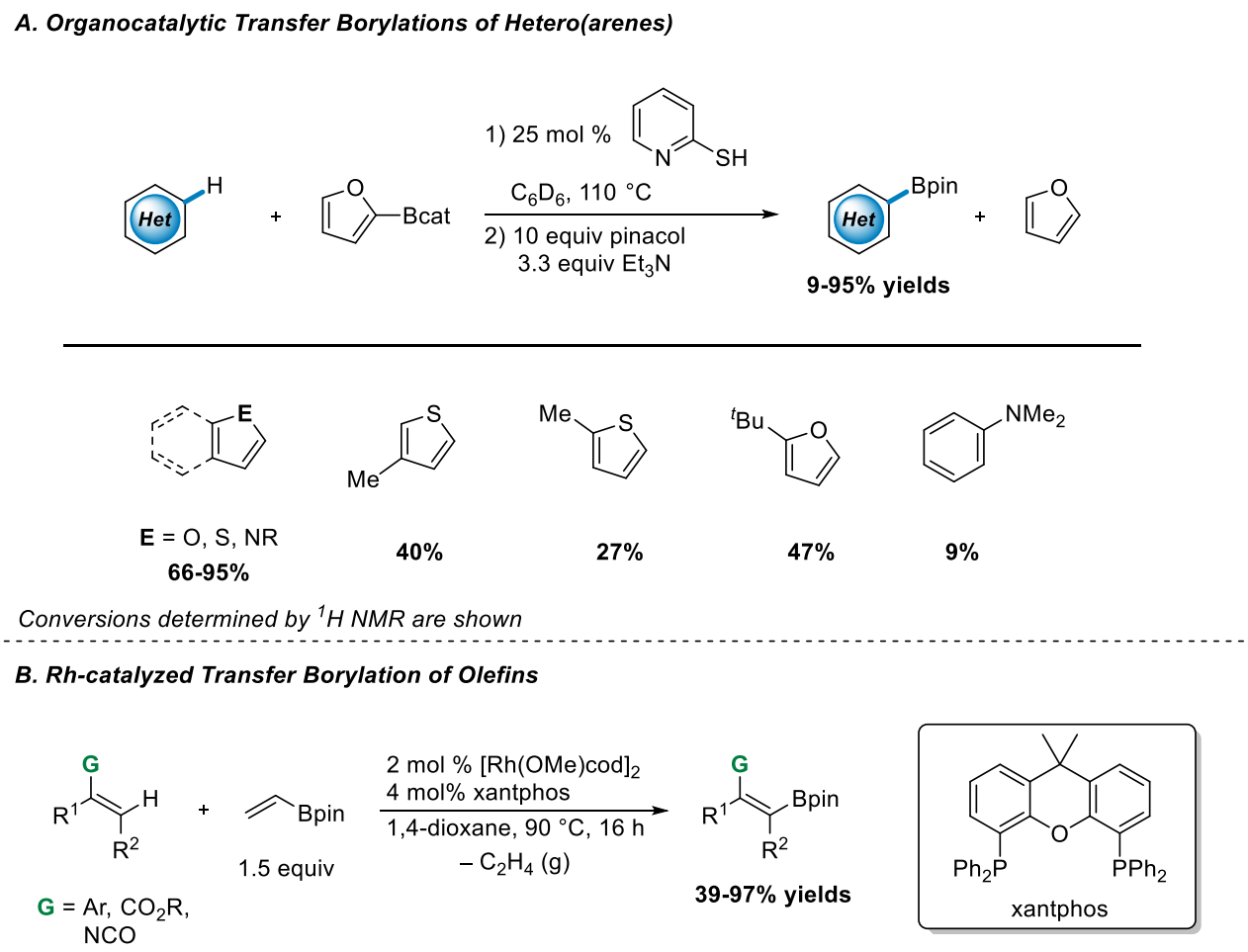

Figure 3.1.1. Known examples of transfer borylation chemistry

The Dydio group demonstrated a rhodium catalyst bearing the xantphos ligand is effective for the transfer borylation of alkenes (**Figure 3.1.1B**) from vinylBpin with excellent functional

group tolerance, regio- and stereoselectivity. The reaction in this case is mildly exergonic ($\Delta G° = -0.57$ kcal·mol^{-1}) and is primarily driven by release of ethylene. They propose an unprecedented β-boryl elimination to form the active Rh^{I} boryl from vinylBpin. The olefins after transfer borylation also have high *E*-selectivity due to faster β-hydride elimination in the product forming step of the cycle. This Rh-catalyzed process operates under kinetic control and is not driven by the thermodynamics of the borylated products, opposite to Fontaine's organocatalytic transfer borylation.

Importantly, these two examples serve as the only two reports of transfer borylation chemistry reported. They lay the foundational concepts for understanding how these catalytic systems operate in addition to the attractive features of isodesmic functionalizations. Herein, the first example of an Ir-catalyzed transfer borylation and product isomerization process is described. Investigations into the catalyst structure and a mechanism distinct from the canonical CHB is proposed to account for the transfer borylation.

3.2. Results and Discussion

Scheme 3.2.1. Initial observation of selectivity difference

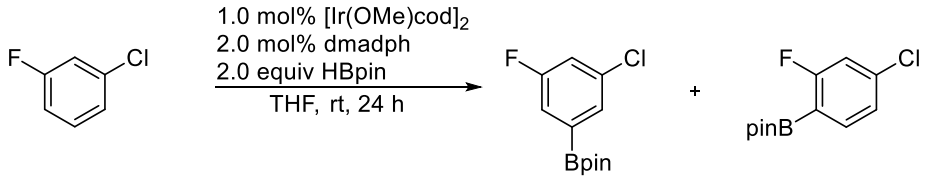

entry	system	time (h)	% conversion	m:o to F
1	closed	24	>99	6.9:1.0
2	open[a]	24	>99	5.0:1.0

[a] Data from reference [5]. Ratios of products were determined by ^{19}F NMR analysis.

The initial work that lead to this observation was in the borylation of 3-fluorochlorobenzene (**Scheme 3.2.1**). The initial work investigating dmadph was to first replicate

the results of prior studies investigating the ligand. The meta-selectivity of the reaction I performed was superior to the results found previously. The only difference experimentally was that previous reactions were performed in well plates that would not fully seal, and any pressure generated during the reaction could escape. To examine whether hydrogen pressure generated during the reaction affected the observed selectivity, the borylation was run in an open system and a closed system under a constant pressure of hydrogen (**Scheme 3.2.2**).

Scheme 3.2.2. Borylation of fluoroarenes in open and closed systems[a]

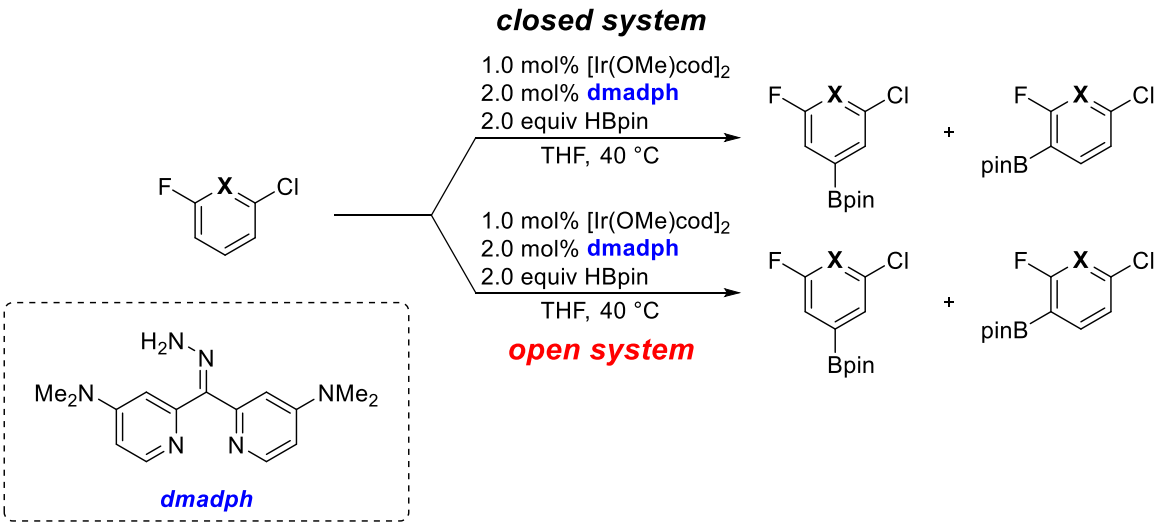

X = C

entry	system	time (h)	% conversion	m:o to F
1	closed (5 bar H_2)	1	>99	7.3:1.0
2	open	5	95	4.0:1.0

X = N

entry	system	time (h)	% conversion	m:o to F
1	closed (5 bar H_2)	1	>99	>20:1
2	open	5	95	8.0:1.0

[a]Reaction conditions: fluoroarene (1.0 mmol), HBpin (2.0 mmol) or B_2pin_2 (1.0 mmol), $[Ir(OMe)cod]_2$ (1.0 mol %), ligand (2.0 mol %), solvent (2.0 mL). Ratios of products were determined by ^{19}F NMR analysis.

The borylation for 3-fluorochlorobenzene resulted in the same behavior as previously observed, with the open system decreasing further in meta-selectivity. While this decrease in selectivity is moderate, borylation of a substrate that is more selective for meta-to-F functionalization resulted in an even larger shift in the selectivity. The borylation of 2-chloro-6-

fluoropyridine in an open system decreased the selectivity to 8.0:1.0 with the meta isomer as the major product, which is a substantial shift in the selectivity of the reaction. This is the *first* observation of selectivity dependence on hydrogen pressure in iridium-catalyzed C–H borylations.

With this in mind, we wondered if hydrogen pressure also affected the regioselectivity in the borylation of fluorobenzene (**Scheme 3.2.3**). The reaction was monitored over time by ^{19}F and ^{11}B NMR to assess both the regioselectivity and conversion respectively. After 2 h, the borylation was essentially complete (82% conversion) and the regioselectivity was found to 1.5:5.7:1.0 of the *ortho:meta:para* borylated isomers. At 3h, the conversion was determined to be 98%, and the mixture was isolated (mass balance = 0.218 g). It is generally understood that C–H scission is rate-limiting in iridium-catalyzed CHBs, and thus the product distribution should not change after functionalization. Prolonged heating of the reaction for 24 h, however, resulted in the product distribution changing to a nearly equimolar mixture (1.0:1.6:1.0 *ortho:meta:para*, mass balance = 0.220 g) of the borylated isomers. The reaction was repeated in an open system and after 24 h of heating, the regioselectivity remained nearly identical to what was observed after 1 h. These results suggest that hydrogen pressure is responsible for the product redistribution.

Due to the regioisomer distribution changing over time, this suggests a thermodynamic equilibrium is operative. If this is true, the thermodynamic stabilities of the products should correspond to the ratio of products observed after equilibration. To assess this, the thermodynamic stability of the borylated isomers of fluorobenzene were calculated using DFT with B3LYP/6-31G (d,p) basis set (**Figure S3.3)**. Unsurprisingly, all three isomers have nearly equivalent ground state energies, and thus the ratio of products can be approximated to be 1:1:1. This ratio is nearly reached in the borylation of fluorobenzene with dmadph in **Scheme 3.2.3**. Prolonged heating (72 h) of the reaction did not further change the regioisomer distribution, nor did increased heating at 80 °C.

The experimental ratio of products, although, are in near agreement with those predicted. This provides evidence that the transfer borylation process is thermodynamically controlled as opposed to the kinetically controlled CHB.

Scheme 3.2.3. Borylation of fluorobenzene over time[a]

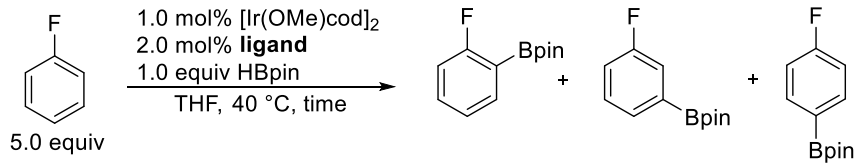

closed system

entry	ligand	time (h)	%conversion	o : m : p to F ratio
1	**dmadph**	2	82	1.5 : 5.7 : 1.0
2	**dmadph**	24	>99	1.0 : 1.6 : 1.0
3	dmadpm	2	15	1.0 : 6.1 : 1.0
4	dmadpm	24	43	1.1 : 6.3 : 1.0
5	dtbpy	2	75	3.5 : 5.2 : 1.0
6	dtbpy	24	>99	3.6 : 5.0 : 1.0

open system

ligand	time (h)	%conversion	o : m : p to F ratio
dmadph	24	>99	1.3 : 4.6 : 1.0

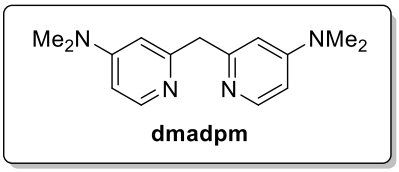

[a]Ratios of products were determined by ^{19}F NMR analysis.

To probe if this behavior is unique to dmadph or if hydrogen pressure also affects regioselectivity with other ligands, the borylation was repeated with the analogous dipyridylmethane ligands and dtbpy (**Scheme 3.2.3**). For all other ligands examined, the regioselectivity observed initially was essentially the same as that observed after full consumption of pinacolborane as expected. These experiments demonstrate that the regioselectivity shift is unique to dmadph and that hydrogen pressure is causing this behavior.

When considering mechanistically how the regioisomer distribution is changing over time, there are two possibilities that could occur. The regioisomers could be scrambling from some isomerization process (i.e. olefin chain walking)[6], and the boryl group remains on the substrate. The second possibility is that the boryl is removed from the substrate back to the metal via oxidative addition or sigma bond metathesis and the substrate is borylated again in a transfer

borylation type process. To probe the possibility of either, the experiments in **Scheme 3.2.4** were carried out. The borylation of 2-methylthiophene occurs first very rapidly (<15 min for full consumption of HBpin) and fully consumes the borylating reagent. After full conversion, 3-fluorophenylBpin was added to the mixture. If the regioisomers were observed due to isomerization, all borylated isomers of fluorobenzene should be observed and *only* mono-borylated thiophene. Conversely, if it is a transfer borylation process, all isomers of fluorobenzene should be observed in addition to the di-borylated isomer of the more electronically activated thiophene. The reaction performed with dmadph gave evidence of the latter, as 46% of the thiophene was di-borylated and all isomers of fluorobenzene were observed. When the reaction was performed in an open system, there was no di-borylation detected by ^{1}H NMR and only the 3-borylated isomer of fluorobenzene as was found when dtbpy was used as the ligand.

Scheme 3.2.4. Probing for transfer borylation[a]

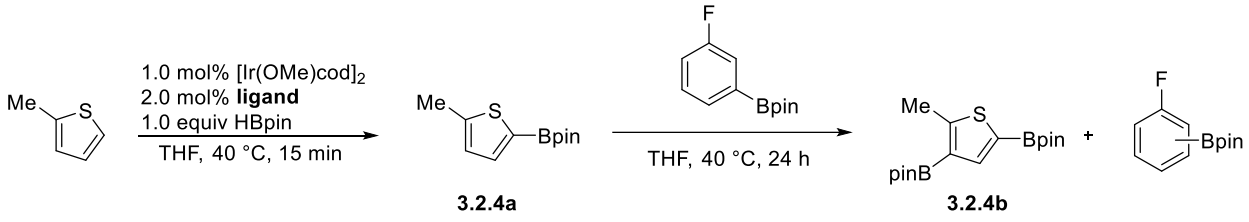

entry	ligand	ratio of *o*:*m*:*p* to F mono-borylated isomers	%**3.2.4b**	%conversion (based on HBpin)
1	**dmadph**	1.7 : 3.5 : 1.0	46	>99
2	dtbpy	0 : >99 : 0	<1	>99

[a]See SI for full experimental details.

3.3. Investigating the Catalyst Structure

With these unusual effects of hydrogen pressure and evidence of transfer borylation, the catalyst itself was investigated. An NMR tube study of the borylation of pentafluorobenzene was performed to study the ligand identity and to observe any catalyst resting states to understand the system. The aromatic region of the ^{1}H NMR shows a mixture of several ligand species within

solution (**Figure 3.3.1**). There is a significant amount of the hydrazone-boronate adduct in solution that also remains throughout the reaction indicating that the ligand is not fully binding to the metal during catalysis. One major species was present that does not correlate with the free ligand, adduct, or iridium hydrazido complex and the intensity of the resonances gradually increased over the course of the reaction. The integration of the exchangeable N–H proton in the ^{1}H NMR being less than one in addition to the ^{11}B resonance at δ 19.7 ppm suggests that it is partially *N*-borylated in solution. Accordingly, the possible structures of this species are proposed in **Figure 3.3.3**. With the observation of iridium boryls in ^{11}B (δ 33.9 ppm), the oxidation state of iridium could be either +3 or +5 where the Ir^{V} complex bears two additional Bpin or H ligands and the Ir^{III} complex does not. Furthermore, with partial *N*-borylation of the ligand observed, none of the proposed structures can be ruled out. Analysis of the hydride region of the ^{1}H NMR (**Figure 3.3.2**) was particularly complicated as multiple hydrides were observed throughout the course of the reaction. After 1.5 h, however, a hydride resonance observed at δ -8.39 ppm was identified as the corresponding Ir–fluoroaryl complex after C–H activation due to its apparent overlapping triplet of triplet of doublets (ttd) splitting pattern. This assignment was confirmed via $\{^{1}H\}^{19}F$ where it collapsed into a singlet. A similar Hg complex, $HgH(C_6F_5)$, was also reported[7] with a ttd splitting pattern. This is a significant observation, suggesting that the intermediate Ir–aryl is a resting state for the catalyst thus altering the inherent mechanism by which borylation occurs.

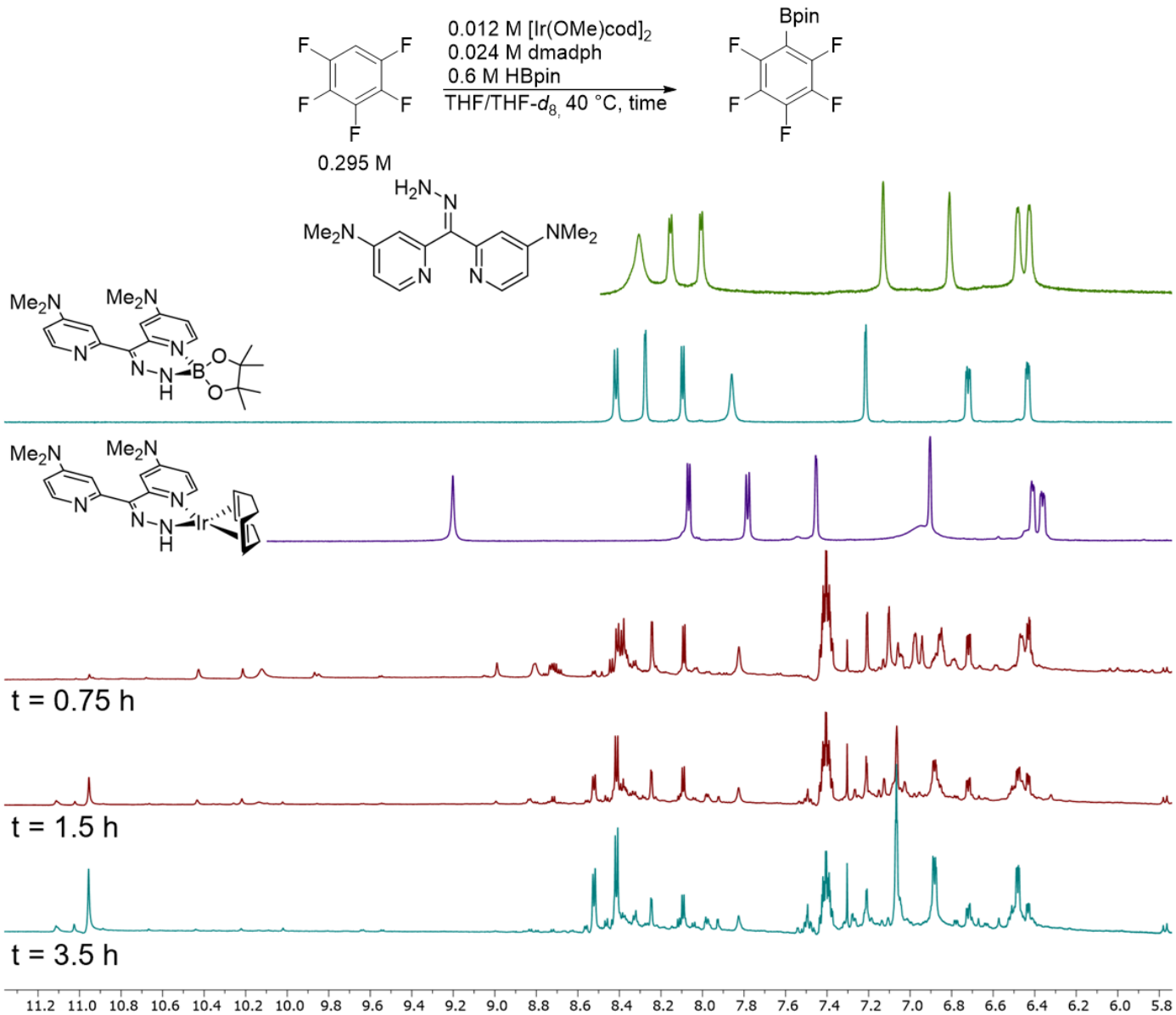

Figure 3.3.1. ^{1}H NMR (THF-d_8) comparison of the aromatic region in pentafluorobenzene borylation

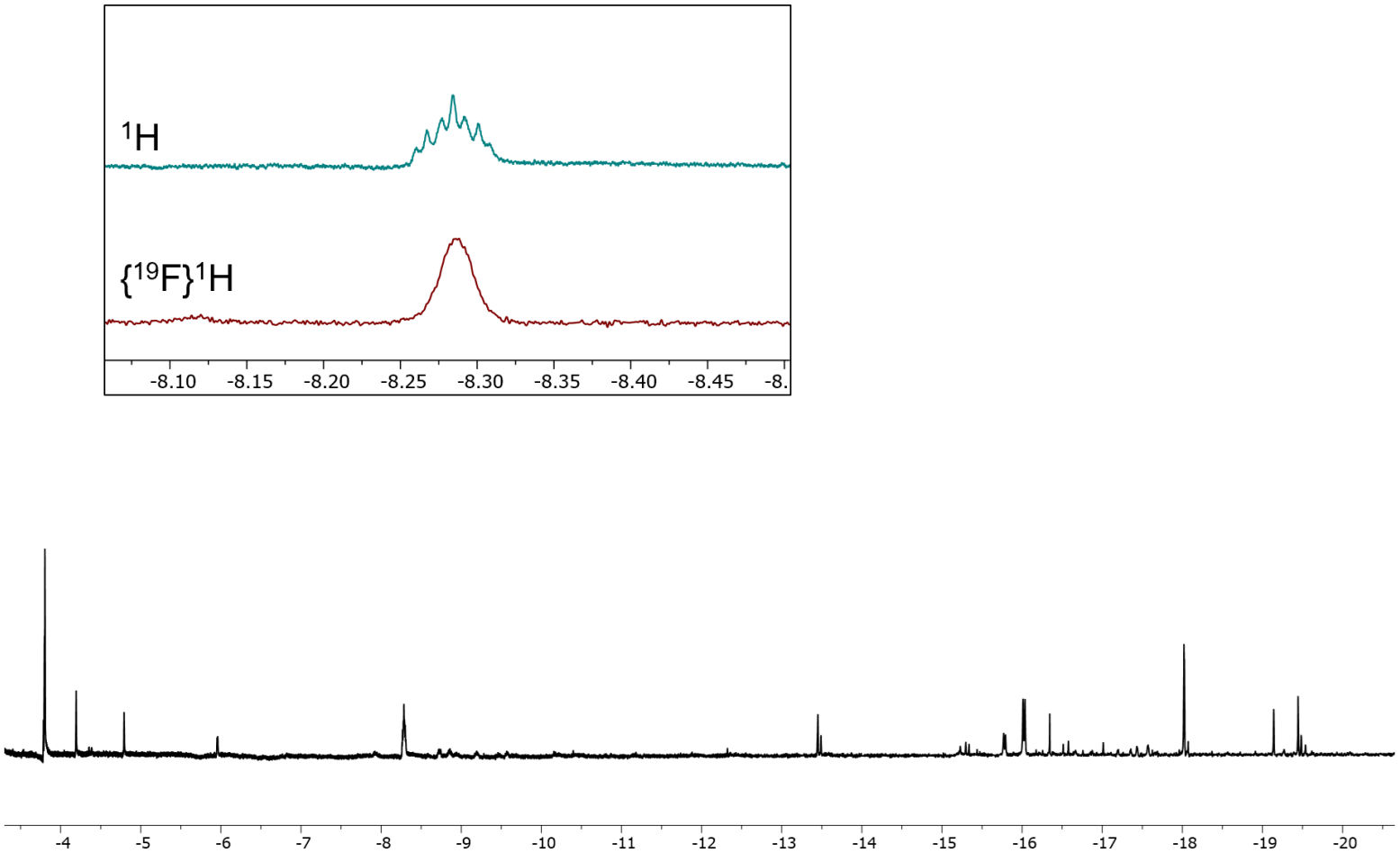

Figure 3.3.2. ^{1}H NMR (THF/THF-d_8) of the hydride region. Inset is a comparison of the ^{1}H and $\{^{19}F\}^{1}H$ of the hydride split into a ttd

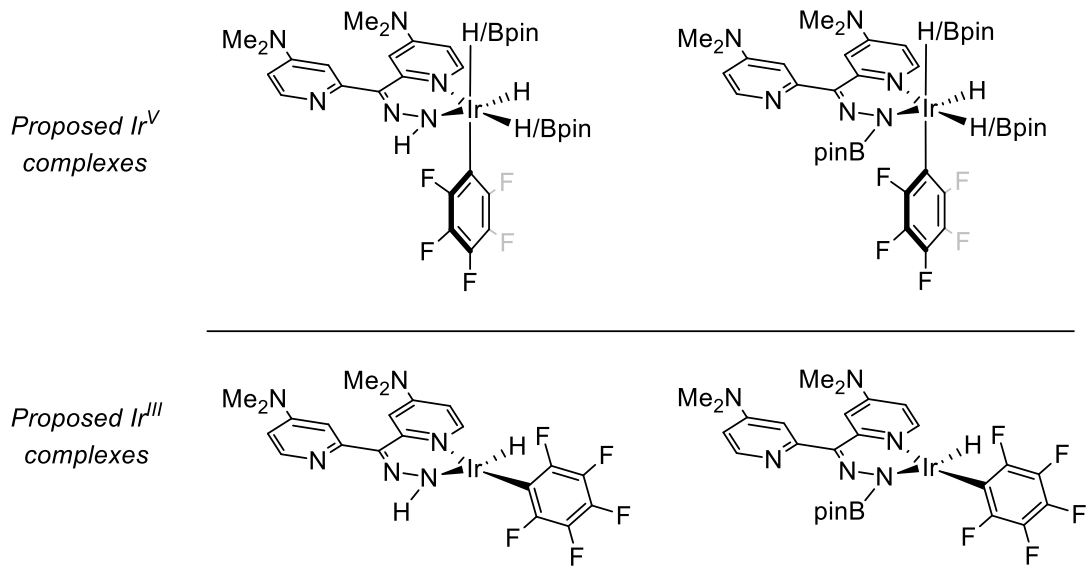

Figure 3.3.3. Proposed structures of species observed during catalysis

The Ir^{I} hydrazido was then reacted with 1 equivalent of pinacolborane (**Scheme 3.3.2**) to see if the catalyst could be further assembled, and the Ir^{III} hydridoboryl complex could be isolated. In practice, this reaction was more complicated than a simple oxidative addition of HBpin to iridium as intractable mixtures of products formed upon reaction. Strong bubbling after addition of HBpin to the solution indicated evolution of hydrogen, thus *N*–borylation competed with the oxidative addition. The ^{11}B NMR of the mixture after drying showed evidence of a 3-coordinate N–B bond (δ 24.9 ppm), an iridium boryl (δ 38.5 ppm), and a 4-coordinate boron species (δ 5.2 ppm). The 4-coordinate species is likely not the hydrazone-boronate adduct as the resonance is downfield shifted by nearly 2 ppm compared to the isolated adduct. The 3-coordinate boron resonance was also observed in the NMR tube borylation of pentafluorobenzene at the same chemical shift and is tentatively assigned as the *N*-borylated Ir^{I} hydrazido complex. Due to their instability, the products could not be separated and isolated.

Scheme 3.3.2. Reaction of Ir^{I} hydrazido with pinacolborane

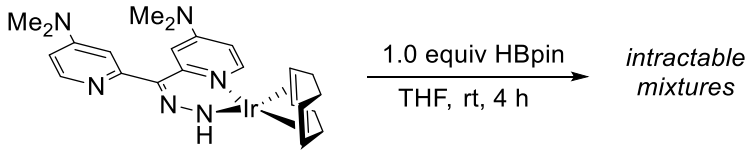

Qualitative KIE Study of dmadph.

The catalytic manifold was examined through a KIE experiment to determine if a large, primary kinetic isotope effect is observed similar to the Hartwig[8] system with dtbpy and our previous studies on dmadpm.[9] In both cases, large primary kinetic isotope effects were observed ($k_H/k_D > 3.5$) suggesting that C–H scission is rate limiting. If no KIE ($k_H/k_D = 1.0$) or an inverse kinetic isotope effect ($k_H/k_D < 1.0$) were observed, a different mechanism where C–H scission is not rate limiting, is engaged using dmadph.

Scheme 3.3.3. KIE determination in a parallel conversion experiment of C_6H_6 and C_6D_6

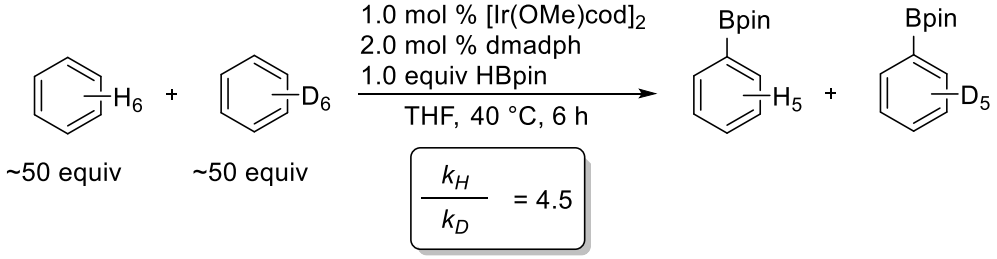

Utilizing the improved method developed and described by Miller,[9] a GC-MS method with a slow temperature ramp and a long isothermal plateau was able to separate the protiated products from the deuterated to determine the relative KIE from the reaction in **Scheme 3.3.3.**. The relative KIE was found to be 4.5, which is on the order found with dmadpm but lower than the k_H/k_D of 5.0 found by Hartwig. These experiments support that C–H activation when using dmadph is still rate limiting. Thus, it is probable that C–H activation and borylation operate under the canonical Ir^{III}/Ir^{V} catalytic cycle, but the transfer borylation chemistry operates in a separate, distinct mechanism.

3.4. Conclusions

In summary, the first example of an Ir-catalyzed transfer borylation enabled by the dipyridyl hydrazone ligand, dmadph, is described. The H_2 pressure generated during catalysis was found to be a requirement for both the functional group transfer chemistry and product isomerization. Kinetic isotope effect experiments demonstrated that for the C–H activation and borylation, C–H scission is rate-limiting and likely operates according to the accepted mechanism for CHB. NMR studies during catalytic borylation identified an Ir–fluoroaryl complex as a resting state of the catalyst for either the CHB or the transfer borylation chemistry, though the KIE studies support that it is a resting state for the latter.

3.5. Experimental

3.5.1. General Information

Pinacolborane (HBpin) (97% stabilized with 1% triethylamine) was purchased commercially and used as received without further purification. The iridium catalyst, bis(η^4-1,5-cyclooctadiene)-di-μ-methoxy-diiridium (I), $[Ir(OMe)(cod)]_2$, was prepared by a literature procedure.[11]

All substrates were obtained commercially. Liquid substrates were purified by distillation and solid substrates were purified by sublimation or recrystallization.

All reactions were prepared in 3.0 mL Wheaton microreactor vials equipped with stir bars and pressure caps in a glovebox under a nitrogen atmosphere and then transferred to a preheated aluminum block outside of the glovebox. THF and *n*-hexane were obtained from wet stills refluxing over sodium and benzophenone. Methylene chloride and acetonitrile were obtained from dry stills according to the literature procedure.[12]

Reactions were monitored by ^{19}F NMR, and crude reaction ratios were verified by ^{1}H NMR or ^{19}F NMR for fluorine containing substrates. NMR spectra were recorded on a Varian 500 MHz DD2 Spectrometer equipped with a 1H-19F/15N-31P 5mm Pulsed Field Gradient (PFG) Probe. Spectra were taken in deuterated solvents referenced to residual solvent signals in ^{1}H NMR and $^{13}C\{^{1}H\}$ NMR. $^{13}C\{^{1}H\}$ NMR resonances for the boron-bearing carbon atom were not observed due to quadrupolar relaxation. NMR spectra were processed for display using the MNova software with only phasing and baseline corrections applied. For all NMR spectra, no peaks were manually corrected, suppressed or altered in any form, and unprocessed fids are available upon request.

Silica used for purification of crude material was standard laboratory grade 230 - 400 mesh designed for flash chromatography applications. Purification of crude materials on a 1 mmol scale was achieved by standard flash chromatography methods employing 2-3 g silica gel plugs in small chromatography columns of dimension approximately 2 x 30 cm. The concentrated crude materials were dissolved in a minimum amount of solvent, applied to the silica gel with a Pasteur pipette and eluted into test tubes. Compounds that eluted were visualized by spotting on TLC plates and irradiating with 254 nm UV light.

3.5.2. Hydrogen Pressure Experiments

General procedure for borylations under H_2 pressure (A):

In a nitrogen-filled glovebox, a 3.0 mL Wheaton pressure vial equipped with a stir bar was charged with a 1.0 mL THF solution of $[Ir(OMe)cod]_2$ (6.6 mg, 0.01 equiv). To this solution, pinacolborane (0.290 mL, 2 mmol, 2.0 equiv) was added with a syringe while stirring, turning the light-yellow solution into a golden orange. Then, in a small test tube, a 1.0 mL THF solution of dmadph (5.6 mg, 0.02 equiv) was made and added to the iridium solution with a syringe and the solution immediately turned dark red in color. Last, the substrate (1 mmol) was added neat to this solution and capped. The vial was then removed from the glovebox and transferred into a Parr reactor vessel fitted with a glass reactor liner and a stirbar and immediately capped. The vessel was filled with H_2 and evacuated three times. Then, H_2 at the desired pressure was filled into the vessel and stirred. Upon returning, the vessel was evacuated, and the reaction mixture was transferred to a 20 mL scintillation vial using CH_2Cl_2 and the volatiles were removed under reduced pressure and the crude mixture was analyzed by ^{1}H, ^{19}F, and ^{11}B NMR.

General procedure for open-system borylation (B):

In a nitrogen-filled glovebox, a 10 mL Schlenk flask equipped with a stir bar was charged with a 1.0 mL THF solution of $[Ir(OMe)cod]_2$ (6.6 mg, 0.01 equiv). To this solution, pinacolborane (0.290 mL, 2 mmol, 2.0 equiv) was added with a syringe while stirring, turning the light-yellow solution into a golden orange. Then, in a small test tube, a 1.0 mL THF solution of dmadph (5.6 mg, 0.02 equiv) was made and added to the iridium solution with a syringe and the solution immediately turned dark red in color. Last, the substrate (1 mmol) was added neat to this solution and capped with a septum. The flask was transferred out of the glovebox and attached to a N_2 line. Under positive N_2 pressure, a reflux condenser was attached, and the flask was immediately submerged

in a preheated oil bath at 40 °C and stirred. When the reaction finished, the crude reaction mixture was transferred to a 20 mL scintillation vial using CH_2Cl_2 and the volatiles were removed under reduced pressure and the crude mixture was analyzed by ^{1}H, ^{19}F, and ^{11}B NMR.

Borylation of 2-chloro-6-fluoropyridine under H_2 pressure

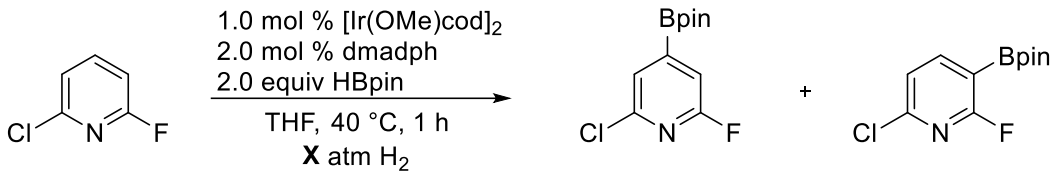

Borylation was performed according to general procedure **A** at 40 °C under 5 atm of H_2 for 1 h. For full spectral characterization, see pages 41–42. The ratio of regioisomers was determined to be >20:1.0 meta:ortho to fluorine by ^{19}F NMR. The conversion determined by ^{19}F NMR was >99%.

Open system borylation of 2-chloro-6-fluoropyridine

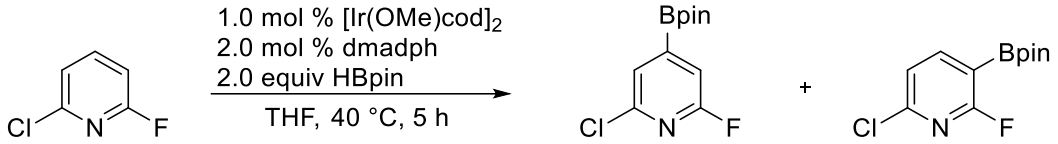

Borylation was performed according to general procedure **B** at 40 °C for 5 h. For full spectral characterization, see pages 41–42. The ratio of regioisomers was determined to be 8.0:1.0 meta:ortho to fluorine by ^{19}F NMR. The conversion determined by ^{19}F NMR was 95%.

Borylation of 3-fluorochlorobenzene under H_2 pressure

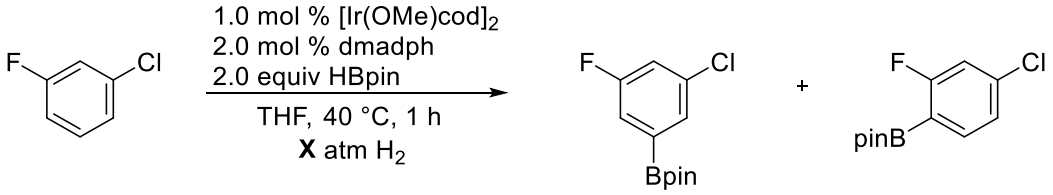

Borylation was performed according to general procedure **A** at 40 °C under 5 atm of H_2 for 1 h. For full spectral characterization, see pages 45–46. The ratio of regioisomers was determined to be 7.3:1.0 meta:ortho to fluorine by ^{19}F NMR. The conversion determined by ^{19}F NMR was >99%.

Open system borylation of 3-fluorochlorobenzene

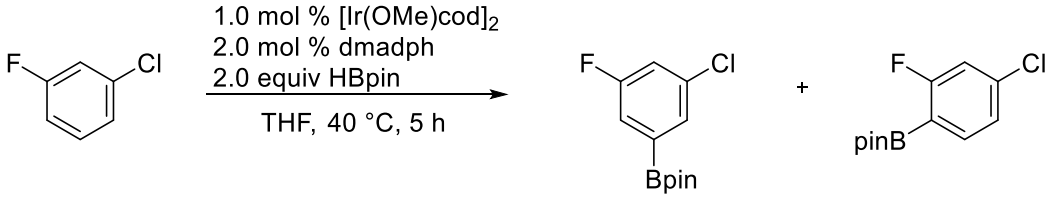

Borylation was performed according to general procedure **B** at 40 °C for 5 h. For full spectral characterization, see pages 45–46. The ratio of regioisomers was determined to be 4.0:1.0 meta:ortho to fluorine by ^{19}F NMR. The conversion determined by ^{19}F NMR was 95%.

General procedure for the borylation of fluorobenzene (C)

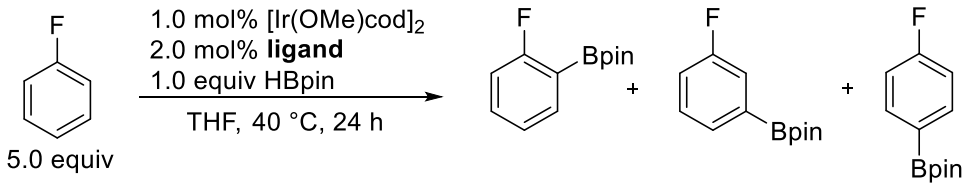

In a nitrogen-filled glovebox, a 3.0 mL Wheaton pressure vial equipped with a stir bar was charged with a 1.0 mL THF solution of $[Ir(OMe)cod]_2$ (6.6 mg, 0.01 equiv). To this solution, pinacolborane (0.290 mL, 2 mmol, 2.0 equiv) was added with a syringe while stirring, turning the light-yellow solution into a golden orange. Then, in a small test tube, a 1.0 mL THF solution of the ligand (0.02 equiv) was made and added to the iridium solution with a syringe and the solution immediately

turned dark red in color. Last, fluorobenzene (96 µL, 1.0 mmol) was added to this solution and capped. The reaction was heated at 40 °C and stirred in an aluminum heating block on top of a stir plate outside of the glovebox. Reactions were monitored by ^{19}F and ^{11}B spectroscopies. After 24 h, the volatiles were evaporated, and the crude reaction mixtures were analyzed by ^{19}F, ^{1}H, and ^{11}B NMR. The results are summarized below in **Figure S1**.

entry	ligand	time (h)	%conversion	o : m : p to F ratio
1	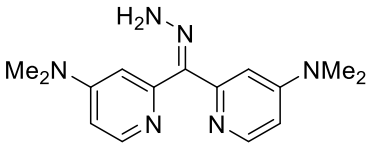 dmadph	24	>99	1.0 : 1.6 : 1.0
2	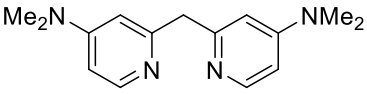 dmadpm	24	43	1.1 : 6.3 : 1.0
3	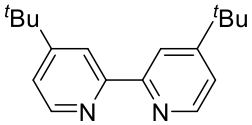 dtbpy	24	>99	3.6 : 5.0 : 1.0

Figure S3.1. Ligand screen for the borylation of fluorobenzene according to general procedure C. Regioselectivities and conversions determined by ^{19}F NMR.

Open system borylation of fluorobenzene

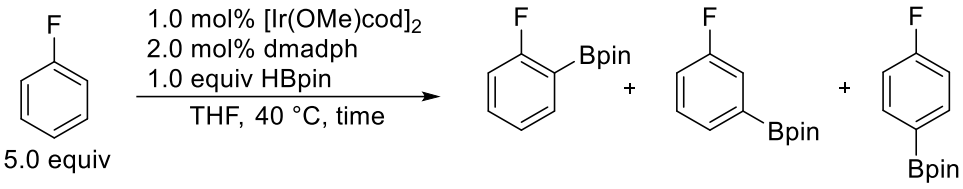

1.3 : 4.6 : 1.0

Borylation was performed according to general procedure **B** at 40 °C for 24 h. For full spectral characterization, see pages 53–54. The ratio of regioisomers was determined to be 1.3:4.6:1.0 of

ortho:meta:para to fluorine by ^{19}F NMR. The conversion determined by ^{19}F and ^{11}B NMR was >99%.

3.3.3. NMR Tube Borylations

Borylation of 2,3,4,5-tetrafluorotoluene

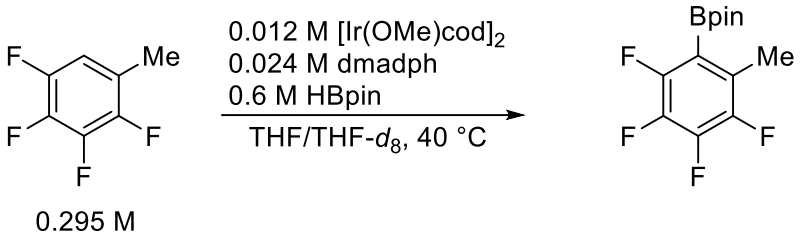

In a N_2 filled glovebox, $[Ir(OMe)cod]_2$ (0.0070 g, 0.01 mmol), dmadph (0.0060 g, 0.02 mmol), were weighed into separate test tubes. Then, 1.0 mL of THF was added to both test tubes. To the solution of Ir, HBpin (300 µL, 2 mmol) was added and shaken briefly, turning the light-yellow solution into a golden-yellow. The solution of Ir and pinacolborane was then pipetted into the solution of dmadph and transferred into a scintillation vial with a stir bar. The combined solution was stirred vigorously for 5 minutes, turning the solution dark red. Using a microsyringe, 400 µL of the combined solution was added to a J-young tube, followed by 2,3,4,5-tetrafluorotoluene (30 µL, 0.18 mmol) and 0.3 mL of THF-d_8. The J-young was capped, inverted and thoroughly mixed. The tube was then transferred into a preheated oil bath at 40 °C and monitored by ^{1}H, ^{19}F, and ^{11}B NMR. The conversion at 6 h determined by ^{19}F NMR analysis was 13%.

Notes: *While the reaction did not proceed as readily as the borylation of pentafluorobenzene (vide infra), the aromatic region of the NMR revealed that a similar species as to the one being proposed in the following section is generated. See* ***Figure S14****.*

Borylation of pentafluorobenzene

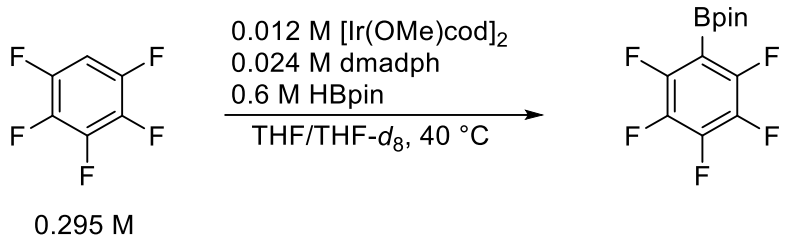

In a N_2 filled glovebox, $[Ir(OMe)cod]_2$ (0.0070 g, 0.01 mmol), dmadph (0.0060 g, 0.02 mmol), were weighed into separate test tubes. Then, 1.0 mL of THF was added to both test tubes. To the solution of Ir, HBpin (300 µL, 2 mmol) was added and shaken briefly, turning the light-yellow solution into a golden-yellow. The solution of Ir and pinacolborane was then pipetted into the solution of dmadph and transferred into a scintillation vial with a stir bar. The combined solution was stirred vigorously for 5 minutes, turning the solution dark red. Using a microsyringe, 400 µL of the combined solution was added to a J-young tube, followed by pentafluorobenzene (20 µL, 0.18 mmol) and 0.3 mL of THF-d_8. The J-young was capped, inverted and thoroughly mixed. The tube was then transferred into a preheated oil bath at 40 °C and monitored by ^{1}H, ^{19}F, and ^{11}B NMR. Conversion after 3.5 h was determined to be 90% via ^{19}F NMR. After the reaction completed, the NMR tube was placed into a –40 °C freezer. Upon returning to the NMR tube after two days, white solids precipitated from solution. These solids were taken up in $CDCl_3$ and analyzed by ^{1}H, ^{11}B, and ^{19}F NMR.

Notes: *Mass balance for isolation of the solid material was not taken due to the NMR tube breaking. With no prior knowledge of the stability of the products, NMR analysis was immediately performed. The solids contained a mixture of the Ir complex and C_6F_5Bpin.*

In the aromatic and hydride regions of the ^{1}H NMR, an Ir–fluoroaryl complex was identified and the proposed structures are shown below. The tentatively assigned ^{1}H, ^{11}B and ^{19}F NMR resonances are given for the proposed structures.

Proposed Ir^{V} complexes

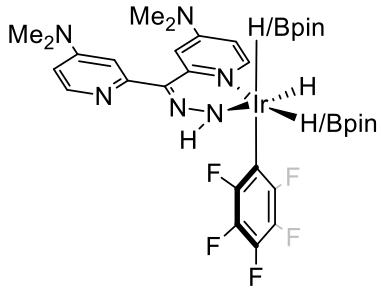

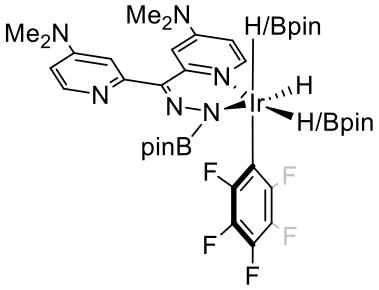

Proposed Ir^{III} complexes

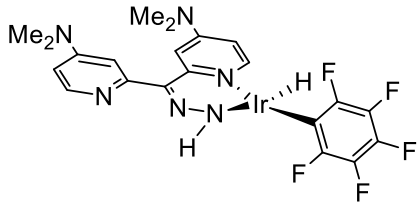

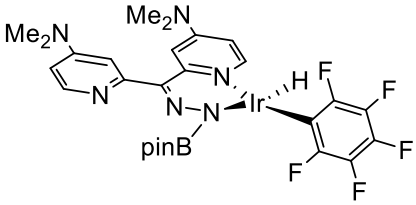

^{1}H NMR (500 MHz, $CDCl_3$) of Ir–fluoroaryl complex δ 11.12 (s, 1H), 8.54 (d, J = 5.9 Hz, 1H), 8.41 (d, J = 7.0 Hz, 1H), 6.89 (d, J = 14.0 Hz, 2H), 6.65 (d, J = 6.3 Hz, 1H), 6.29 (d, J = 5.1 Hz, 1H), 3.08 (s, 6H), 2.99 (s, 6H), 0.95 (s, 6H), 0.90 (s, 6H), -8.24 – -8.33 (m, 1H)*.

Note: The hydride integral was <1, and this may be due to rapid exchange with residual D_2O.

^{11}B NMR (160 MHz, $CDCl_3$) of Ir–fluoroaryl complex δ 22.5 (br s), 2.9 (br s).

^{19}F NMR (470 MHz, $CDCl_3$) δ -116.40, -131.43, -134.39.

3.3.4. KIE Experiment

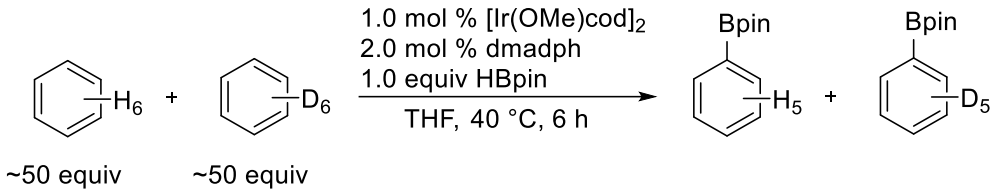

In a N_2 filled glovebox, $[Ir(OMe)cod]_2$ (0.004 g, 0.06 mmol), dmadph (0.003 g, 0.011 mmol), were weighed into separate test tubes. Then, 1.0 mL of THF was added to both test tubes. To the solution of Ir, HBpin (15.0 µL, 0.10 mmol) was added and shaken briefly, turning the light-yellow solution into a golden-yellow. The solution of Ir and pinacolborane was then pipetted into the solution of dmadph and transferred into a Wheaton vial with a stir bar. The combined solution was stirred vigorously for 5 minutes, turning the solution dark red. Last, benzene (0.46 mL, 5.2 mmol) and d_6-benzene (0.50 mL, 5.2 mmol) were added to the combined solution. The vial was capped and taken out of the glovebox and transferred to a preheated aluminum block at 40 °C. The reaction was monitored by GC-MS and ^{11}B NMR. The conversion determined by ^{11}B NMR was >99% at 6 h.

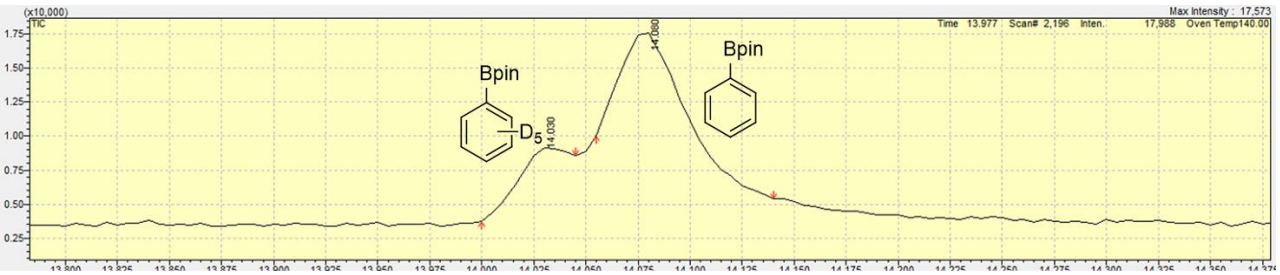

Peak#	Ret.Time	Start Tm	End Tm	m/z	Area	Area%	Height	Height%	A/H	Mark
1	14.032	14.000	14.045	TIC	3519	17.16	1919	17.94	1.83	
2	14.078	14.055	14.140	TIC	16991	82.84	8777	82.06	1.94	

Figure S3.2. GC-MS trace of the crude reaction mixture at t = 6 h

3.3.5. Experiments Probing for Transfer Borylation

Transfer borylation of 2-methylthiophene with dmadph

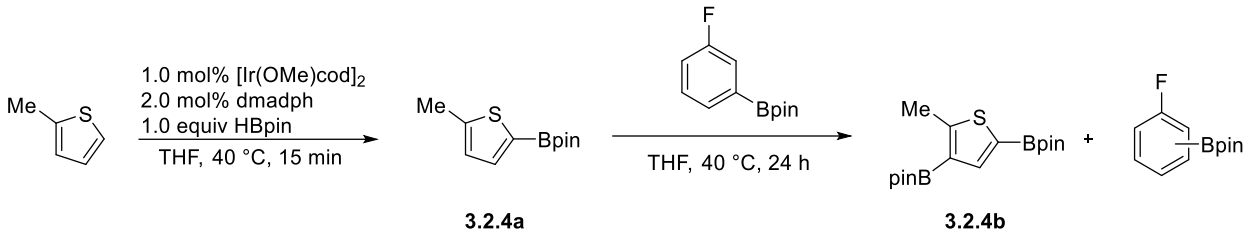

ligand	ratio of *o*:*m*:*p* to F mono-borylated isomers	%**3.2.4b**	%conversion (based on HBpin)
dmadph	1.7 : 3.5 : 1.0	46	>99

In a nitrogen-filled glovebox, a 3.0 mL Wheaton pressure vial equipped with a stir bar was charged with a 1.0 mL THF solution of $[Ir(OMe)cod]_2$ (6.6 mg, 0.01 equiv). To this solution, pinacolborane (0.145 mL, 1 mmol, 1.0 equiv) was added with a syringe while stirring, turning the light-yellow solution into a golden orange. Then, in a small test tube, a 1.0 mL THF solution of dmadph (5.3 mg, 0.02 equiv) was made and added to the iridium solution with a syringe and the solution immediately turned dark red in color. Last, 2-methylthiophene (98 µL, 1.0 mmol, 1.0 equiv) was added to this solution and capped. The reaction was heated at 40 °C and stirred in an aluminum heating block on top of a stir plate outside of the glovebox for 15 min. The vial was removed from the block, and 2-(3-fluorophenyl)-4,4,5,5-tetramethyl-1,3,2-dioxaborolane (0.2204 g, 1.0 mmol, 1.0 equiv) was added and the vial immediately capped and heated at 40 °C for 24 h. After 24 h, the volatiles were evaporated, and the crude reaction mixtures were analyzed by ^{19}F, ^{1}H, and ^{11}B NMR. ^{19}F NMR analysis showed all three isomers of mono-borylated fluorobenzene (1.7 : 3.5 : 1.0 of the o:m:p isomers) and fluorobenzene. For full characterization of all isomers of borylated fluorobenzene, see pages 53–54**.** ^{1}H NMR analysis revealed 46% of the 3,5-diborylated 2-methylthiophene and 54% of the mono-borylated 5-Bpin-2-methylthiophene.

Note: *Products were not isolated, and crude reaction mixtures after drying were analyzed. Both 3.2.4a*[13] *and 3.2.4b*[13] *matched previously reported literature values.*

^{1}H NMR (500 MHz, $CDCl_3$) of 3.2.4a δ 7.40 (d, *J* = 3.4 Hz, 1H), 6.81 – 6.79 (m, 1 H), 2.49 (s, 3H), 1.29 (s, 12H).

^{11}B NMR (160 MHz, $CDCl_3$) of 3.2.4a δ 30.6 (br s)

^{1}H NMR (500 MHz, $CDCl_3$) of 3.2.4b δ 7.79 (s, 1H), 2.67 (s, 3H), 1.27 (s, 12H), 1.26 (s, 12H).

^{11}B NMR (160 MHz, $CDCl_3$) of 3.2.4b δ 30.6 (br s)

Transfer borylation of 2-methylthiophene with dtbpy

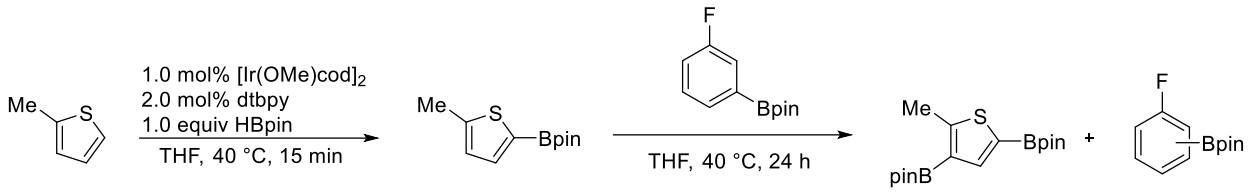

ligand	ratio of *o*:*m*:*p* to F mono-borylated isomers	%**3.2.4b**	%conversion (based on HBpin)
dtbpy	0 : >99 : 0	<1	>99

In a nitrogen-filled glovebox, a 3.0 mL Wheaton pressure vial equipped with a stir bar was charged with a 1.0 mL THF solution of $[Ir(OMe)cod]_2$ (6.6 mg, 0.01 equiv). To this solution, pinacolborane (0.145 mL, 1 mmol, 1.0 equiv) was added with a syringe while stirring, turning the light-yellow solution into a golden orange. Then, in a small test tube, a 1.0 mL THF solution of dtbpy (5.6 mg, 0.02 equiv) was made and added to the iridium solution with a syringe and the solution immediately turned dark red in color. Last, 2-methylthiophene (98 µL, 1.0 mmol, 1.0 equiv) was added to this solution and capped. The reaction was heated at 40 °C and stirred in an aluminum heating block on top of a stir plate outside of the glovebox for 15 min. The vial was removed from the block, and 2-(3-fluorophenyl)-4,4,5,5-tetramethyl-1,3,2-dioxaborolane (0.2204 g, 1.0 mmol, 1.0 equiv) was added and the vial immediately capped and heated at 40 °C for 24 h. After 24 h,

the volatiles were evaporated, and the crude reaction mixtures were analyzed by ^{19}F, ^{1}H, and ^{11}B NMR. ^{19}F NMR analysis showed only starting material and deborylated fluorobenzene. ^{1}H NMR analysis revealed no diborylation of the thiophene and only monoborylated **3.2.4a**.

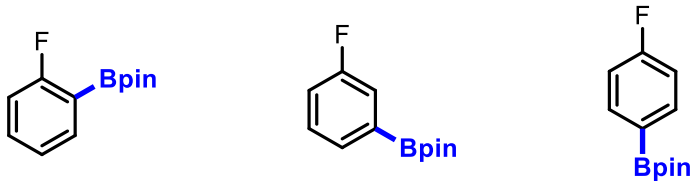

energy (kcal•mol^{-1})	-737.365	-737.620	-737.621

Figure S3.3. Calculated ground state energies of borylated fluorobenzene isomers

3.3.6. NMR Data

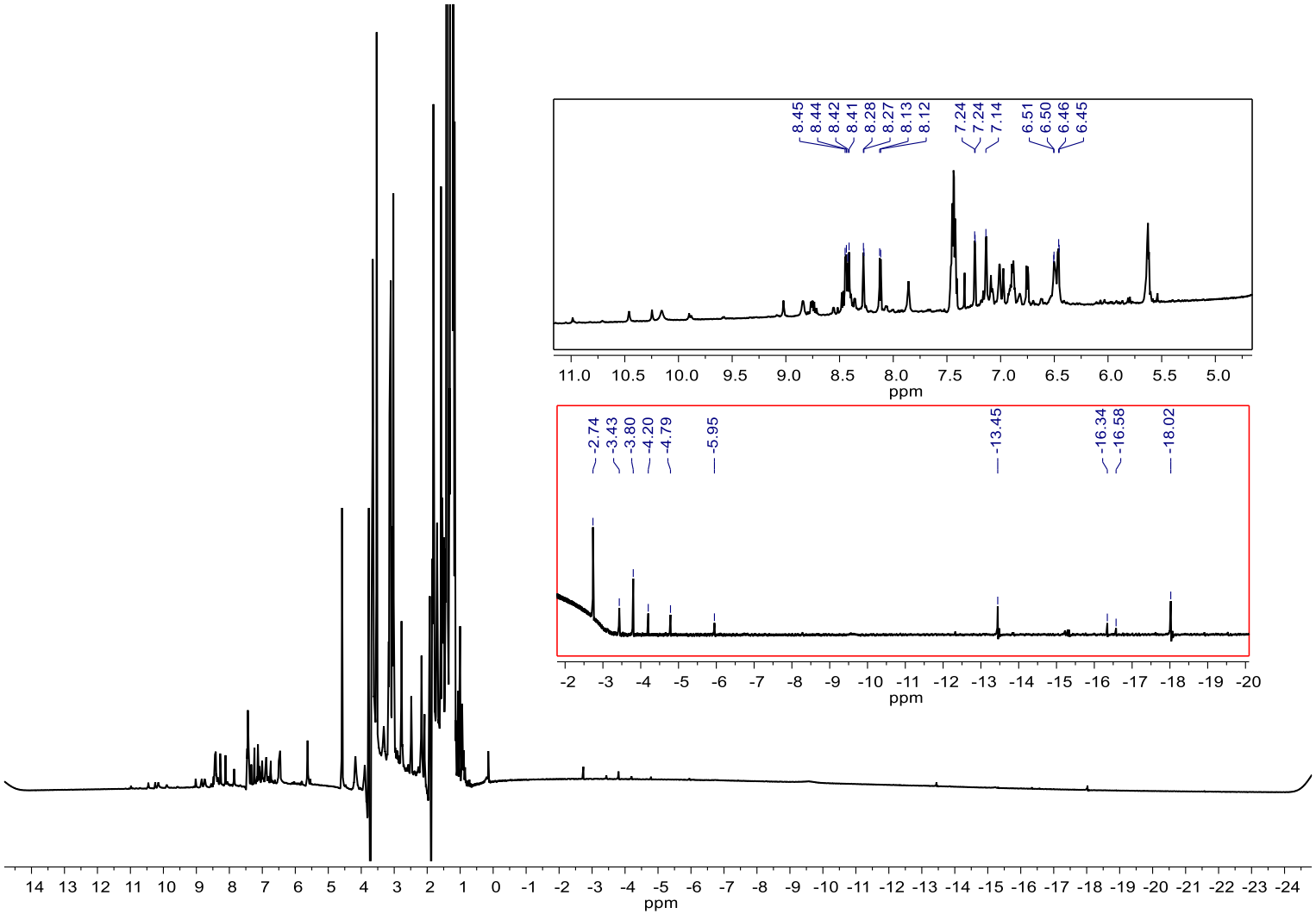

^{1}H NMR (500 MHz, 1:1 THF/THF-d_8) of pentafluorobenzene borylation at t = 1.5 h. Top inset shows the aryl region expanded. Bottom inset in red is the hydride region expanded.

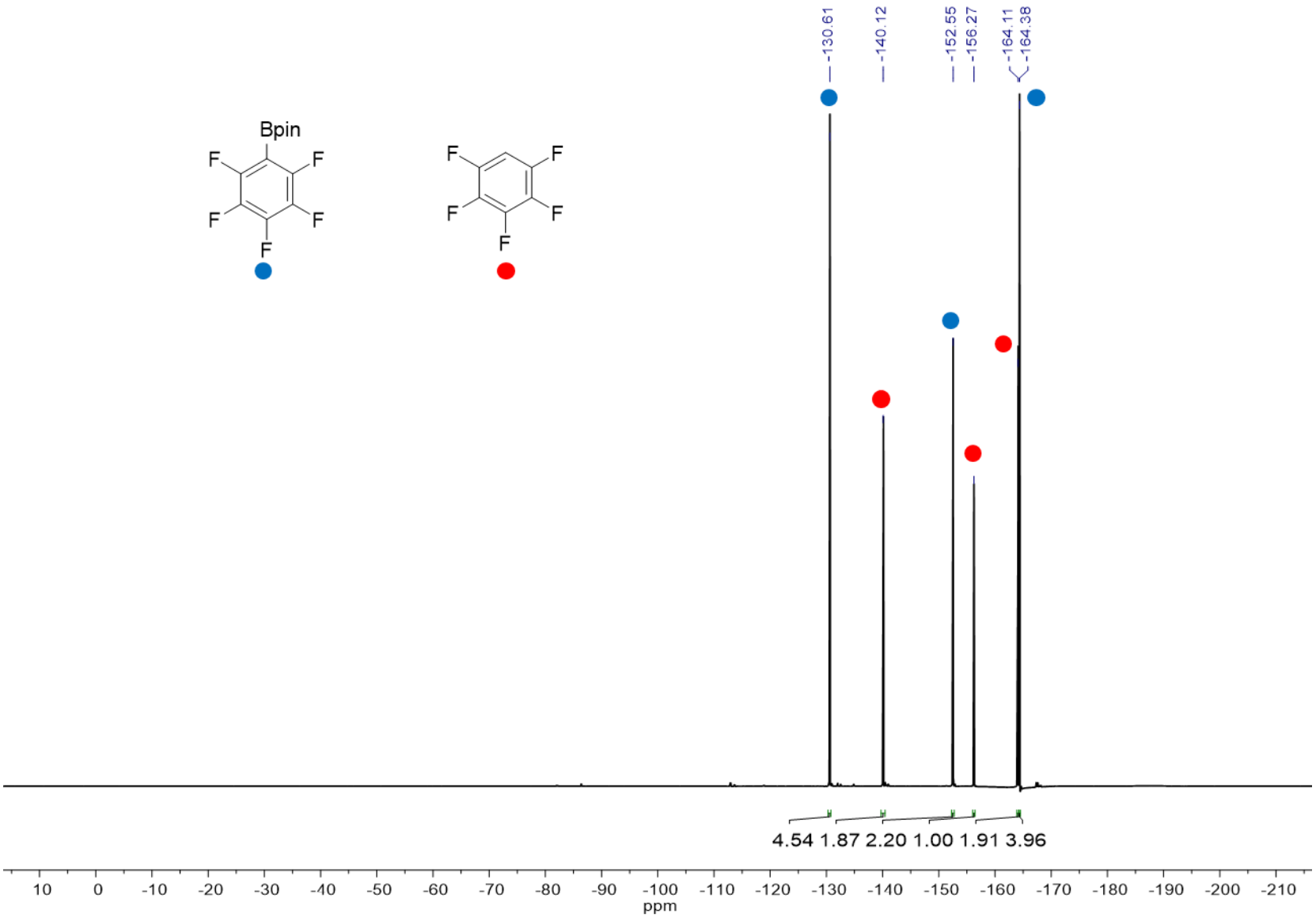

^{19}F NMR (470 MHz, 1:1 THF/THF-d_8) of pentafluorobenzene borylation at t = 0.75 h.

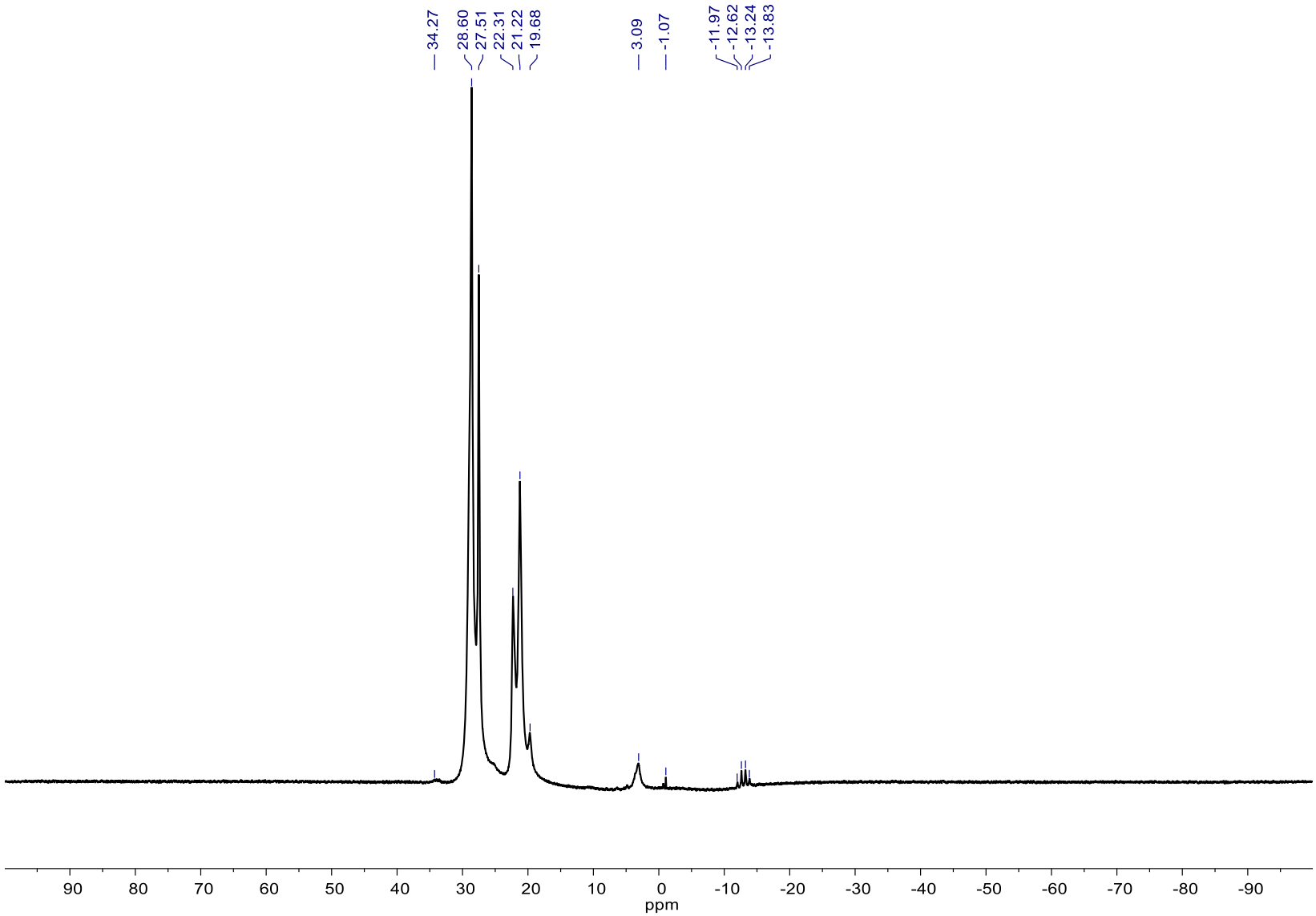

^{11}B NMR (160 MHz, 1:1 THF/THF-d_8) of pentafluorobenzene borylation at t = 0.75 h.

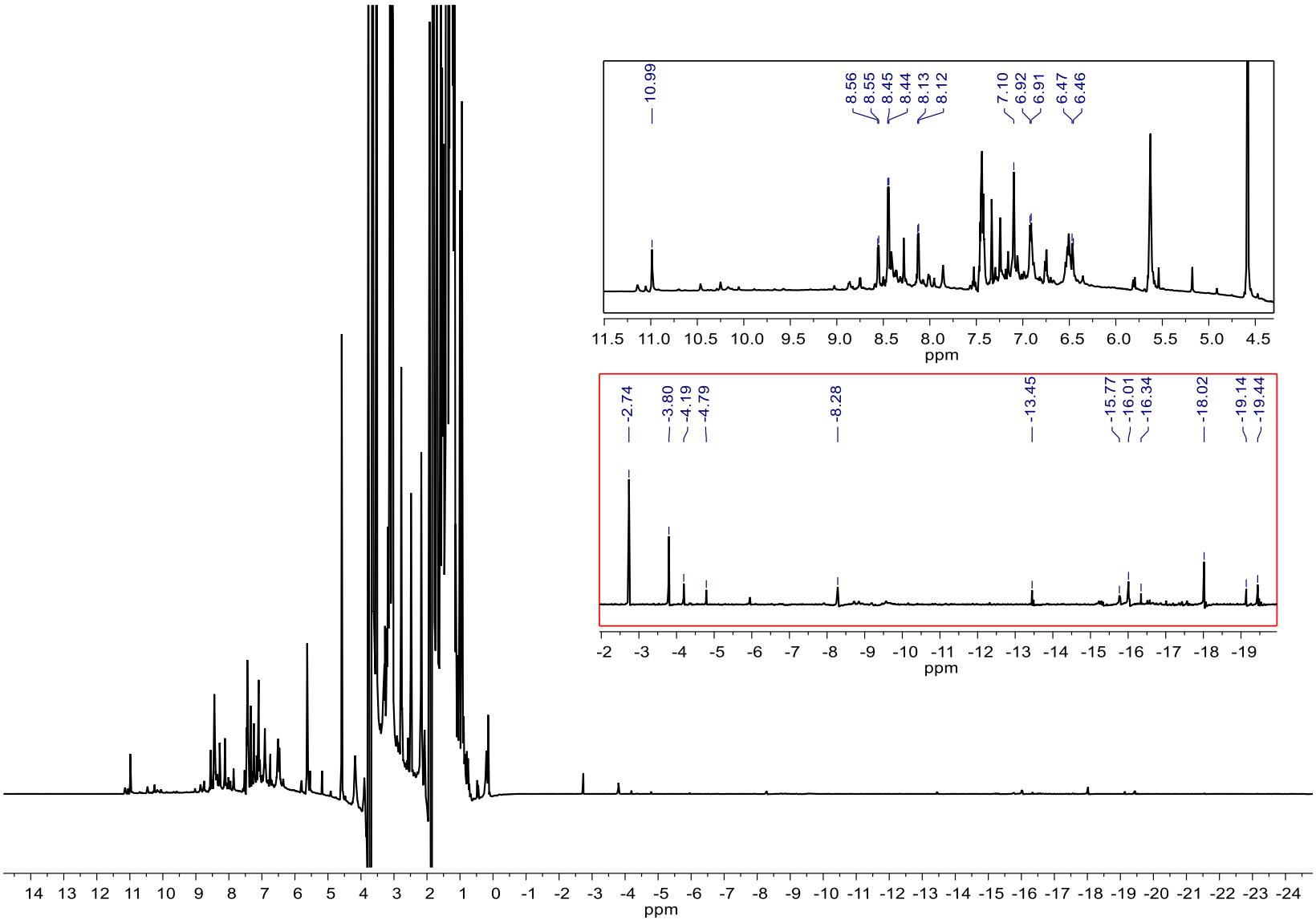

^{1}H NMR (500 MHz, 1:1 THF/THF-d_8) of pentafluorobenzene borylation at t = 1.5 h. Top inset shows the aryl region expanded. Bottom inset in red is the hydride region expanded.

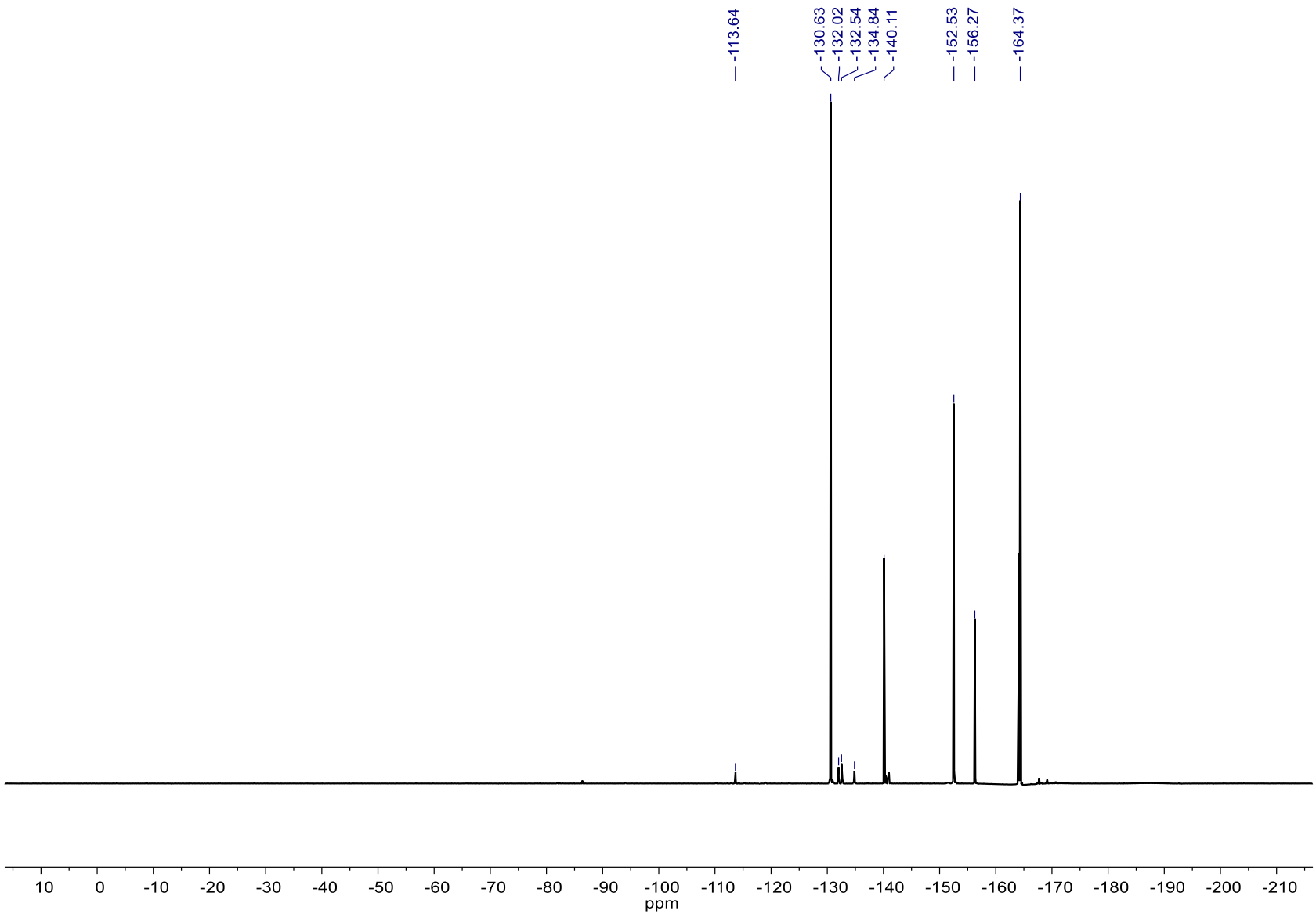

^{19}F NMR (470 MHz, 1:1 THF/THF-d_8) of pentafluorobenzene borylation at t = 1.5 h.

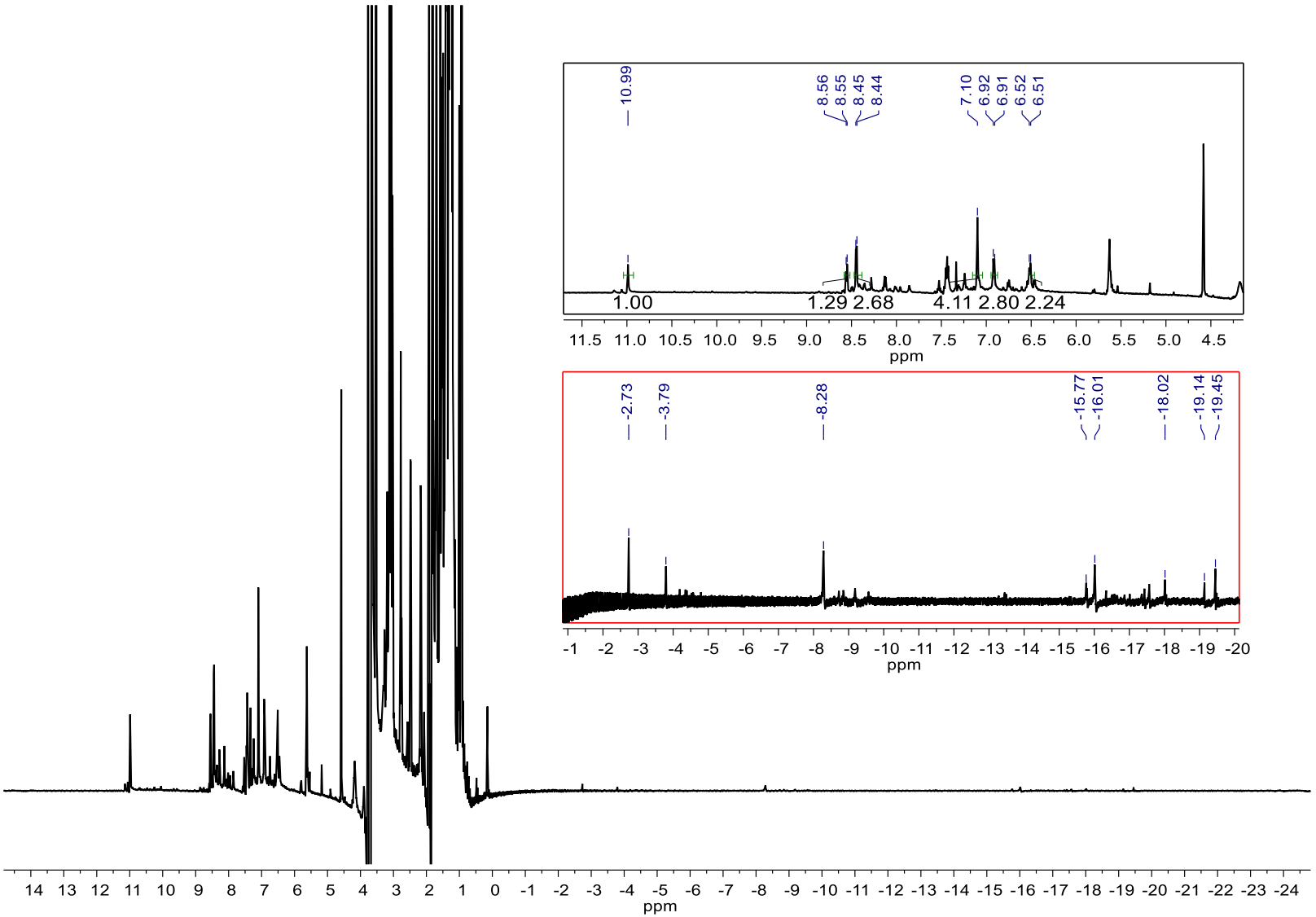

^{1}H NMR (500 MHz, 1:1 THF/THF-d_8) of pentafluorobenzene borylation at t = 3.5 h. Top inset shows the aryl region expanded. Bottom inset in red is the hydride region expanded.

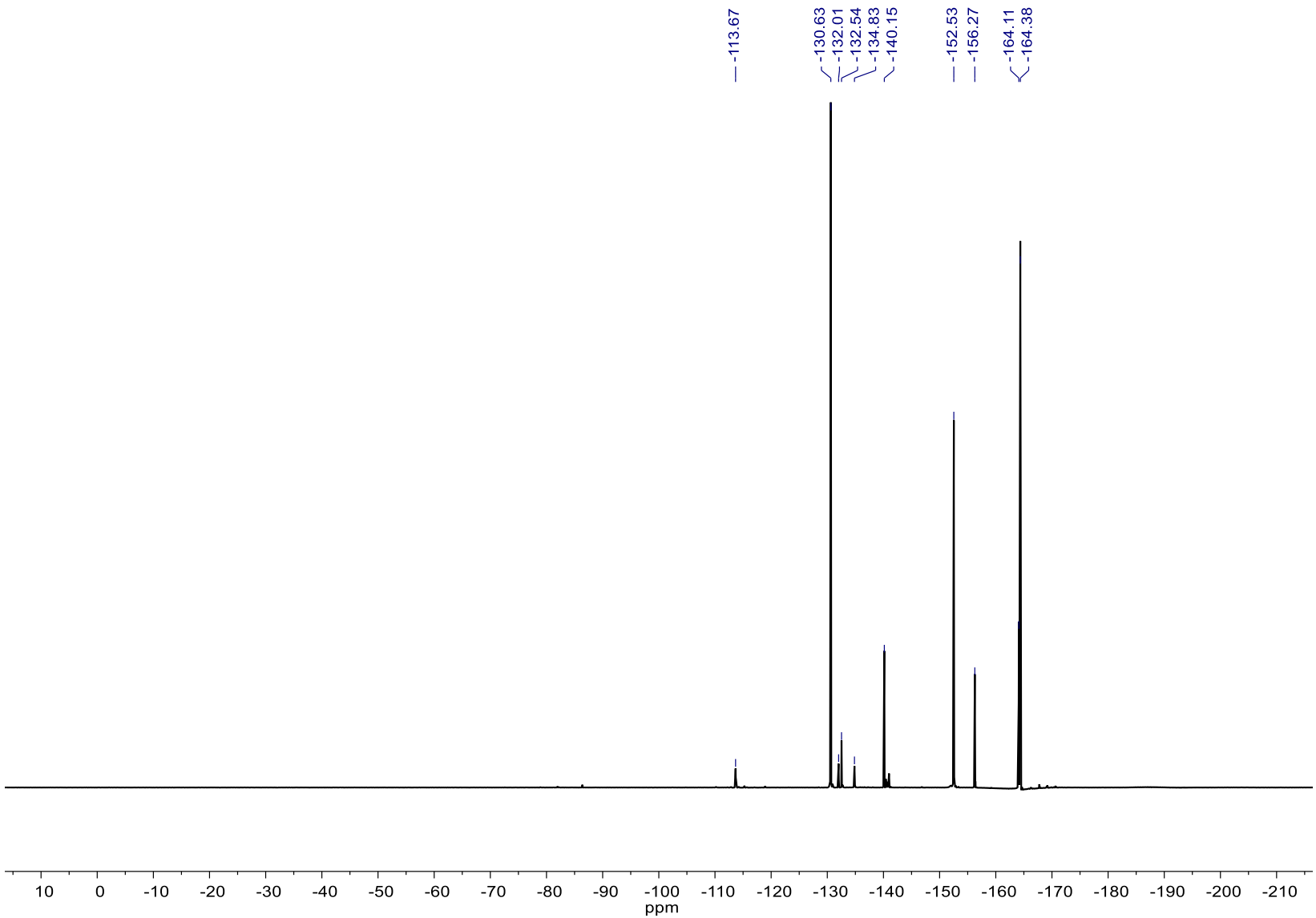

^{19}F NMR (470 MHz, 1:1 THF/THF-d_8) of pentafluorobenzene borylation at t = 3.5 h.

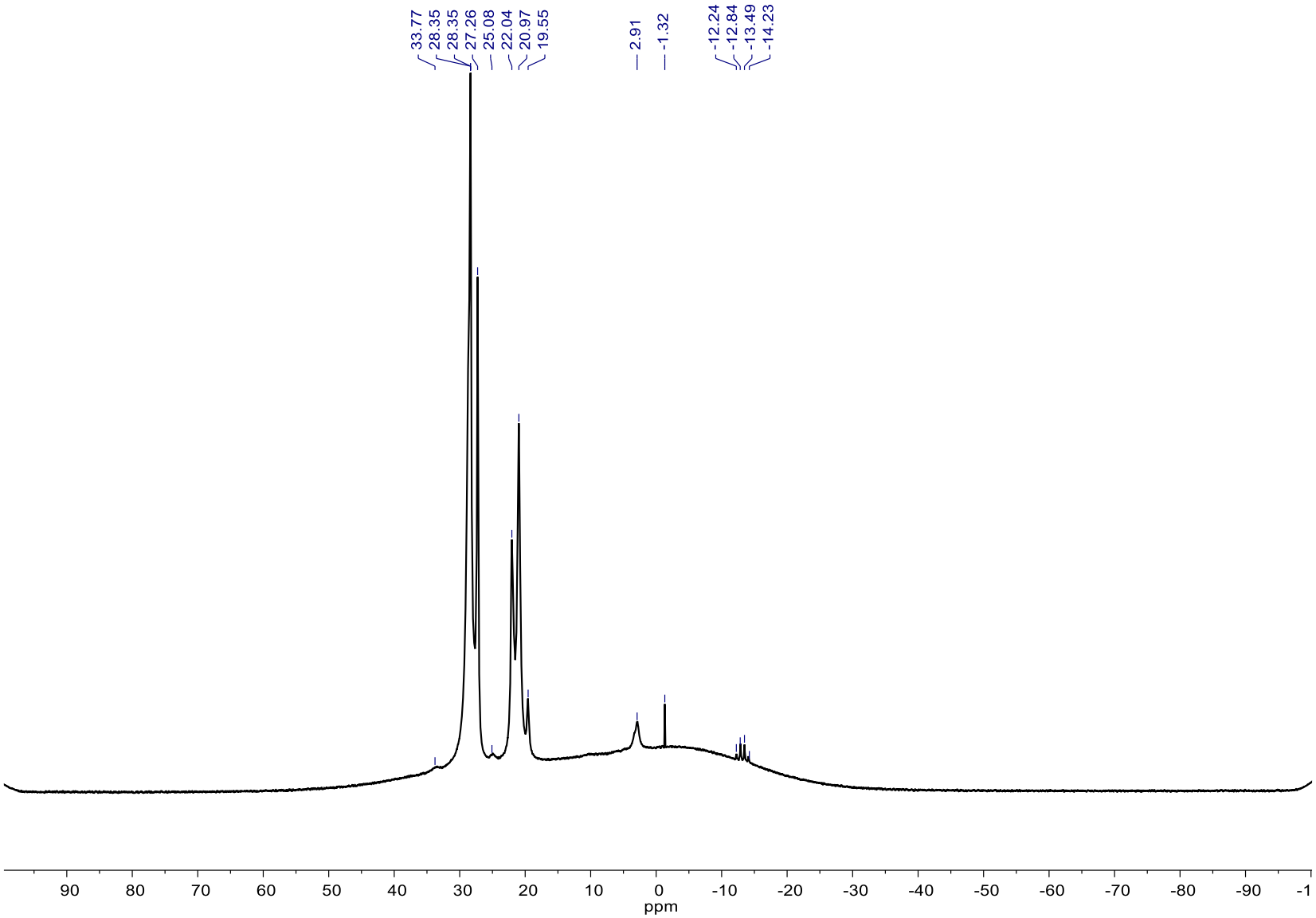

^{11}B NMR (160 MHz, 1:1 THF/THF-d_8) of pentafluorobenzene borylation at t = 3.5 h.

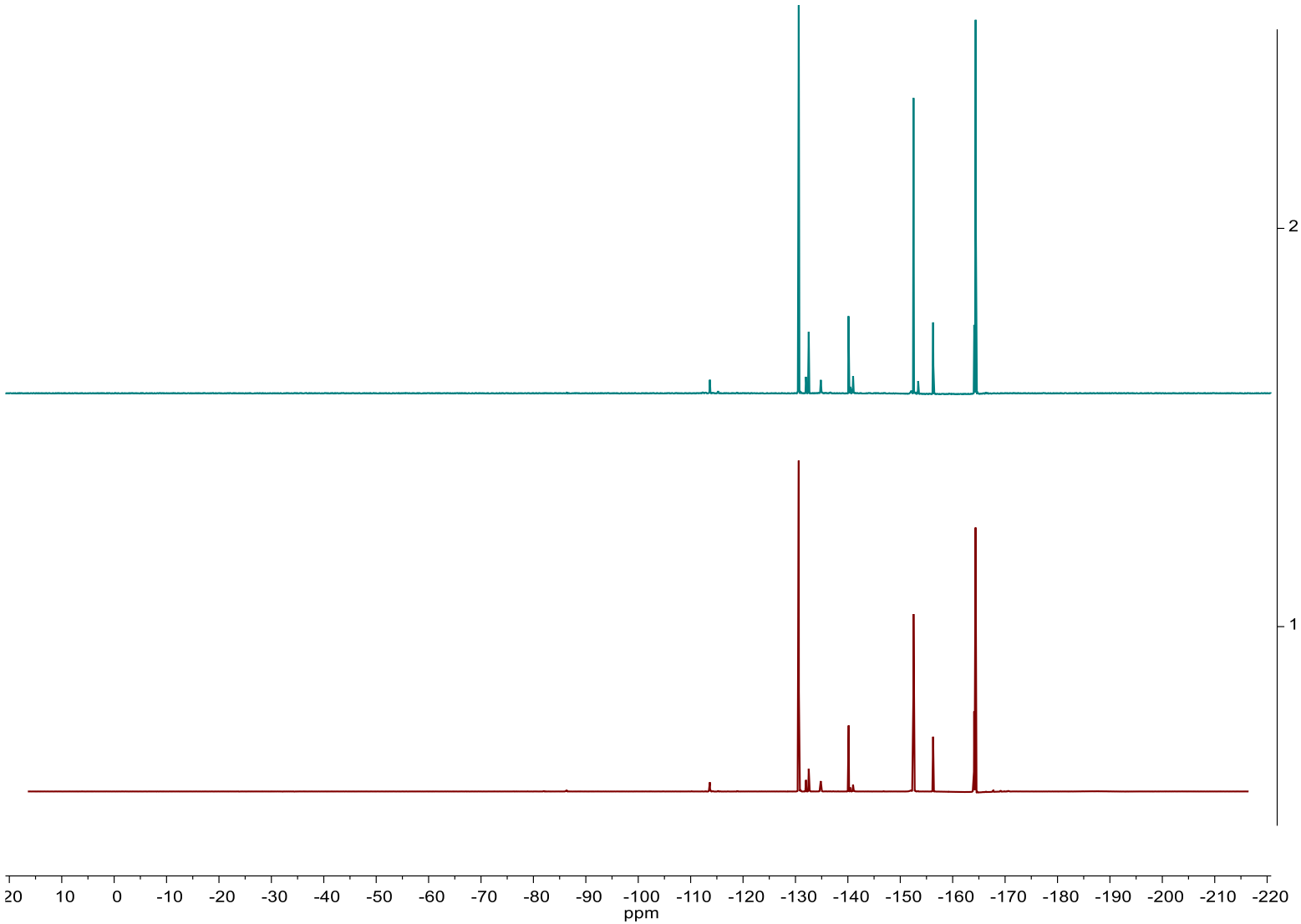

^{19}F NMR (470 MHz, 1:1 THF/THF-d_8) stacked plot of pentafluorobenzene borylation at t = 3.5 h. Top spectrum is $\{^1H\}^{19}F$ and the bottom is ^{1}H coupled.

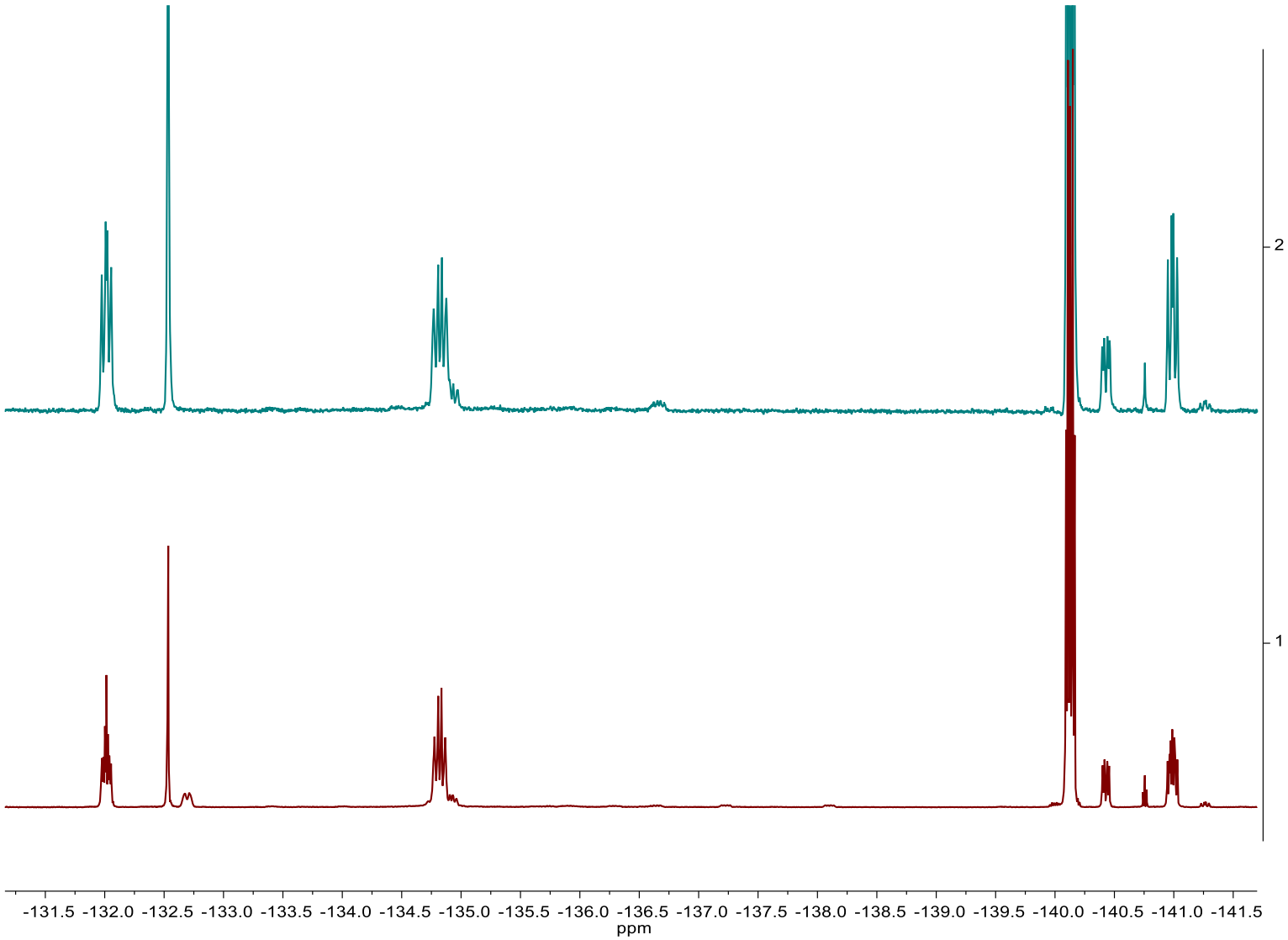

^{19}F NMR (470 MHz, 1:1 THF/THF-d_8) stacked plot of pentafluorobenzene borylation at t = 3.5 h. Top spectrum is {^{1}H}^{19}F and the

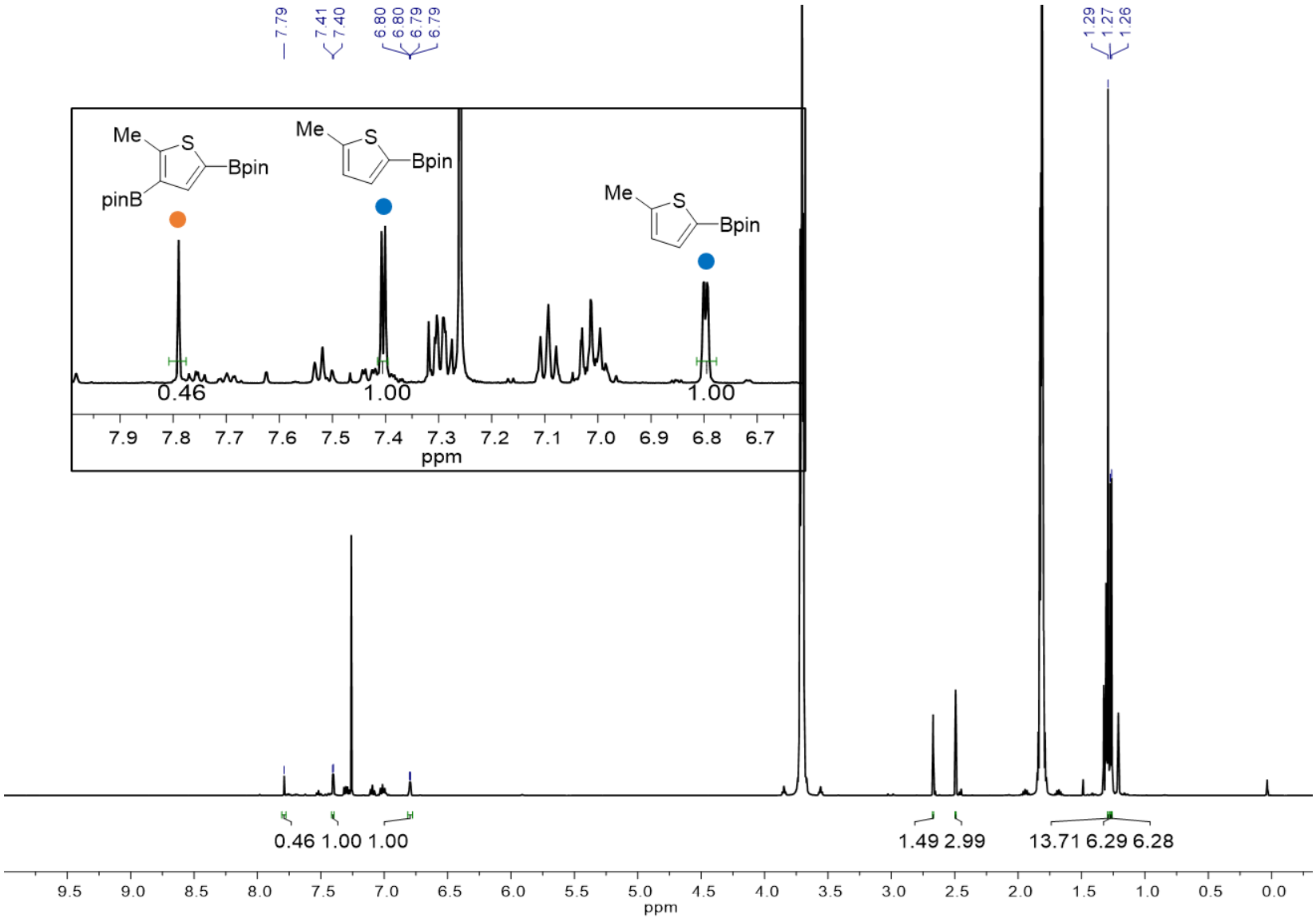

^{1}H NMR (500 MHz, $CDCl_3$) of the crude reaction mixture from the transfer borylation of **3.2.4a** and **3.2.4b**

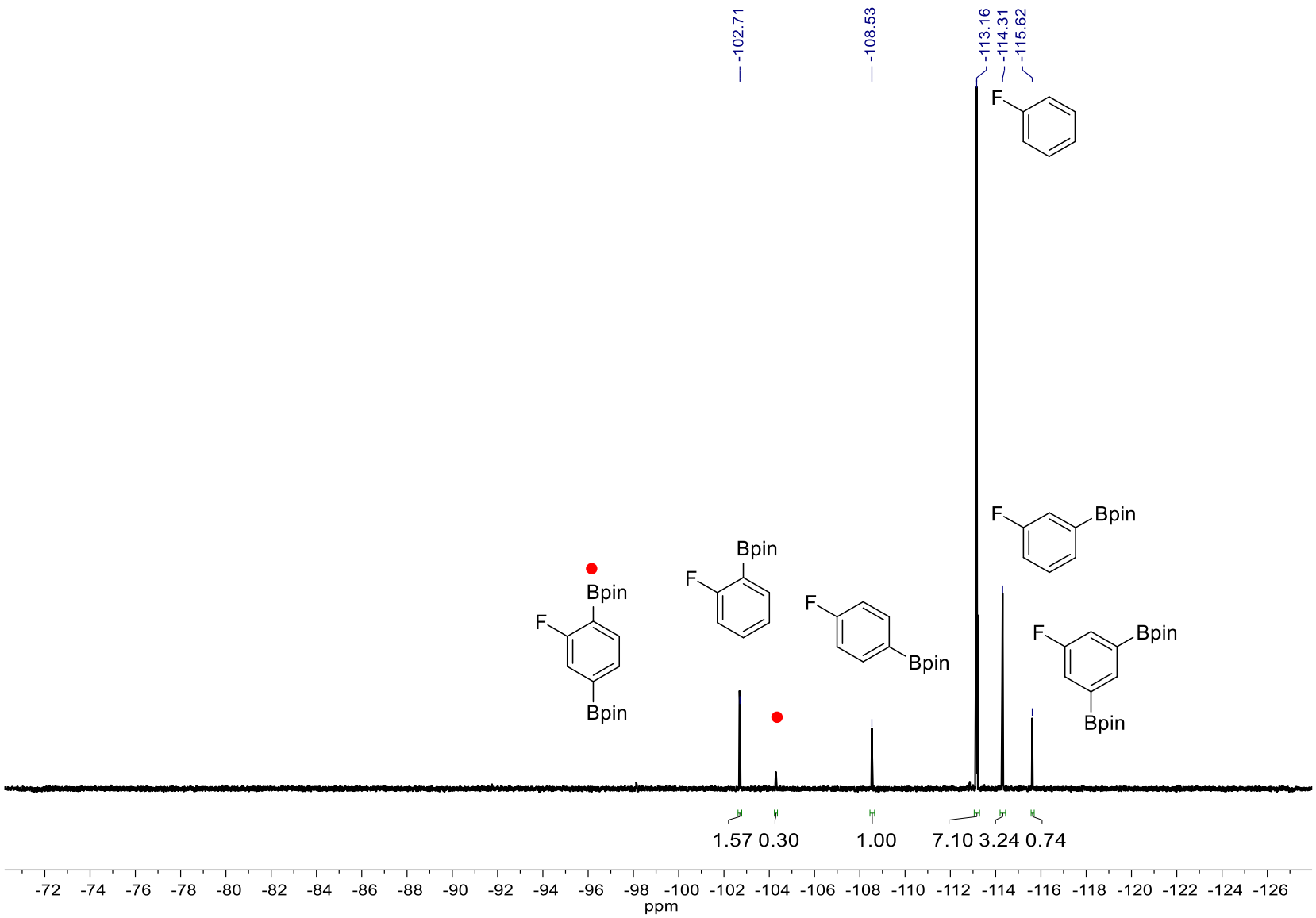

^{19}F NMR (470 MHz, $CDCl_3$) of the crude reaction mixture from the transfer borylation of **3.2.4a** and **3.2.4b**

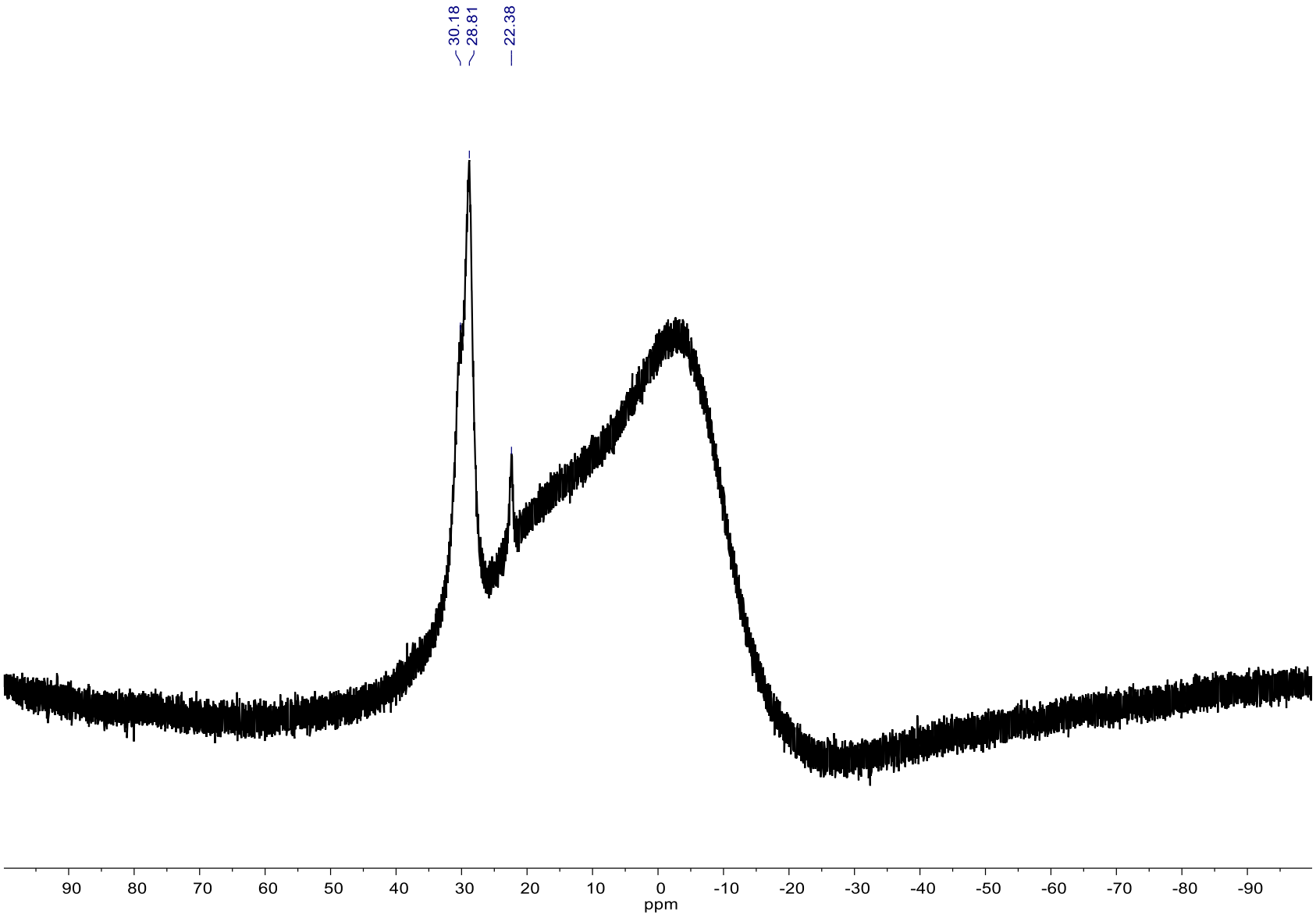

^{11}B NMR (160 MHz, $CDCl_3$) of the crude reaction mixture from the transfer borylation of **3.2.4a** and **3.2.4b**

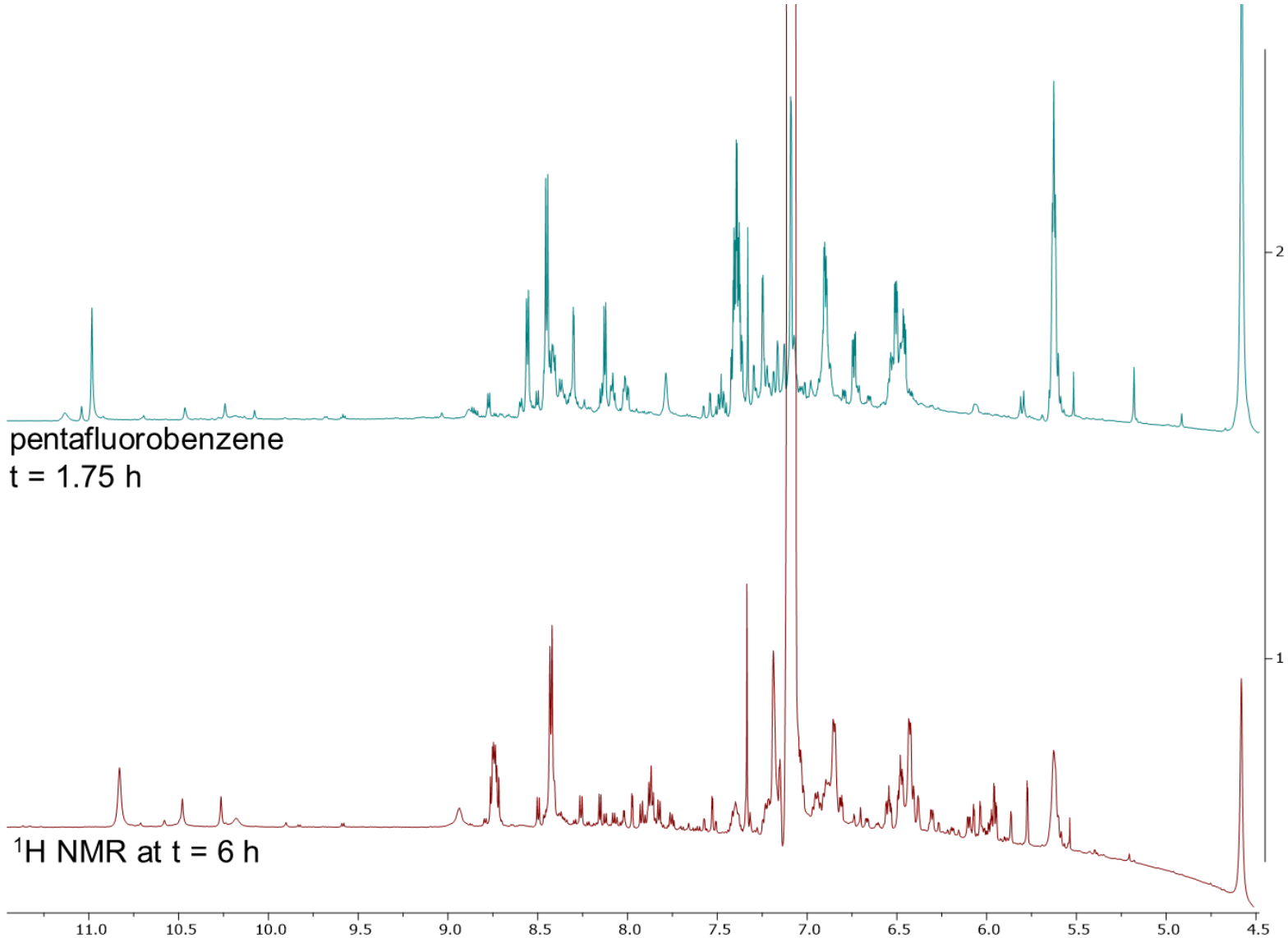

^{1}H NMR (500 MHz, THF/THF-d_8) stack plot of the crude reaction mixture from the borylation of tetrafluorotoluene (bottom) and that observed from the borylation of pentafluorobenzene

REFERENCES

(1) Rochette, É.; Desrosiers, V.; Soltani, Y.; Fontaine, F.-G. Isodesmic C-H Borylation: Perspectives and Proof of Concept of Transfer Borylation Catalysis. *J. Am. Chem. Soc.* **2019**, *141* (31), 12305–12311.

(2) Desrosiers, V.; Garcia, C. Z.; Fontaine, F.-G. Boron Recycling in the Metal-Free Transfer C–H Borylation of Terminal Alkynes and Heteroarenes. *ACS Catal.* **2020**, *10* (19), 11046–11056.

(3) Veth, L.; Grab, H. A.; Martínez, S.; Antheaume, C.; Dydio, P. Transfer C–H Borylation of Alkenes under Rh(I) Catalysis: Insight into the Synthetic Capacity, Mechanism, and Selectivity Control. *Chem Catalysis* **2022**. https://doi.org/10.1016/j.checat.2022.02.008.

(4) Légaré, M.-A.; Courtemanche, M.-A.; Rochette, É.; Fontaine, F.-G. Metal-Free Catalytic C-H Bond Activation and Borylation of Heteroarenes. *Science* **2015**, *349* (6247), 513–516.

(5) Dannatt, J. E. Advancing Frontiers in Reactive and Selective Iridium C–H Borylation Catalysis and Targeted Silsesquioxane Synthesis. Ph.D. Dissertation, Michigan State University, 2019.

(6) Guo, L.; Dai, S.; Sui, X.; Chen, C. Palladium and Nickel Catalyzed Chain Walking Olefin Polymerization and Copolymerization. *ACS Catal.* **2016**, *6* (1), 428–441.

(7) Craig, P. J.; Needham, M. I.; Ostah, N.; Stojak, G. H.; Symons, M.; Teesdale-Spittle, P. Nuclear Magnetic Resonance and Mass Spectra of Organomercury Hydrides and Deuterides. *J. Chem. Soc. Dalton Trans.* **1996**, No. 2, 153–156.

(8) Boller, T. M.; Murphy, J. M.; Hapke, M.; Ishiyama, T.; Miyaura, N.; Hartwig, J. F. Mechanism of the Mild Functionalization of Arenes by Diboron Reagents Catalyzed by Iridium Complexes. Intermediacy and Chemistry of Bipyridine-Ligated Iridium Trisboryl Complexes. *J. Am. Chem. Soc.* **2005**, *127* (41), 14263–14278.

(9) Miller, S. L. PART A: Iridium Catalyzed C-H Borylation of Arenes; Engineering Selectivity by Ligand Design. Ph.D. Dissertation, Michigan State University, 2017.

(10) Uson, R.; Oro, L. A.; Cabeza, J. A.; Bryndza, H. E.; Stepro, M. P. Dinuclear Methoxy, Cyclooctadiene, and Barrelene Complexes of Rhodium(I) and Iridium(I): Kirschner/Inorganic. In *Inorganic Syntheses*; Kirschner, S., Ed.; Inorganic Syntheses; John Wiley & Sons, Inc.: Hoboken, NJ, USA, 1985; Vol. 231, pp 126–130.

(11) Pangborn, A. B.; Giardello, M. A.; Grubbs, R. H.; Rosen, R. K.; Timmers, F. J. Safe and Convenient Procedure for Solvent Purification. *Organometallics* **1996**, *15* (5), 1518–1520.

(12) Cai, M.; Luo, C.; Xu, C.; Huang, B. Recyclable Pd2dba3/XPhos/PEG-2000 System for Efficient Boryl-ation of Aryl Chlorides: Practical Access to Aryl Boronates. *Synthesis* **2022**, *54* (05), 1339–1346.

(13) Kallepalli, V. A.; Gore, K. A.; Shi, F.; Sanchez, L.; Chotana, G. A.; Miller, S. L.; Maleczka, R. E., Jr.; Smith, M. R., III. Harnessing C–H Borylation/Deborylation for Selective Deuteration, Synthesis of Boronate Esters, and Late Stage Functionalization. *J. Org. Chem.* **2015**, *80* (16), 8341–8353.